FUNCTIONAL GENOMICS OF MICRORNA-DIRECTED REGULATION OF TUMORIGENESIS IN HUMAN CANCER CELLS

DUYGU SELÇUKLU

A thesis submitted to National University of Ireland, Galway
For the degree of Doctor of Philosophy

Genetics & Biotechnology Lab
Centre for Chromosome Biology
School of Natural Sciences
September 2011

Under the supervision of Prof Charles Spillane

Table of Contents

List of Figures

List of Tables

Declaration

Data described in this thesis are the result of my work, which has been carried out in the Genetics and Biotechnology Lab, Department of Biochemistry, University College Cork (UCC) from October 2007 to January 2010 and in the Genetics and Biotechnology Lab, Centre for Chromosome Biology, National University of Ireland Galway (NUIG) from January 2010 to September 2011. The material is not substantially similar to any other work that has been submitted for any other degree or qualification at NUIG or any other university.

Abbreviations

A	Amper
Ab	Antibody
amp	ampicillin
AGO	Argonaute
BLAST	Basic Local Alignment Search Tool
bp	base pairs
BP	Biological Process
BSA	Bovine Serum Albumin
cDNA	Complementary Deoxyribonucleic Acid
CLL	Chronic Lymphocytic Leukemia
Ct	Cycle threshold
DGCR8	DiGeorge syndrome Critical Region gene 8
DLBCL	Diffuse large B-cell lymphoma
DMEM	Dulbecco's minimum Essential Medium
DMSO	Dimethyl Sulfoxide
DNA	Deoxyribonucleic Acid
DNase	Deoxyribonuclease
DOC	Deoxycholate
dNTP	Deoxyribonucleotide Triphosphate
E2	Estradiol
EDTA	Ethylenediaminetetraacetic Acid
EMT	Epithelial-Mesenchymal Transition
Em	Emission
EtOH	Ethanol
ER	Estrogen Receptor
Ex	Excitation
FBS	Fetal Bovine Serum
g	centrifuge gravity force
GO	Gene Ontology
hr	hour
IL-6	Interleukin-6

IPA	Ingenuity Pathway Analysis
IVT	In Vitro Transcription
KEGG	Kyoto Encyclopedia of Genes and Genomes
LB	Lysogeny Broth
MCF-7	Michigan Cancer Foundation - 7
MCS	Multiple Cloning Site
MDDC	Monocyte-Derived Dendritic Cells
min	minute
mRNA	messenger RNA
miRNA	microRNA
miRNP	miRNA Ribonucleoprotein complex
miPPR	Putative Promoter Regions of miRNA
MMP	Matrix metalloproteinases
MS	Multiple Sclerosis
NCBI	National Center for Biotechnology Information
ng	nano gram
nm	nano meter
nM	nano Molar
nt	nucleotide(s)
PBS	Phosphate Buffered Saline
PCR	Polymerase Chain Reaction
PLB	Passive Lysis Buffer
PR	Progesterone Receptor
Pri-miRNA	Primary microRNA
Pre-miRNA	Precursor microRNA
PVDF	Polyvinylidene Fluoride
qPCR	quantitative PCR
RIN	RNA Integrity Number
RISC	RNA-Induced Silencing Complex
RNA	Ribonucleic Acid
RNase	Ribonuclease
RNU6B	Small Nuclear U6 B
RT-PCR	Reverse Transcription Polymerase Chain Reaction

rpm	revolution per minute
RQ	Relative Quantification
SAP	Shrimp Alkaline Phosphatase
SCC	Squanmous Cell Carcinoma
SDM	Site Directed Mutagenesis
SDS-PAGE	Sodium Dodecyl Sulfate- Polyacrylamide Gel Electrophoresis
SILAC	Stable Isotope Labeling with Amino acids In Cell culture
siRNA	Small Interfering RNA
stRNA	small temporal RNA
SNP	Single Nucleotide Polymorphism
STS	Staurosporine
TBS-T	Tris Buffered Saline-Tween 20
Taq	*Thermus aquaticus*
Tm	melting Temperature
TSS	Transcription Start Site
µg	micro gram
µl	micro litre
UCSC	University of California, Santa Cruz
UTR	Untranslated Region
V	Volt

Conferences and Presentations

Practical Courses

- EMBL Practical Course on Next-Generation Sequencing, June 2010, Heidelberg, Germany

Poster Presentations

- Irish Association of Cancer Research Annual Meeting, March 2007, Cork, Ireland
- 39th European Human Genetics Conference, June 2007, Nice, France, Conference Fellowship
- Joint Health Research Day to incorporate Cork University Hospital Annual Research Day, June 2007, College of Medicine and Health UCC, Cork, Ireland, Best Poster Award
- Epigenetics and New Therapies in Cancer, Spanish National Cancer Centre, November 2007, Madrid, Spain
- EMBO young scientist forum, 2008, Istanbul, Turkey
- Irish Association of Cancer Research Annual Meeting Feb 2008, Newcastle, Ireland, Best Poster Award
- Genomes to Systems, The Consortium for the latest post-genome developments, March 2008, Manchester, UK
- ESF Symposium, Non-Coding RNAs: Computational Challenges and Applications, April 2008, Antalya, Turkey, Conference Fellowship
- ESF Workshop and Symposium, Advanced large scale gene expression profiling, May 2008, Turku, Finland, Conference Fellowship
- 40th European Human Genetics Conference, June 2008, Barcelona, Spain, Conference Fellowship
- Keystone, miRNAs and cancer, June 2009, Colorado, USA
- Apoptosis Symposium, ARC, August 2010, NUI, Galway, Ireland

Oral Presentations

- ESF Workshop and Symposium, Advanced large scale gene expression profiling, focus on miRNAs, ChIP-on-chip and whole genome sequencing, May 2008, Turku, Finland
- Genome Instability and cancer seminar, December 2008, NUI, Galway, Ireland

Publications

Peer-reviewed publications

Selcuklu SD, Donoghue MTA, Spillane C (2009) Mir-21 as a key regulator of oncogenic processes, Biochem Soc Trans 37: 918-925

Selcuklu SD, Yakicier MC, Erson AE (2009) An investigation of microRNA genes mapping to genomic instability regions in breast cancer, Cancer Genet Cytogenet., 189(1):15-23.

Selcuklu SD, Spillane C (2008) Translational epigenetics: clinical approaches to epigenome therapeutics for cancer, Epigenetics 3: 107-112

Selcuklu SD, Yakicier MC, Erson AE (2007) Identification and Characterization of microRNA in genomic instability regions of breast cancer, European Human Genetics Conference, France, Abstract in Proceedings of European Journal of Human Genetics, Vol 15(1): 162

Selcuklu SD, Yakicier MC, Erson AE. (2007) MIRN21 (microRNA 21), Atlas Genet Cytogenet Oncol Haematol. Available online.
URL: http://AtlasGeneticsOncology.org/Genes/MİRN21ID44019ch17q23.html

Manuscripts in preparation

Selcuklu SD, Donoghue MTA*, Gomes MS*, Kovvuru P, Muniyappa MK, Enright A, Spillane C (2011) Mir-9 targets oncogenes to regulate proliferation and apoptosis in breast cancer cells. Target Journal: Brisitsh Journal of Cancer

Selcuklu SD, Akman HB*, Donoghue MTA*, Gomes MS, Yakicier MC, Erson-Bensan AE, Spillane C (2011) Cross talk between mir-21 and STAT3 signaling. Target Journal: The Journal of Biological Chemistry

Selcuklu SD, Donoghue MTA, Spillane C (2011) Estradiol regulated JAG1 targeting by mir-21 in breast cancer cells. Target Journal: PLos One

Selcuklu SD, Gomes MS, Fort A, Mahe E, Spillane C (2011) CSDAP1 acts as mir-9 decoy in MCF-7 cells. Target Journal: RNA

Selcuklu SD, Donoghue MTA*, Gomes MS*, Fort A, Mahe E, Spillane C (2012) Genome-wide microarray profiling and functional analysis of mir-9* in breast cancer cells. Target Journal: Molecular Cell

Acknowledgements

This research was funded by The Irish Research Council for Science, Engineering & Technology (IRCSET), Cancer Research Ireland (CRI), Thomas Crawford Hayes Trust Fund (NUIG) and Health and Research Board (HRB), Ireland.

I'm grateful to my external examiner; Dr. Tamas Dalmay (UEA,UK) and my internal examiner and PhD Graduate Research Committee member; Dr. Howard Fearnhead (NUIG, Ireland) for their invaluable comments and suggestions in in my PhD oral examination. I also thank Dr. Howard Fearnhead for providing the MDA-MB-231 cell line and to Prof. Rosemary O'Connor (UCC, Ireland) for providing the MCF-7 cell line. The LARP1 antibody was a generous gift from Dr. Sarah Blagden (Imperial College, UK) and JAG1 antibody was a generous gift from Prof. Finian Martin (UCD, Ireland). I thank Prof. Michael J Kerin and Dr. Roisin Dwyer (Surgery Dept., NUIG hospital) for kindly providing the primary breast cancer samples.

I thank all the Spillane lab members, especially Dr. Prasad Kovvuru, Grace Martin, Dr. Mohan K. Muniyappa, and Kristina Rehmet. Also many thanks go to Dr. Peter McKeown for his invaluable suggestions during my PhD and for proofreading my thesis.

Many thanks to colleagues who helped me with the experiments over the four years; Sharon O'Sullivan and Elise Mahe, especially Matheus Gomes, Antoine Fort and Begum Akman Tuncer for their patience and great help with the experiments. Also, I thank Dr. Mark Donoghue for the bioinformatics support. Moreover, I'm grateful to all dinner club members: Antoine Fort, Martin Braud, Angela Mina Vargas, Mark Donoghue and Peter McKeown for their friendship and making my life in Ireland more fun and enjoyable.

I would like to express my sincere gratitude to my Master's degree supervisor Assist. Prof Elif Erson-Bensan (METU, Turkey) who inspired me to pursue

cancer research and continuously supported me since I have known her. Without her inspiration and encouragement I would never have considered a career in science.

I am deeply grateful to my supervisor Prof. Charles Spillane for inspiring me with his great vision and enthusiasm for science and research. I would like to express special thanks to him for continuous support and providing me with a great research environment and making this PhD thesis possible.

Special thanks to my dear love, Dr. Mark Donoghue, for his endless support by every means possible, for being the joy and inspiration in my life and always being there for me. Most importantly, I'm thankful to him for being my best friend and making life easier for me. I love you and am looking forward to starting a new life with you.

Last, but not least, it is impossible to express how grateful I am to my mum; Hanife Selcuklu and to my dad; Soner Selcuklu who supported me wherever I go and whatever I do, even if I was thousands of miles away. They have been my mentors throughout my life teaching me to never give up and always follow my dreams. Without them I would be lost. Annecigim ve Babacigim, iyi ki varsiniz, iyi ki benim ailemsiniz. Sizi cok seviyorum.

Abstract

In the past few decades, microRNAs emerged as key regulators of gene expression in many fundamental biological processes such as development and differentiation as well as diseases. There are thousands of microRNAs that have been discovered, and while plenty of them have been linked to diseases such as cancer, there is still much to discover; their genome-wide targets and functions to elucidate their potential as cancer biomarkers and therapeutic targets. This study provides an investigation of genome-wide effects of three microRNAs; mir-21, mir-9 and mir-9*, their functional roles and direct targets in breast cancer transcriptome.

Consistent with the previous reports, the oncogenic activity of mir-21 in breast cancer cells has been confirmed. Microarray analysis of the knockdown of mir-21, a well-known oncomir shown in many cancer types, identified downregulation of the JAK-STAT pathway. A possible autoregulatory loop with direct interaction of mir-21 and STAT3 has been identified. In addition, a direct communication between mir-21 and JAG1 that involves estrogen signaling has been identified in breast cancer cells. Mir-9 is known to be frequently hypermethylated and downregulated in cancer samples. Functional analysis of mir-9 overexpression showed decreased cell proliferation and increased apoptosis. Microarray analysis of mir-9 expression restoration in cancer cells revealed many predicted targets as differentially regulated. A total of seven direct targets have been confirmed of which two of them involved in the anti-proliferative activity of mir-9. Moreover, a gene/pseudogene pair has been identified as direct mir-9 targets. CSDAP1, pseudogene of CSDA, acts as mir-9 decoy in MCF-7 cells. Mir-9* is processed as the minor product of MIRN9 precursor which also generates mir-9. Its expression is lower than mir-9 in cancer cells although shows higher expression in MCF-7 cells compared to normal breast tissue. Functional analysis of mir-9* overexpression revealed an oncogenic potential in breast cancer cells. Mir-9*

overexpressing cells showed faster cell proliferation, migration and more invasiveness. Microarray profiling of mir-9* overexpression identified many predicted targets as differentially regulated. Twelve of selected direct or indirect targets have been confirmed.

Using microarray profiling, this study elucidates genome-wide effects of three microRNAs. Functional experiments revealed further insights regarding the phenotypic effects of microRNA dosage perturbations and direct targets of microRNAs in cancer cells. This study demonstrates the importance of microRNA dosage (expression levels) in cancer cells highlights the potential of microRNAs as biomarkers in cancer and contributes to the microRNA and cancer literature through identification of novel microRNA: mRNA interactions in cancer cells.

CHAPTER 1: Introduction

1.1. MicroRNAs: biogenesis and gene regulation

MicroRNAs are small ,18-25nt in length, non-coding RNAs classified as novel gene regulators found in many species [2]. The first microRNA was discovered in 1993 by Victor Ambros and his colleagues at Harvard University as a small RNA, lin-4 that does not code for a protein but regulates lin-14 gene which has a role in developmental timing in C.elegans [3]. Because of the role in developmental timing these small RNAs were first named as small temporal RNAs (stRNAs).Then they were re-named as 'MicroRNAs' and with the growing body of experiments and discoveries by other labs it was found that microRNAs are conserved throughout the evolution and are specific to certain cell types in plants [4], Drosophila [5], human [6], *C.elegans* [3] and in viruses [7].

MicroRNAs are transcribed as capped and polyadenylated full length long primary transcripts (pri-miRNAs) usually by Pol II [8], [9]. However there are some experimental evidences suggesting that some microRNAs are transcribed by Pol III [10], [2]. Pri-miRNAs undergo maturation steps first by being cleaved by RNaseIII enzyme Drosha into a stem loop or hairpin loop precursor intermediate (pre-miRNA) [11] which is 70-80 nt long and has a 5′ phosphate and ~2 nt 3′ overhang at the base [11, 12]. Pre-miRNA is transported from nucleus to cytoplasm by Exportin5 [13].After transport to cytoplasm another RNaseIII enzyme, Dicer, recognizes this stem loop precursor and cleaves it to ~20-22 nt miRNA:miRNA duplex. One of the strands is less stable (minor form or star form) and the other strand is more stable (major form) and incorporated into a RISC (RNA-induced silencing complex) protein complex miRNP [14], [15] and guided to imperfect complimentary mRNA 3'UTR regions by Argonaute (AGO) proteins [16], [11], [17] **(Figure 1.1)**.

Although guide strands are mostly associated into RICS and guided to targets, recently, there are cases experimentally validated that passenger strands are also functional (may not be completely degraded) and can be

incorporated into RISC to target genes dependent on their expression, stability and microenvironment [18, 19].

Some recent works demonstrated a significant accumulation of numerous star forms (miRNA*) compared to their corresponding miRNAs during some developmental stages of the silkworm [20]. Moreover another study on *D. melanogaster* suggested a regulatory role for the miRNA* strand [19]. In addition to being found in the Ago complex, these miRNA* include some conserved seed matches. This activity of target regulation by some miRNA* species seems to be related with their degree of nucleotides conservation with the mature form of the miRNA duplex [21, 22]. On this basis, conserved miRNAs* are likely selected for being loaded into the RISC and therefore be able to repress a lot of genes as well as their partner miRNAs. Mature miRNAs are designated with organism prefix and number suffix (i.e. hsa-mir-101 for ***H****omo* ***sa****piens* microRNA-101) and less stable miRNAs (also known as minor forms) are designated with a star next to number suffix (i.e. microRNA-101*) [23]. Naming of mature miRNAs (major/star forms) has been recently changed to suffixes for the hairpin strand (i.e. -3p or -5p).

The most recent microRNA database, mirBase Registry Release 17 (April 2011) (http://microrna.sanger.ac.uk/sequences/) [23] lists 16,772 entries including precursor and mature miRNA products, in primates, rodents, birds, fish, worms, flies, plants and viruses. Of these 1424 precursors and 1902 mature forms belong to humans. MiRNAs are predicted to regulate a large number of genes in human genome (about 30% of all genes) [24], [25]. They can be expressed in a cell and tissue specific manner [26]. They regulate gene expression post-transcriptionally via different mechanisms; mostly by binding imperfect complementary regions in 3' UTR of target genes [3], [27-29]. Recent findings showed that microRNAs can bind to 5' UTR, promoter or coding regions as efficiently as binding the 3' UTR to repress the mRNAs [30, 31]. However, 3'UTR binding still dominates the experimental findings.

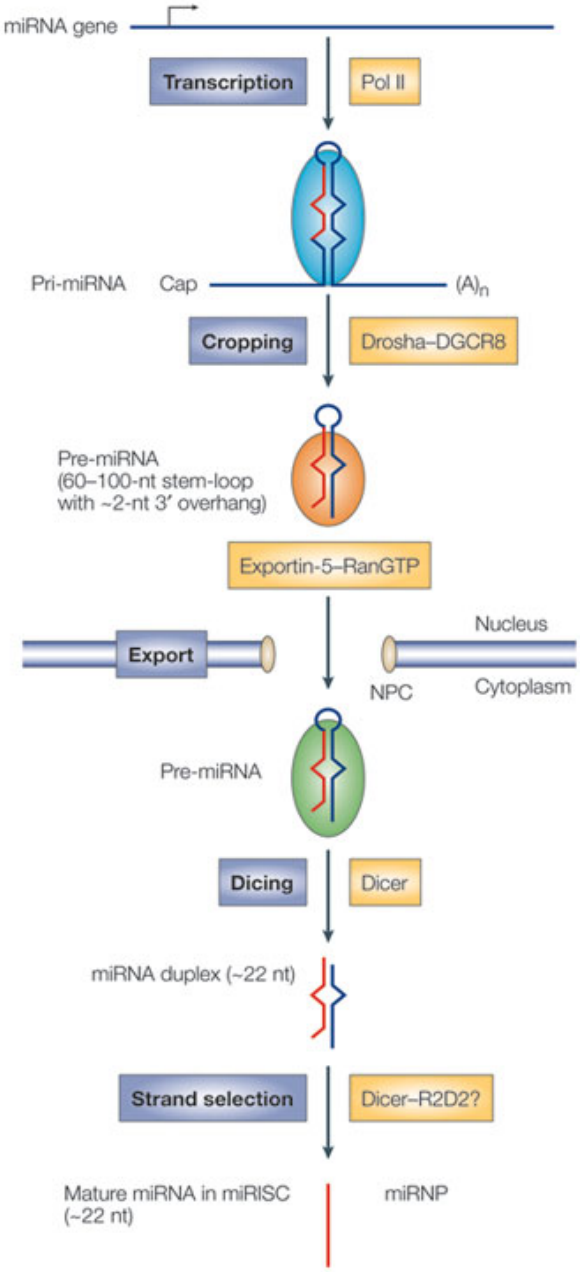

Figure 1.1: MicroRNA biogenesis

Chart explaining steps of microRNA biogenesis process starting with transcription of microRNA gene followed by cropping, export, and dicing and strand selection. Figure was taken from [32].

MicroRNAs can cause translational repression if they have imperfect complementarity to 3'UTR regions or they can induce mRNA cleavage if they have sufficient (or perfect) complementarity to 3' UTR regions [33]**.** In mammals, translational repression has been implicated as a major pathway but mRNA cleavage has also been shown to occur [34], [35] although it is more common phenomenon observed in plants [36], [37]. Besides translational repression and mRNA cleavage [2] , some other miRNA-mediated gene regulation pathways models are also proposed [38], [39], [40]. First, via post-initiation mechanisms; microRNAs repress translation by blocking elongation or by promoting ribosome drop-off. Second, via co-translational protein degradation; the nascent polypeptide chain is degraded co-translationally by an unknown protease. Third, initiation mechanisms; Argonaute loaded miRNAs interfere with early translation before elongation by competing for the cap structure, inhibiting ribosomal subunit joining or deadenylation. Last, via mRNA decay; miRNAs trigger deadenylation and decapping of the mRNA target **(Figure 1.2)** although this could be an independent silencing mechanism or a consequence of translational repression [41].

Previous studies suggested that protein down-regulation by microRNAs was due to decreased translation [3], [42]. However, recent findings indicate that microRNAs can decrease amount of cellular mRNAs, destabilize them by imperfect complementation via removal of poly A tails of mRNAs, which is not necessary in translational repression [43], [38]. Although decreasing protein levels by translational repression is known to be a common mechanism of microRNA mediated targeting [3], studies suggest that microRNAs can reduce mRNA levels endogenously [44], by rapid mRNA deadenylation as previously described [38], [39].

After discovery of regulation of lin-14 gene by lin-4 and let-7 miRNAs, gene regulation by miRNAs was investigated in detail for better understanding of the mechanism. One of the significant feature of miRNA:mRNA binding is 6-8nt long sequences from 5' end of the miRNA called 'seed'. Seed sequences are proven to be a common phenomenon

required for mRNA recognition however recently some studies showed it is not a strict rule and there can be other determinants in microRNA:mRNA pairing [45]. Many computational methods have been developed based on predicting miRNA:mRNA complementarities, conservation of microRNAs and/or target regions across species and a seed sequence match. Some of the commonly accessed online tools include TargetScan [24], PicTar [46] and MiRanda [47].

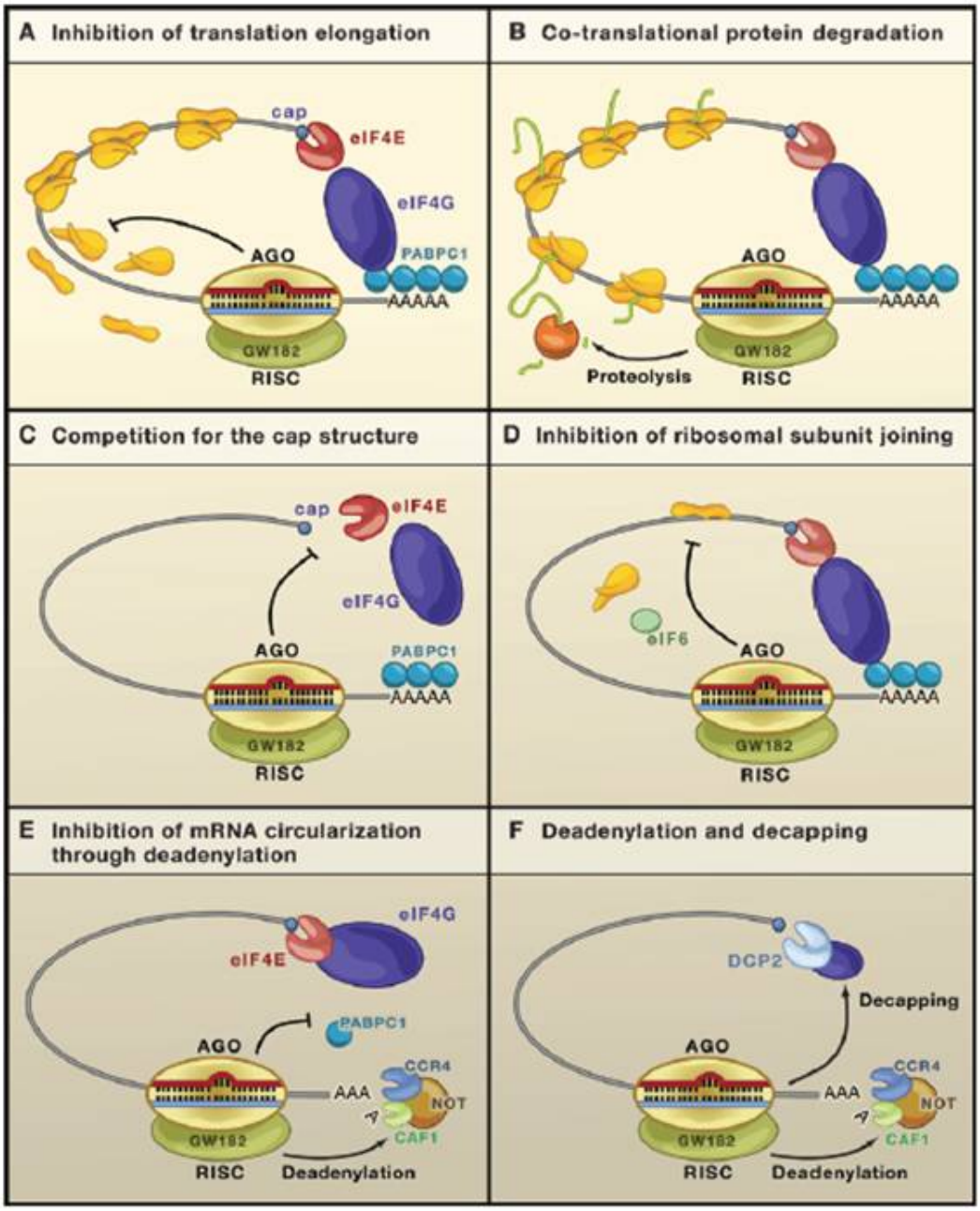

Figure 1.2: MicroRNA mediated gene regulation.

Six proposed mechanisms of microRNA directed gene regulation (A-F). Figure was taken from [41].

1.2. MicroRNAs and cancer

Since the discovery of microRNAs, research activity on this class of non-coding RNAs has dramatically accelerated due to their involvement in regulation of a wide range of cell and developmental processes such as cell proliferation, differentiation and apoptosis [48-50]. Disruptions of miRNA:target gene regulation including genomic instability and impaired miRNA processing have been associated with a growing range of cancers [51], [52]. More than 50% of human microRNAs genes are located in fragile sites and in the regions that are often associated with cancer, which provided an early indication of the potential importance of microRNAs in cancer [1], [53].The first link between miRNAs and cancer was reported by Calin et al. when researching the chromosome locus 13q14, which is deleted frequently in B-cell chronic lymphocytic leukemia (CLL) cases. They found that mir-15a and mir-16-1, which are located on the chromosome locus 13q14, are downregulated or deleted in ~68% of CLL cases [54] indicating how miRNA deregulation can initiate tumorigenesis via direct or indirect regulation of genes involved in cancer **(Figure 1.3)**. Since this discovery, extensive research on miRNAs' expression levels between healthy tissues and tumor tissues has been carried out, showing abnormal expression of miRNAs in numerous cancers [55],[56].

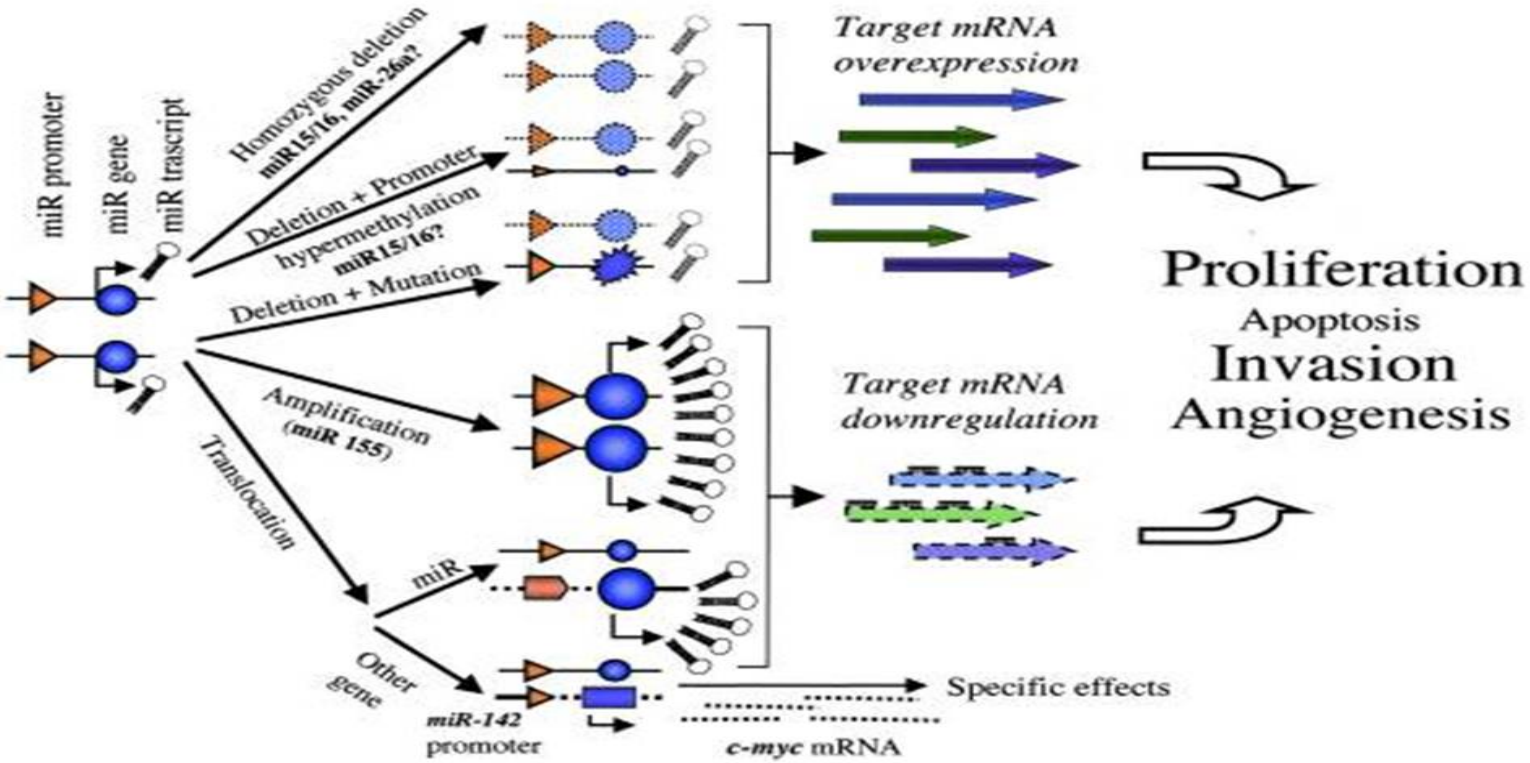

Figure 1.3: MicroRNA deregulation contributes to cancer

MiRNA deregulation I (amplification, translocation, deletion, mutation etc.) causes target overexpression or downregulation that may induce malignant transformation. Figure was taken from [1]

Cancer is a disease associated with increased cellular proliferation and decreased levels of apoptotic function [57, 58]. MiRNAs have been shown to have the ability to function as oncogenes or tumor suppressors **(Table 1-1)** as the amplification/overexpression or deletion/downregulation of many miRNAs has been linked with tumorigenesis. This leads to increased proliferation, increased invasion, increased angiogenesis and a decrease in apoptosis [59]. These miRNAs are often classed as oncomirs [59].

Oncomirs can act as negative regulators of tumor suppressor genes and genes involved in apoptosis, thus leading to tumor development [60, 61]. The mir-17-92 family is just one example of a miRNA acting as an oncogene [53], where its overexpression is found in various cancers, such as prostrate, breast and pancreas cancer [62]. On the other hand, some miRNA can act as tumor suppressors. For instance, as previously mentioned, mir-15a and mir-16-1 are examples of tumor suppressors that when deleted cause cellular proliferation and tumorigenesis in a vast majority of CLL patients [54]. Let-7, which was originally discovered in *Caenorhabditis elegans*, is essential for cellular proliferation and development [63]. In mammals, the let-7 was shown to have complementary binding sites in 3'UTR of the oncogene RAS, where it acts as a tumor suppressor. In lung cancer, a down-regulation of let-7 has shown increased protein expression of RAS [64]. A poor prognosis and increased lung cancer progression is often linked with decreased let-7 expression [65]. In breast cancer, let-7 was found to regulate estrogen receptor alpha triggering apoptotic process [66].

Up to date, involvement of microRNAs in tumorigenesis have been implicated in targeting genes with significant functions in cancer pathways such as angiogenesis or cell signaling [67], [6]. Involvement of microRNAs and their deregulation in cancer have been attributed to its target gene functions. Among thousands of target genes predicted, few of them were experimentally confirmed. For instance, hsa-mir-21 has been shown to regulate tumor growth and apoptosis through regulating genes directly or

indirectly that are involved in cancer pathways (i.e. *PTEN, BCL-2, PDCD4, TPM1, etc*) [68-70]. Also, hsa-mir-17-5p regulates E2F1 expression and hsa-mir-15 and hsa-mir-16 downregulate BCL-2 and induce apoptosis [64], [71, 72], hsa-mir-142 has been found to target *c-myc* (myelocytomatosis viral oncogene), hsa-mir-20a targets *E2FI*, hsa-mir-19a targets *PTEN*. [59], [73]. On the other hand, in a study of Bommer et al, hsa-mir-34 is reported to be targeted by p53 tumor suppressor gene in human and mouse cells. It has been considered as "significant downstream effector of p53 function" and it is suggested that its inactivation might contribute to certain cancer types [74].

While deregulation of a miRNA:mRNA targeting relationship will have obvious implications for cancer if the target gene is an oncogene or tumor suppressor, it is also possible for miRNA deregulation to cause indirect (secondary) effects on the expression levels of key genes or pathways implicated in cancer. MicroRNAs were found to be powerful discriminators of classified human cancers as they show different expression patterns in different cancer types [75]. Additional to individual miRNA studies, genome wide microarray profiling in poorly differentiated tumor samples by comparing mRNA profiling versus microRNA profiling showed that microRNA expression profiles classified 12 of 17 tumor samples whereas mRNA expression profiles could discriminate only 1 of 17 samples despite the fact that mRNA array contains 15,000 genes but miRNA array contained 200 genes [76]. MicroRNA microarray study by Iorio et al, 2005 analyzed breast cancer tumors and cell lines and showed that compared to normal breast tissue, hsa-mi125b, hsa-mir-145, hsa-mir-21 and hsa-mir-155 were significantly deregulated in breast cancer. MicroRNA expression profiling was clustered and breast cancer samples were clearly differentiated from normal samples also according to bio-pathological features. They found let-7, mir-125b, mir-145 down-regulated, whereas mir-155 and mir-21 were up-regulated [77]. In recent studies on microRNAs and breast cancer some microRNAs were deregulated at genomic level as well as expression level. For example, in a CGH study on 283 microRNAs in ovarian cancer, breast cancer and melanoma they

identified common microRNAs deregulated in three cancer types as well as some microRNAs unique to a certain cancer type. They showed copy number changes of microRNAs in 72.8 % of breast cancer samples [78]. In addition to microRNAs suggested to be correlated with breast cancer, hsa-mir-21 have been found to be amplified and overexpressed and involved in many cancer types indicating an oncogenic role [68], [69], [79], [80]. In terms of comparison of miRNA expressions in breast cancer cell lines and tumors, Mattie et al, 2006 analyzed many microRNAs in 10 breast tumors (ErbB2+) and SKBR3 cell line (ErbB2+). They suggested that unique sets of microRNAs are associated with phenotypic status of breast cancer samples such as ErbB2 status (+/-) different expression levels of 56 microRNAs in SKBR3 cell line and breast tumors [81].

1.3. Mir-21 as a key regulator of oncogenic processes

This section is adapted from the peer-reviewed publication:
Selcuklu SD, Donoghue MTA, Spillane C (2009) Mir-21 as a key regulator of oncogenic processes, Biochem Soc Trans 37: 918-925

1.3.1. MicroRNA-21 gene and transcript (MIRN21, mir-21)

Mir-21 was one of the first microRNAs detected in the human genome [8] and is known by a number of synonyms (hsa-mir-21, MİR21, mir-21, miRNA21). Mir-21 displays a strong evolutionary conservation across a wide range of vertebrate species in mammalian, avian and fish clades. In *Homo sapiens*, the *MIRN21* gene (DNA of pre-mir-21) is located on chromosome 17 (55273409-55273480 [+], intergenic) residing within the 10th intron of the gene *TMEM49* (trans-membrane protein-49 also known as vacuole membrane protein-1) [82] **(Figure 1.4)**. Fujita et al., 2008 have demonstrated that a primary transcript containing mir-21 (i.e. pri-mir-21) is independently transcribed from a conserved promoter that is located within the intron of the overlapping protein coding gene, *TMEM49* [83].

Table 1-1: Well known Oncogenic and Tumor Suppressor MicroRNAs

Oncogenic microRNAs	cancer type	reference
mir-21	breast, colon, pancreas, lymphoma, prostate, liver, stomach, glioblastoma	[61, 84-91]
mir-17-92	lymphoma, breast, pancreas, stomach, lung, colon	[53, 87, 92, 93]
mir-155	CLL, AML, lung, breast	[87, 94-96]
mir-372/373	Testicular germ cell	[97]
Tumor suppressor microRNAs	**cancer type**	**reference**
let-7 (-a,-b,-c,-d)	breast, lung	[64, 94, 98-100]
mir-34 (-a,-b,-c)	pancreatic, colon, breast	[101-104]
mir-29 (-a,-b,-c)	CLL, AML, lung, breast, cholangiocarcinoma	[88, 89, 94, 98, 105, 106]
mir-125(-a,-b)	breast	[107, 108]
mir-15a/mir-16-1	CLL	[109-111]

Precursor Sequence: 5′-UGUCGGGUAGCUUAUCAGACUGAUGUUGACUGUU GAAUCUCAUGGCAACACCAGUCGAUGGGCUGUCUGACA-3′

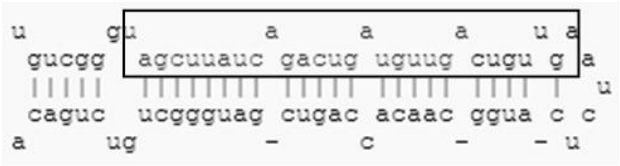

Major Mature Sequence (hsa-mir-21): 5’-UAGCUUAUCAGACUGAUGUUGA-3’
Minor Sequence (hsa-mir-21*): 5’- CAACACCAGUCGAYGGGCUGU-3’

Figure 1.4: MIRN21 gene

Location, sequence and folding of the precursor MİRN21 gene (pre-mir-21) on chr17q23.1) (55273409-55273480, (+)) (Chromosome figure taken from UCSC Human Genome Browser, version Mar.2006). Sequences of major (mir-21) and minor (mir-21*) forms of the mature microRNA. Sequences were taken from miRBase:
http://microrna.sanger.ac.uk/sequences/

Cai et al., 2004 examined several human microRNAs and found that microRNAs are derived from capped and polyadenylated primary precursors (pri-miRNA). In the case of mir-21, they were able to clone a 3433 nt full-length pri-mir-21 from which mature mir-21 is derived. The pri-mir-21 transcript contained a consensus “AAUAAA” polyadenylation signal between nucleotides +3394 to +3399 [112]. The stem-loop precursor of mir-21 (pre-mir-21) resides between nucleotides +2445 to +2516 on the 3433 nt full-length pri-mir-21**.** A computational algorithm developed by Fujita et al., 2008 to search for microRNA putative promoter regions (miPPRs) predicted such miPPRs for mir-21 (miPPR-21) in the 900bp upstream of the transcription start site (TSS) previously reported by Cai et al., 2004. Using primer extension approaches in HeLa and HL-60 mammalian cell lines, Fujita et al., 2008 demonstrated that mir-21 transcription was initiated 30bp downstream of conserved TATA box in miPPR-21, after PMA (phorbol 12-myristate 13-acetate) treatment (which induces mir-21 expression in the HL-60 line). However, the previously described transcriptional start site (TSS) for mir-21 [8] was not detectable before or after the PMA treatment [83].

The primary mir-21 transcript (Pri-mir-21) transcribed by Pol II is processed by the nuclear RNAse III enzyme, Drosha and DGCR8 (dsRNA binding protein) in the nucleus [113] forming the 72-nt long stem-loop precursor (pre-mir-21) which is located to cytoplasm by the enzyme Exportin5 [13]. Following transport to cytoplasm another RNase III enzyme, Dicer, recognizes this stem loop precursor and cleaves it to yield a 22 nt miRNA:miRNA duplex. One of the strands (minor hsa-mir-21*) is degraded, and the single stranded mature miRNA destined for regulatory activity (predominant hsa-mir-21) is incorporated into a RISC (RNA-induced silencing complex)-like protein complex miRNP [14] and guided to any target mRNAs (mainly 3’UTR regions) containing targets of imperfect complementarity [16]. While some miRNAs (e.g. let-7) are deeply conserved across species, there are also miRNAs that are species or clade specific. In the case of mir-21, multiple sequence alignments of the precursor and mature mir-21 regions shows that both sequences are

highly conserved across many species, possibly suggesting a deeply conserved role for mir-21 in gene regulation **(Figure 1.5).**

Species abbreviations used in **Figure 1.5**: mmu = *Mus musculus*, rno = *Rattus norvegicus*, dre = *Danio rerio*, ssc = *Sus scrofa*, mml = *Macaca nemestrina*, age = *Ateles geoffroyi*, ppa = *Pan paniscus*, fru = *Fugu rubripes*, tni =*Tetraodon nigroviridis*, bta = Bos Taurus, gga = *Gallus gallus*, mdo = *Monodelphis domestica*, cgr = *Cricetulus griseus*, oan = *Ornithorhynchus anatinus*, cfa = *Canis familaris*.

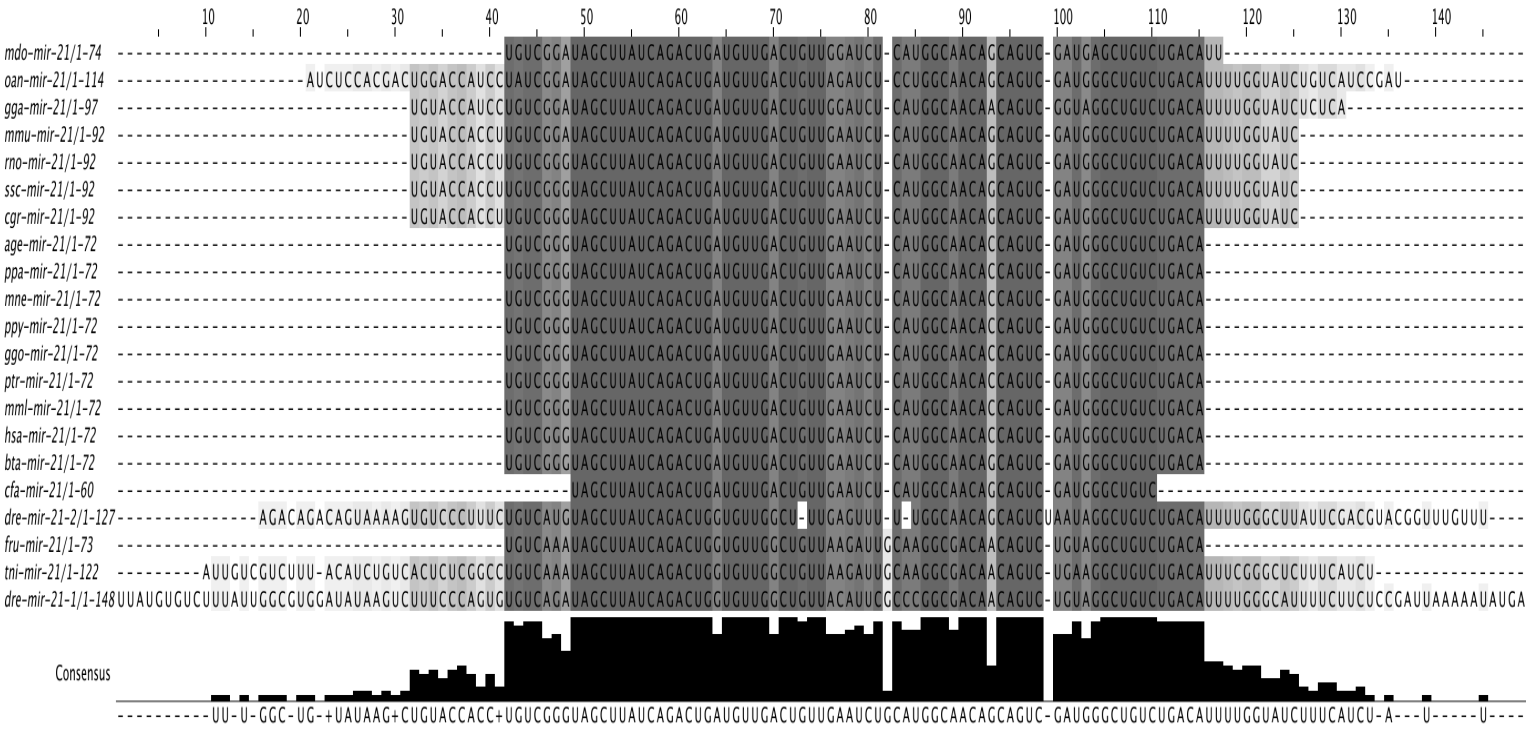

Figure 1.5: Evolutionary conservation of the mir-21 precursor (pre-mir-21).

Conservation across 21 vertebrate species spanning mammals, avian and fish. The RNA sequence of each mir-21 precursor in each species is aligned with all of the other mir-21 homologs in a Clustal W2 multiple sequence alignment.

1.3.2. Overexpression of mir-21 is associated with many forms of cancers

The discovery of multiple miRNAs and the advent of high-throughput transcriptome profiling approaches for miRNAs have facilitated comparative analysis of miRNA expression profiles in tumors and cell lines associated with cancer, with those of normal cells/tissues. Strikingly, mir-21 has been found to be over-expressed in the vast majority of cancer types analyzed [84], although one study has found that inhibition of mir-21 expression was associated with increased cell growth in cancer cells [114].

Transcript profiling studies of miRNA expression levels across tumor samples or cancer cell lines have revealed that mir-21 is upregulated in cell lines/tissues specific to glioblastoma [68], breast cancer [77], [115], lung cancer [116], [98], stomach cancer [116], esophageal cancer [117]; prostate cancer [116], colon cancer [116], [118], ovarian carcinoma [119], cholangiocarcinoma [120], B-cell lymphoma [121], hepatocellular carcinomas [122], [123], cervical cancer [124], uterine leiomyomas [125], head and neck cancer [126], chronic lymphocytic leukemia [127], pancreas cancer [116], [128], squanmous cell carcinoma (SCC) of the tongue [129] and papillary thyroid carcinoma [130]. Similarly, an analysis of 157 miRNAs across breast cancer tissues, demonstrated that mir-21 is highly overexpressed in breast tumors [69]. Another study showed that overexpression of mir-21 in primary breast cancer samples is associated with advanced clinical stage, lymph node metastasis and poor prognosis [131]. However, while such studies clearly demonstrate that mir-21 is deregulated in samples where cancer is at an advanced stage; such studies do not prove any causal role for mir-21 in cancer etiology. From a functional perspective, the entire field of cancer research is challenged by the nature of cancer itself due to the difficulty of identifying and profiling samples which are at the earliest stages of cancer initiation and development (i.e. single cell or few cell stages) [132]. Nonetheless, such

studies to identify miRNA profiles associated with specific cancer types are very useful for classifying cancers based on miRNA profiles and for identification of cancer specific “biomarkers” that can be used in cancer diagnosis and treatment assessment.

1.3.3. Functional demonstrations that mir-21 is an oncomir

While there has been extensive miRNA profiling of cancer versus normal tissues and cells, which have identified mir-21 as a key molecule (or biomarker) associated with a wide range of cancers, there have been fewer functional studies that demonstrate cause-effect relationships between mir-21 and neoplastic transformation. The following provide an overview of functional studies (e.g. Assaying function after mir-21 knockdown by antisense inhibitors) conducted with mir-21 to date that strongly suggests that mir-21 has oncogenic activity.

- Knockdown of mir-21 in cultured glioblastoma cells triggers activation of caspases and leads to increased apoptotic cell death, suggesting that expression of mir-21 can act as an anti-apoptotic factor [68].

- Knockdown of mir-21 in breast cancer MCF7 cells led to suppression of cell growth *in vitro* and tumor growth in the xenograft mouse model. Cell growth suppression was accompanied by increased apoptosis and decreased cell proliferation (possibly due to downregulation of Bcl2 protein expression) [69].

- Knockdown of mir-21 in metastatic breast cancer MDA-MB-231 cells significantly reduced invasion and lung metastasis [133].

- Knockdown of mir-21 in hepatocellular cancer cells increased expression of the phosphatase and tensin homolog (PTEN) tumor suppressor, and decreased tumor cell proliferation, migration, and invasion. Increase of

mir-21 expression in hepatocellular cancer cells led to increased tumor cell proliferation, migration, and invasion [123].

- In colorectal cell lines, an inverse correlation of mir-21 and the tumor suppressor Pdcd4-protein has been observed [70]. Knockdown of mir-21 leads to an increase in Pdcd4 protein levels and reduced invasiveness, while mir-21 overexpression led to increased invasiveness and metastasis [70].

- Increasing mir-21 expression in myeloma cells (in the absence of IL-6) significantly reduced their apoptosis levels [134].

- In a screen of miRNAs in HeLa cells treated with a library of miRNA inhibitors, it has been found that along with other miRNAs, mir-21 inhibition caused a decrease in cell growth [114].

- Antisense inhibition of mir-21 caused significant apoptotic cell death in neuroepithelial cells through significant activation of caspases detected by pan-caspase assay. Mir-21-antisense treated cultures also showed high LDH release as an indication of apoptotic cell death [135]. Mir-335-antisense treated neuroepithelial cells showed resistance to apoptosis after ethanol treatment and prevented cell death caused by mir-21 suppression indicating antagonistic effect of mir-335 to mir-21 [135].

- Using RT-PCR to detect expression of mature mir-21, Qian et al., 2008 were able to detect mir-21 expression in 344 fresh tumor samples collected from patients diagnosed with primary breast cancer. Considering features such as disease stage, tumor grade, histology, hormone receptor status and lymph node involvement they found association of high mir-21 expression with aggressiveness of the disease, high tumor grade, negative hormone receptor status, poor disease-free survival in early stage patients and ductal carcinoma but no clinical value for prognosis.

Overall these studies indicate that knockdown of the expression of mir-21 can lead to functional effects clearly linked with cancer initiation and progression. Such studies suggest that mir-21 has some oncogenic activity, which if removed inhibits the development of cancer-associated phenotypes in cell lines.

1.3.4. What downstream pathways and genes are regulated by mir-21?

While it is known that mir-21 is over-expressed in cancer cells/tissues and has oncogenic activity in terms of neoplastic transformation, little is known regarding the genes and pathways downstream that are regulated by mir-21, particularly those which if deregulated can trigger neoplastic cellular growth.

Much of the early efforts to identify downstream targets of microRNAs have been based on bioinformatic target prediction algorithms, and the number of predicted miRNA target genes vastly outnumbers the number of miRNA target genes that have been actually validated in wet-lab experiments [136]. This is evident from the fact that there are over 600 known miRNAs potentially (i.e. based on bioinformatics) targeting up to 30% (more than 5300 genes) of protein-coding genes in the human genome [24], yet there are only 461 experimentally validated miRNA:target gene demonstrations in TarBase [137].

A number of tumor suppressor genes have been found to be targeted by mir-21 supporting its proposed oncogenic role in cancer **(Figure 1.6)**. A study using 2D proteomics, luciferase reporter analysis and Western blot assays to screen for translational suppression of target genes due to mir-21 has validated the tumor suppressor gene *tropomyosin-1 (TPM1)* in breast cancer as a target of mir-21 [138]. Target validation studies in breast cancer samples (cell lines and tumors) and colorectal cancer cells on putative mir-21 targets have demonstrated a link between mir-21

expression levels and the p53 tumor suppressor, and also demonstrated that the tumor suppressors *Programmed Cell Death 4 (PDCD4)* and *maspin* are targets of mir-21 [139], [133], [70]. Other candidate targets of mir-21 that have been recently validated include the *PTEN* tumor suppressor in hepatocellular cancer cells [123] and *SPRY2* [140] which is also known to induce up-regulation of *PTEN* [141]. In addition, an indirect positive regulation of *BCL-2* by mir-21 has also been shown in breast cancer [142].

A growing body of mir-21 targets are now being validated, including recent studies in glioblastoma cells and cervical cancer cell lines, which identified a range of mir-21 targeted genes (including the *HNRPK* and *TAp63* genes which are components of the p53, TGF-B and mitochondrial apoptosis pathways [143]. Recently, it has been shown that in glioma cells mir-21 negatively regulates MMPs (matrix metalloproteinases) inhibitors, which causes activation of MMPs and so invasiveness of cancer cells [144].

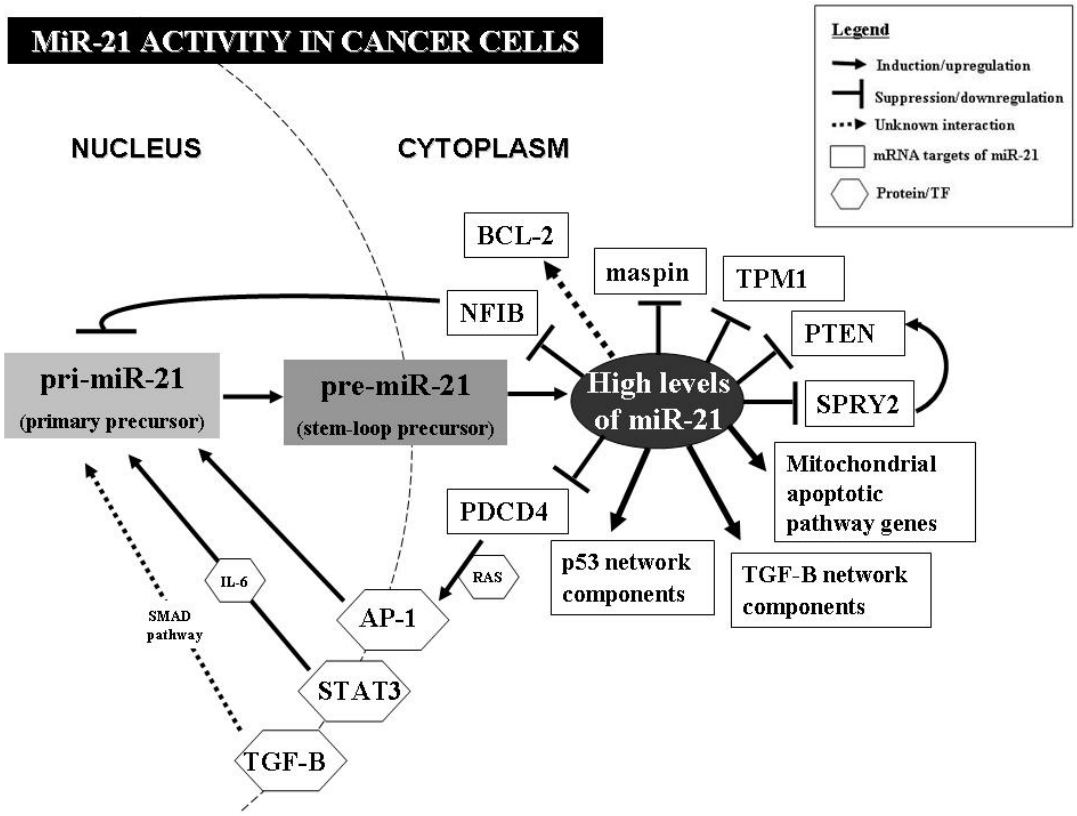

Figure 1.6: Mir-21 activity in cancer cells

Schematic representation of validated targets and interactions of mir-21 in cancer cells based on current literature.

Microarray studies investigating effects of knockdown of mir-21 in the breast cancer cell line MCF7 has identified a range of 737 genes whose mRNA levels are affected (402 genes upregulated, 335 genes downregulated) by loss of mir-21 [139]. The advent of stable isotope labeling by amino acids in cell culture (SILAC) approaches for the identification of targets of miRNAs is indicating that when miRNA targeting occurs, in most instances there is both a knockdown in the levels of the mRNA transcript and the protein [145], [146], [147]. This indicates that microarray based approaches in combination with techniques to assay protein levels will be of use for identification of the downstream genes and gene networks regulated by miRNAs in different cell line backgrounds.

1.3.5. What upstream pathways and genes regulate mir-21?

The functional identification of regulatory genes upstream of microRNAs, which are responsible for controlling the spatial and temporal expression of specific miRNAs, is also in its early stages. In this regard, a study investigated the possible involvement of *STAT3* in regulation of microRNA genes by bioinformatic analysis of evolutionary conserved putative STAT3 binding sites in regulatory regions of microRNAs genes. STAT3 (Signal transducer and activator of transcription 3) is a transcription factor mediating IL-6 signaling and shown to be involved in cellular transformation and oncogenesis. Amongst the analyzed microRNAs, the mir-21 gene region contained 2 consensus STAT3 binding sites ~800bp upstream of its transcription start site, both of which are highly conserved in vertebrates [134]. Also, it was shown that mir-21 expression is controlled by an upstream enhancer element containing these two containing evolutionarily conserved STAT3 binding sites. Induction of mir-21 expression by IL-6 requires STAT3, implicating mir-21 in the oncogenic potential of STAT3 [134].

Chromatin immunoprecipitation experiments in human myeloma cells (XG-1) have demonstrated that STAT3 is recruited to the mir-21 regulatory

region in response to IL-6. This was validated by inhibition of mir-21 promoter activity (decreased primary mir-21 transcript levels) after STAT3 knockdown. The experiments demonstrated that mir-21 gene transcription is controlled by IL-6, which requires STAT3 regulation of mir-21 upstream enhancer [134]. These recent findings regarding regulation of mir-21 may indicate cooperation of STAT3 and mir-21 in tumorigenesis. The transcription factor AP-1 is known to be an important regulator of cell proliferation, apoptosis and invasion [148], [149], and has also been shown to activate mir-21 transcription [83]. Bioinformatic approaches have revealed highly conserved potential AP-1 binding sites in mir-21 primary transcript (pri-mir-21), suggesting that mir-21 is a possible transcriptional target of AP-1. AP-1 induced-expression of mir-21 causes downregulation of mir-21 target, *PDCD4*, which is required for stimulation of AP-1 in response to the RAS oncoprotein. This indicates an autoregulatory loop between PDCD4 and mir-21 for controlling AP-1 activity in RAS-transformed cells. One of the AP-1 binding sites has been validated by functional assays as the major RAS-responsive element of the mir-21 gene promoter. AP-1-induced mir-21 expression causes upregulation of rat thyroid cell growth and downregulation of mir-21 targets; tumor suppressor genes PDCD4 and PTEN [150], [83].

In a separate analysis of endogenous mir-21 expression, Qian et al., 2008 determined that transforming growth factor-beta (TGF-b1) upregulates mir-21 expression. They found positive correlation of high mir-21 expression with TGF-b1 in tumor samples that may indicate regulation of mir-21 expression by TGF-b1. This finding is in concordance with a recent report indicating upregulation of mir-21 expression by TGF-b1 through the SMAD signal transduction pathway [151], [82].

1.3.6. Mir-21 as a cancer biomarker

A wide range of studies have now shown that microRNAs can act as more powerful cancer biomarkers (e.g. for cancer type, prognosis, responsiveness to therapy) than messenger RNAs (mRNAs) or proteins [120], [116], [77], [125]. For instance, overexpression of mir-21 in pancreatic endocrine and acinar tumors is strongly associated with both a high Ki67 cell proliferation index, and presence of liver metastasis [152]. Recently, it has been demonstrated that high mir-21 expression is associated with poor survival and poor therapeutic outcome of colon adenocarcinomas [153].

Analysis of the effects of anti-cancer chemotherapeutic agents (e.g. 5-fluorouracil, gemcitabine) in relation to microRNAs has demonstrated that inhibition of mir-21 increased sensitivity to gemcitabine induced apoptosis [120], while mir-21 expression is increased in response to cellular treatment with 5-FU [154], [155]. Pioneering studies are now underway whereby combinatorial approaches to cancer treatment based on modulation of miRNAs (such as mir-21) in conjunction with conventional therapeutics (e.g. tumor necrosis factor-related apoptosis inducing ligand S-TRAIL, or libraries of anticancer compounds) are showing promise [156, 157].

Mir-21 was also detected in biological fluids such as in serum. High mir-21 expression was found in serum samples of large B-cell lymphoma (DLBCL) patients compared to healthy control samples. Also they showed that mir-21 expression in disease samples was associated with relapse-free survival but not overall survival [158]. These approaches are highlighting the potential use of microRNAs as non-invasive diagnostic markers in cancer.

1.3.7. Conclusions

The discovery of the important role of miRNAs in cancer has opened up a new era of cancer investigations that take into account new and emerging knowledge regarding the RNA signaling systems within eukaryotic cells such as mammalian cells. Among the many microRNAs already identified as regulators of neoplastic transformation, invasion and metastasis, mir-21 has emerged as a key miRNA (oncomir), which is deregulated in many cancers. While there are many predicted targets of microRNAs identified by in online tools, only a handful are validated for miRNAs such as mir-21 **(Figure 1.6)**.

Even less known regarding the regulatory networks miRNAs (operating in union or in concert) are embedded within. Moreover, tissue specific expression of microRNAs and combinatorial effects of different microRNAs on a particular target gene have to be taken into account for more comprehensive understanding of miRNA functioning. Hence, understanding in healthy cells, tissues and individuals how mir-21 is regulated and how mir-21 regulates downstream target genes will be a prerequisite for rational design of cancer therapeutic strategies based on modulation of mir-21 expression. Nonetheless, even with available knowledge and resources, it is clear that studies on microRNA expression profiling and targets in cancer samples are proving worthwhile for developing effective cancer biomarkers for diagnosis and individualized medicine (e.g. how biomarkers can give an indication for likely response of a cancer patient or cohort to a specific drug or treatment). Depending on the cancer and its stage of development, therapeutics can target specific stages and types of tumors. The involvement of miRNAs in all stages of cancer development from initiation, to progression and metastasis opens the possibility for miRNA-targeted or miRNA-based therapeutics. Examples of such therapeutics include silencing oncomirs or gene therapy approaches based on re-expression of microRNAs that are downregulated in cancer cells.

MiRNAs such as mir-21 have heralded a new era of research on “RNA signaling pathways” which now have to be elucidated and related to what we know regarding more conventional protein signaling pathways. The integration of such research into a systems-based understanding of genetic nodes, networks and graphs that underlie normal and neoplastic cell division should allow for the identification of new approaches for cancer diagnosis and therapy.

1.4. Mir-9: Gene and regulation

1.4.1. Description of MIRN9 gene

MIRN9 (MicroRNA-9 or mir-9) was first identified in drosophila species and is highly conserved from flies to humans except *C.elegans* [159]. Mir-9 is encoded in three distinct genomic loci mir-9-1, mir-9-2, mir-9-3 on chromosome 1, 5 and 15 **(Figure 1.7)**. Mir-9-1 is located in the second intron of the CLorf61 gene encoding CROC4 protein, mir-9-2 is located in the last exon of the annotated overlapping BC036480, AX746931, and CR599257 non-coding genes and mir-9-3 gene is located within the first intron of the non coding CR612213 gene (UCSC Genome Browser). It was recently shown that the transcription of mir-9-2 gene is directed by an unidentified promoter that displays unique exonic location compared to other host genes [160]. Although they are located in separate locations in the genome all three precursor generate the same mature mir-9 and mir-9* sequences **(Figure 1.7)**. Despite this, the adjacent sequences are moderately conserved at two loci (chromosome 1 and 5) and strongly differ at chromosome 15 indicating independent transcriptional regulation or processing of each transcript.

Mature mir-9, a well-conserved 23 nucleotides microRNA, was shown to be involved in development and diseases [161-163]. Mir-9 was initially

discovered as brain (neuronal progenitor cells) specific microRNA [164, 165] where it is highly expressed and functioning in brain development and neural cell differentiation [165, 166]. Tissue specific detection of mir-9 identified the pre-mir-9-2 as highly expressed in mouse embryos at embryonic stage10.5 compared to pre-mir-9-1 and pre-mir-9-3 [167]. Similarly, pre-mir-9-2 was highly expressed in human neural progenitor cells while pre-mir-9-1 was undetected [168]. Both mir-9 and mir-9* showed a similar expression pattern in corticogenesis reflecting their co-transcription and co-maturation from the same genetic unit. However slightly greater reduction of mir-9* compared mir-9 was observed between E21 to adult stage indicating difference in processing and stability [164]. Mir-9 and mir-9* showed some quantitative differences in association with polyribosomes. Mir-9 showed a higher proportion of association with polyribosomes compared to mir-9* [164]. This suggests a complex regulatory mechanism where mir-9 could be favored for access to target sites.

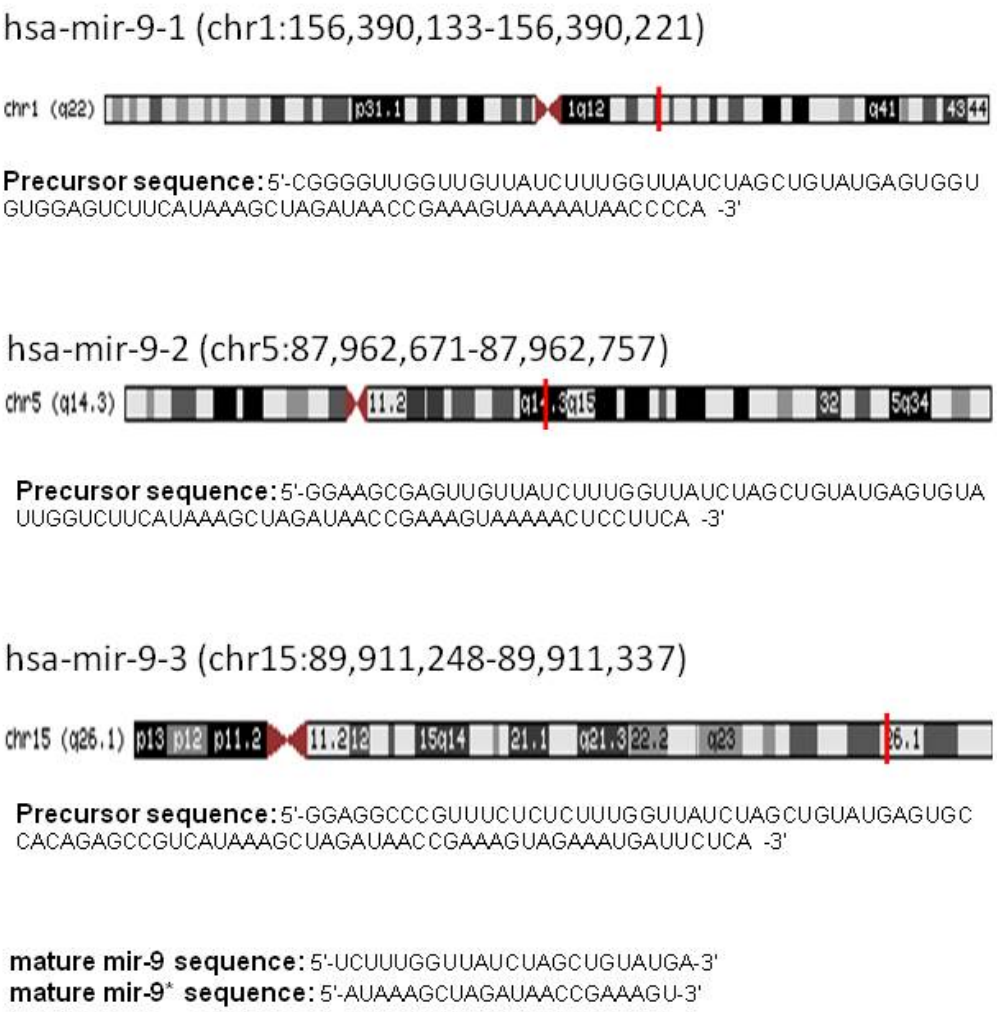

Figure 1.7: MIRN9 precursor and mature forms

Location and sequence of three MIRN9 precursors (hsa-mir-9-1, hsa-mir-9-2 and hsa-mir-9-3) and mature forms mir-9 and mir-9* processed from all three precursors are shown. Chromosome figures were taken from UCSC Genome Browser and sequences were taken from miRBase.

1.4.2. Epigenetic and transcriptional regulation of MIRN9 in cancer

Many miRNAs display developmental stage or tissue specific expression, which if perturbed can cause diseases [77] [169, 170]. Although mir-9 was identified as brain/neuron specific microRNA, later it was described as one of the significant microRNAs in regulation of carcinogenesis. MicroRNAs expression can be subject to epigenetic control through modulation of chromatin structure [171-173]. For instance, in a study, mir-9 (specifically mir-9-1) was epigenetically inactivated through aberrant CpG island hypermethylation and transcriptionally repressed in primary human breast cancer specimens [174].

Similarly, many other independent studies showed that mir-9-1 was methylated in cancer cells such as pancreatic cancer [175], colorectal cancer [176], renal cell carcinoma for mir-9-1 and mir-9-3 [163] and hepatocellular carcinoma for mir-9-1 and mir-9-2 [177]. In addition, hypermethylation of mir-9 was shown in other cancer samples metastasized from colon, melanoma and head and neck [178]. On the other hand, together with other miRNAs, mir-9-1, mir-9-2 and mir-9-3 were identified as unmethylated all the time in normal tissues indicating that hypermethylation of these microRNAs being cancer-specific [178].

1.4.3. Pseudogenes as microRNA decoys

In 2007, Ebert *et al.* introduced the term “microRNA sponges” as an alternative approach to chemically modified antisense oligonucleotides to inactivate miRNAs [179]. MicroRNA sponges are miRNA decoys with several miRNA binding sites and are expressed from plasmids or chromosomal insertions. Since these miRNA sponges inhibited miRNA activity effectively, specifically “target” miRNAs, the possibility that such endogenous inhibitors exist was raised. The first discovery was a non-coding RNA found in *Arabidopsis thaliana* whose function was to reduce a miRNA-mediated response to an environmental stress [180].

More recently, non-coding pseudogenes were shown to act as miRNAs sponges in mammalian cells. Pseudogenes are in essence DNA sequences that correspond to functional genes but they cannot be translated due to premature stop-codon and several injuries in their sequence. PTEN Pseudogene 1 (PTENP1) was targeted and downregulated by the same miRNAs (mir-19b and mir-20a) as its functional gene PTEN in DU145 prostate cancer cells [181]. Silencing of the 3'UTR part of PTENP1 by siRNA lead to an increase of the cell proliferation showing a tumor suppressive activity for this pseudogene; moreover its locus is often lost in cancers [181].

1.5. Cancer cell lines as models

Cell line models have been widely used for research on molecular biology of breast cancer and identification of novel biomarkers and drug targets prior to clinical studies [182]. The advantage of using cell lines as cancer models is that they are easy to grow, genetically manipulate and apply functional assays on. Cell lines represent the snapshot state of the tumor at the time of the biopsy and it was shown that injecting the cell lines into nude mice generated tumor and histopathology results correlated to origin of the tumor [183] [184].

Breast cancer is not a simple but genetically and genomically heterogeneous disease, with distinct pathological features, genetic instabilities and diverse prognosis [185]. One of the major challenges in breast cancer research is to find one representative model that mimics all types of breast cancer, which is not possible. Some molecular profiling studies have shown that none of the cell lines are completely representative of the primary tissues however in some studies a panel of cell lines showed the similar heterogeneity observed in primary breast cancer [182, 186, 187]. Similarly, panel of [188] cell lines were shown to retain the phenotypic (receptors) and genotypic (mutations) properties of

the tumors which they were derived from for a long time [189] [190]. These indicate that cell lines can be reliable models when used under the right conditions [183, 191].

MCF-7 is an estrogen positive (ER+) cell line that was derived by Michigan Cancer Foundation (which also gives its name) in 1973 [192]. It is one of the most recognized and routinely used model cell lines for researching breast cancer. A study on determining the identity of cell lines with the known cancer pathologies of showed that there is a similarity of the pattern of gene expression triggered by estrogen treatment in MCF-7 cell line and in the xenografts in mice [193, 194].

1.6: The aim, objectives and the outline of the thesis

Cancer is leading cause of death worldwide. According to world statistics (published by GLOBOCAN: International agency for research on cancer) there are around 13 million new cancer incidences excluding non-melanoma skin cancers [195].

Breast cancer is the most frequent cancer among women with an estimation of 1.38 million new cancer cases diagnosed (2008) that is 23% of all cancers **(Figure 1.8)**. It is the most common cancer both in developed and developing countries [196] yet molecular biology of breast cancer has still have many unknowns and detailed investigation should be done for early diagnosis and better therapeutics. For the past few decades, exponentially increasing evidence suggest that microRNAs are actively involved in regulation of diseases such as cancer. A simple PubMed Central (http://www.ncbi.nlm.nih.gov/pubmed/) search on articles published on microRNAs and cancer proves how fast this field is growing **(Figure 1.9)**. However, there are thousands of microRNAs identified in humans, each having probably hundreds of individual targets that could lead cancer cell progression or death. This makes microRNA research one

of major areas in investigating molecular biology of cancer and therapeutics.

The aim of this thesis is to focus on three microRNAs; mir-21, mir-9 and mir-9* using microarray profiling approach to identify their targets and phenotypic effects on breast cancer cells. Mir-21 and mir-9 are reported to be involved in regulation of breast tumorigenesis but there are still much to discover about their genome-wide effects and individual targets to elucidate how they role in cancer growth. Mir-9* on the other hand has only handful of reports. It is processed from the same precursor with mir-9, thus it needs to be further investigated to identify whether it involves in breast cancer regulation as its duplex partner mir-9.

1.6.1. Chapter 1 objective

- To provide a review of the literature on miRNAs and cancer with special reference to mir-21, mir-9, mir-9* and pseudogenes.

1.6.2. Chapter 2 objectives

- To determine the genome wide effects on transcript levels when mir-21 levels are depleted in MCF-7 breast cancer cell line.
- To determine whether mir-21 targets STAT3 and is involved in an autoregulatory loop with STAT3.

In chapter 2, the genome wide effects of mir-21 depletion by microarray profiling are investigated. Identification of JAK-STAT pathway as sensitive to mir-21 levels raised STAT3 as the key regulator of the pathway and as the predicted target of mir-21 so that it could serve as an intermediary link for mir-21 to communicate to the pathway. Therefore, the possible interaction between mir-21 and STAT3 as a part of autoregulatory loop is investigated.

1.6.3. Chapter 3 objectives

- To determine whether mir-21 targets JAG1 in breast cancer cells
- To investigate the interplay between Estradiol, mir-21 and JAG1 in estrogen responsive and non-responsive breast cancer cell lines

In chapter 3, JAG1 is identified as one of the top scoring predicted targets of mir-21 predicted by many online tools available. JAG1 and mir-21 have been shown to be involved in breast carcinogenesis and both are regulated by estrogen (17-beta-estradiol) oppositely. This raises the hypothesis that the possible interaction between mir-21 and JAG1 might be regulated by estrogen and the outcome of the interaction in ER+ or ER- cells could be different. Thus, the effects of 17-beta-estradiol on mir-21 and JAG1 levels and interaction in MCF-7 (luminal, ER+) and MDA-MB-231 (basal, ER-) cells are investigated.

1.6.4. Chapter 4 objectives

- To test the phenotypic effects of mir-9 overexpression on breast cancer cell growth
- To determine the genome-wide effects of mir-9 overexpression on MCF-7 breast cancer cells
- To identify direct targets of mir-9
- To test whether mir-9 direct targets contribute in activity of mir-9 in regulating tumorigenesis
- To test whether CSDAP1 as a pseudogene of CSDA, is targeted by mir-9 and acts as mir-9 sponge.

In chapter 4, the genome wide effects of mir-9 overexpression are investigated by microarray profiling. Mir-9 is expressed in low levels in cancer cells and overexpression of it could be a potential therapeutic approach but the genome wide effects need to be identified to define the potential outcomes of mir-9 replacement in the cancer cells. The functional effect on cancer cells and direct targets of mir-9 are identified and tested further to elucidate the contribution of mir-9 directed regulation of these

genes in breast tumorigenesis regulation. In addition, a gene/pseudogene pair (CSDA/CSDAP1) is identified to be downregulated by mir-9 overexpression in microarray analysis. The similar UTR and conservation of mir-9 binding sites make them ideal targets of mir-9. The maintained expression of CSDAP1 holds a great potential to be a mir-9 decoy that leads to less suppressed CSDA expression. Therefore, the interaction of mir-9 with CSDA and CSDAP1, the changes in the expression levels of the pair in mir-9 overexpressing MCF-7 cells is investigated.

1.6.5. Chapter 5 objectives

- To test the phenotypic effects of mir-9* overexpression on breast cancer cell growth
- To determine the genome-wide effects of mir-9* overexpression on MCF-7 breast cancer cells
- To identify direct targets of mir-9* and to elucidate the possible interactions as a consequence of mir-9* expression restoration in cancer cells

In chapter 5, similar to chapter 2 and 4, genome wide effects of mir-9* overexpression is investigated by microarray profiling. Unlike mir-9, an oncogenic potential of mir-9* is identified and its direct targets are investigated to gain insights into how mir-9* regulate breast tumorigenesis.

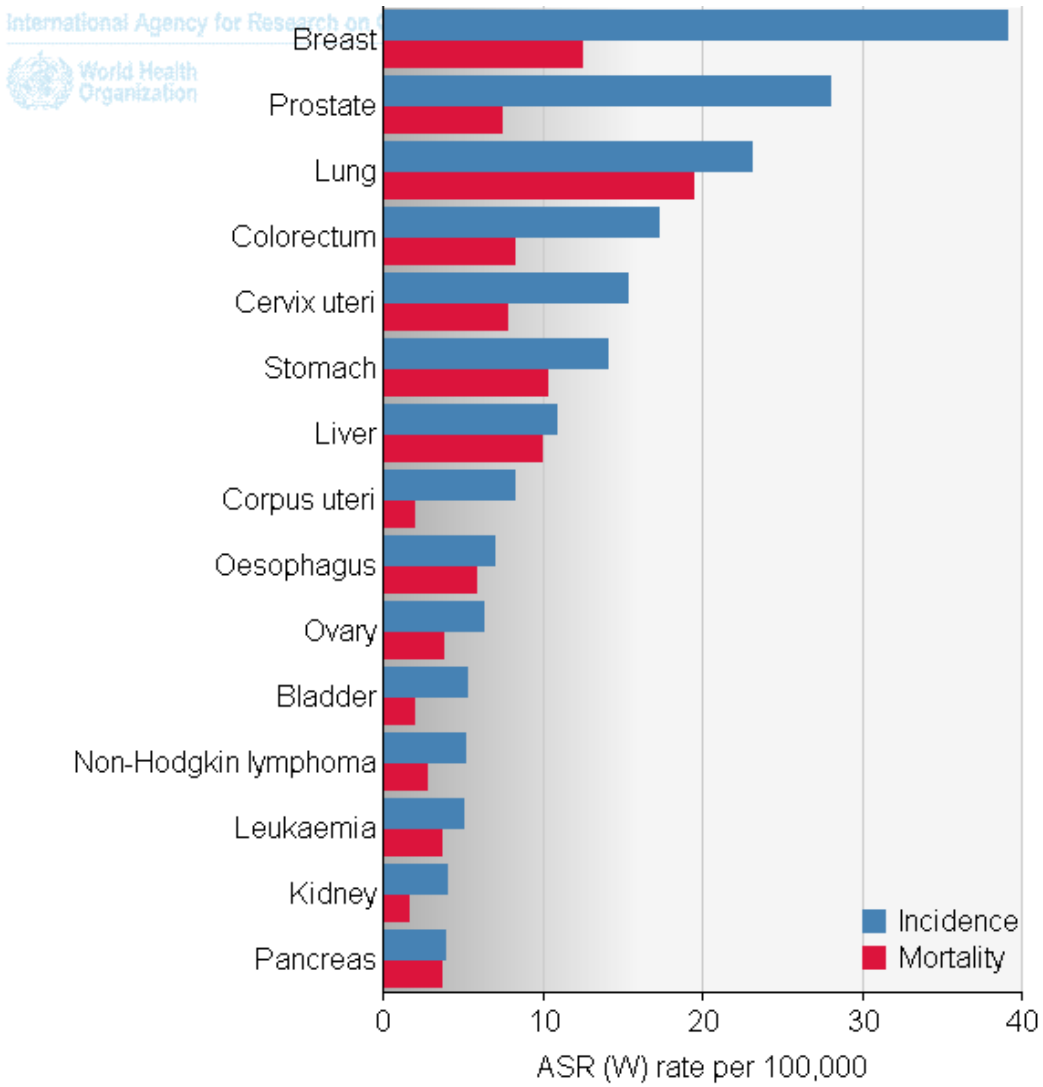

Figure 1.8: Worldwide most frequent cancers.

Frequency of cancers in both men and women in 2008 analyzed by GLOBOCAN.

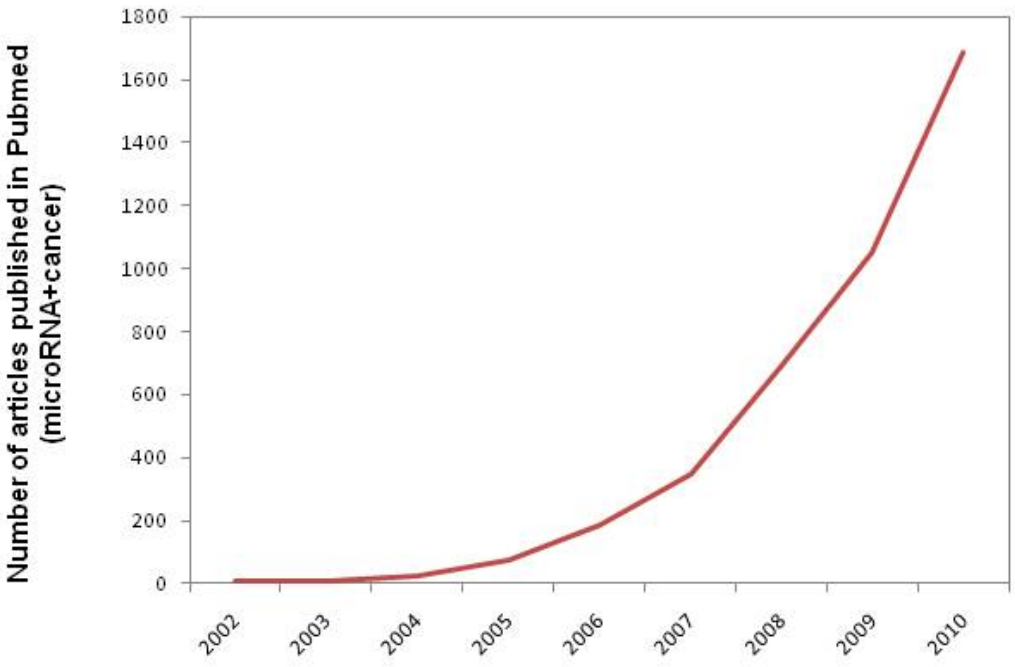

Figure 1.9: Number of articles listed in PubMed Entrez for microRNA & cancer between 2001 and 2010.

CHAPTER 2: Microarray profiling of mir-21 sensitive MCF-7 transcriptome and investigation of STAT3 and mir-21 interaction

2.1. Background: Significance of mir-21 in cancer

Some microRNAs have been shown to act as genuine oncogenes and directly induce tumorigenesis: they are named as 'oncomirs'. A recent study on an *in vivo* model of mir-21-induced pre-B-cell lymphoma introduced a phenomenon called 'oncomir addiction' where despite the multistep nature of malignant transformation, single oncogenic targets have potential as cancer therapeutics and mir-21 is one of these [61].

In addition to the previously validated oncogenic activity of mir-21 (mentioned in Section 1.3), recent studies dating from 2009 to 2011 strengthen the potential and significance of mir-21. With the help of novel technological advancements such as next-generation sequencing [197], *in situ* hybridization [198] [199] and other techniques [200] mir-21 is now considered as a cancer biomarker and a drug target.

Besides tumor tissue samples, the use of minimally invasive biomarker assays such as detection of microRNAs in body fluids (circulating microRNAs) has been reported recently. Quantitative approaches identified mir-21 as one of the significantly elevated microRNAs in plasma of patients with pancreatic cancer [201], non-small cell lung cancer [202], gastric cancer [203] and in blood samples of prostate cancer patients [204]. Elevated mir-21 levels have been detected in serum samples of hepatocellular carcinoma [205] and pancreatic cancer [206], in non-small cell lung cancer with poor prognosis [207], in bone marrow samples of breast cancer patients as a prognostic marker for cancer recurrence [208] and in pancreatic cyst fluid in pancreatic adenocarcinoma [209]. All these studies show that circulating mir-21 has great potential in the early diagnosis of cancer [210-215].

The role of mir-21 in cancer progression has been established by a large amount of research [216, 217]. Many clinical studies have shown that that mir-21 can be used as a biomarker for many metastatic primary tumors,

poor prognosis [218, 219] and drug resistance [220-222]. Its overexpression is associated with malignant transformation in many cancer types [223-226] and its knockdown has been shown to cause decreased cell proliferation and invasion and also increased apoptosis [227-231].

Up to date, numerous tumor suppressor genes have been identified as direct targets of mir-21. For example, in prostate cancer, MARCKS related protein (MRP), which is known to decrease cell migration, is a direct target of mir-21 [232] as well as MARCKS itself [233]. Additionally, a cell cycle gene, BTG2, in human laryngeal carcinoma [234], bone morphogenetic protein receptor II (BMPRII) in prostate cancer, RHOB; a known tumor suppressor, in hepatocellular cancer and breast cancer cell lines [235]. Moreover, RECK, the membrane-anchored protease regulator, was shown in many different cancer types as mir-21 target [236]. Thyroid hormone receptor beta (THRB) in thyroid carcinoma [237] and tumor suppressor gene P12 CDK2AP1 in head and neck squamous carcinoma [238] were also recently reported as direct targets of mir-21.

In association to breast cancer, mir-21 is one of the most significant deregulated microRNAs. Mir-21 expression was found to be negatively correlated with expression of its target PTEN in ductal carcinoma of the breast and its overexpression was associated with lymph node positivity, higher proliferation index and an aggressive phenotype [239]. An inverse correlation of mir-21 expression and its previously shown targets PDCD4, TM1 and PTEN was found in breast cancer [240]. Quantitative analysis of mir-21 in breast cancer samples showed significant upregulation compared to controls [241].

As mentioned in the **section 1.3.5,** other upstream pathways may affect the expression of mir-21. For instance, Bone morphogenetic protein-6 (BMP-6), which is an inhibitor of breast cancer epithelial-mesenchymal transition (EMT), has been shown to inhibit mir-21 transcription by binding to the E2-box and AP-1 sites in the mir-21 promoter (miPPR-21) [242].

Mir-21 was also shown to be upregulated by the MAPK (ERK1/2) pathway upon Her2/Neu stimulation [243], by the TGF-beta pathway in breast cancer cells [244] and by androgen (via AR binding to miPPR-21) in prostate cancer cells [245]. Moreover, mir-21 was found to be induced by the EGFR signalling pathway in lung cancer [246], by all-trans-retinoic acid (ATRA) in ER+ breast cancer cells [247] and by NFkB in gastric cancer cells [248], in mouse mammary adenocarcinomas and human ovarian carcinomas via AKT2 [249], by Ras in human thyroid cancers and non-small-cell lung cancers [250]. In contrast to mir-21 induction, downregulation of mir-21 by Polyphenon-60 (green tea extract) [251] and estradiol (E2) by activating estrogen receptor in MCF-7 [252] has also been described.

Moreover, AP-1, in response to RAS, was shown to induce mir-21 expression and mir-21 targets PTEN and PDCD4 are downregulated in an AP-1- and mir-21-dependent fashion [253]. As mentioned earlier, TGF-B induces mir-21 expression. A recent study showed that mir-21 overexpression also increases TGF-beta levels in colon cancer cells [254] which may indicate the presence of a regulatory loop. Taken together, these many findings demonstrate the oncogenic activity and potential of mir-21 as a drug target in cancer cells.

2.1.1. Aim

Despite the well known oncogenic activity and of mir-21 and its individual targets, the mechanisms of mir-21-directed cancer pathways are not fully understood at the genome-wide level

The aim of this chapter is to identify genome-wide effects on the transcriptome of mir-21 knockdown (depletion) using a breast cancer model, the MCF-7 cell line. This involves investigating pathways, networks and individual genes as direct or indirect targets of mir-21: in other words, defining the mir-21-sensitive transcriptome.

A whole genome microarray profiling approach coupled with detailed analysis of direct and indirect interactions of mir-21 with cancer-relevant pathways and genes was used to investigate the potential outcomes of mir-21 depletion in the MCF-7 breast cancer genome.

2.2. Materials and Methods

All the step-by-step protocols, primer sequences and recipes used in this thesis are listed in Appendices and corresponding sections are cross-referenced in the text.

2.2.1. Tissue culture and reagents

All tissue culture work was performed under the tissue culture laminar flow cabinet (SafeFAST Elite, FASTER, Mason Technologies) sterilized with UV, wiped with 80 % v/v EtOH (ethanol) before and after use, regularly wiped with 10 % v/v bleach solution (stock: 10 % w/v Chloropol, Water Technology Ltd.) once a month. All items, before placing in the hood, were sprayed with 100 % ethanol and wiped.

Adherent (monolayer) breast cancer cell line MCF-7 (obtained from Prof. Rosemary O'Connor's lab, UCC) and hepatocellular carcinoma cell line HepG2 (obtained from Anita Talbot, Michael Cairns' lab, NCBES, NUIG) were cultured in Dulbecco's modified Eagle's medium (DMEM, Sigma, UK, #D6429) supplemented with a final concentration of 10 % v/v fetal bovine serum (FBS, Sigma, UK, #F7524) and a final concentration of 100 U/ml of penicillin and streptomycin (P/S, Sigma, UK, #P0781). The DMEM media prepared was named as 'complete DMEM'. Cultures were maintained at 37˚C and 5 % v/v CO_2 incubator (Galaxy 170S, New Brunswick, Eppendorf).

Firstly, frozen stocks of cells removed from liquid nitrogen storage were immediately thawed at 37 ˚C in a water bath to prevent damaging by DMSO (Sigma, UK, #D2650) in the media that cells were stored in. Thawed cells were mixed with DMEM complete medium and seeded in T25 (25 cm^2, Sarstedt, Germany, # 83.1810.002) tissue culture flasks. The following day, cells were replaced with fresh complete medium to clear DMSO from the media they were growing in. After 2-3 days, cells were

washed with 1X Phosphate Buffer Saline (PBS, Sigma, UK, #P4417) to remove the metabolic wastes and old medium was replaced with a fresh complete medium.

1X Trypsin-EDTA (Sigma, UK, #T4174) solution was used to detach the cells from the flasks when they had reached 80% confluency by incubating at 37˚C for 5 min. The detached cells were mixed with complete medium to inactivate Trypsin and the Trypsin/cell suspension was centrifuged for 5 min at 1000 rpm. The pellet was resuspended in fresh medium and transferred into T175 flasks (75 cm^2, Sarstedt, Germany, #83.182.002). Once the cells had reached 80% confluency in these larger flasks they were counted by staining samples of cells using tryphan blue (Sigma, UK, #T8154). Viable cells were discriminated from dead ones using FastRead102 disposable counting slides (Immune Systems, UK, #BVS100) under an inverted microscope.

Sub-culturing of the cells was done based on the doubling time of each cell line with 1:5 and 1:3 ratios for MCF-7 and HepG2 cells, respectively. Grown cells were detached as described above and appropriate numbers of cells were seeded to tissue culture plates (96 well, 24 well or 6 well) for the experiment. Remaining cells were stored by mixing with freezing medium (10% DMSO in FBS) with equal volume of cells (final concentrations of 5% DMSO, 45% FBS and 50% DMEM) in cryovials (CryoPure, Sarstedt, Germany, #72.380.004). Cells were kept at -80˚C overnight and transferred to liquid nitrogen for long-term storage. Human Recombinant IL-6 (Peprotech, UK, #200-06) was used in a final concentration of 5 ng/ml in treatments. For IL-6 treatments, phenol red-free DMEM (Sigma, UK, #D5921) was prepared with 10% FBS-charcoal stripped Sigma, UK, #F6765).

2.2.2. Antibodies

Polyclonal STAT3 primary antibody (rabbit, #9132), phospho-STAT3 (Tyr705) antibody (rabbit, # 9131) and BCL2L1 antibody (BCL-xL, rabbit, #2762) were purchased from Cell Signaling Technology, USA. Monoclonal Beta-Actin primary antibody (mouse, #A3854) and secondary antibodies (anti-rabbit A6667, anti-mouse A0168) were purchased from Sigma, USA. Polyclonal JAK1 antibody (rabbit, #GTX101955S) was purchased from GeneTex, US.

2.2.3. Mir-21 overexpression construct

To study the functions of miRNAs in cells, expression of microRNAs can be mimicked by precursor PCR amplification and cloning into mammalian expression vectors. To study the mir-21 overexpression effect on MCF-7 cells, precursor mir-21 sequence (pre-mir-21) located at chr17: 55,273,409-55,273,480 together with ~200 bp of upstream and downstream flanking sequences was obtained from the UCSC genome Browser.

Specific primers were designed to amplify the target region (490 bp) from human genomic DNA (Roche, UK, # 11 691 112 001). These primers were manually designed **(protocol: A.4.1.)** to include suitable restriction enzyme (RE) sites to allow restriction digestion and cloning into the pcDNA3 mammalian expression vector (5446bp, Invitrogen, USA, #A-150228) **(vector map: A.5.1.)**. The region was amplified by PCR using genomic DNA as a template. The PCR reaction mixture and program are shown **(Table 2-1)**. Amplified products were cloned into HindIII-EcoRI RE sites of the vector. Direct cloning of the insert was performed **(protocol: A.3.3.)**. The construct was designated as pc-21 **(Figure 2.1).** Following sequence confirmation (GATC, Germany) of the construct, midiprep plasmid isolation was performed using NucleoBond Xtra Midi kit (Macherey-Nagel, MN, Germany, #740410.50) **(protocol: A.3.14.)**. Mir-21

was knocked down using antisense-mir-21 oligonucleotides with 2'O-methyl modification (anti-mir-21) (Integrated DNA Technologies, IDT, USA) at final concentrations of 50 nM in all transfections.

Table 2-1: PCR reaction conditions and program to amplify inserts for vector cloning

1X PCR master mix	
5X flexi buffer	10 µl
dNTP mix (2.5 mM)	1 µl
Fwd primer (10 µM)	5 µl
Rvs primer (10 µM)	5 µl
Nuclease-free water	32.75 µl
GoTaq Polymerase (5U/µl)	0.25 µl
DNA (50 ng /µl)	1 µl
$MgCl_2$ (25 mM)	3 µl
TOTAL	50 µl

Thermal Cycler Program:

95˚C	3:00 min	
95˚C	0:30 min	x33
60˚C	0:30 min	
72˚C	0:30 min	
72˚C	10:00 min	
10˚C	Hold	

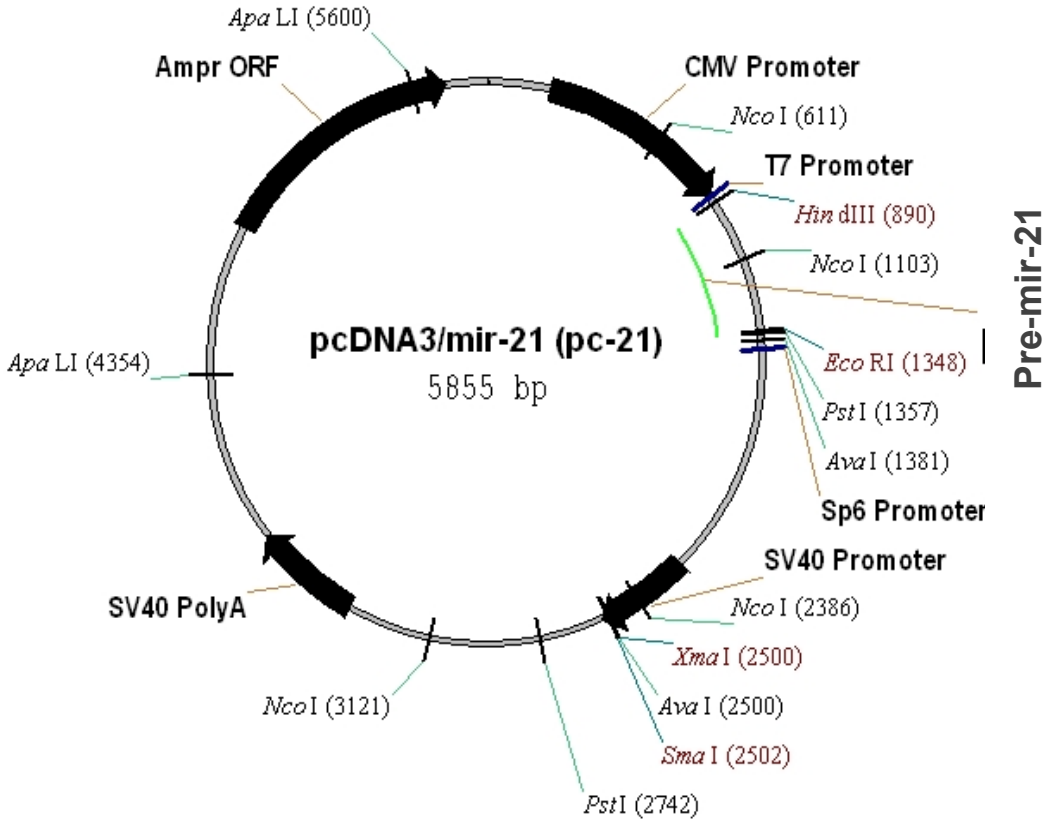

Figure 2.1: Pre-mir-21 DNA sequence cloned into expression vector. Pre-mir-21 with ~ 200nt upstream and downstream flanking sequences was amplified by PCR and cloned into the pcDNA3 mammalian expression vector (shown in green).

2.2.4. pMIR-STAT3 luciferase reporter constructs

To test whether mir-21 targets the STAT3 3'UTR, pMIR-REPORT miRNA expression reporter vector containing the firefly luciferase gene (Ambion, USA, #5795) was used **(vector map: A.5.3.)**. The genomic region of STAT3 containing its full length UTR (2.4 kb containing both mir-21 putative binding sites 1&2) was amplified by PCR using human genomic DNA and cloned into the SpeI/MluI restriction sites of pMIR-REPORT vector. Sub-cloning into TOPO PCR vector was performed **(protocol: A.3.4.)**. The insert was released by double digestion and gel extracted, together with the double digested vector. Following ligation and transformation, selected colonies were tested by colony PCR to confirm the presence of the insert **(protocol: A.3.4.).** Selected positive colonies were grown in LB-amp broth; miniprep plasmid isolation was performed and sent for sequencing confirmation. The correct clone as confirmed by sequencing was designated as **pMIR-STAT3^{UTR} (Figure 2.2)**.

Mutant constructs lacking complementarity with mir-21 seed sequences were cloned using specific primers (Quikchange Primer design) designed using Quikchange XL kit (#200516, Agilent Technologies, USA). Positive clones (as confirmed by sequencing) were designated as pMIR-STAT3$^{UTR\Delta1}$ (seed region 1 deleted), pMIR-STAT3$^{UTR\Delta2}$ (seed region 2 deleted) and pMIR-STAT3$^{UTR\Delta1/2}$ (seed regions 1&2 deleted) **(Figure 2.3).**

Table 2-2: Site Directed Mutagenesis PCR Reaction

1X SDM PCR master mix (Stratagene)	
10X buffer	5 µl
dNTP mix (10 mM)	1 µl
Fwd primer (10 µM)	0.8 µl
Rvs primer (10 µM)	0.8 µl
Nuclease free water	39.4 µl
Quick solution	3 µl
Plasmid (15 ng/µl)	1 µl
PfU Turbo enzyme	1 µl
TOTAL	51 µl

Thermal Cycler Program:

95˚C	2:00 min	
95˚C	1:00 min	X18
65˚C	1:00 min	
68˚C	14:00 min (2 min/kb)	
68˚C	7:00 min	
10˚C	Hold	

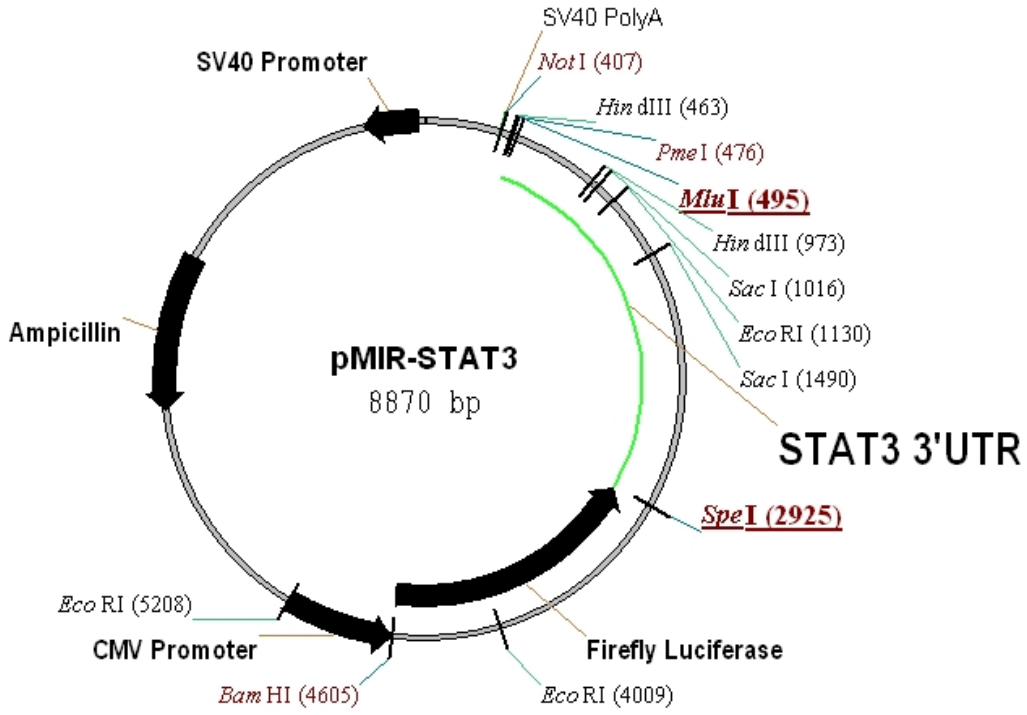

Figure 2.2: pMIR-STAT3 luciferase construct map.

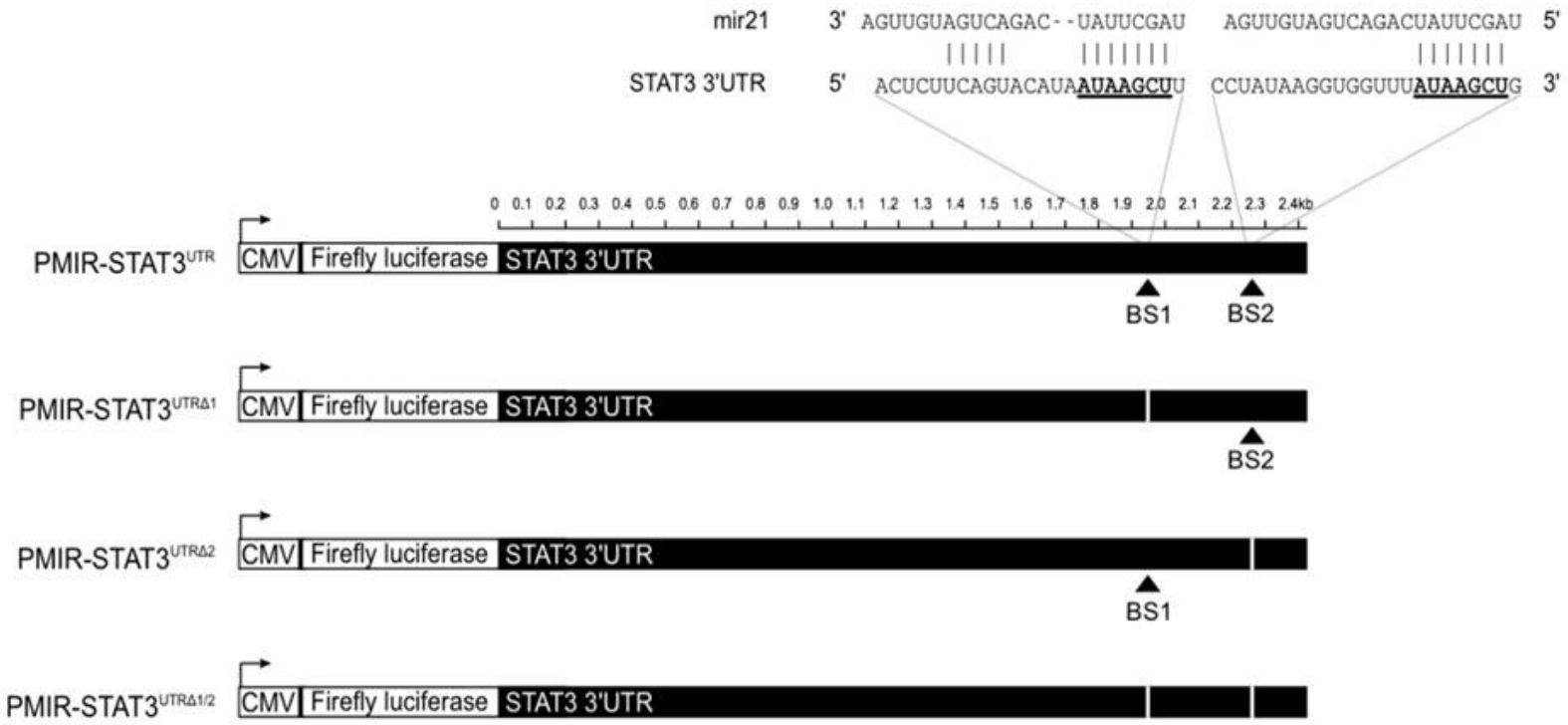

Figure 2.3: pMIR-STAT3 luciferase reporter constructs design.

2.2.5. Transfections

All the transfections were performed in tissue culture laminar flow cabinet. The day before transfection, cells were grown, detached, counted and required numbers of cells were seeded into tissue culture plates (10^3 cells for 96-well, 10^3 cells for 24-well and $2x10^5$ cells for 6-well plates). The next day, cells were washed with 1X PBS and placed in complete DMEM medium without Pen/Strep. Transfection mixtures were prepared in OPTIMEM-I medium (Gibco, USA, #31985-047) using the liposome based transfection agent (Lipofectamine 2000, Invitrogen, USA, #11668-027) according to manufacturer's protocol **(protocol: A.3.10.)**.

For overexpression and knockdown of mir-21, MCF-7 cells were seeded into 6-well plates. The next day, 1 μg of pcDNA-21 or pcDNA empty vector and 50 nM of anti-21 or anti-control (scrambled) oligonucleotides were transfected. Cells were harvested 24, 48 and 72 hours post-transfection.

For luciferase experiments, pRL-SV40 renilla luciferase vector (Promega, USA, #E2231) **(vector map: A.5.4.)** was used to normalize transfection efficiencies. 300 ng of each pMIR-STAT3-UTR construct or empty vector control pMIR-REPORT were co-transfected with 3 ng of Renilla vector (300 ng: 1 ng ratio for firefly: renilla) in 24 well plates (in the presence and absence of IL-6). 24hr post-transfection cells were assayed for luciferase expression.

For STAT3 overexpression experiments, cells were plated into 6-well plates the day before transfection and serum starved for 4 hours before being transfected in DMEM medium without phenol red or Pen/Strep. Cells were transfected with 1 μg of the appropriate construct in the presence or absence of IL-6 (5 ng/ml). Cells were harvested 48 and 72 hours post-transfection.

2.2.6. RNA isolation

Total RNA and small RNAs were isolated from cells in one fraction using the Nucleospin miRNA kit (Macherey-Nagel, MN, Germany, #740971.250) **(protocol: A.3.13.)**. RNA samples were always kept on ice and visualized on 1% agarose gels for integrity. Quantity measurements were performed on the NanoPhotometer system (Implen, Germany). Total RNA samples were immediately stored at -80˚C or cDNA synthesis was performed.

2.2.7. Quantitative RT-PCR analysis of mir-21

Separate RT-PCR reactions were performed for microRNAs and mRNAs. MicroRNA RT-PCR was performed using Taqman Assays and the microRNA reverse transcription kit (Applied Biosystems, ABI, UK, #4366596). Taqman assays are based on stem-loop primers, which selectively bind to specific microRNAs and reverse, transcribe. This is followed by a quantitative PCR amplification step using specific probes **(Figure 2.4)**. 10 ng of total RNA was used as a starting material for all miRNA RT reactions. In parallel to this, the same RNA material was used for another RT reaction using primers specific for RNU6B (U6 small RNA), which was used as a housekeeping control for normalization. The reaction was prepared in 0.2 ml PCR 8-strip tubes, briefly centrifuged in a bench-top mini centrifuge and run in thermal cycler (PTC-200, MJ Research) **(Table 2-3).** cDNA reactions were followed by quantitative PCR using probes specific for mir-21 (supplied in Taqman mir-21 assay kit) and RNU6B and AmpliTaq Gold enzyme already included in the 2X universal master mix (ABI, UK, #M14814). cDNA was diluted with sterile water in a 1:3 ratio (e.g. 10 µl cDNA + 20 µl water for a final volume of 30 µl); diluted cDNA was used in PCR performed on the thermal cycler as before **(Table 2-4)**.

Data analysis was performed using the software supplied with the detection system. This was based on the relative quantification (RQ)

method (ΔΔCt analysis) that measures the change in expression in the target sample (treated) compared to a calibrator sample (untreated). Endogenous control is used for normalization without measuring the exact copy of the template to avoid the need for a standard curve. The ΔΔCt method formula is shown in **Table 2-4**.

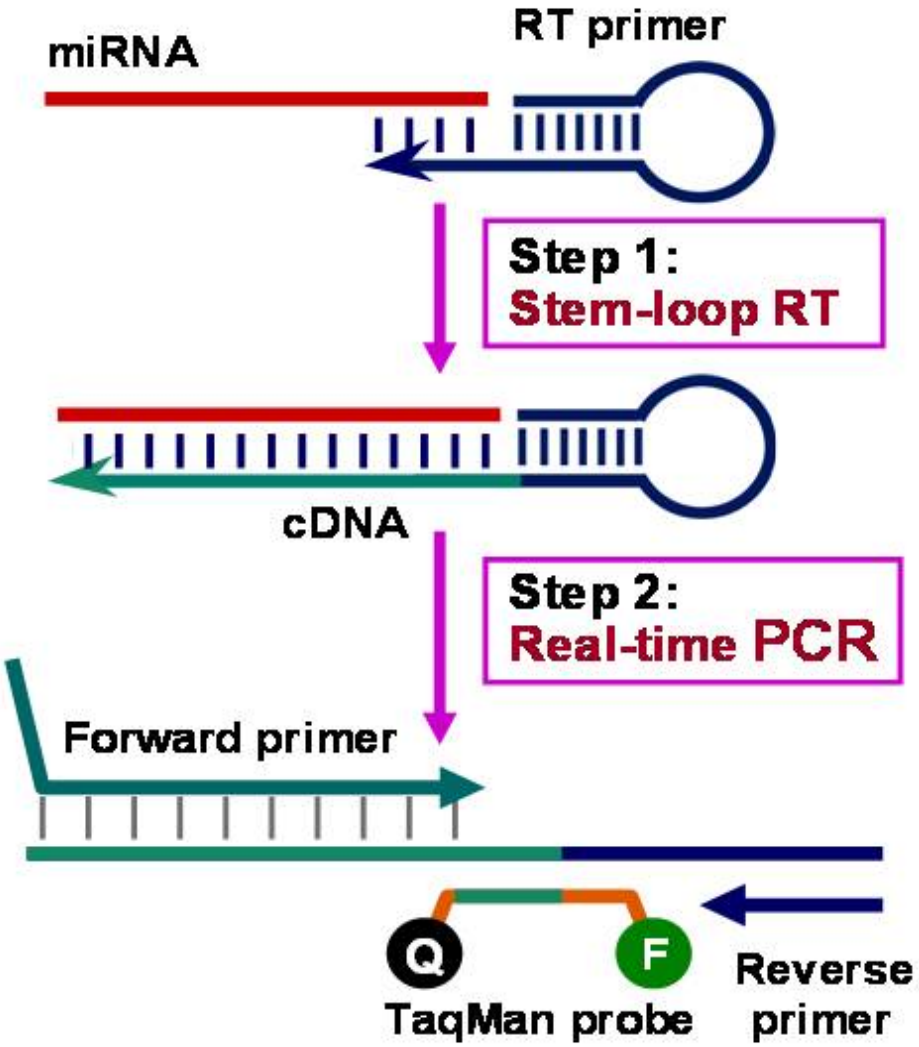

Figure 2.4: Taqman microRNA RT-PCR.

RT primers specific for detection of mir-21 and RNU6B (U6 small RNA, housekeeping control) were used in reverse transcription reactions. This figure is adapted from www.appliedbiosystems.com.

Table 2-3: MicroRNA Reverse Transcription reaction and program

1X cDNA synthesis mix (Taqman, ABI)	
10X buffer	1.5 µl
dNTP mix	0.15 µl
RT Primer mix	3 µl
Total RNA (5 ng/µl)	2 µl
Nuclease free water	7.16 µl
RNase Inhibitor (20 U/µl)	0.19 µl
MultiScribe enzyme (50 U/µl)	1 µl
TOTAL	15 µl

Thermal Cycler Program:

16˚C	30:00 min
42˚C	30:00 min
85˚C	5:00 min
10˚C	Hold

Table 2-4: MicroRNA PCR amplification

1X PCR mix (Taqman, ABI)	
Taqman MicroRNA Assay probe	0.5 ul
cDNA (1:3 dilution)	0.7 ul
Taqman 2X Universal master mix	5 ul
Nuclease free water	3.8 ul
TOTAL	10 ul

Thermal Cycler Program:

95˚C	10:00 min	
95˚C	00:15 min	X39
60˚C	1:00 min	
10˚C	Hold	

$2^{-\Delta\Delta Ct}$ method

$\Delta Ct = Ct_{Gene} - Ct_{housekeeping}$

$\Delta\Delta Ct = \Delta Ct_{treated} - \Delta Ct_{untreated\ (ref)}$

2.2.8. Quantitative RT-PCR analysis of mRNAs

For cDNA synthesis of total RNA for detection of mRNAs, the First Strand cDNA synthesis kit was used (Revert-aid H-minus, Fermentas, USA, #K1632). Initially, primers specific for exon-exon junction regions were designed to avoid any possible DNA contamination interfering with the results. Manually selected primes were first tested for specificity using the NCBI-primer BLAST program, and Sigma DNA calculator (http://www.sigma-genosys.com/calc/DNACalc.asp) was used to check the melting temperatures (Tm), GC content, tendency to primer-dimer formation and product length (which is optimal at 80-120 bp). Based on this, further arrangements were done using both primer sequences so that both had a similar Tm, around 50 % GC content and no or weak primer dimers. Finally, the primers were tested in UCSC *in silico* PCR program to check the possible DNA amplicon (usually ranged between 5-10 kb). Regular PCR was initially performed to check the specificity of the primers. 1 µg of total RNA was used as a starting material and oligo-dT primers were used in the reaction. These reactions were prepared in 0.2 ml PCR tubes and run on a standard thermal cycler **(Table 2-5)**.

Following cDNA synthesis, cDNA was diluted 1:5 with nuclease-free water and amplified by PCR using the SYBR Green assay system (Jumpstart Taq Ready mix for qPCR, Sigma, USA, #S4438) in 96-well opaque plates **(Table 2-6).** Plates were sealed with optically clear seals and centrifuged briefly at 1000 rpm. The reaction was then run on a CFX96 real time thermal cycler (Bio-Rad, USA). Melt curve analysis was performed in each PCR reaction to test the specificity of the primers and the amplicon. Results giving double peaks (double amplicons) or primer dimers (represented by a peak at 75˚C) were excluded from the analysis. Data analysis was performed using the software supplied by the detection system based on the relative quantification method (ΔΔCt analysis) as described for detection of microRNAs**.** Melt-curve analysis was performed at the first usage of the primes to make sure they gave a single peak at

80-85˚C as an indication of amplification and specificity. B2MG, GAPDH and Actin genes were used as housekeeping controls in normalizations and relative quantifications.

2.2.9. Luciferase Reporter Assay

24 hours after transfection with UTR constructs in 6-well plates, cells were lysed in Passive Lysis Buffer and transferred to 96-well opaque plates. Luciferase Assay Buffer II and Stop-Glo buffers were added by the automated injector system (dual injector) **(protocol: A.3.8.)**. Normalized luciferase activity was measured and analyzed in Modulus Microplate Luminometer (Turner Biosystems). Results were represented in bar graphs as the mean of triplicate experiments with +/- SEM (standard error of mean). Statistical significance was analyzed by Student's t-test ($p<0.05$) considered as significant as labeled with asterix (*) on top of the data bars.

Table 2-5: First-strand cDNA synthesis

1X cDNA synthesis mix (Revertaid H-minus, Fermentas)	
Total RNA (200 ng/µl)	5 µl
OligodT Primer	1 µl
Nuclease free water	6 µl
5X Reaction Buffer	4 µl
RiboLock RNase inhibitor (20 U/µl)	1 µl
dNTP mix (10 mM)	2 µl
M-MuLV Reverse Transcriptase (200 U/µl)	1 µl
TOTAL	20 µl

Thermal Cycler Program:

42˚C	60:00 min
70˚C	05:00 min
10˚C	Hold

Table 2-6: Sybr Green qPCR

1X Sybr green PCR (Sybr mix, Sigma)	
Sybr green assay (2X)	5.5 μl
Fwd Primer (10 μM)	1 μl
Rvs Primer (10 μM)	1 μl
Nuclease free water	1.5 μl
cDNA (1:5 dilution)	1 μl
TOTAL	10 μl

Thermal Cycler Program:

95˚C	10:00 min	
95˚C	0:15 min	X39
60˚C	1:00 min	
Plate Read		
95˚C	0:10 min	
Melt curve, Increment 0.5 ˚C 65-95˚C	0:05	
Plate Read		

$2^{-\Delta\Delta Ct}$ method

$\Delta Ct = Ct_{Gene} - Ct_{housekeeping}$

$\Delta\Delta Ct = \Delta Ct_{treated} - \Delta Ct_{untreated\ (ref)}$

2.2.10. Cell Proliferation (acid phosphatase) assay

24 hours after transfection with pcDNA-21or pcDNA empty vector, MCF-7 cells were transferred into 96-well tissue culture plates for cell proliferation measurements. At 48 and 72hr post-transfection time points, p-nitrophenol phosphate substrate (Sigma, USA, #P4744) **(recipe: A.2.2.)** was added onto cells. Following 2hr incubation at 37˚C, the reaction was stopped by addition of 1N NaOH. Using the plate reader, absorbance was measured at 405 nm (ref: 620 nm) to assess the phosphatase production as an indication of cell proliferation activity **(protocol: A.3.6.)**

2.2.11. Viability and Caspase-3/7 (ApoTox-Glo) Assay

For viability, cytotoxicity and caspase-3/7 activation analysis, the ApoTox-Glo Triplex Assay was used (Promega, USA, #G6320) according to manufacturer's protocol **(protocol: A.3.7.)**. Two differential protease biomarkers (to detect live and dead cells) were simultaneously added onto cells and fluorescence measurements were taken after 1hr incubation at 37˚C (viability: $400_{Ex}/505_{Em}$ and cytotoxicity: $485Ex/520_{Em}$). The viability readings across wells were normalized by viability to cytotoxicity ratio of each well (live/dead cells).

Following viability and cytotoxicity measurements, the caspase-3/7 substrate (containing luminogenic DEVD-peptide substrate and recombinant thermostable luciferase) was added onto cells. Following 1hr incubation at room temperature, luminescence measurements were taken to determine caspase-3/7 activation as an indication of apoptosis. Apoptosis readings across wells were normalized by caspase-3/7 to viability ratio of each well.

2.2.12. Protein extraction and western blotting

Cells were washed with 1X PBS and harvested using cell scrapers (Sarstedt, Germany, #83.1832), centrifuged at 1000 rpm for 5 min and pellets resuspended in protein lysis buffer **(recipe: A.2.1.)**. After incubation on ice for 20 min, samples were centrifuged at 10,000rpm for 15 min to remove any insoluble material. Quantification was performed by protein assay (Bio-Rad, USA, #500-0006) using BSA to generate a standard curve **(protocol: A.3.11.)**.

30 µg protein was mixed with 6X protein loading buffer **(recipe: A.2.1.)**, heated at 95˚C for 5 min, loaded into 10 % SDS-PAGE and transferred onto a PVDF membrane (Westran CS, #10485288, Whatman, UK) by semidry transfer (Bio-Rad, USA) All primary antibodies were used in 1:1000 dilutions made up in 5% BSA in 0.1% TBS-Tween-20. Primary incubations were performed overnight at 4°C with gentle rocking. Secondary antibodies were used at a 1:10,000 dilution in 5% milk TBS-T for 2hr at room temperature. Blots were visualized with enhanced chemiluminescence (ECL Plus Kit, Perkin Elmer, USA, #NEL101001EA) using the G:Box Chemi imaging system (Syngene, UK).

2.2.13. Microarray Profiling and Data Analysis

MCF-7 cells were treated with anti-21 (50 nM), Scrambled control (50nM) or untreated in 6 well plates. Samples were processed and hybridized onto GeneChip Human Genome U133 plus 2.0 arrays (Affymetrix, USA, #520065) in duplicates **(protocol: A.3.16.).** Microarray profiling was performed at the BilGen Microarray Core Facility (Bilkent University, Turkey).

Microarray Analysis Quality assessment of the hgu133plus2 arrays was performed using the arrayQualityMetrics package in Bioconductor [255, 256]. One array failed several tests and was therefore removed, leaving

duplicates for each condition. The remaining arrays were normalized using the RMA method provided in the Bioconductor Affy package [257]. Probe set-to-locus mappings for the arrays were provided by the hgu133plus2.db package [258]. Probe sets matching no or few loci were filtered out. Also, redundant probe sets that represent the same locus several times were counted only once (using the probe set with the greatest interquartile range) using the featureFilter function in the Genefilter package [259].

Differentially expressed genes were identified using linear modeling and moderated t-tests using the LIMMA package [260]. T-tests were performed for anti-mir-21 vs. untreated and scrambled vs. untreated. Any genes displaying differential expression in both tests were discarded as displaying a non-specific effect caused by the introduction of an oligonucleotide to the cell. Adjusted p-values were calculated using the FDR method [261]. Confidence thresholds of adjusted p-value < 0.05 and fold change > log2 (1.5) were used. Hypergeometric testing for enrichment of GO and KEGG terms in the set of differentially expressed genes was performed using the Bioconductor packages GOStats and Category [262, 263]. Enrichment was tested separately for the upregulated and down-regulated gene sets and results are reported as unadjusted p-values.

2.3. Results

2.3.1. Mir-21 overexpression induces an increase in cell proliferation

Knockdown of mir-21 has previously been shown to decrease cell proliferation and induce apoptosis in cancer cells [68, 69, 114]. To test the opposite effect of overexpression of mir-21 on cell proliferation and apoptosis, dosage of mir-21 in MCF-7 cells was increased using the pcDNA-21 (pc-21) precursor plasmid, which is processed into the active mature form of mir-21 when expressed. qRT-PCR analysis performed at 48 hours post-transfection showed that the levels of mir-21 increased up to 5 fold compared to MCF-7 cells transfected with the empty pcDNA vector **(Figure 2.5).**

In cells overexpressing mir-21, a cell proliferation assay was performed at three time points, 24, 48 and 72hr after transfection. Data from each time point was normalized to the result of treatment with the corresponding empty plasmid (pcDNA). After 48hr of mir-21 overexpression the cell proliferation rate was significantly increased as measured by phosphatase production **(Figure 2.6),** consistent with previous studies of the activity of mir-21 in cancer cells [264, 265].

2.3.2. Mir-21 knockdown decreases cell viability and increases caspase-3/7 production

To test the effect of mir-21 knockdown prior to microarray analysis, anti-21 or anti-ctr transfected MCF-7 cells (with a final anti-21 concentration of 50 nM) were analyzed for viability, cytotoxicity and caspase-3/7 production using the ApoTox-Glo triplex assay [266]. Viability results were represented as ratios of viability readings/ cytotoxicity readings as a live/dead cell ratio to normalize the well-to-well differences. Relative to anti-ctr treated cells, anti-21 treated MCF-7 cells showed decreased

viability after 48 hours of transfection **(Figure 2.7A)**. On the other hand, caspase-7 production decreased in cells in which mir-21 had been deleted by anti-21 treatment, indicating the presence of apoptosis **(Figure 2.7B)**.

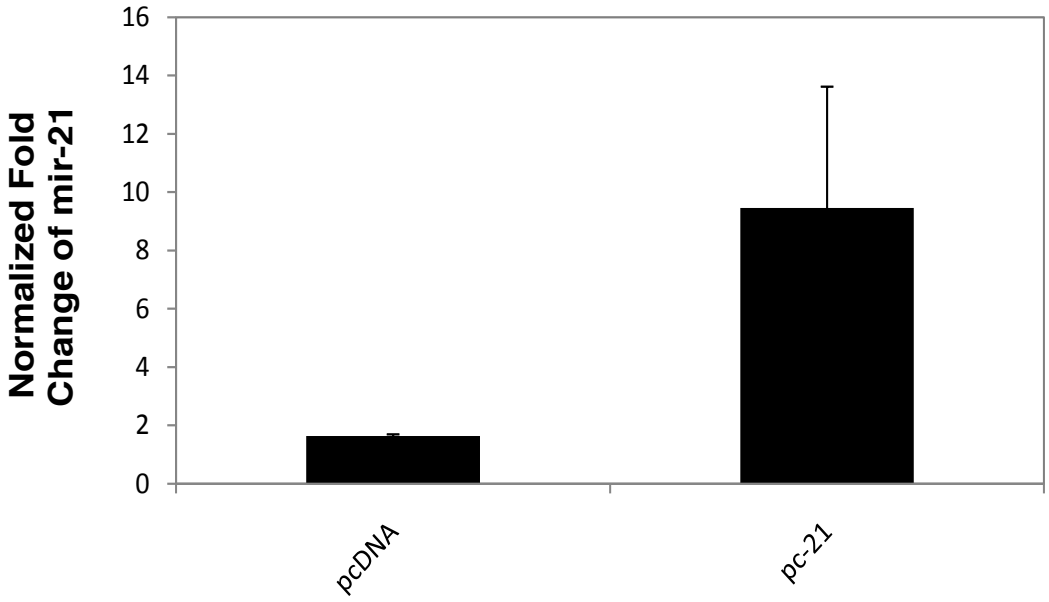

Figure 2.5: Relative fold expression of mir-21 in pc-21 or pcDNA transfected MCF-7 cells.

Mir-21 expression is showed an approximate fivefold increased in MCF-7 cells overexpressing the pc-21 vector compared to an empty pcDNA vector control.

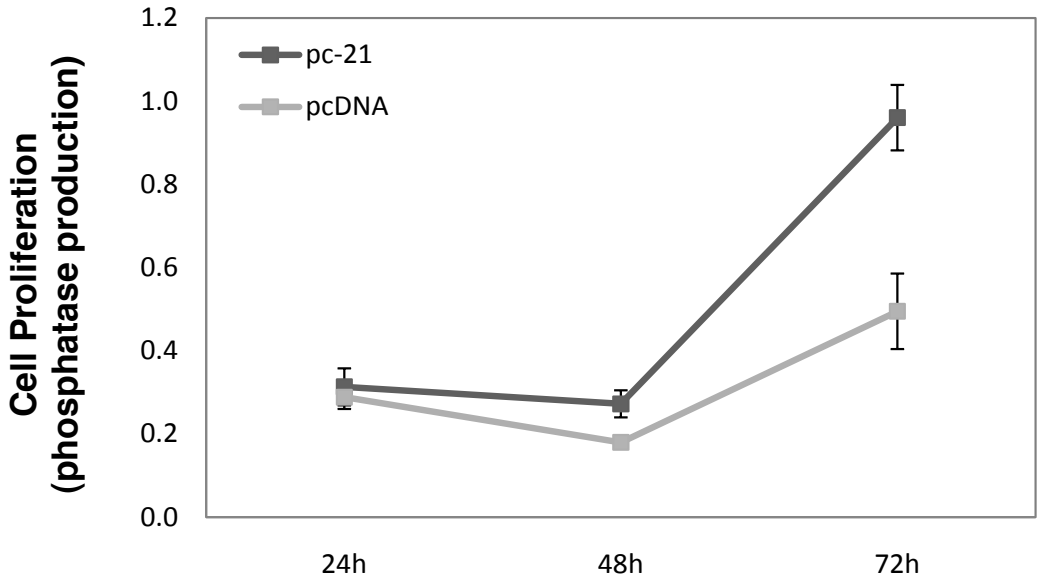

Figure 2.6: Mir-21 overexpressing cells (pc-21) grow faster compared to mock-treated controls.

P-nitrophenol fluorescence was measured at 420 nm with reference background subtraction at 620 nm. Cell growth at 72hr is indicated by increased phosphatase production in pc-21 transfected cells when compared to cells transfected with empty pcDNA vectors.

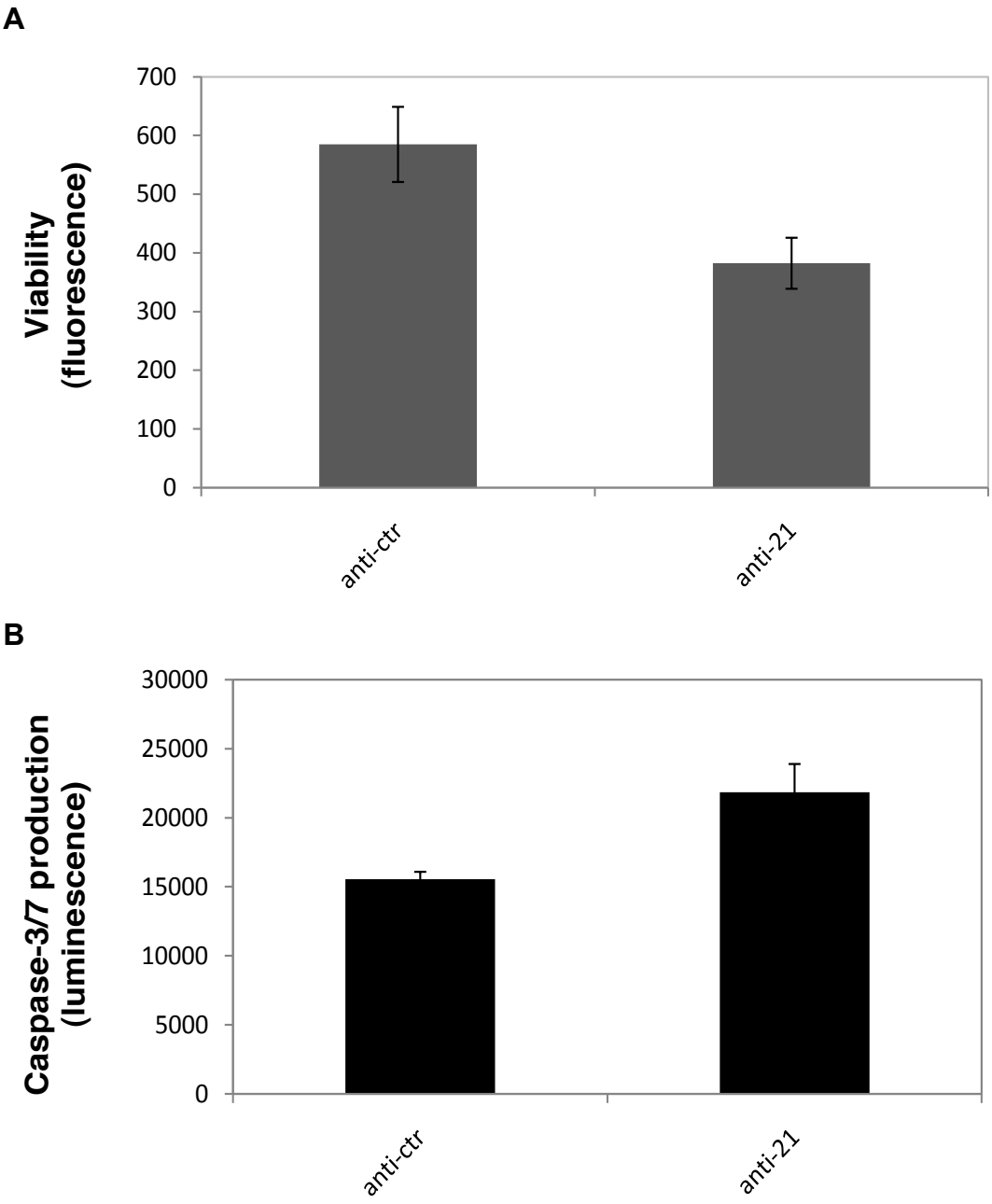

Figure 2.7: Functional effect of mir-21 depletion on MCF-7 cells.

A) Decreased viability and **B)** increased caspase-7 production in MCF-7 cells with depleted mir-21 levels.

2.3.3. Microarray analysis identifies cancer-associated pathways and genes which are deregulated in MCF-7 cells depleted in mir-21

As an overexpressed microRNA oncomir, miR-21 has high potential as a drug target for use in clinical studies. However, understanding the genome-wide impacts of mir-21 expression is important for understanding cancer cell phenotypes triggered by modulation of mir-21 levels.

To investigate the global effects of mir-21 depletion on gene expression in cancer cells, transcript levels in MCF-7 cells were determined by microarray analysis on cells treated with anti-21 or anti-ctr (scrambled) or left untreated in independent duplicates. The results showed that a total of 404 genes were differentially expressed at the mRNA level following anti-21 treatment (with cut offs of $p<0.05$ and fold change>1.5). Of these genes, 136 were upregulated and 268 were downregulated in anti-21 treated cells compared to anti-ctr treated or untreated cells **(Figure 2.8)**.

Among the differentially expressed genes identified, GO enrichment analysis showed many involved in migration, cell movement, invasion, apoptosis and survival, all with significant p-values **(Table 2-7)**.

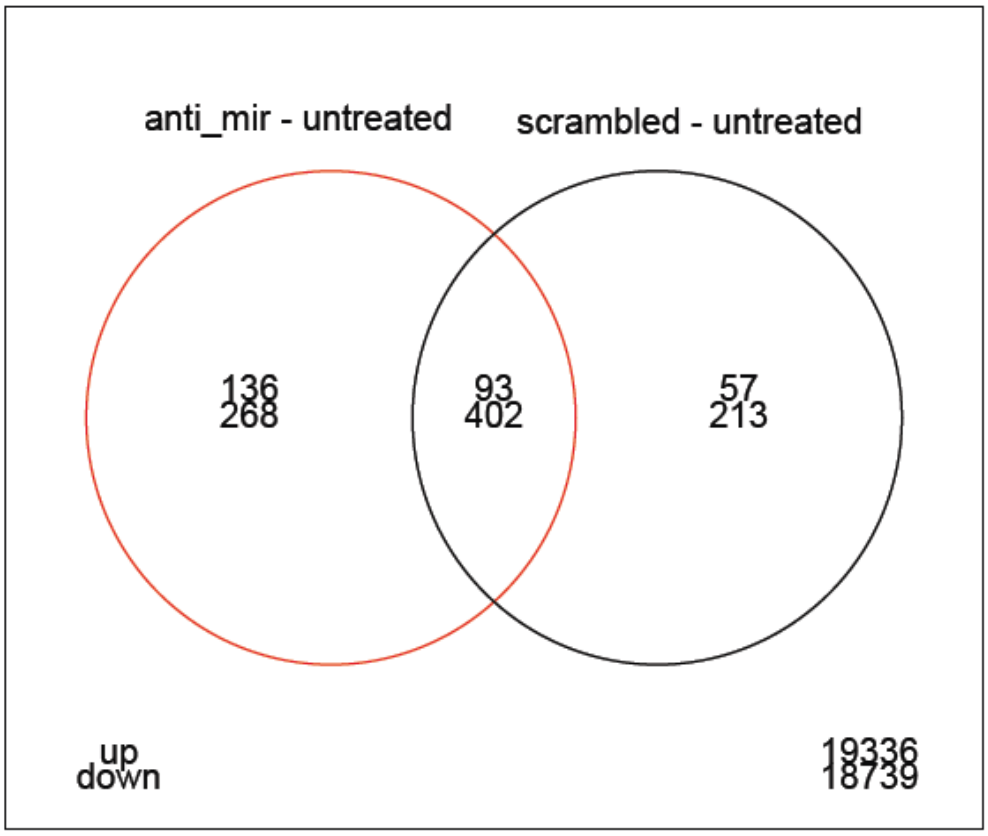

Figure 2.8: Venn diagram of differentially expressed genes identified in microarray data analysis.

Anti-21 or anti-ctr (scrambled) treated samples were compared to untreated MCF-7 cells. After elimination of off-target effects (scrambled oligonucleotide or anti-ctr), 136 upregulated and 268 downregulated genes were identified as anti-21-specific differentially expressed genes.

Category	Function	Function Annotation	P-value	Molecules	#Molecules
Cellular Movement	migration	migration of breast cancer cell lines	4.17E-02	GFBP3,ITGB5,NRP1,PLAUR,PTK2, SERPINE1, VEGFA	7
Cellular Movement	migration	migration of cancer cells	1.16E-01	TGB5,NRP1,S100A2, VEGFA	4
Cellular Movement	cell movement	cell movement of cell lines	9.79E-02	ADM,BMP7, FOS,ITGB5,NRP1,PLAUR, PTK2, SERPINE1, SOCS2,STARD13,TP63, VEGFA	12
Cellular Movement	movement	movement of breast cancer cell lines	4.17E-02	GFBP3,ITGB5,NRP1,PLAUR,PTK2, SERPINE1, VEGFA	7
Cellular Movement	movement	movement of cancer cells	1.16E-01	TGB5,NRP1,S100A2, VEGFA	4
Cellular Movement	invasion	invasion of tumor cells	1.16E-01	AKT2,BTC,PLAUR,PTK2	4
Cellular Movement	invasion	invasion of cancer cells	1.16E-01	AKT2,PLAUR,PTK2	3
Cell Morphology	morphology	morphology of breast cancer cell lines	1.16E-01	ADM,FOS,SMARCE1	3
Cancer	apoptosis	apoptosis of tumor cell lines	4.15E-02	ADM,AKT2,BCL2L1, BMP7, CSNK1A1, DDIT4,FGFR2,FOS,HIPK2,IGFBP3,ITGB5,ITPK1, MAPT, MXD1,NRP1,PARVA, PLAUR, PLK2, PPID, PTK2, RASD1, SMARCE1, SRPX, TNFRSF25,TP63, VEGFA, ZFYVE16	27
Cancer	apoptosis	apoptosis of breast cancer cell lines	1.01E-01	ADM,AKT2,BCL2L1, DDIT4,IGFBP3,PLK2, SMARCE1,TNFRSF25,TP63	9
Cancer	migration	migration of breast cancer cell lines	4.17E-02	GFBP3,ITGB5,NRP1,PLAUR,PTK2, SERPINE1, VEGFA	7
Cancer	movement	movement of breast cancer cell lines	4.17E-02	GFBP3,ITGB5,NRP1,PLAUR,PTK2, SERPINE1, VEGFA	7
Cancer	proliferation	proliferation of breast cancer cell lines	1.15E-01	BMP7,BTC,FOS,IGFBP3,PTPRG,SERPINE1,VEGFA	7
Cancer	morphology	morphology of breast cancer cell lines	1.16E-01	ADM,FOS,SMARCE1	3
Cancer	attachment	attachment of breast cancer cell lines	1.16E-01	PLAUR,SERPINE1	2
Cell Death	apoptosis	apoptosis of breast cancer cell lines	1.01E-01	ADM,AKT2,BCL2L1, DDIT4,IGFBP3,PLK2, SMARCE1,TNFRSF25,TP63	9
Cell Death	survival	survival of breast cancer cell lines	1.16E-01	AKT2,BCL2L1, ID4,IGFBP3	4
Cellular Growth and Proliferation	proliferation	proliferation of breast cancer cell lines	1.15E-01	BMP7,BTC,FOS,IGFBP3,PTPRG,SERPINE1,VEGFA	7
Reproductive System Disease	migration	migration of breast cancer cell lines	4.17E-02	GFBP3,ITGB5,NRP1,PLAUR,PTK2, SERPINE1, VEGFA	7
Reproductive System Disease	movement	movement of breast cancer cell lines	4.17E-02	GFBP3,ITGB5,NRP1,PLAUR,PTK2, SERPINE1, VEGFA	7
Reproductive System Disease	cell death	cell death of breast cancer cell lines	4.52E-02	ADM,AKT2,BCL2L1, DDIT4,IGFBP3,PLK2, PPID, SMARCE1,TNFRSF25,TP63,VEGFA	11
Cell-To-Cell Signaling and Interaction	binding	binding of breast cancer cell lines	1.16E-01	GFBP3,ITGB5,SERPINE1	3
Cell-To-Cell Signaling and Interaction	attachment	attachment of breast cancer cell lines	1.16E-01	PLAUR,SERPINE1	2
Gene Expression	transcription	transcription of p63 response element	1.16E-01	TP63	1
Tumor Morphology	development	development of breast carcinoma	1.16E-01	TBX2,VEGFA	2

Table 2-7: GO enrichment of differentially expressed genes (up/down) identified in microarray

2.3.4. The JAK-STAT pathway is sensitive to mir-21 levels

To identify pathways sensitive to mir-21 dosage, KEGG pathway analysis of differentially expressed genes identified in microarray analysis was performed. A significant enrichment of eight downregulated genes related to the JAK-STAT signaling pathway was detected (AKT2, BCL2L1, IFNAR, IL-20, JAK1, JAK2, SOCS2 and SOS1) **(Figure 2.9)**. Seven of these genes (all except SOS1) showed significant decreases ranging from 15 to 80 % of mRNA levels in the cells depleted for mir-21 compared to anti-ctr treated cells, all of which were validated by quantitative real time PCR analysis (qRT-PCR). **(Figure 2.10)**.

In addition, JAK1 showed decreased protein levels in anti-21 transfected cells depleted in mir-21 and increased protein levels in pc-21 transfected cells overexpressing mir-21, both compared to corresponding controls (anti-ctr and pcDNA) **(Figure 2.11)**. BCL2L1 showed decreased protein levels in anti-21 transfected cells compared to anti-ctr transfected MCF-7 cells **(Figure 2.11)**. No detectable results were obtained for BCL2L1 western blot in pc-21 or pcDNA transfected samples.

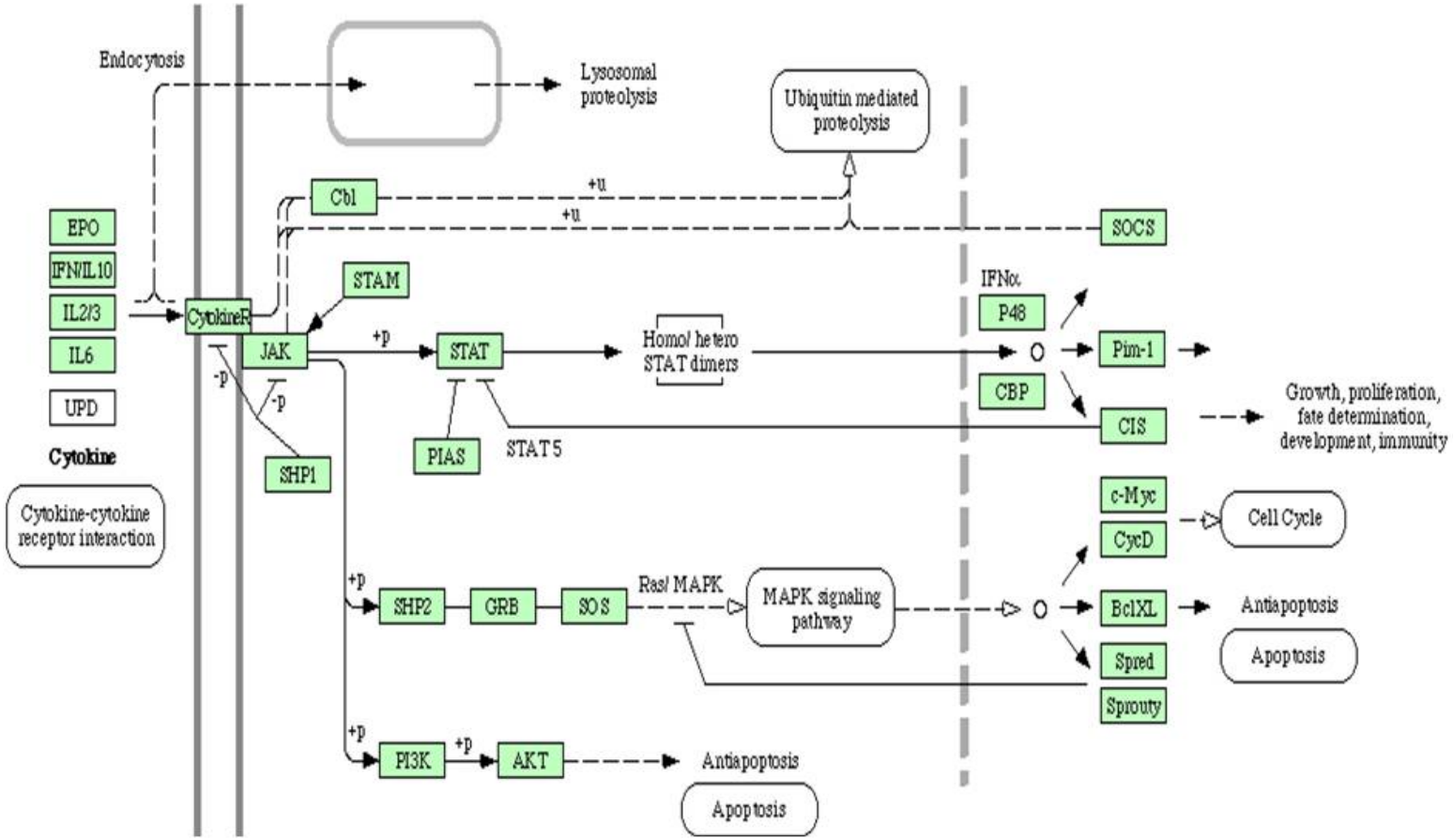

Figure 2.9: JAK-STAT pathway (KEGG).

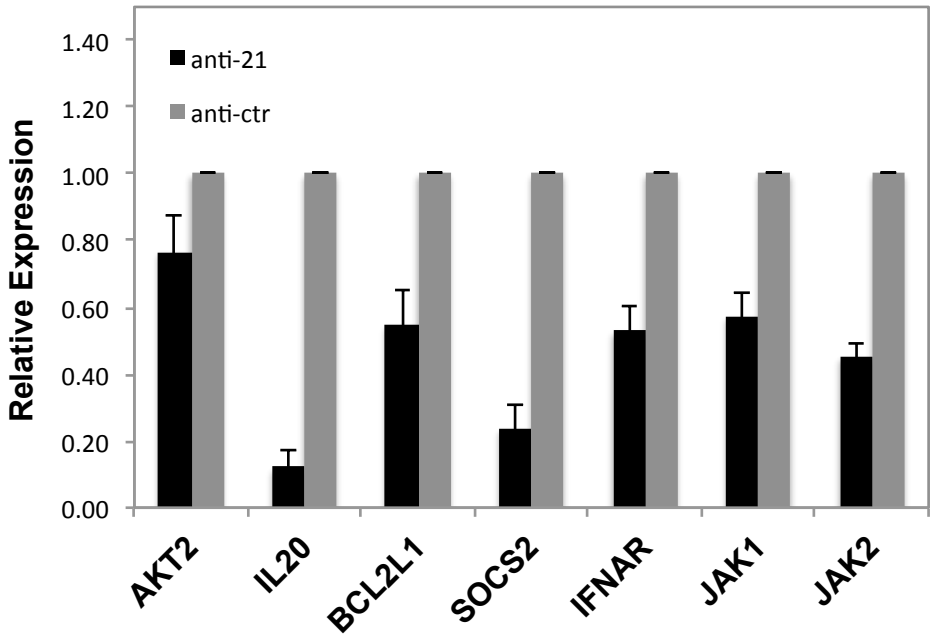

Figure 2.10: qRT-PCR validation of seven downregulated JAK-STAT pathway genes.

Quantitative RT-PCR (qRT-PCR) analysis confirms seven genes involved in the JAK-STAT pathway are downregulated. Relative fold changes (±SD) were normalized to housekeeping control (GAPDH) and compared to anti-ctr (set to one).

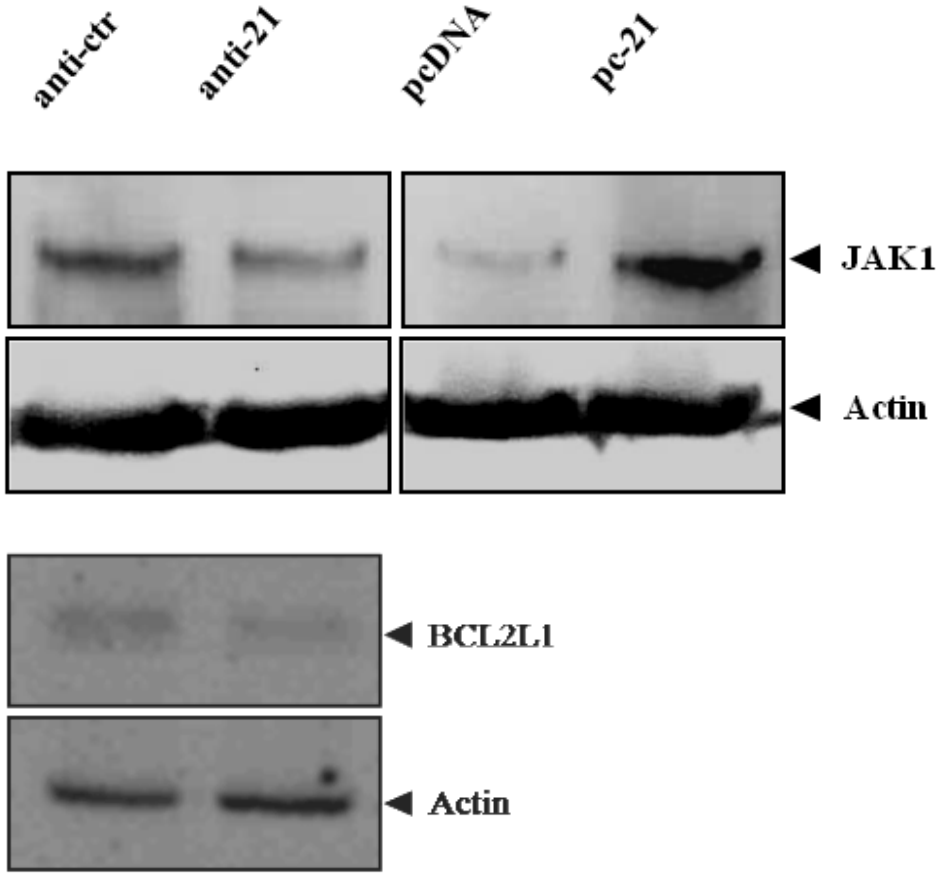

Figure 2.11: JAK1 and BCL2L1 protein levels are positively correlated with mir-21 dosage.

Western blotting of total protein levels of JAK1 and BCL2L1 in MCF-7 cells treated with anti-21, pc-21 or controls as showed. Actin was used as a loading control (lower lanes).

2.3.5. Mir-21 and STAT3 mRNA levels show positive correlation

To investigate how mir-21 communicates with the JAK-STAT pathway, a predicted miRNA target search was performed using available online prediction tools (TargetScan, MiRanda and PicTar). Amongst the components of the JAK-STAT pathway that were detected to be downregulated after anti-21 treatment, none were listed as predicted targets using these miRNA prediction algorithms. Although STAT3 had not been identified as a differentially expressed gene by microarray analysis, TargetScan predicted it to be a target of mir-21 with two putative sites in its 3'UTR **(Figure 2.12)**.

STAT3 is a well-known transcription factor that mediates the effects of interferons and other cytokines by combining signaling events at the cell surface to direct gene regulation [267]. It is constitutively activated (phosphorylated and overexpressed) in multiple human cancers including breast, ovarian, prostate, leukemia, and lymphoma [268, 269]. STAT3 plays a pivotal transcriptional role in cancer cell progression, differentiation, and survival by driving the expression of its target genes, including those that code for anti-apoptotic proteins such as Mcl-1 and BCL2L1, and the cell cycle regulators cyclin D1 and c-myc [270].

As a key transcription factor acting within the JAK-STAT pathway, STAT3 expression was tested by qRT-PCR analysis and found to be upregulated 2-6 fold in cells overexpressing mir-21 (pc-21) compared to mock cells (pcDNA) **(Figure 2.13)**. In addition, a positive correlation was observed also at the protein level. Western blot analysis of STAT3 in MCF-7 cells transfected with anti-21, pc-21 or controls (anti-ctr, pcDNA) showed decreased STAT3 protein in anti-21 transfected and increased STAT3 protein in pc-21 transfected cells compared to controls **(Figure 2.14)**.

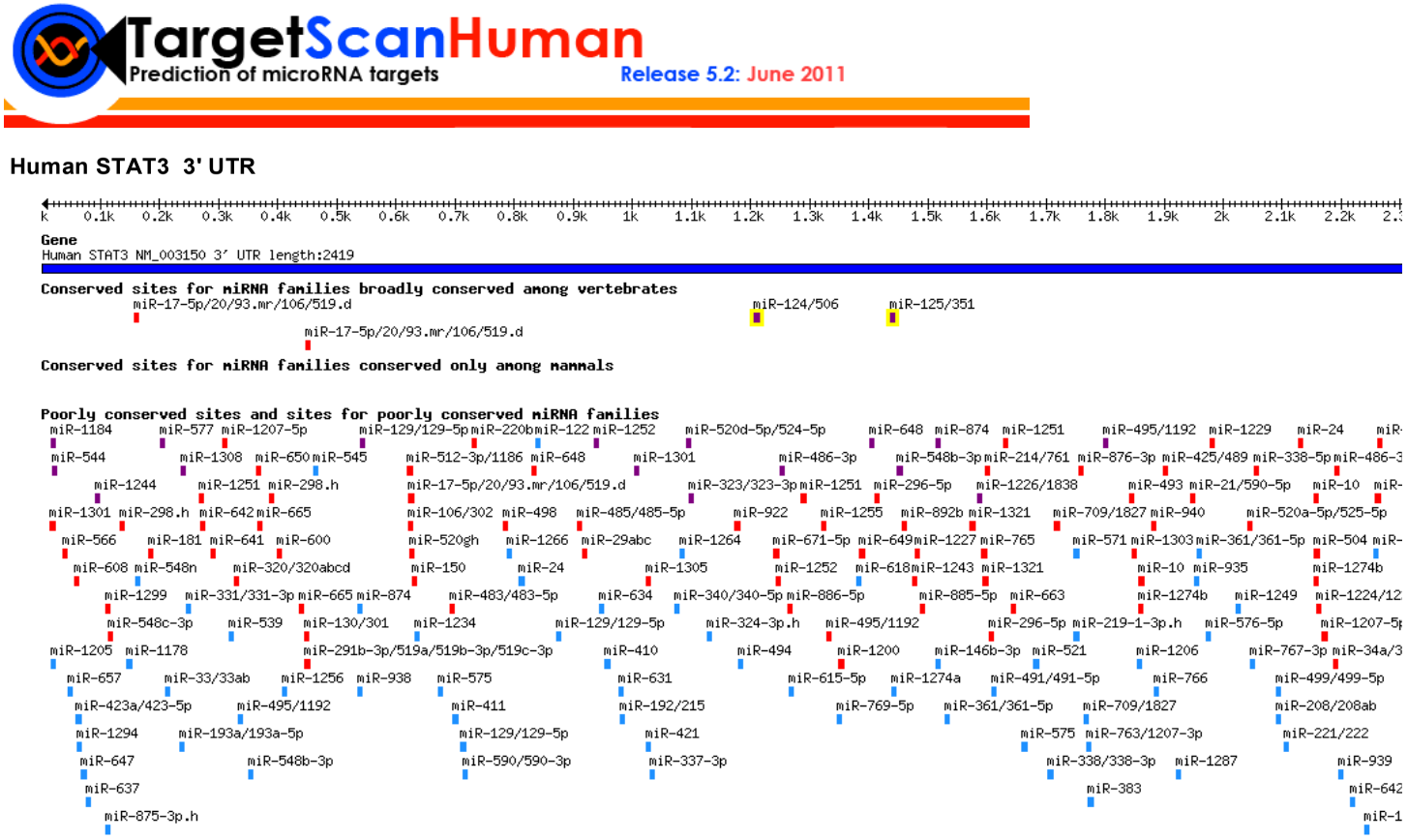

Figure 2.12: STAT3 3'UTR with predicted microRNA binding sites from TargetScan.

Two putative mir-21 binding sites are highlighted in boxes. Screenshot taken from www.targetscan.com

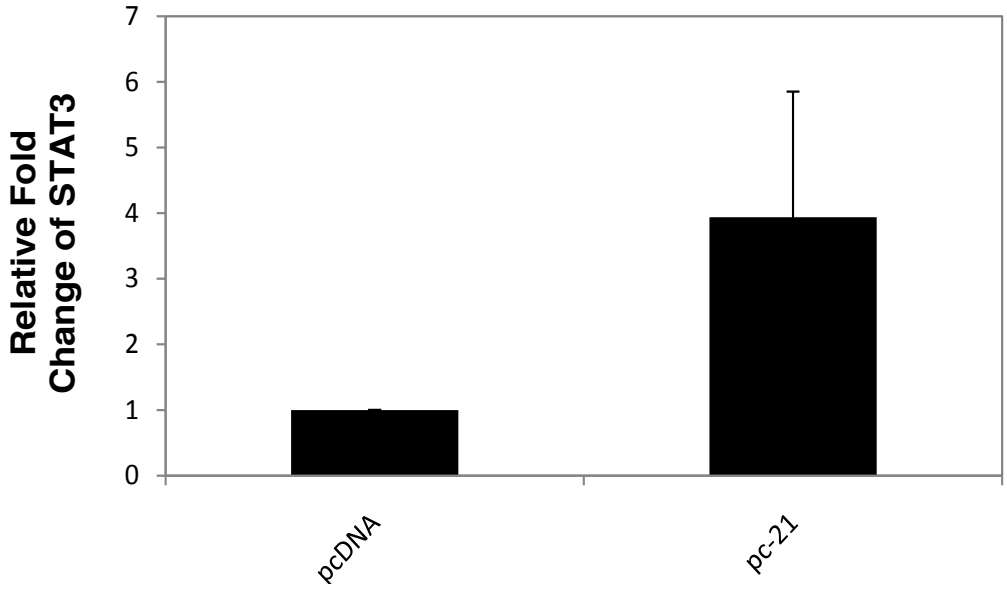

Figure 2.13: Mir-21 overexpression increases STAT3 mRNA levels
Quantitative RT-PCR (qRT-PCR) analysis of STAT3 shows positive correlation in mir-21 dosage and STAT3 expression. Graph represents relative fold change in STAT3 levels normalized to housekeeping gene GAPDH and compared to pcDNA empty vector control (set to 1).

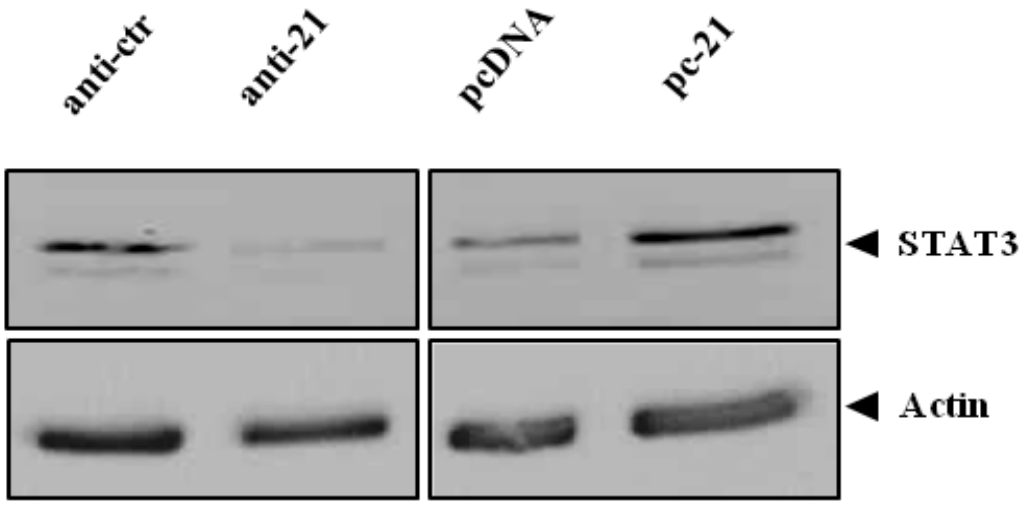

Figure 2.14: Mir-21 dosage positively correlates to STAT3 protein levels.

STAT3 protein levels determined by western blot analysis in MCF-7 cells as shown. Actin was used as loading control (lower lane).

2.3.6. IL-6 stimulation causes STAT3 Tyr-phosphorylation

STAT3 has recently been shown to regulate the expression of some microRNAs through binding to promoters such as that regulating the miR-17/92 gene cluster [271], and the promoters of mir-181b-1 and mir-21 [134]. This binding occurs in response to IL-6 mediated phosphorylation activation and in the case of mir-21, also in response to IFN stimulation [272]. IL-6-activated STAT3, which undergoes Tyr-phosphorylation, was found to induce mir-21 expression via two binding sites in the mir-21 promoter in hepatocellular carcinoma cells, including HepG2 [134]. A positive correlation between expression levels of STAT3 and miR-21 that also involves PTEN, AKT, NFKB and IL-6 has recently been reported [273]. Moreover, decreased STAT3 and p-STAT3 expression is observed in glioblastoma cells treated with anti-21 inhibitor or with taxol that blocks cell division and used in cancer treatments [274].

Since STAT3-mediated mir-21 induction has previously been reported from hepatocellular carcinoma cells [29], STAT3 phosphorylation via IL-6 stimulation was tested in HepG2 cells. Consistent with previous reports, a time-course of IL-6 treatment in HepG2 cells showed Tyr705 phosphorylation of STAT3 after just five minutes when compared to untreated controls **(Figure 2.15)**. On the other hand, non-phosphorylated STAT3 levels showed no significant change after 5 min, 1hr, 4hr or even 24 hr of IL-6 treatment **(Figure 2.15)**. After 48hr and 72hr of IL-6 treatment, STAT3 phosphorylation was maintained whilst non-phosphorylated STAT3 protein levels showed a slight increase in the presence of IL-6 **(Figure 2.15)**.

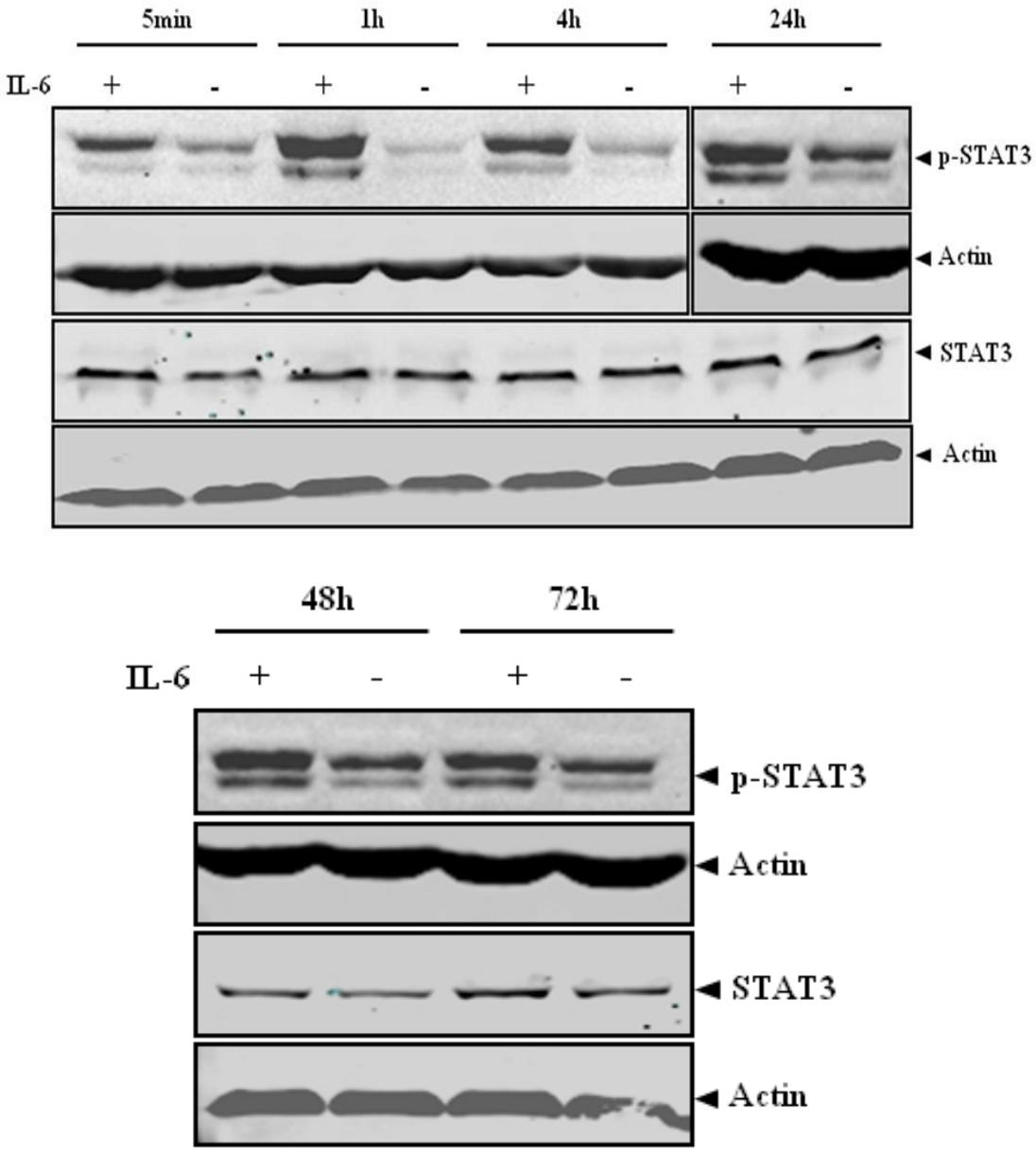

Figure 2.15: IL-6 phosphorylates STAT3.

Western blot analysis of p-STAT3 and STAT3 in HepG2 cells at different time points (5 min, 1hr, 4hr, 24hr, 48hr and 72hr) with IL-6 (5 ng/ml) or without IL-6 stimulation. Actin was used as loading control (lower lanes).

2.3.7. IL-6 stimulation causes mir-21 and STAT3 upregulation

To test the effects of IL-6 stimulation on mir-21 and STAT3 mRNA expression in HepG2 cells, IL-6 was added to cells that were harvested and endogenous/induced levels of mir-21 and STAT3 measured.

An increase in mir-21 expression was observed after 1hr of IL-6 stimulation, which continued to increase until the 48hr time point. Addition of IL-6 at the 48hr time point restored mir-21 levels by 72hr. In the absence of exogenous IL-6 treatment, mir-21 levels remained lower compared to treated cells **(Figure 2.16A)**.

Similarly, STAT3 expression was increased after 4hr and all later time points except that at 48hr, where mir-21 expression also showed no change. In the absence of exogenous IL-6 treatment, STAT3 expression showed no significant change **(Figure 2.16B).**

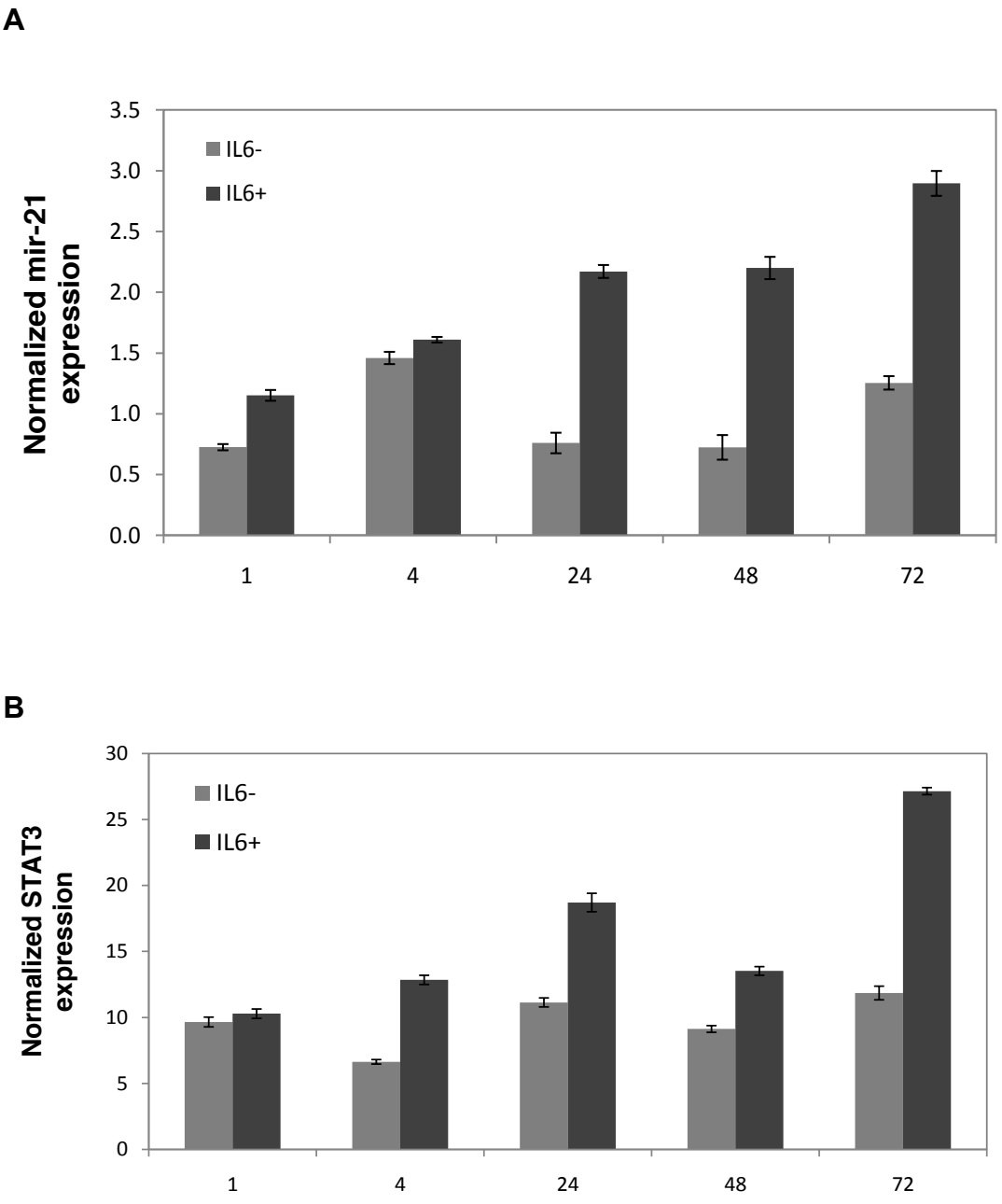

Figure 2.16: Mir-21 and STAT3 mRNA levels are induced by IL-6.

Time course qRT-PCR analysis shows induction of mir-21 and STAT3 mRNA induction by IL-6 (5 ng/ml). β-Actin was used in normalizations.

2.3.8. Mir-21 binds to putative sites in the STAT3 3'UTR

To test whether the two putative mir-21 binding sites in the STAT3 3'UTR are targeted by mir-21 or not, luciferase reporter constructs for the STAT3 3'UTR were generated and tested for luciferase gene expression in the presence or absence of IL-6. These constructs were designed so that each represents the full length wild-type STAT3 3'UTR (UTR) but with deletions of either the binding site 1 seed sequence (del1), binding site 2 seed sequence (del2) or both (del1/2).

In MCF-7 cells, the wild-type STAT3 3'UTR transfected samples showed a significant decrease (approximately 80 %) compared to pMIR empty vector control **(Figure 2.17A)** both in the presence or absence of IL-6. Luciferase expression was restored partially when the cells were transfected with deleted UTR constructs. For all of the del1, del2 and del1/2 transfected samples, luciferase expression was restored by approximately 20 % in the presence of IL-6 (IL-6+) whereas in the absence of IL-6 (IL-6-) this recovery rose 30%. Del1/2 transfected samples showed no change in luciferase expression in either the presence or absence of IL-6 **(Figure 2.17A).**

In HepG2 cells, the wild-type STAT3 3'UTR showed significantly decreased luciferase expression of approximately 50 % compared to pMIR empty vector control both in the presence and absence of IL-6 **(Figure 2.17B)**. In the presence of IL-6 (IL-6+), del1 and del2 transfected samples showed restoration of luciferase expression by approximately 20%, whereas the del1/2 transfected sample showed a slight decrease compared to the wild-type UTR transfected sample. On the other hand, in the absence of IL-6 (IL-6-) no significant change in luciferase expression was observed for del1 transfected sample while a slight decrease was observed for the del2 and del1/2 transfected samples **(Figure 2.17B)**.

A

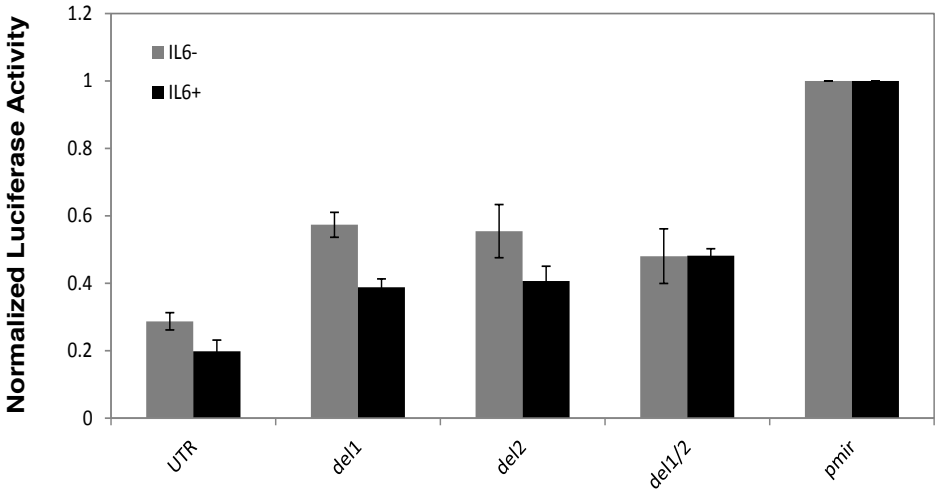

B

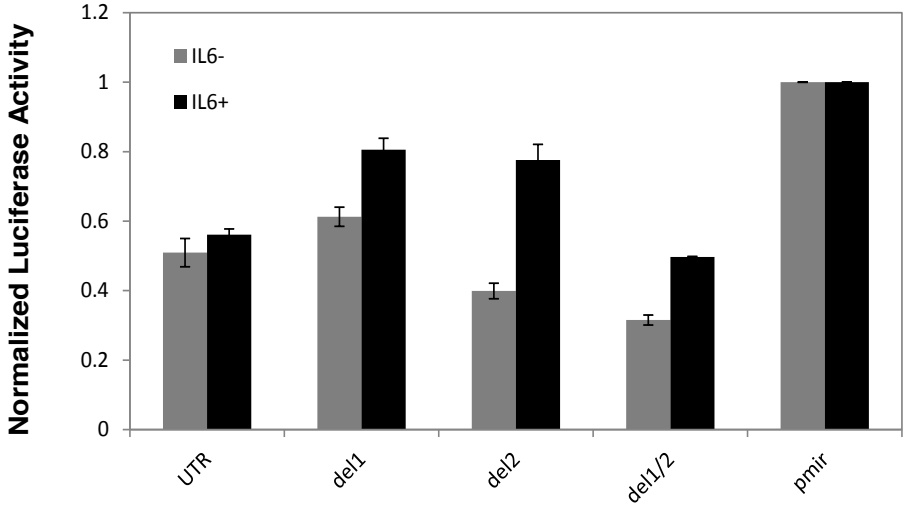

Figure 2.17: Mir-21 binding sites on STAT3 3'UTR are active.

Luciferase expression was detected in **A)** MCF-7 **B)** HepG2 cells transfected with pMIR-STAT3-UTR constructs showing response to perturbation of mir-21 binding sites in the presence or absence of IL-6 (5 ng/ml).

2.4. Discussion

Mir-21 has an oncogenic activity in cancer cells

The overexpression of mir-21 in many cancer types when compared to normal cells is well known. To test the effects of increased mir-21 dosage in MCF-7 cells, mir-21 overexpression was induced and cell proliferation analyzed. Cell proliferation was significantly increased in treated cells after 48 hours of mir-21 overexpression **(Figure 2.6)**. This is the first report to show that MCF-7 cells have the capacity to express higher levels of mir-21 without toxic effects and confirms the proliferative effect of increased mir-21 expression. On the other hand, consistent with previous studies, loss-of function (knockdown) studies for mir-21 showed decreased cell viability and increased caspase-7 activity, which indicates apoptosis in cancer cells **(Figure 2.7)**. These experiments confirmed the established proliferative activity of mir-21 and represented a positive control for the cell system used in this study prior to genome-wide studies.

Despite the overwhelming evidence of oncogenic activity of mir-21, the mechanism of how mir-21 regulates cancer pathways across the cell has not been fully described yet. This raises several questions such as whether mir-21 is solely an oncogenic microRNA (oncomir) selectively targeting tumor suppressors, or whether targeting mir-21 could potentially cause secondary effects due to altered activity of downstream pathways that are not intended therapeutic targets.

Mir-21 depletion downregulates JAK-STAT pathway

To test the wider effects of mir-21 depletion, microarray profiling was performed on MCF-7 cells. Analysis of these data compared to controls identified many differentially expressed genes relevant to cancer (GO, functional annotations) indicating direct or indirect involvement of mir-21 in cancer pathways. In addition to affects on individual genes, KEGG

pathway analysis identified the JAK-STAT pathway to be significantly downregulated in cells in which mir-21 was knocked down. Since the JAK-STAT pathway has previously been linked to cancer and this study has found it to be responsive to mir-21 depletion, the link between mir-21 and the JAK-STAT pathway was investigated further.

Eight downregulated genes were identified as associated with the JAK-STAT pathway (AKT2, BCL2L1, IFNAR1, IL20, JAK1, JAK2, SOCS2 and SOS1). All, except SOS1, were validated using qRT-PCR. This positive correlation between mir-21 and activity of the JAK-STAT pathway indicates an indirect regulation by mir-21, possibly via an intermediary target, with the assumption that miRNAs negatively regulated mRNA expression. Not to dismiss the possibility that mir-21 might be directly binding and upregulating these genes, as was previously reported in a few cases [275, 276], online target prediction programs were screened for possible direct binding sites. None of the genes encoding members of the pathway were listed as predicted targets using the algorithms available. Therefore, the possibility of mir-21 directly regulating a master regulator that then communicated to the JAK-STAT pathway was considered.

STAT3 plays a pivotal transcriptional role in cancer cell progression, differentiation, and survival by up-regulating genes, including those that encode for anti-apoptotic proteins such as Mcl-1 and Bcl-x_L, and the cell cycle regulators cyclin D1 and c-Myc [270]. Although IL20, IFNAR1, JAK1 and JAK2 are upstream effectors of STAT3 signalling, AKT2, SOCS2 and BCL2L1 are downstream targets of activated STAT3. STAT3 was identified as a predicted mir-21 target with two putative binding sites located in the 3'UTR. Moreover, IL-6-mediated STAT3 directed regulation of mir-21 has been reported [134] which could potentially indicate the existence of an autoregulatory loop between mir-21 and STAT3 if mir-21 can be shown to directly regulate STAT3 via its 3'UTR.

Mir-21 and STAT3 expression levels are positively correlated

The decrease observed in some of the JAK-STAT pathway genes that are downstream of STAT3 may make STAT3 one of the candidate intermediary targets of mir-21 to communicate to downstream members of the JAK-STAT pathway. STAT3-mediated mir-21 induction was previously reported in hepatocellular carcinoma cell lines which include HepG2. Therefore, subsequent experiments also made use of HepG2 cells.

First, STAT3 was confirmed to be phosphorylated by IL-6 in HepG2 cells at different time-points. STAT3 was phosphorylated after a few minutes of IL-6 stimulation indicating a rapid response and this phosphorylation was maintained until 72hr post-treatment. Non-phosphorylated STAT3 protein levels showed no change until 48 hr of IL-6 treatment. On the other hand, at 48hr and 72hr time-points, IL-6 stimulation caused a slight increase in STAT3 protein levels compared to untreated cells. This is also consistent with a report indicating that IL-6 directs unphosphorylated STAT3 (U-STAT3) accumulation in these cells [277] in addition to causing phosphorylation of STAT3.

Moreover, HepG2 cells were tested for mir-21 and STAT3 mRNA expression at the time-points at which IL-6 stimulation occurred. Consistent with previous findings [134, 273], mir-21 expression increased with IL-6 treatment until the 48hr time point when it stabilized. Following the addition of extra IL-6 to the system at the 48hr time point, mir-21 expression reached its highest levels at 72hr, confirming the effect is due to the activity of IL-6 **(Figure 2.16A)**. Without IL-6 treatment, mir-21 showed stable expression, which again indicates that induction of mir-21 is due to IL-6. Similarly, STAT3 expression gradually increased until the 48hr time-point when it showed a slight decrease; however, addition of extra IL-6 at 48hr led to restored STAT3 expression at 72hr indicating that IL-6 caused upregulation of STAT3 mRNA **(Figure 2.16B)**.

Overall, these results confirm that mir-21 and STAT3 have positive correlation of expression induced by IL-6 stimulation in HepG2 cells. In addition to IL-6-mediated STAT3 phosphorylation, a possible induction of STAT3 mRNA and protein expression by IL-6 stimulation was identified.

To test the possible relationship between mir-21 and STAT3 in more detail, mir-21 was overexpressed in MCF-7 cells using the pc-21 construct. Overexpression of mir-21 increased STAT3 mRNA levels. No differential expression of STAT3 had been identified by microarray which could be due to a short STAT3 mRNA half-life. Alternatively, STAT3 expression may be temporally regulation in a way that could not be detected at the time point at which the cells were harvested for microarray analysis.

Taken together, these findings indicate that there is a positive correlation between levels of mir-21 and STAT3 which are enhanced by, but not restricted to, IL-6 **(Figures 2.16-17)**.

Mir-21 communicates with STAT3 via putative mir-21 binding sites

To investigate whether the two putative mir-21 binding sites in the STAT3 3'UTR are active, luciferase reporter assays were performed in both HepG2 and MCF-7 cell lines. Four different constructs were generated such that they represent wild type STAT3 3'UTR (pMIR-STAT3^{UTR}), mir-21 binding site 1 inactivated (BS1 deleted; pMIR-STAT3$^{UTR\Delta1}$), mir-21 binding site 2 inactivated (BS2 deleted; pMIR-STAT3$^{UTR\Delta2}$) and mir-21 binding sites 1 and 2 inactivated (BS1/2 deleted; pMIR-STAT3$^{UTR\Delta1/2}$). These constructs allowed the identification of either individual or combinatorial effects of the two putative sites **(Figure 2.2)**. The luciferase expression in these constructs was investigated in the presence of IL-6.

In MCF-7 cells, deletion of either or both binding sites increased the target expression compared to wild type UTR construct. This indicates that the presence of mir-21 binding sites keeps the target expression suppressed.

In other words, mir-21 binds to both sites and downregulates the target expression. Presence of IL-6 caused more suppression of the target, possibly due to IL-6-mediated mir-21 induction. This was confirmed by treatment with the del1/2 construct in which mir-21 has no communication to the UTR, which showed no difference between presence and absence of IL-6 **(Figure 2.17A).**

On the other hand, in HepG2 cells, only del1 and del2 constructs restored the target expression to certain levels, but a slight decrease in luciferase target expression was observed following treatment with the 1/2del construct. These results may indicate that mir-21 binding to these sites requires a certain context or molecular signature depending on the cell type. So, absence of both mir-21 binding sites may have different effects on target expression in different cell lines. Similar to the results obtained in MCF-7, target expression showed similar profiles in the absence of IL-6 as in IL-6 presence but the target expression was more suppressed, probably due to increased mir-21 expression and increased binding potential **(Figure 2.17B)**.

To sum up, luciferase assay results showed that mir-21, when it binds to two putative sites of the STAT3 3'UTR, limits the expression of the target. This may indicate the presence of a feedback loop. Taken together with the positive correlation between the levels of miR-21 and STAT3 observed in gain-of function experiments, these data indicate a complex relationship that may involve an oscillatory temporal regulation of mir-21 and STAT3. Indeed, a recent study on mir-21 and STAT3 identified a positive feedback loop that involves PTEN, AKT, NFkB and IL-6 [278]. The activation of STAT3 by IL-6 induced mir-21 expression which lead to PTEN inhibition. This lead to increased NF-kB activity which is required to maintaine this transformed state [278]. Therefore, the dominance of this positive feed-back loop can lead to increased STAT3 levels upon mir-21 overexpression. On the other hand, the direct communication of mir-21 and STAT3 via 3'UTR targeting shown here can be the mechanism less prominent and act as the fine-tuning of STAT3 and mir-21 levels whilst the

positive feed-back loop keeps the STAT3 and therefore mir-21 levels high to maintain the transformed state in cancer cells.

Based on these experiments, the results indicate that the putative mir-21 binding sites in the STAT3 3'UTR are active and limit STAT3 expression, especially in the presence of IL-6. Although there is no strong evidence obtained to indicate a linear relationship between mir-21 and STAT3 expression levels, mir-21 and STAT3 are in communication and STAT3 respond to mir-21 dosage changes positively. This communication should be investigated further in detail to identify the regulatory rules and speculate a model loop that could be a potential therapeutic target.

CHAPTER 3: Interplay between 17-beta-Estradiol (E2), mir-21 and JAG1 in breast cancer cells

3.1. Background: JAG1 functions in cancer

The JAG1 gene encodes a ligand important for the Notch intercellular signaling pathway and for angiogenesis [279]. Notch signaling is important for development and tissue homeostasis and is activated in many human cancers and key in maintaining the homeostasis of stem cells and progenitor cells [280]. Mutations in JAG1 gene have been linked to Alagille syndrome in many studies [281-283] and it has been studied as a therapeutic target for MS (Multiple Sclerosis) [284]. JAG1 is also reported to be involved in EMT (epithelial mesenchymal transition) induced by TGF-B in epithelial cells [285]. JAG1 is expressed throughout embryonic development in tissues such as the nervous system as well as in cancer cells and has been identified as an evolutionarily conserved target of the WNT/ß-catenin signaling pathway [280] [286].

JAG1 is one of the genes that contain putative binding sites for mir-21 as predicted by many online tools such as TargetScan, PicTar and MiRanda. JAG1 is downregulated by mir-34a and mir-21 at the protein level in human monocyte-derived dendritic cells (MDDC), which regulates their differentiation [287]. In contrast to this post-transcriptional repression effect, an increase in JAG1 mRNA levels has been also reported during MDDC differentiation, which suggests the hypothesis that high expression levels of JAG1 could be required for maintaining MDDC differentiation where microRNAs are post-transcriptionally regulating JAG1 protein levels to provide a balanced expression of JAG1 for proper functioning. The lack of association between JAG1 mRNA and protein has been described [288].

3.1.1. Aim

Downregulation of JAG1 has been shown to occur in human mesenchymal stem cells (hMSCs) that are induced to differentiate into neural cells [289]. Also in *in vitro-in vivo* model of E2-induced (Estradiol)

transformed MCF-10F cells JAG1 was downregulated compared to the parental cell line [290]. In contrast, high levels of JAG1 were observed in oral squamous cell carcinoma cells [291] and its levels are associated with poor prognosis in breast cancer samples [292, 293], as well as with high tumor grade, and with ER and PR negativity [288]. Similarly, a recent study on breast cancer cell lines showed that triple negative (ER/PR/Her minus) cell lines (i.e. MDA-MB-231) showed higher expression of JAG1 compared to ER+ cell lines such as MCF-7 and T47D which indicates that, in the absence of ER/PR/Her stimulation, activation of Notch signaling by JAG1 promotes growth [294]. On the other hand, in a cDNA microarray study, MCF-7 cells treated with 17-beta-Estradiol showed upregulation of JAG1 mRNA [295]. In contrast, mir-21 is found to be downregulated by 17-beta-Estradiol (E2) via promoter binding in MCF-7 cells [252] although a contradictory finding exists [296]. Taken together, these studies indicate that JAG1 and mir-21 expression levels may be affected by estrogen signaling (via E2 stimulation) in opposite directions and that both JAG1 and mir-21 levels are variable in cells depending on ER status of the cells.

Therefore, in this chapter the aim is to investigate and compare the interaction between mir-21 and JAG1 in ER+ and ER- breast cancer cell lines (MCF-7 and MDA-MB-231, respectively) to clarify the effects of estrogen signaling (17-beta-Estradiol) on this interaction.

3.2. Materials and Methods

3.2.1. Tissue culture and reagents

Human breast cancer cell line MCF-7 and lung cancer cell line and MDA-MB-231 (obtained from Dr. Howard Fearnhead's lab, NCBES, NUIG) were cultured as described before in **section 2.2.1.** For 17-Beta-Estradiol (E2) treatments (Sigma, USA, #E2758), cells were maintained in DMEM without phenol red, supplemented with 5% charcoal stripped FBS (Sigma, UK, #F6765). Cells were treated with 17-Beta-Estradiol (resuspended in ethanol) to a final concentration of 10 nM or with absolute EtOH as control. At 24hr post-treatment cells were harvested. Cells were maintained as previously described in **section 2.2.1.**

3.2.2. JAG1 3'UTR reporter constructs and luciferase assay

The 3'UTR region (632 bp) harbouring the mir-21 binding sites as well as several other miRNA binding sites was amplified from human genomic DNA by PCR **(primers: A.4.1.)**. This region was selected to minimise the number of predicted miRNA binding sites to allow the other miRNA binding sites to be eliminated so that the individual effect of mir-21 binding on JAG1 3'UTR regulation could be identified in isolation. Amplified PCR product was directly cloned into SpeI/HindIII restriction sites located in the pMIR-REPORT luciferase vector and designated as pMIR/JAG1-UTR **(protocol: A.3.3.)**. Mutated construct lacking the mir-21 seed region was cloned using Quikchange II SDM kit (Agilent Technologies, USA.) and designated as pMIR/JAG1-UTRdel **(primers: A.4.1.)**. Constructs were confirmed by sequencing and purified using the midiprep plasmid purification kit. Luciferase assays and data analysis were performed as described in **section 2.2.9**.

3.2.3. Transfections and RNA isolation

For luciferase experiments, MCF-7 and MDA-MB-231 cells were co-transfected with 300ng of each plasmid (pMIR/JAG1-UTR or pMIR/JAG1-UTRdel) and 1 ng of renilla vector using Lipofectamine 2000 reagent in 24-well tissue culture plates **(protocol: A.3.10.)**. For qRT-PCR analysis, cells were transfected with 50 nM anti-21 or anti-control oligonucleotides and 1ug of pcDNA-21 or pcDNA empty vector in 6-well tissue culture plates **(section 2.2.3.)**. 48hr post-transfection cells were harvested and total RNA was isolated using miRNA isolation kit according to manufacturer's instructions **(protocol: A.3.13.).** Quality of RNA was checked by 1% Agarose gel electrophoresis and quantified by NanoSpectrophotometer.

3.2.4. Quantitative RT-PCR

For quantitative PCR analysis of mir-21, Taqman assays were used as described in **section 2.2.7**. For quantitative PCR analysis of JAG1, 1ug of total RNA was reverse transcribed using the Revertaid H-minus first strand cDNA synthesis kit. SYBR Green-based detection was used in quantification of JAG1 mRNA, TFF mRNA (as E2 control) and Beta-Actin mRNA (as housekeeping control for normalization) as described in **section 2.2.8 (primers: A.4.2.)**. PCR was performed on the CFX96 system. Relative quantification results were generated automatically using the system software ($2^{-\Delta\Delta Ct}$ method).

3.2.5. Protein extraction and western blotting

Following treatments and transfections, cells were harvested and proteins were isolated as previously described in **section 2.2.12**. 30ug protein mixed with 6X protein loading buffer **(recipe: A.2.1.)**, heated at 95˚C for 5min, loaded into 10% SDS-PAGE and transferred into PVDF membrane

(Westran CS, #10485288, Whatman, UK) by wet transfer method **(protocol: A.3.12.)**. JAG1 (Jagged-1) primary antibody (rabbit, #sc-8303, Santa Cruz Biotechnology, USA) and Beta-Actin primary antibody (mouse, #A3854, Sigma, UK) were used in 1:1000 dilutions in 5% BSA in 0.1% TBS-Tween-20 overnight at 4°C with gentle rocking. Secondary antibodies, anti-rabbit (#A6667, Sigma, UK) and anti-mouse #A0168, Sigma, UK), were used in 1:10,000 dilution in 5% milk TBS-T for 2 hours at room temperature with gentle shaking. Blots were visualized with enhanced chemiluminescence (ECL Plus Kit, Perkin Elmer, USA, #NEL101001EA) using G:Box Chemi imaging system (Syngene, UK).

3.3. Results

3.3.1. The mir-21 binding site in JAG1 3'UTR is highly conserved and operational in MCF-7 cells

Using the online tools TargetScan, PicTar and MiRanda, the top scoring fifty predicted targets for mir-21 were identified. From these, JAG1 was selected for downstream analysis because all three programs predicted it and it was previously implicated in cancer [297] . Mir-21 has one predicted binding site in JAG1 3'UTR. The binding site contains the complementary 8-mer mir-21 seed region '*ATAAGCTA*'. The conservation of this sequence was tested using Multiple Sequence Alignment of 20 species **(Figure 3.1)**. This analysis showed that the seed region of mir-21 is highly conserved in all species tested except for one nucleotide mismatch in the 5' end of the seed region ('U' instead of 'A') in frog. (*Xenopus tropicalis*).

To determine if the JAG1 3'UTR is directly targeted by mir-21 via its putative binding site, a luciferase reporter assay was performed using the JAG1 3'UTR and mutated 3'UTR constructs, in both MCF-7 and MDA-MB-231 cells **(Figure 3.2)**. Luciferase activity was decreased in pMIR-JAG1-UTR-transfected MCF-7 cells compared to pMIR empty vector. This decrease might be due to combinatorial effects of all miRNAs that are expressed and have complementarity to the 3'UTR, or to other regulatory elements. The repression of the UTR was restored to levels close to those shown by pMIR empty vector when the cells were transfected with the construct lacking themir-21 binding site (PMIR/JAG1-UTRdel). This change was statistically significant compared to UTR construct (Student's t-test $p<0.05$). The restoration indicates a strong binding capacity and competitiveness of mir-21 on JAG1 3'UTR (at position 1233-1239 as predicted by TargetScan v5.1) in MCF-7 cells.

On the other hand, there was no repression effect observed on JAG1 3'UTR in MDA-MB-231 cells. The levels of luciferase activity remained similar in presence or absence of mir-21 seed region (PMIR/JAG1-UTR or PMIR/JAG1-UTRdel) which shows the inability of mir-21 in regulating JAG1 3'UTR in MDA-MB-231 cells in a context dependent manner **(Figure 3.3)**.

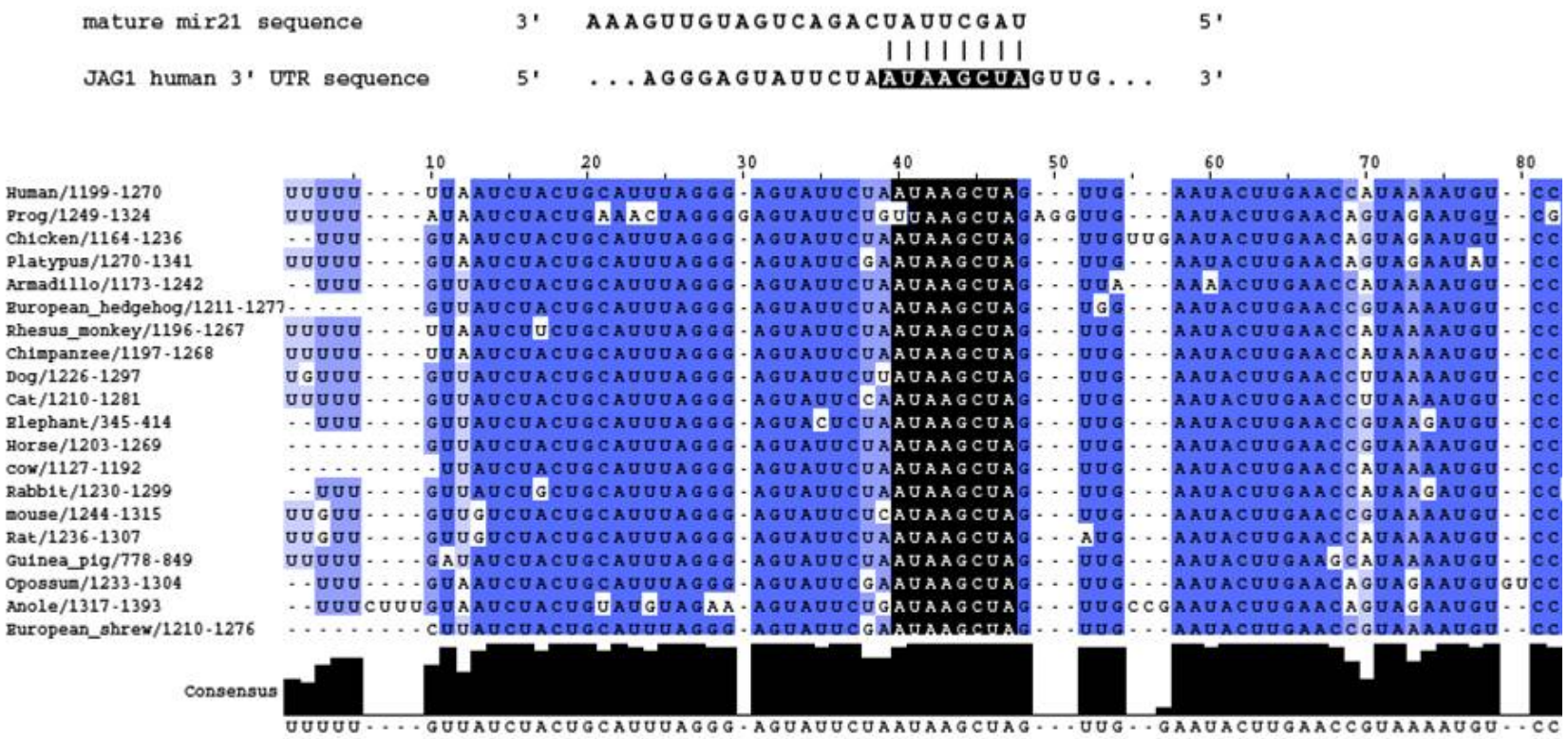

Figure 3.1: Multiple Sequence alignment of JAG1 UTR and mir-21 binding site in 20 species.

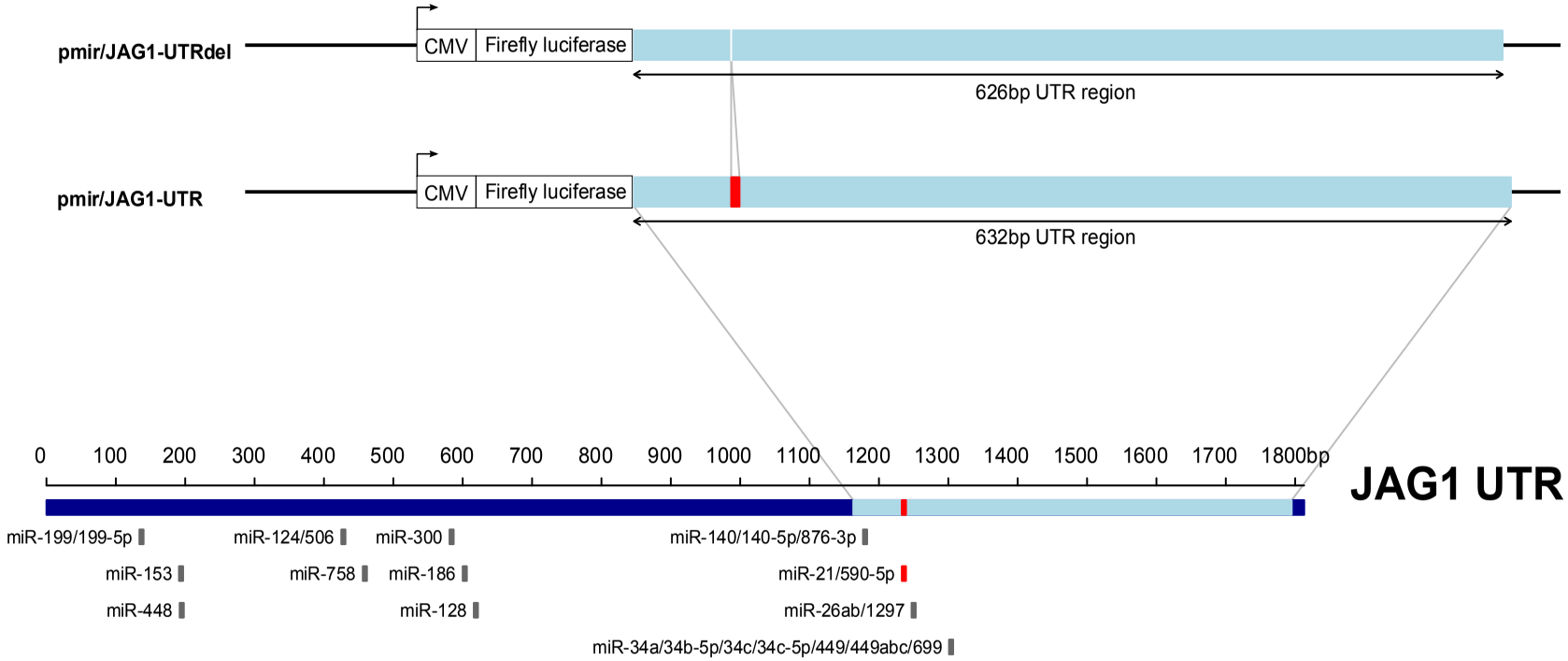

Figure 3.2: pMIR-JAG1-UTR constructs design.

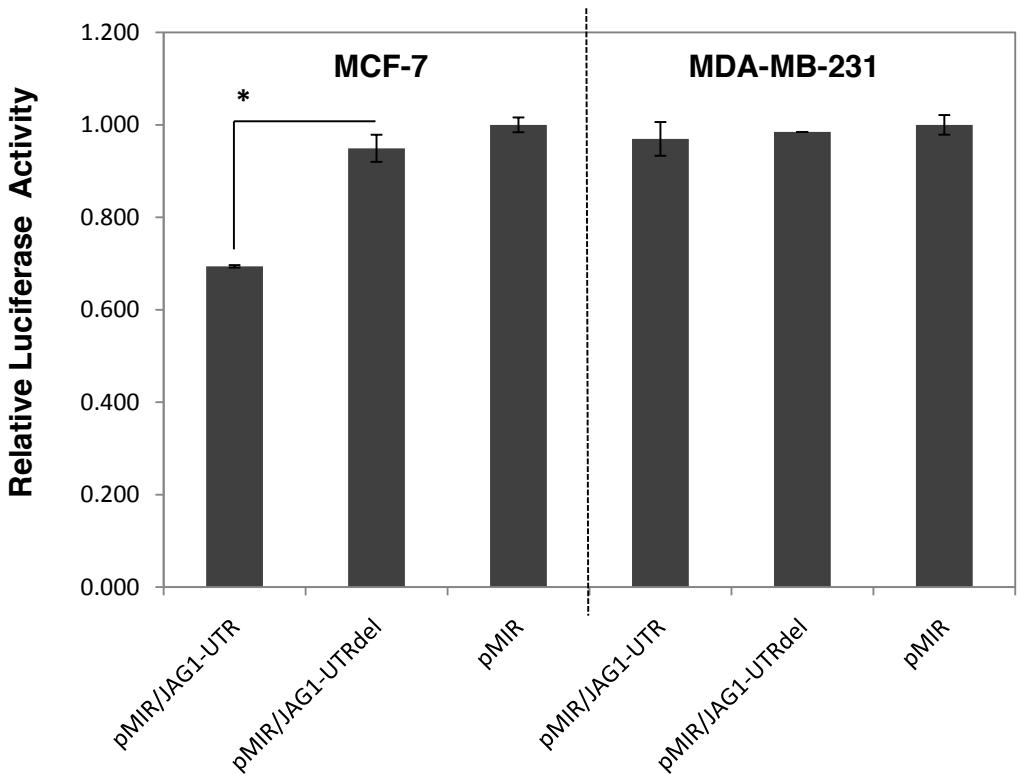

Figure 3.3: Luciferase activity is reduced in MCF-7 but not in MDA-MB-231.

Luciferase assay was performed for JAG1 3'UTR and JAG1-3'UTRdel transfected MCF-7 and MDA-MB-231 cells. Student's t-test analysis shows significant ($p<0.05$) downregulation in luciferase expression in Pmir/JAG1-UTR transfected MCF-7 cells.

3.3.2. Mir-21 and JAG1 expression levels are negatively correlated

To identify the relative levels of JAG1 in MCF-7 and MDA-MB-231 cells, qRT-PCR analysis was performed. GAPDH was used as a housekeeping control for normalization and results are represented relative to MCF-7 cells (set to 1). MDA-MB-231 cells showed less JAG1 expression (approximately half) compared to MCF-7 cells **(Figure 3.4)**.

To test whether mir-21 dosage correlates with JAG1 levels, the dosage of mir-21 in MCF-7 was decreased (by use of anti-21) and the dosage of mir-21 in MDA-MB-231 cells was increased (by use of pc-21). qRT-PCR analysis of JAG1 showed that in MCF-7 cells decreased mir-21 expression caused increased JAG1 levels compared to control (anti-ctr) **(Figure 3.5A)**. This effect was confirmed at protein level by western bloting **(Figure 3.5B)**. On the other hand, increased mir-21 expression in MDA-MB-231 cells by plasmid-based mir-21 overexpression (pc-21) led to decreased JAG1 expression compared to control (pcDNA) **(Figure 3.6)**.

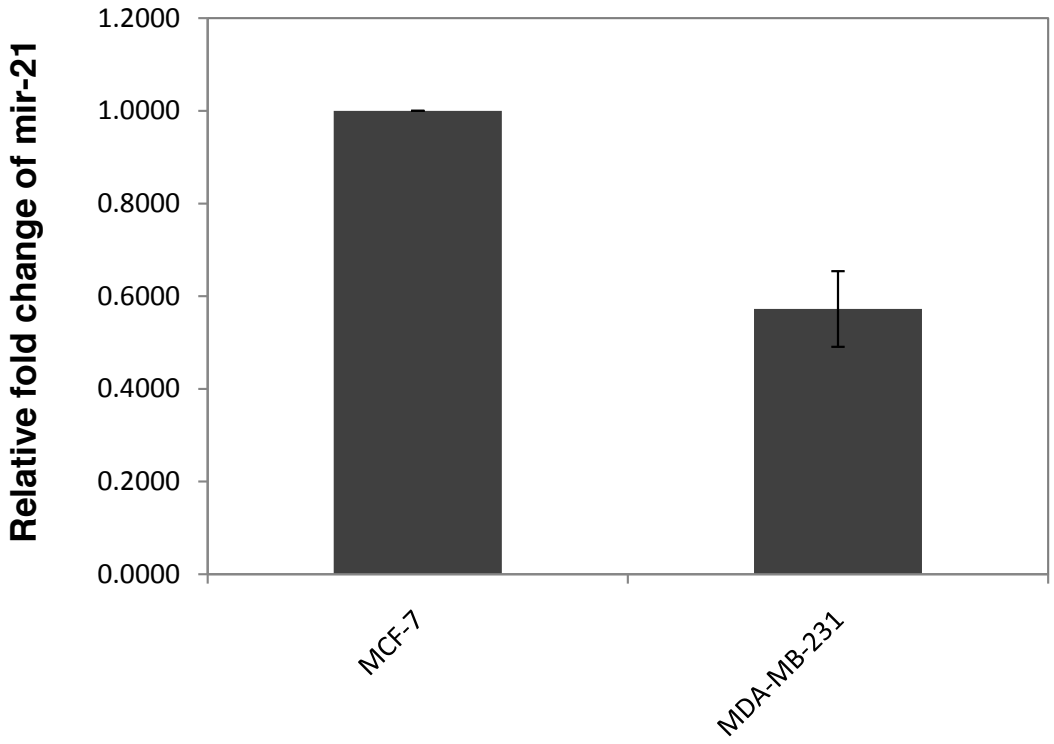

Figure 3.4: Mir-21 is expressed in lower levels in MDA-MB-231 compared to MCF-7.

qRT-PCR analysis of endogenous mir-21 expression is shown in MCF-7 and MDA-MB-231 cells. RNU6B was used as housekeeping control in data normalizations.

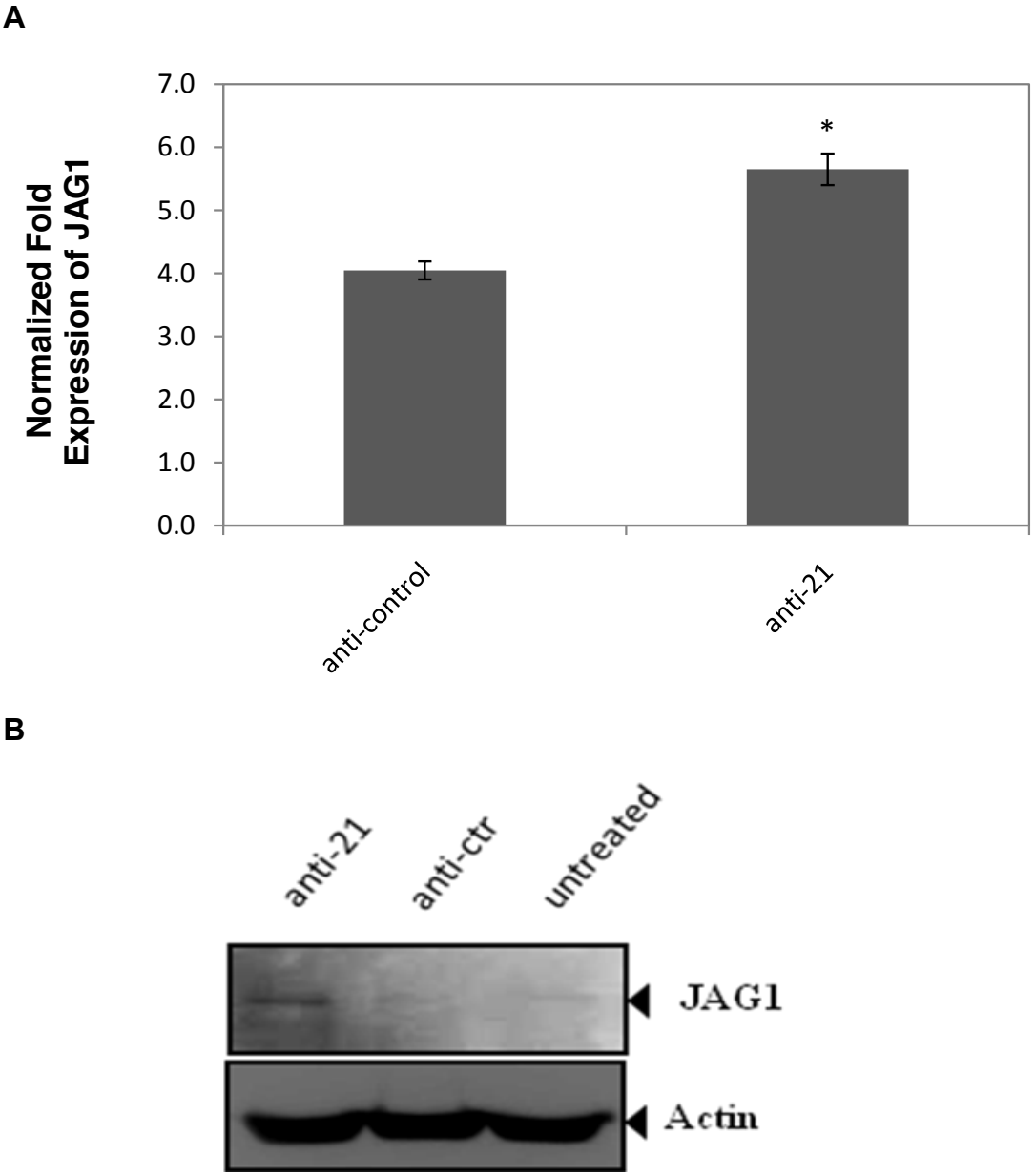

Figure 3.5: JAG1 mRNA and protein levels increase in mir-21 depleting MCF-7 cells.

A) qRT-PCR analysis of JAG1 **B)** western blotting analysis of JAG1 protein in anti-control or anti-21 treated MCF-7 cells are shown. Statistical analysis (student's t-test) showed significant upregulation of JAG1 mRNA expression in anti-21 treated cells compared to anti-control ($p<0.001$).

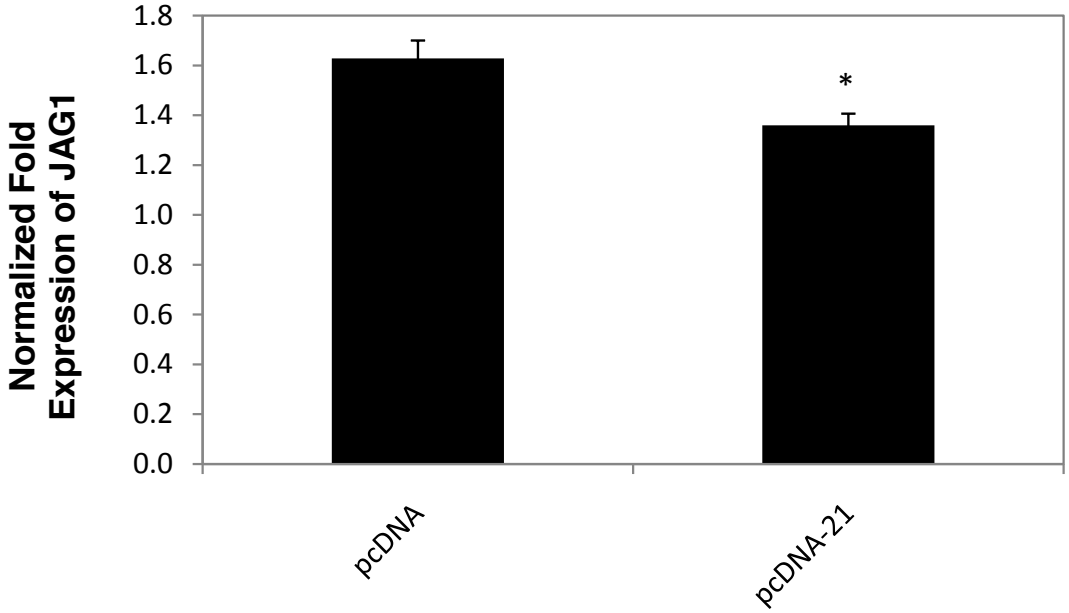

Figure 3.6: JAG1 mRNA levels decrease in mir-21 overexpressing MDA-MB-231 cells.

qRT-PCR analysis of in pc-21 or pcDNA treated MDA-MB-231 cells are shown. Statistical analysis (student's t-test) showed significant downregulation of JAG1 mRNA expression in pc-21 treated cells compared to pcDNA ($p<0.05$).

3.3.3. Mir-21 dosage interferes with JAG1 3'UTR targeting

To confirm that changes in JAG1 mRNA levels (which responded to mir-21 dosage) are due to enhanced or limited access of mir-21 to the binding sites on the JAG1 3'UTR, a luciferase assay was performed on MCF-7 and MDA-MB-231 cells expressing mir-21 in different dosages.

JAG1 UTR constructs (pMIR/JAG1-UTR or pMIR/JAG1-UTRdel or pMIR empty vector) were co-transfected with anti-21 (or anti-ctr) oligonucleotides in MCF-7 cells and pc-21 (or pcDNA control) in MDA-MB-231 cells to change the levels of mir-21 in each cell line in opposite directions. Luciferase assay was performed to test changes in target gene expression. In MCF-7 cells, knockdown of mir-21 (anti-21) slightly increased luciferase activity in pMIR/JAG1-UTR transfected cells compared to anti-ctr **(Figure 3.7)**. On the other hand, in MDA-MB-231 cells, compared to pcDNA empty vector control, overexpression of mir-21 (pc-21) significantly decreased the luciferase activity of pMIR/JAG1-UTR **(Figure 3.7)**.

Taken together, these results show that mir-21 dosage has an effect on JAG1 levels in MCF-7 and MDA-MB-231 cells. JAG1 targeting by mir-21 in MCF-7 cells can be perturbed by depleting mir-21 by anti-21 whereas mir-21 directed JAG1 regulation can be switched on in MDA-MB-231 cells by overexpressing mir-21 by pc-21.

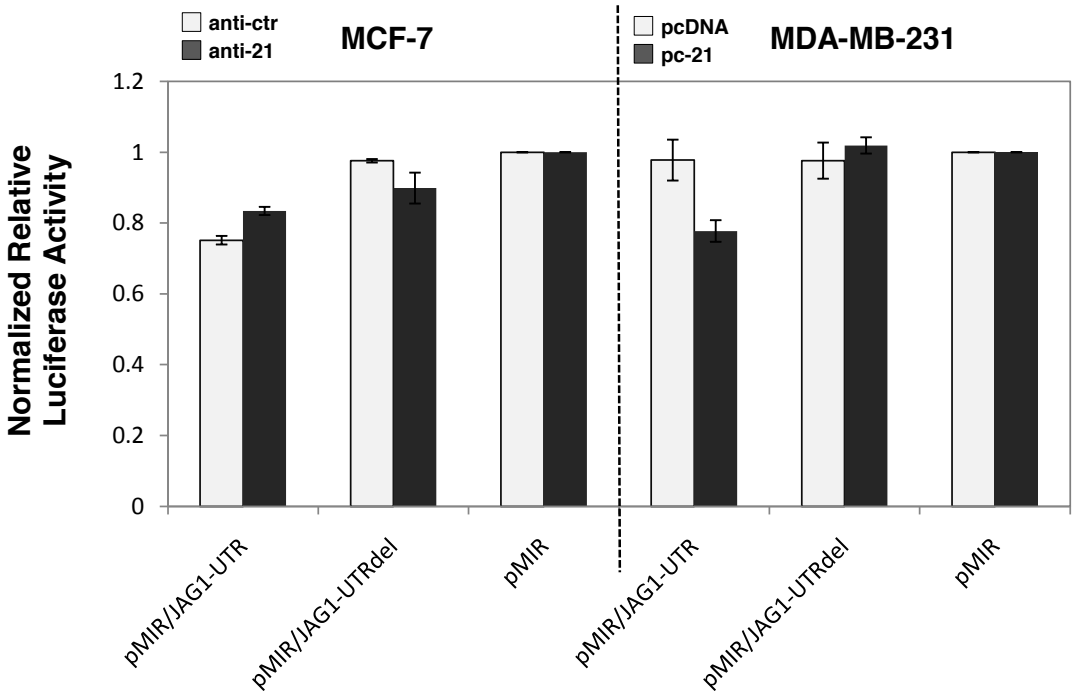

Figure 3.7: Mir-21 dosage determines mir-21/JAG1 interaction

Luciferase analysis of JAG1 3'UTR constructs in MCF-7 and MDA-MB-231 cells co-transfected with anti-21 or pc-21, respectively compared to controls show restored or suppressed luciferase expression.

3.3.4. Mir-21 and JAG1 expression levels display an inverse correlation in ER+ and ER- cells

To investigate whether E2 is involved in mir-21/JAG1 targeting, the levels of mir-21 and JAG1 in MCF-7 and MDA-MB-231 cells were tested by qRT-PCR performed before and after E2 treatment. The activity of E2 was tested and confirmed by qRT-PCR analysis of the estrogen-responsive biomarker TFF1. TFF1 was expressed in untreated MCF-7 cells and was undetectable in MDA-MB-231 cells. E2 treatment significantly increased TFF1 expression in MCF-7 cells whereas MDA-MB-231 cells were non-responsive **(Figure 3.8)**.

qRT-PCR analysis of mir-21 showed relatively low levels of mir-21 expression in untreated MDA-MB-231 cells compared to untreated MCF-7 cells (E2-) **(Figure 3.9).** Mir-21 expression in untreated MCF-7 and MDA-MB-231 cells was shown previously (**Figure 3.4**). E2 treatment significantly decreased mir-21 levels in MCF-7 cells (E2+) whereas MDA-MB-231 cells were again non-responsive **(Figure 3.9)**.

On the other hand, endogenous levels of JAG1 were relatively high in untreated MDA-MB-231 cells compared to untreated MCF-7 cells (E2-) **(Figure 3.10A)**. E2 treatment increased JAG1 levels significantly in MCF-7 as expected, whereas the ER- cell line MDA-MB-231 was not responsive to estrogen (E2+) **(Figure 3.10A)**. The response of JAG1 expression induced by Estradiol (E2) treatment in MCF-7 cells was also confirmed to be dosage-dependent at the protein level **(Figure 3.10B)**.

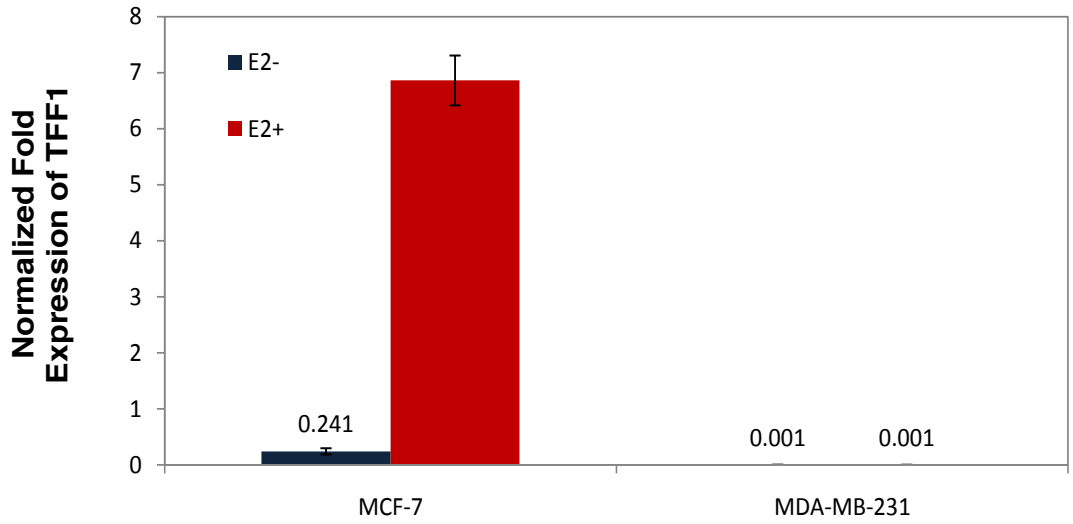

Figure 3.8: Estrogen marker TFF1 mRNA expression is induced in MCF-7 cells by Estradiol treatment.

qRT-PCR analysis of estrogen marker TFF1 is shown in MCF-7 and MDA-MB-231 cells treated with Estradiol (E2) (10 nM).

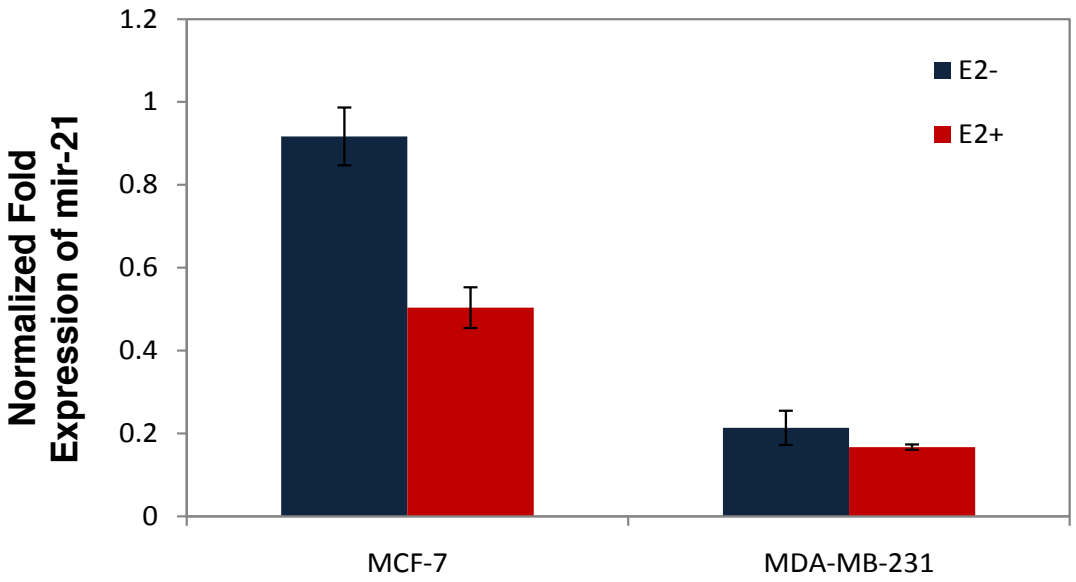

Figure 3.9: Mir-21 expression is suppressed by Estradiol treatment in MCF-7 cells

qRT-PCR analysis of mir-21 is shown in MCF-7 and MDA-MB-231 cells treated with Estradiol (E2) (10 nM).

A

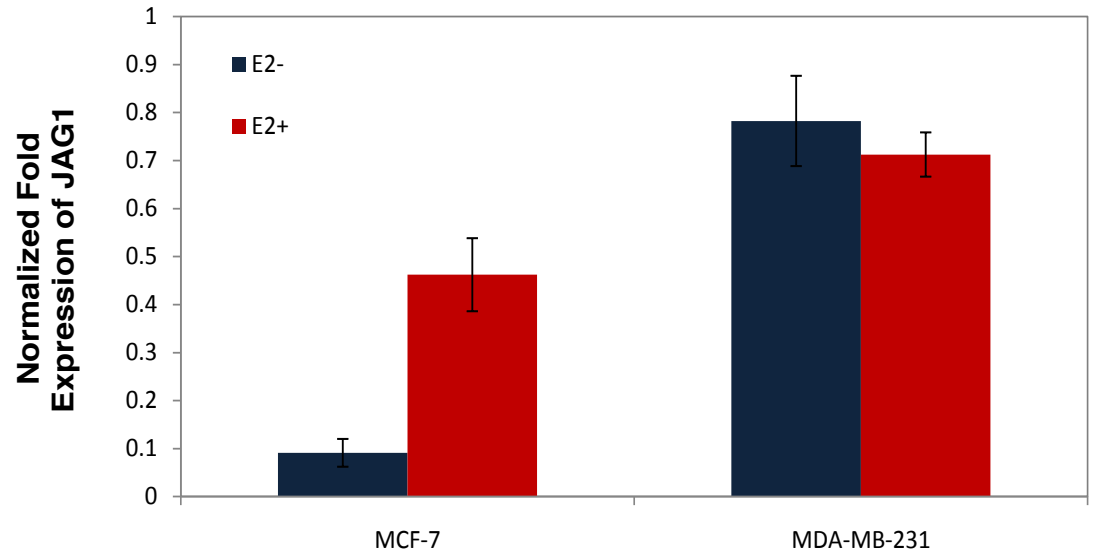

B

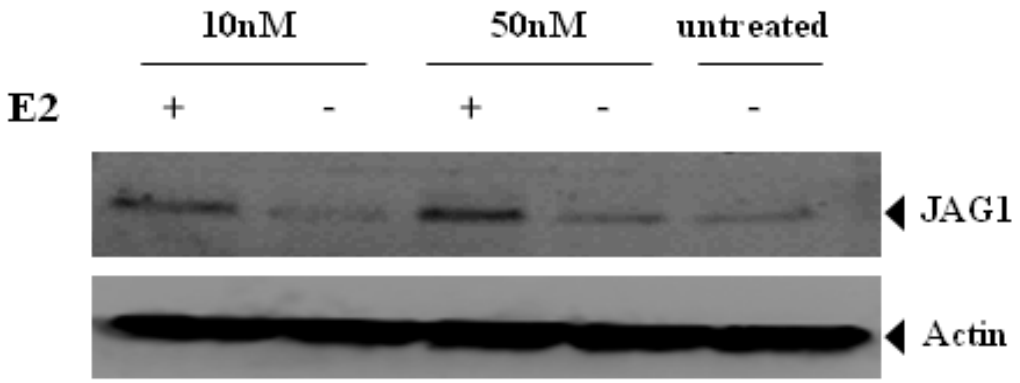

Figure 3.10: Expression of JAG1 mRNA and protein increases Estradiol treated MCF-7.

A) qRT-PCR analysis of JAG1 mRNA is shown in Estradiol treated (E2) MCF-7 and MDA-MB-231 cells and **B)** western blot analysis of JAG1 protein expression in MCF-7 cells treated with two dosages of E2 (10 nM and 50 nM). Actin was used as loading control (lower lane).

3.3.5. Estradiol interferes with mir-21 and JAG1 3'UTR targeting

To test whether E2 treatment enhances JAG1 expression due to decreased mir-21 expression and release of mir-21 binding from JAG1 3'UTR, luciferase assay was performed in cells treated with E2, or on untreated controls.

The results showed that, in MCF-7 cells in the absence of Estradiol (E2-), JAG1 3'UTR was suppressed compared to JAG1 3'UTRdel where mir-21 has no binding site **(Figure 3.11A)**. On the other hand, addition of E2 (E2+) in MCF-7 cells restored the suppression of the JAG1 3'UTR to similar levels seen for JAG1 3'UTRdel **(Figure 3.11A)**. For MDA-MB-231 the effect was not significant **(Figure 3.11B).**

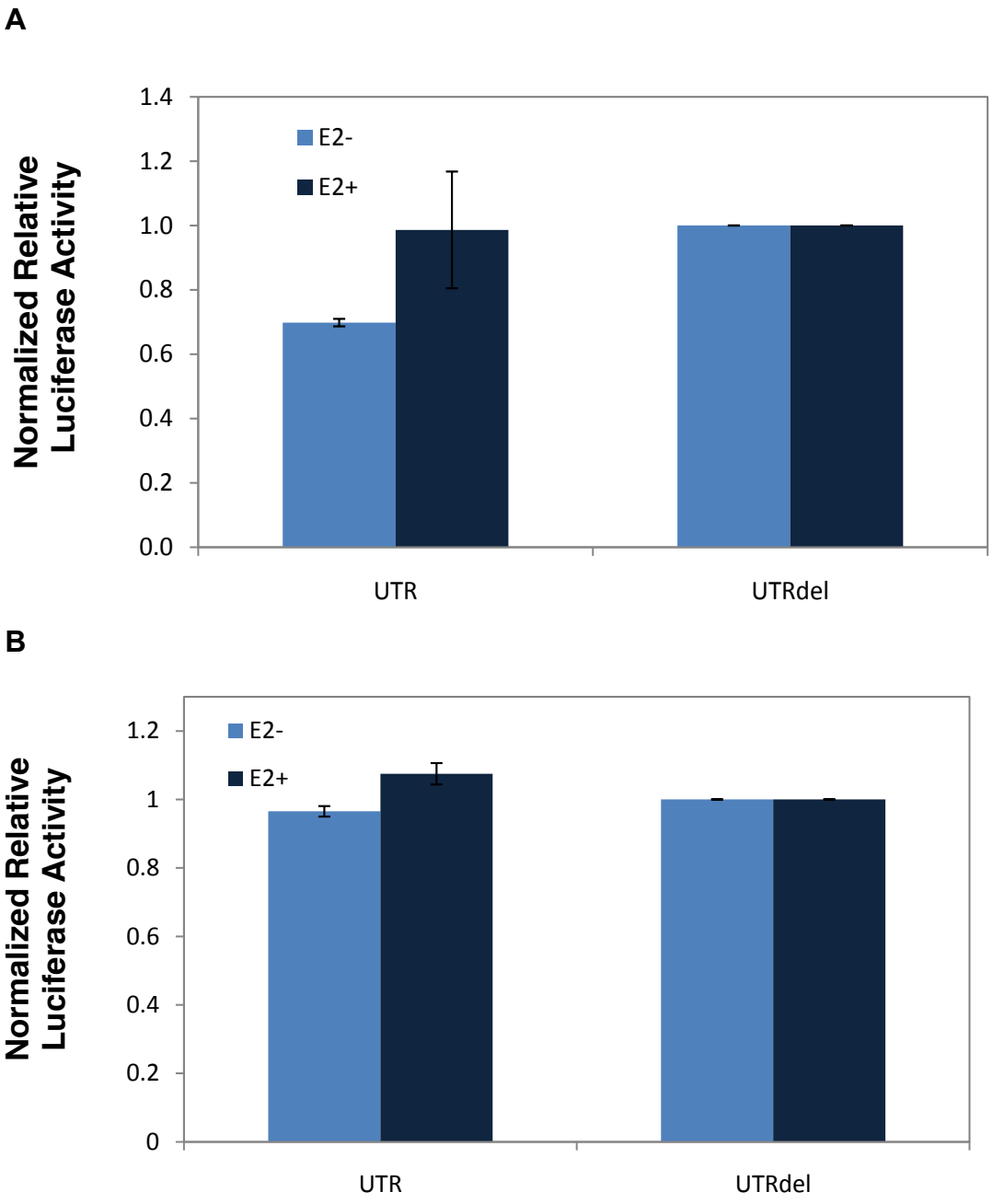

Figure 3.11: Estradiol increases luciferase expression of JAG1 3'UTR construct in MCF-7.

Luciferase analysis in **A)** MCF-7 cells **B)** MDA-MB-231 cells treated with E2 (E2+) (10 nM) or untreated (E2-) are shown.

3.4. Discussion

Mir-34 and mir-21 targeting of JAG1 was recently demonstrated in dendritic cells [287]. Mir-21 [298] and JAG1 [292, 293] have also been independently reported to be involved in cancer. In this chapter, targeting of JAG1 by mir-21 in the context of cancer cells, and the relationship between mir-21 dosages, JAG1 and Estradiol (E2) in cancer cells were investigated. MCF-7 and MDA-MB-231 cells were chosen as different types of breast cancer models: non-invasive ER+ and invasive ER-, respectively.

Estrogen signaling is very important in cell fate especially in the context of breast cancer progression and therapies [299{Tyson, 2011 #1905]}. Both tumor-promoting [300, 301] and pro-apoptotic [302], [303] effects of estrogen have been reported. Many estrogen receptor antagonists such as Fulvestrant [304], Tamoxifen [305] are used to control breast cancer progression. Although the action mechanisms of these drugs are well established it is still important to elucidate how estrogen signaling affects gene regulation, including microRNA/mRNA interactions in cancer cells.

Mir-21 targets JAG1 in MCF-7 but not in MDA-MB-231 cells

To confirm that the JAG1 3'UTR binding site is targeted by mir-21 in breast cancer cells, a construct containing part of the JAG1 3'UTR (PMIR/JAG1-UTR) was generated. The rationale for cloning a 632 bp region of the 3'UTR was to clone the minimum possible number of other miRNA binding sites with maximum length covering 3'UTR region in the luciferase reporter construct. This construct contained three miRNA binding sites in addition to that for mir-21 (mir-26ab/1297, mir-140-5p/876-3p and mir-34a/34b-5p/34c-5p/449/449abc/699). Transfection of PMIR/JAG1-UTR into MCF-7 cells caused a significant decrease in luciferase expression **(Figure 3.3)** indicating that the JAG1 3'UTR region is regulated by putative miRNAs or other regulatory elements. Since the

3'UTR is available for all the putative microRNAs listed above, the decrease can be attributed to either the individual or combinatorial activity of all these microRNAs, including mir-21.

To test the individual contribution of mir-21 to the decrease of target expression, another construct was generated with the mir-21 seed region deleted (PMIR/JAG1-UTRdel). The individual effect of mir-21 on JAG1 3'UTR was confirmed by restoration of luciferase expression to similar levels as the PMIR empty vector control when cells were transfected with PMIR/JAG1-UTRdel **(Figure 3.3)**. This demonstrates that mir-21 has a strong binding capacity and has a regulatory effect on the JAG1 3'UTR since mir-21 is one of the microRNAs showing highest expression among many tested miRNAs in MCF-7 breast cancer cells (www.microrna.org).

On the other hand, no significant effect was observed on luciferase expression in MDA-MB-231 cells transfected with PMIR/JAG1-UTR compared to PMIR/JAG1-UTRdel or PMIR empty vector control **(Figure 3.3)**. This indicates a cellular 'context-dependent' mir-21-directed regulation of JAG1, in other words a selective miRNA targeting, in two different breast cancer cell lines.

Lower levels of mir-21 in MDA-231 relative to MCF7 may explain the lack of targeting of JAG1 in MDA-231.

To investigate the reason why mir-21 is not targeting JAG1 3'UTR in MDA-MB-231 cells but does target in MCF-7 cells, the endogenous levels of mir-21 were determined. Mir-21 levels were much lower in MDA-MB-231 cells relative to MCF-7 cells indicating an endogenous mir-21 dosage difference in the two cell lines. To show that mir-21 dosage affects JAG1 mRNA expression, anti-21 oligonucleotides or pc-21 overexpression plasmids were used to decrease or increase mir-21 levels, respectively. As expected, mir-21 dosage inversely correlated with JAG1 levels in both cell lines. These results indicate an inverse relationship in mir-21 and JAG1 expression levels where mir-21 transcriptionally regulates JAG1.

To confirm that the change of JAG1 mRNA levels is due to perturbed mir-21 dosage and binding, luciferase reporter assays were performed on MCF-7 and MDA-MB-231 cells with decreased or increased mir-21 dosage in each cell line, respectively. The results confirmed that in both cell lines mir-21 dosage affects the mRNA levels of the target gene, in this case JAG1 3'UTR. These data indicate that the endogenous levels of mir-21 in MDA-MB-231 are not sufficient for JAG1 3'UTR targeting. Instead, mir-21-directed JAG1 3'UTR targeting can be "switched on" by ectopically increasing mir-21 levels. Similarly, mir-21-directed JAG1 3'UTR targeting can be interrupted by decreasing mir-21 levels in MCF-7 cells. Although this is (to the author's knowledge) the first report showing that changing the dosage of a microRNA can switch on or off a microRNA: mRNA interaction, similar dosage-dependent complexity in selective microRNA targeting has occasionally been reported, mostly due to tissue specific expression of microRNAs [306-308].

JAG1 is known to be expressed more highly in lymph node-negative cancer cells with lymphatic invasion [288] and JAG1 levels can affect invasion of cancer cells [309, 310]. Taken together, the results in this study indicate that lower levels of mir-21 can allow JAG1 mRNA levels to be higher in MDA-MB-231 cells, possibly contributing to the highly invasive nature of this cell line.

Although mir-21 is known to be an oncomir and has been reported to promote invasiveness [231], the dosage (i.e. levels) of mir-21 in cells is important in fine-tuning mRNA levels of its targets. In this way, lower mir-21 expression could potentiate expression of potential targets are involved in oncogenic processes which include JAG1. Despite some reports that have found higher expression of mir-21 in MDA-MB-231 cells compared to MCF-7 cells [311], others found that endogenous mir-21 levels are higher in MCF-7 cells compared to MDA-MB-231 cells [133, 231], including this study. On the other hand, one study reported that anti-*mir-21* had no effect on the growth of MDA-MB-231 *in vitro* whereas a significant decrease in growth was observed in MCF-7 cells. This was proposed to be linked to

the different genetic and epigenetic backgrounds of the two cell lines [133]. The inconsistencies in the findings of different groups using the same cell lines could also be also due to generation of different passages of lines over many years that are grown in different labs under different conditions [191, 312].

Mir-21 and JAG1 expression levels behave oppositely in response to Estradiol stimulation

There are few studies which have investigated JAG1 levels in tumor samples, and some have found discrepancies between the levels of mRNA and protein expression in tumor samples [293] [288]. This indicates that JAG1 could be regulated differentially at mRNA and protein levels. There are also recent reports showing higher levels of JAG1 mRNA in aggressive breast tumors as a determinant of poor prognosis [288]. In addition, higher JAG1 mRNA levels has been linked to aggressiveness of the tumor triple negative state, (TN; ER/PR/Her2 -) whereas luminal (ER+/Her2-) or Her2+ cell lines such as MCF-7 displayed less JAG1 expression levels [294]. Especially, BRCA1- mutant breast cancers (mostly ER-) are associated with higher JAG1 levels compared to BRCA2-associated tumors, which have a predominant luminal phenotype [313]. These findings correlate with the results presented in this chapter where highly invasive MDA-MB-231 cells showed higher JAG1 expression compared to non-invasive MCF-7 cells. A study on estrogen and JAG1 reported that 17-beta-Estradiol (E2) promoted JAG1 expression up to six-fold in MCF-7 cells [295]. On the other hand, inhibition of estrogen activity by Estradiol decreased mir-21 levels where mir-21 levels were found to be higher in ER+ cells [252].

Consistent with these findings, in this study, JAG1 mRNA levels increased with 17-beta-Estradiol (E2) treatment in MCF-7 cells. As expected, JAG1 mRNA levels were non-responsive to E2 stimulation in ER- MDA-MB-231 cells. Mir-21 expression levels, on the other hand, decreased with 17-beta-Estradiol (E2) treatment in MCF-7 cells. Mir-21 expression, similar to

JAG1, showed no change in response to E2 in MDA-MB-231 cells. The effect of E2 on mir-21/JAG1 targeting in MCF-7 cells was confirmed by luciferase assays. Due to E2-directed reduced mir-21 expression, wild-type JAG1 3'UTR luciferase expression was restored in MCF-7 cells.

Mir-21 targeting of JAG1 is mir-21 dosage dependent and interfered with by Estradiol stimulation

These results show that targeting of JAG1 by mir-21 is dependent upon the mir-21 dosage (i.e. the steady state levels of the microRNA). Increasing or decreasing mir-21 levels can control the mir-21/JAG1 interaction in MCF-7 and MDA-MB-231 cells. Mir-21 and JAG1 expression levels show an inverse correlation in both of these cell lines. Moreover, mir-21 and JAG1 interaction in ER+ MCF-7 cells is interfered with by 17-beta-Estradiol treatment whereas, in MDA-MB-231 cells, mir-21/JAG1 targeting could be "switched on" by increasing mir-21 levels.

Taken together, (1) the higher expression levels of mir-21 and lower JAG1 expression levels reported in previous studies in ER+ tumors compared to ER- tumors, (2) the estrogen induced expression changes in mir-21 and JAG1, and (3) the regulation of JAG1 mRNA in the ER+ MCF-7 cell line, the results indicate that the association between estrogen (receptor status) and mir-21 levels contribute to modulating JAG1 mRNA levels in MCF-7 cells.

An interaction between microRNA and an mRNA target identified in a specific cell type (i.e. heart, brain, tumor tissue) or stage (i.e. embryonic or differentiated) may not necessarily apply to other cell types and cell stages due to largely unknown context-dependent determinants and tissue-specificity of microRNAs and target genes [116]. Consequently, the contribution of this tight regulation to cancer progression should be investigated in more detail before it is possible to speculate that targeting of JAG1 by mir-21 at the mRNA level is a cancer-relevant phenomenon. This could include investigation of mir-21 and JAG1 interaction in large

number of clinical samples to establish the extent of any link to carcinogenesis as a cause or consequence and in relation to enhancement or interference by other regulatory elements (i.e. hormone receptor status, hormones, other microRNAs, growth factors, etc.).

CHAPTER 4: Genome wide analysis of mir-9 overexpression effects on breast cancer cells

4.1. Background: mir-9 significance in cancer

Mir-9, initially shown to function in neurogenesis [166], is one miRNA recently been implicated in cancer. Although many experiments indicate tumor suppressor activity for mir-9, conflicting results on mir-9 expression make it difficult to classify mir-9 as a tumor suppressor or oncogene (oncomir). This could be due to its heterogeneous expression in different tissues and tumor types [174, 314, 315]. For example, mir-9 has been reported to be overexpressed in brain tumors [18]. It is also induced by MYC in breast cancer cells enhancing metastasis [162, 316] and in mouse mammary tumors [317]. MYC activated mir-9 has been shown to suppress the activity of E-cadherin to promote cell motility and invasiveness. Furthermore, the mir-9 mediated E-cadherin downregulation activates β-catenin signaling pathway causing increased VEGF expression, further leading to induction of angiogenesis. However, downregulation of E-cadherin and activation of β-catenin is not sufficient for mir-9 dependent VEGF up regulation and it has been postulated that other mir-9 targets could enable the VEGF induction by mir-9 [318]. This suggests that elevated expression of mir-9 and downregulation of E-cadherin contributes to EMT and metastasis in breast tumor cells. Additionally, knockdown of mir-9 decreases invasion of hepatocellular carcinoma cells [319].

In contrast to findings indicating overexpression of mir-9 in cancer cells compared to normal cells, some studies identify downregulation of mir-9 in cancer. Microarray profiling of gastric cancer tissues and normal gastric tissues identified mir-9 as downregulated [314]. Decreased expression of mir-9 has been reported in gastric adenocarcinoma [320], ovarian cancer [321, 322] and malignant mesothelioma [323, 324]. Moreover, as mentioned in **section 1.4.2**, epigenetic inactivation of mir-9 gene is observed in many cancer types such as breast cancer [174, 176, 325], colorectal cancer [176] and renal cell carcinoma [163] and other cancer cell lines and tumor tissues [178].

To date, few mir-9 targets have been experimentally validated such as the transcriptional factor REST in Huntington's disease [326] and TLX in neural stem cells [324]. In cancer, CBX7 in human glioma [327], CDX2 in gastric cancer [328], NFKB1 in ovarian cancer [321] and gastric adenocarcinoma [320] and E-Cadherin when induced by MYC [162] were reported as direct targets of mir-9.

Numerous studies have been carried out using plasmid vectors for overexpression of mature microRNAs and studying their functional impact in the cells. Recently, mir-9 was shown to be deregulated in ovarian cancer and gastric adenocarcinoma tissues compared to normal ovarian tissues and normal gastric tissues [320, 321]. In both studies, NF-kB1 displayed higher expression in ovarian cancers and gastric adenocarcinoma tissues compared to normal tissues consistent with deregulation of mir-9 in ovarian cancer and gastric adenocarcinoma tissues. In these studies, overexpression of mir-9 using pcDNA3B/mir-9 showed significant growth inhibition of ovarian and gastric adenocarcinoma cells [320, 321]. However, the suppression of malignant phenotypes could be due to mir-9 or mir-9* or both when overexpressed using pcDNA3/pri-mir-9. The fundamental question of mir-9 precursor overexpression leading to mir-9 or mir-9* expression and their regulation was not addressed in any of the gain of function approaches using mir-9 expression vectors. The individual functional effects of mir-9 and mir-9*, although they are processed from the same precursor, are still unclear.

It is still unclear how the loss of mir-9 contributes to cancer cell growth and how the restoration of mir-9 expression affects the cancer transcriptome. Therefore, in this study, the effects of mir-9 ectopic expression on cell growth and apoptosis were investigated. Global changes in the transcriptome of MCF-7 breast cancer model cell line with novel mir-9 targets were identified using microarray profiling.

4.1.1. Aim

Mir-9, first identified as brain-specific microRNA [164, 329], has been recently shown to be significant also in cancer [174, 322, 327]. Although there are conflicting reports, most of the findings suggest an inactivation or loss of mir-9 activity in cancer cells/tissues, including breast cancer suggesting that restoration of mir-9 expression in cancer cells could hold a therapeutic potential.

Despite the few known targets of mir-9 in cancer cells, a genome-wide investigation of mir-9 expression has not been reported yet. Therefore, it is important to identify the genome-wide effects of mir-9 overexpression on the transcriptome in cancer cells to elucidate possible outcomes of mir-9 expression restoration, and identification of genes and pathways that are sensitive to changes in mir-9 levels. The aim of this chapter is to investigate the phenotypic changes and genome-wide effects on the transcriptome of mir-9 overexpression on breast cancer cells by microarray profiling and to identify direct targets of mir-9 that could contribute to the elucidation of the function of mir-9 in cancer cells.

In addition this chapter also investigates the extent to which pseudogenes can act as miRNA decoys (sponges). The Cold Shock Domain protein A (CSDA) and ANXA2 (Annexin A2) genes are predicted targets of mir-9 (TargetScan). In this study, CSDA, ANXA2 and their corresponding pseudogenes CSDAP1 and ANXAP1, respectively were found to be downregulated in microarray analysis of mir-9 overexpressing MCF-7 cells. The pseudogenes CSDAP1 and ANXA2P1 retained the mir-9 seed region indicating that they can be targeted by mir-9. Therefore, in the final part of this chapter, the aim is to investigate the potential of CSDAP1 and ANXA2P1 as mir-9 decoys (sponges).

4.2. Materials and Methods

4.2.1. Tissue culture, samples and reagents

Human breast cancer cell lines MCF-7, MDA-MB-231, Hs578T, and SUM159PT were cultured and maintained in complete DMEM as described in 2.2.1. Normal breast RNA was used as a control (Ambion, USA, #AM6952) and synthetic oligonucleotides for precursors (pre-9 and pre-ctr) (ABI, UK, #AM17100) were used as final 50nM concentrations in transfections. Primary tumor tissues (breast cancer, n=20) and normal breast tissues (mastopexy, n=5) were obtained from Prof. Michael J Kerin (NUI, Galway University hospital). The cancer samples contained 10 non-metastatic and 10 metastatic primary breast cancer samples (all mixed epithelial). The detailed information on samples is shown in **section A.1.10.**

4.2.2. Ectopic expression of mir-9 and transfections

The mir-9 overexpression construct (pcDNA3/pre-9-1) was previously generated by Dr. Prasad Kovvuru (PhD thesis, Genetics & Biotechnology Lab, UCC, Ireland). The genomic region containing precursor-mir-9-1 located at Chr 1: 153,203,206-153,203,294 was PCR amplified (with additional ~200bp upstream and downstream flanking sequences) using a human genomic DNA template (Roche, US). Amplified products were directly cloned into HindIII/EcoRI restriction sites in a pcDNA3 mammalian expression vector and the construct was designated as pc-9-1 **(section A.1.11.)**. PcDNA3 empty vector was used as a negative control in transfections. One µg of each construct was transfected into cells in 6-well plates using Lipofectamine 2000 reagent according to manufacturer's protocol **(protocol: A.3.10.)**. For the microarray analysis, synthetic oligonucleotides were transfected at two dosages; 12.5nM and 25nm final

concentrations. For other experiments, final concentration of 50 nM was used. Downstream analyses were performed 48hr post-transfection.

4.2.3. RNA isolation and Quantitative RT- PCR

To confirm the levels of mir-9 or target mRNAs pre- or post-transfections, total RNA and small RNAs were isolated from transfected samples using a Nucleospin miRNA kit. For cDNA synthesis, 0.5 µg of total RNA from each sample was reverse-transcribed using a RevertAid H-Minus First Strand cDNA Synthesis Kit. Real-time PCR amplification was performed using SYBR green assays and the reaction was run in a CFX96 system. β-Actin was used as housekeeping gene for normalizations. For mir-9 expression level detection, mature mir-9 specific Taqman primers and probes were used. Small U6 RNA (RNU6B) was used as housekeeping gene for normalizations. Relative quantification of expression was calculated using the $2^{-\Delta\Delta CT}$ method and represented as normalized expression in graphs. t-tests were performed to determine statistically significant expression levels between samples. For microarray samples, RNA integrity number (RIN) was measured using Bioanalyzer (Agilent, UK).

4.2.4. Microarray Profiling and data analysis

MCF-7 cells were transfected with two dosages of pre-9 or pre-ctr synthetic oligonucleotides (1X; 12.5nM and 2X; 25nM) using Lipofectamine 2000 reagent according to manufacturer's protocol. 48hr post-transfection cells were harvested and total RNA was isolated using Trizol reagent (Invitrogen, US). Total RNA was purified by isopropanol precipitation and 100ng of each sample was further processed for hybridization into whole human genome Illumina bead arrays (Illumina, USA) in biological triplicates (by Sanger Institute microarray core facility). All data was variance stabilizing transformed and robust spline normalized using the lumi package in Bioconductor. Differentially expressed genes were identified using LIMMA ($p < 0.05$, fold change > 1.2). Putative

microRNA targets were identified using MAMI microRNA target meta-predictor. Mir-9 seed region enrichment was identified using SylArray using the list of all genes ranked according to t-statistics. Enrichment analysis was performed using hypergeometric tests (conditional tests were used for GO terms).

4.2.5. Western Blot analysis

Following treatment, cells were harvested; protein was isolated and quantified **(protocol: A.3.11.)**. Thirty µg of protein was separated on 8%, 10% or 15% SDS-PAGE according to protein size and transferred into PVDF membrane by the semi-dry transfer method. Blots were stained with Ponceau red (Sigma, USA, Fluka 09276) and blocked in 5% milk TBS-Tween-20 **(protocol: A.3.12).**

Primary antibodies against ANXA2 (rabbit, #GTX100046S), AP3B1 (also known as HPS2) (rabbit, #GTX113878S), MTHFD2 (rabbit, #GTX115482S), MTHFD1L (rabbit, #GTX119126S) and MYC (rabbit, #GTX109636S) were purchased from GeneTex, USA. CCNG1 (rabbit, #AP11209b) and CSDA (mouse, #AT1648a) primary antibodies were obtained from Abgent, USA and SRPK1 (#H00006732-A01) primary antibody was obtained from Abnova, USA. Primary antibody against β-actin (mouse, #A9169) and secondary antibodies anti-rabbit (#A9169) and anti-mouse (#A0168) were purchased from Sigma, UK. All primary antibodies were used in 1:500-1000 dilution in 5% BSA, TBS-0.1% Tween-20 (TBS-T) overnight at 4°C. Secondary antibodies were used in 1:10,000 dilution in 5% milk, TBS-T for 2 hours RT. Immunodetection was performed using enhanced chemiluminescence (ECL Plus Kit, Perkin Elmer) and visualized in G:Box Chemi imaging system (Syngene, UK).

4.2.6. Cell proliferation (Acid phosphatase) and ApoTox-Glo Assays

For cell proliferation, 10^3 cells in 96-well plates were transfected with 1 µg of pcDNA mir-9 precursor constructs (pcDNA-9-1 and pcDNA-9-2). At 24 and 48hr post-transfection wells were washed with PBS, phosphatase substrate was added and absorbance was measured **(protocol: A.3.6.)**. Values were normalized using pcDNA empty vector control.

For viability, cytotoxicity and caspase-3/7 activation analysis, cells were transfected with 50 nM of pre-9 or pre-ctr and 48hr post-transfection, ApoTox-Glo Triplex Assay was used to test the changes in viability and caspase-3/7 activation **(protocol: A.3.7.)**. Well-to-well differences were normalized by taking the ratio of viability to cytotoxicity measurements (live/dead cell) and represented in the graphs as ratio. 1nM of STS (Staurosporine) treatment for 3 hours was used as positive control.

4.2.7. Apoptosis Assay (flow cytometry analysis)

Flow cytometry analysis was performed on the MCF-7 cells stained with Annexin-V and PI fluorescent dyes provided in Annexin-V-Fluos Staining Kit (#11858777001, Roche, USA). MCF-7 cells transfected with 5nM of each siRNA for AP3B1, MTHFD1L, MTHFD2 and siRNA control were stained according to manufacturer's procedure **(protocol: A.3.17.)**. Data analysis was performed (by Prof Rhodri Ceredig, NCBES, NUIG) using the BD FACS Canto machine. Cell populations stained only with Annexin were selected as the gate. The same procedure was performed for PI stained-only, and Annexin & PI stained cells, to determine the borders of each population. Based on these compensations, in each treatment the percentage of cell populations that were apoptotic (Annexin positive, PI negative), necrotic (Annexin & PI positive) or living (Annexin & PI negative) were calculated. In analysis 10000-50000 cells were counted.

4.2.8. Wound healing assay

To test migration of MCF-7 cells, cells were grown to full confluence and wounded by a pipette tip. Following transfection with pre-9 or pre-ctr (50 nM) images of the cells were taken under an inverted microscope at 0hr, 24hr and 48hr. Three replicates of two independent experiments were performed.

4.2.9. Invasion assay

Following transfection of pre-9 or pre-ctr, $2.5x10^4$ cells (in serum starving DMEM medium with 0.1% FBS) were transferred into matrigel invasion chambers, 24-well plate (BD Biosciences, Germany, #354480) containing a matrigel-coated membrane with 0.8μm pore size. 10% FBS containing DMEM was added to the lower compartment and incubated at 37˚C. The non-invaded cells were removed from the insert by a cotton swab. The invaded cells were fixed in 100% methanol, stained by 0.5% crystal violet and counted. The number of stained cells from images was counted from multiple parts of the membrane **(protocol: A.3.9.).**

4.2.10. Luciferase Reporter Assay

For reporter luciferase assays, full length 3'UTRs cloned in pLightSwitch luciferase reporter vectors (Switchgear Genomics, USA) **(vector map: A.5.5.)** for ANXA2, CSDA, AP3B1, CCNG1, MTHFD1L, MTHFD2, LARP1 and SRPK1 were obtained **(vector maps: A.5.6-15)**. Mutations in seed regions of mir-9 were introduced using specific primers **(primers: A.4.1.)** using Quikchange Lightning Site Directed Mutagenesis Kit (Agilent Technologies, USA, #210518-5) **(protocol: A.3.5.)**. 100 ng of each UTR or mutated UTR construct was co-transfected with pre-9 or pre-ctr synthetic oligonucleotides (final concentration of 50 nM) in 24-well tissue culture plates. 48hr transfection, LightSwitch luciferase assay solution

(Switchgear Genomics, USA, #L5010) was added onto cells, incubated for 30 min at room temperature and luminescence was read for two seconds in plate reader **(protocol: A.3.8.)**. Graphs are represented as percentage changes in luminescence in pre-9 treatments, normalized to pre-ctr treatments.

4.2.11. Designing specific primers for qPCR detection and mRNA amplification of pseudogenes

Sequences for gene and pseudogene mRNAs were obtained from NCBI and multiple sequence alignment were performed using ClustalW the in BioEdit software suite. qRT-PCR primers were designed to discriminate the genes from pseudogenes. Primers were selected manually based on the sequence differences between ANXA2 isoforms (1, 2, 3 and 4), ANXA2P1, ANXA2P2 and ANXA2P3 for a product size of 80 to 200 bp. Similarly, to amplify pseudogene mRNAs, primers were selected manually from regions specific to each gene and restriction sites were added to 5' regions. Forward primers contained NheI sites and reverse primers contained AvrII sites together with four extra nucleotides **(primers: A.4.1.)**. Human genomic DNA was used as a template to amplify pseudogene mRNAs and amplified products are digested and cloned into a pLightSwitch luciferase vector (Switchgear genomics, USA).

4.2.12. Cloning of pseudogene mRNAs into pLight luciferase vector

Luciferase UTR constructs for ANXA2 and CSDA were obtained from Switchgear Genomics, USA **(vector maps: A.5.6. and A.5.9.)**. To clone pseudogene mRNAs, PCR amplification was performed and sub-cloned into TOPO PCRII vector. The inserts were released from the sub-clone by double digestion (NheI/AvrII) overnight at 37˚C as well as the pLight empty vector **(protocol: A.3.4.)** and ligation was performed. Colonies were screened by PCR and confirmed by sequencing.

4.3. Results

4.3.1. Quantitative analysis of mir-9 in breast cancer cell line and primary tumors, and mir-9 ectopic expression

Mir-9 was previously reported to be dysregulated in cancer samples compared to normal samples [162, 174, 322]. Both downregulation and upregulation of mir-9 in cancer samples compared to normal samples has also been shown indicating a tissue/context dependent heterogeneous mir-9 expression in different cancer types [162, 174, 322]. To identify the expression levels of mir-9 in breast cancer cell lines, normal breast RNA, normal breast epithelial cell line MCF-10-2A, a small cohort of primary tumor samples (breast cancer, n=16; 8 non-metastatic and 8 metastatic), and normal breast tissues (mastopexy, n=4), a quantitative RT-PCR (Taqman) was performed. Lower levels of mir-9 were observed in breast cancer cell line MCF-7 compared with normal breast epithelial cell line MCF-10-2A. The relative quantities, calculated by the ΔΔCt method using RNU6B small RNA as housekeeping control in normalizations **(Figure 4.1A).**

Analysis of mir-9 expression in primary tumor samples compared to normal tissues showed that 16/20 (80%) of the tumor samples had lower levels of mir-9 **(Figure 4.1B)**. Four tumor samples showed significantly higher levels of mir-9 compared to normal breast tissue samples. In the figure, the mean expression of mir-9 in primary tissue samples (n=16) (pooled) is shown compared the mean expression of mir-9 in normal breast tissue samples (n=4) (pooled), presented with ±SE. Statistical analysis (student's t-test) showed significant downregulation (p=0.029) in 16 primary samples compared to normal samples. The individual expression values for each sample tested are also presented later in this chapter **(section 4.3.9.)**.

For downstream *in vitro* analyses of mir-9 effects, MCF-7 cell line was chosen as model cancer cell line. To ectopically express mir-9 in MCF-7 cells, the mir-9 precursor plasmid (pc-9-1) was used. This construct harbors the mir-9 stem-loop precursor derived from the pri-9-1 locus located on chr1: 156,390,133-156,390,221. In addition to plasmid driven ectopic expression of precursor mir-9, synthetic oligonucleotides to specifically express the mir-9 (pre-9) mature miRNA were used. Mir-9 relative expression increased from 0.003 (pcDNA empty vector control) to 0.967 in pc-9-1 transfected samples whereas synthetic oligonucleotides (pre-9) increased the relative expression from 0.005 (pre-control) to 1.288 **(Figure 4.2)**.

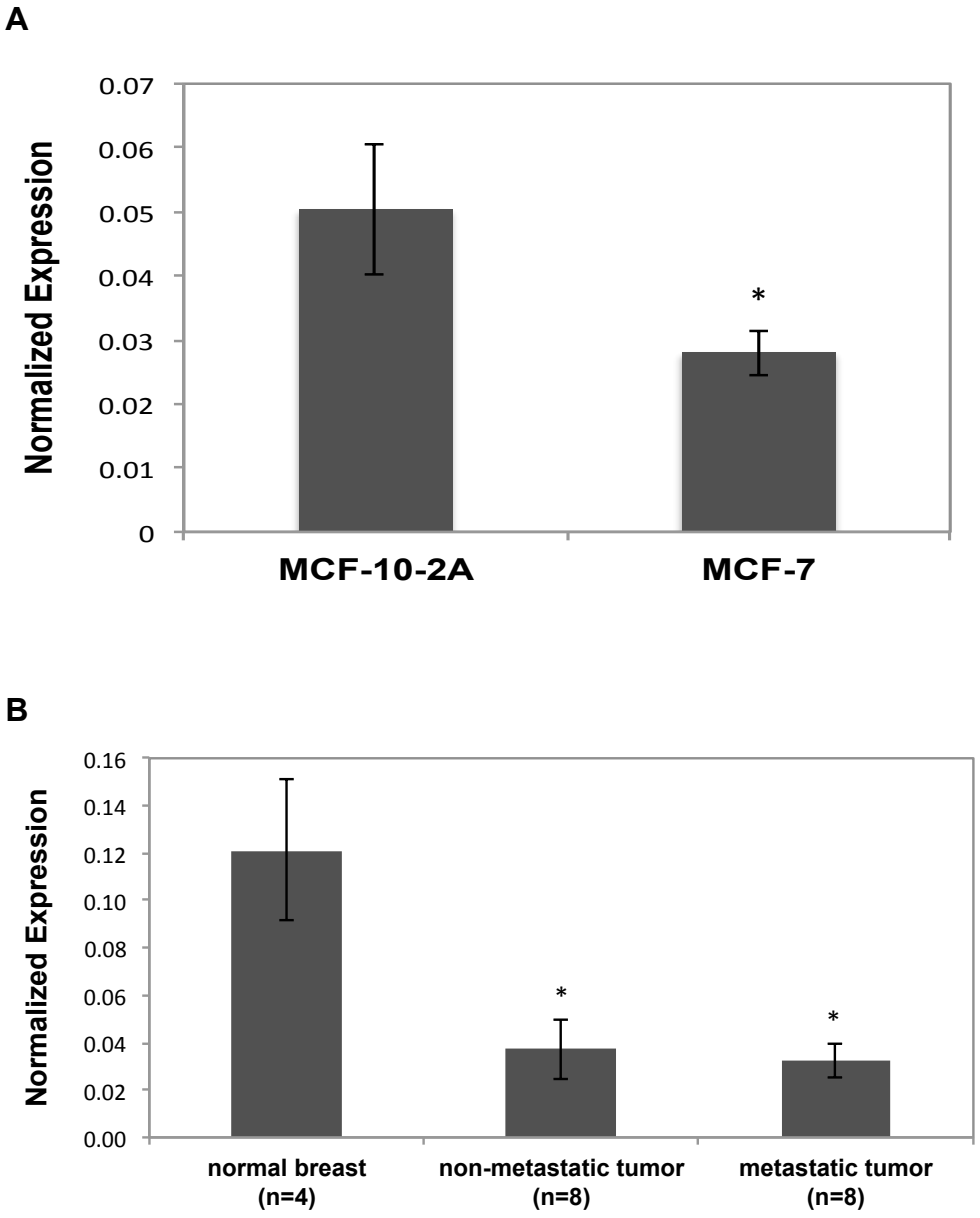

Figure 4.1: Mir-9 expression is downregulated in MCF-7 breast cancer cells and in primary breast tumor samples.

qRT-PCR analysis of mir-9 is shown (Normalized fold expression ±SE). Endogenous levels of mir-9 are detected in **A)** normal breast epithelial cell line MCF-10-2A and breast cancer cell line MCF-7 and in **B)** 16 primary tumors (8 non-metastatic and 8 metastatic) and 4 normal breast tissues. Statistical analysis identified significant downregulation in tumor samples compared to normal tissues ($p<0.05$). RNU6B was used as housekeeping control in normalizations

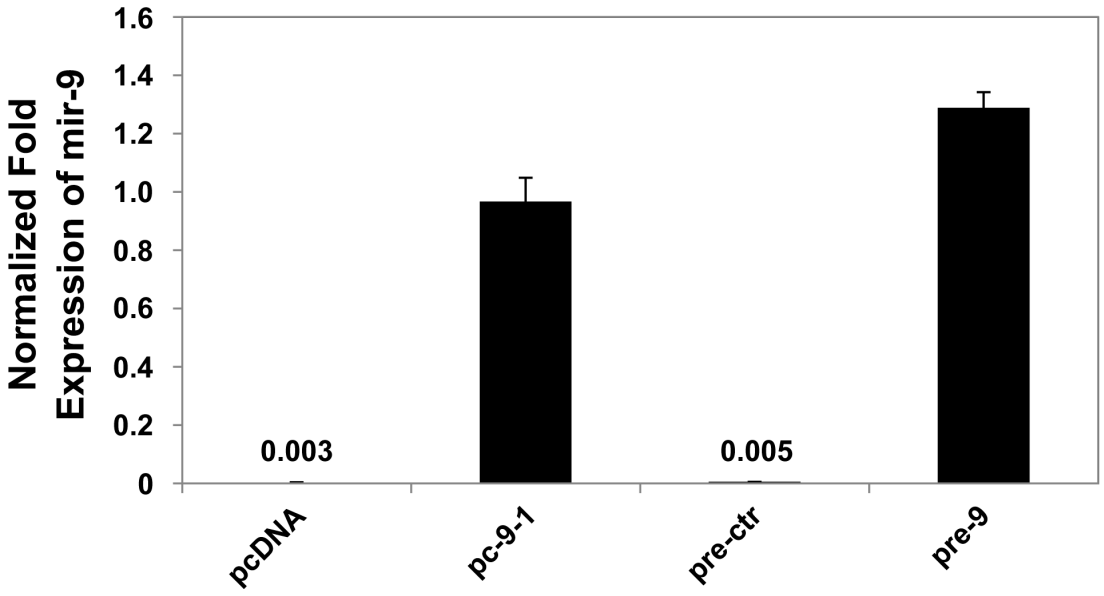

Figure 4.2: Mir-9 can be overexpressed using plasmid or synthetic precursors.

qRT-PCR analysis of mir-9 expression (Normalized fold expression) in MCF-7 cells after overexpression using plasmid based precursor (pc-9-1) or synthetic oligonucleotide (pre-9) as well as corresponding controls; pcDNA and pre-ctr. RNU6B was used as housekeeping control for normalizations.

4.3.2. Mir-9 ectopic expression by plasmid precursor decreases cell proliferation

Cell proliferation and invasion are key phenotypes observed in malignant transformation [58]. Therefore, the effect of mir-9 ectopic expression on tumor cell growth was investigated. Plasmid precursor transfected samples were tested for p-nitrophenol (phosphatase) production as a hallmark of cell proliferation. Cell proliferation decreased significantly in pc-9-1 transfected samples compared to pcDNA control **(Figure 4.3)**. Since stem-loop precursors are processed by intracellular miRNA machinery [330] to generate miRNA duplex with an active mature form (guide strand) and star form (*, star form) plasmid driven expression of miRNA precursors have the potential to ectopically express miRNA star forms as well as mature forms. Recent findings show that MiRNA star forms can be abundantly expressed and function in regulatory networks [331], [22]. Therefore, the phenotypic effects observed from use of stem-loop precursor plasmids can be due to mature and/or star forms. In the samples tested slight increases in the relative expression of mir-9* was observed, data shown in **chapter 5**.

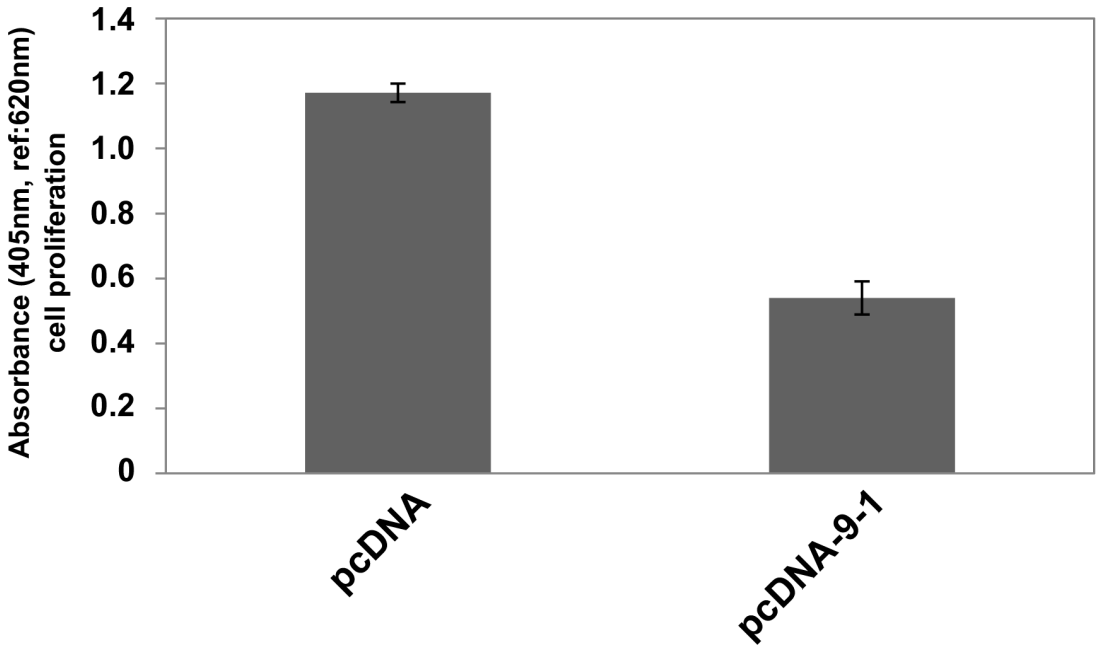

Figure 4.3: pc-9-1 transfection causes decreased cell proliferation in MCF-7 cells.

Acid phosphatase assay (p-nitrophenol production as an indication of cell proliferation) of pcDNA or pc-9-1 transfected MCF-7 cells are shown as absorbance values (405nm; background: 620nm).

4.3.3. Mir-9 ectopic expression by synthetic oligonucleotides decreases cell viability, migration, invasiveness, and increases caspase-3/7 activity

To eliminate the potential effects of mir-9* additional to mir-9 overexpression that could occur in plasmid precursor transfections, pre-9 synthetic oligonucleotides were used to specifically express mir-9 only. Cell viability and caspase-3/7 activity of cells over-expressing mir-9 was measured after 48hr of transfection. The viability measurement by live-cell protease activity (ApoTox-Glo) showed that mir-9 overexpressing cells (pre-9) are less viable compared to pre-ctr (scrambled control) **(Figure 4.4A)**.

Staurosporine (STS) is known to induce apoptosis by activating caspase 3 [332]. 1 nM of STS treatment for 3 hours was used as a control; however it showed no significant change in viability of the cells compared to control **(Figure 4.4A)**. In contrast, caspase-7 activation (measured by analysis of caspase-3/7 substrate activity) increased in MCF-7 cells overexpressing mir-9 (pre-9) compared to pre-ctr **(Figure 4.4B).** 1 nM STS treatment for 3 hours was sufficient to activate caspase-3/7 detection as an indication of apoptosis **(Figure 4.4B)**, which confirms the sensitivity of the detection method.

A

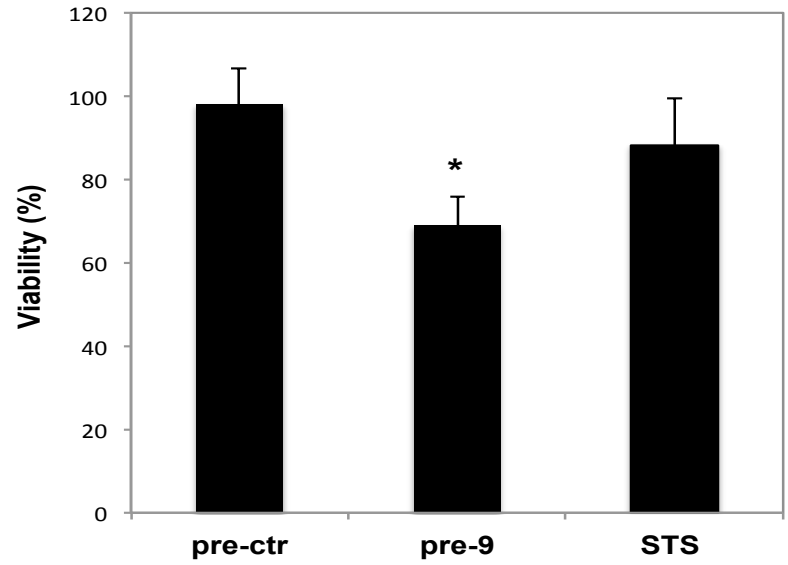

B

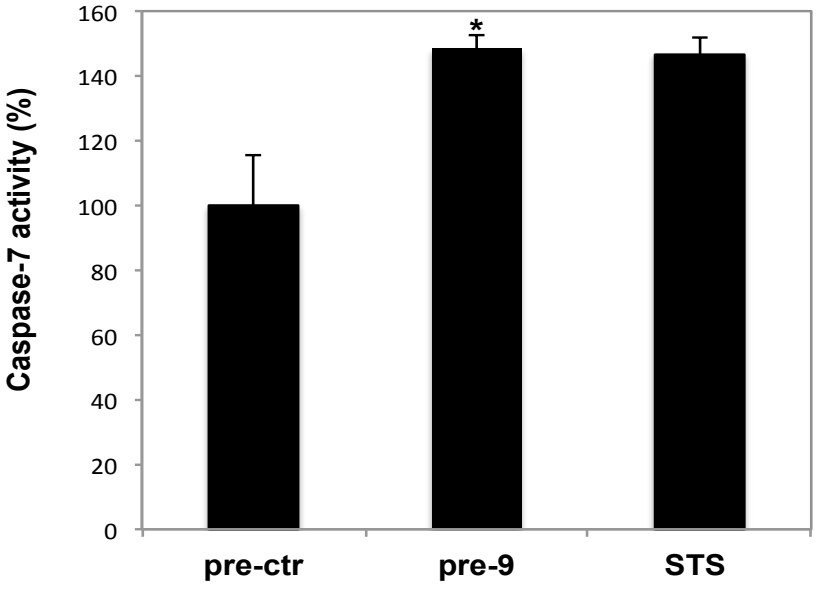

Figure 4.4: Pre-9 transfection decreased viability and increases caspase-7 activity in MCF-7 cells.

ApoTox-Glo analysis of pre-9 or pre-ctr transfections in MCF-7 cells are shown as **A)** Percentage (%) viability (normalized against dead cell number; cytotoxicity) and **B)** Percentage (%) caspase-7 activity as luminescence detected in MCF-7 cells. STS (Staurosporine) apoptotic drug was used as positive control in caspase-7 activation.

In addition to anti-proliferation effects, the migration of MCF-7 cells overexpressing mir-9 (pre-9) was tested compared to pre-ctr. After 48hr of transfection, mir-9 overexpressing cells showed less migration (wound healing) compared to control **(Figure 4.5)**.

To further examine the effects of mir-9, invasion was tested (matrigel invasion assay) in MCF-7 (non-invasive, ER+) and MDA-MB-231 (highly invasive, ER-) cells overexpressing mir-9. No cell invasion was observed in MCF-7 cells (data not shown). However mir-9 overexpression (pre-9) significantly decreased the invasiveness of highly invasive cell line MDA-MB-231 compared to control (pre-ctr). 10X and 20X magnification photos (inverted microscope) are shown in **Figure 4.6A.** Cell count was performed on the images of matrigel and represented as average number of invading cells in graph **(Figure 4.6B)**.

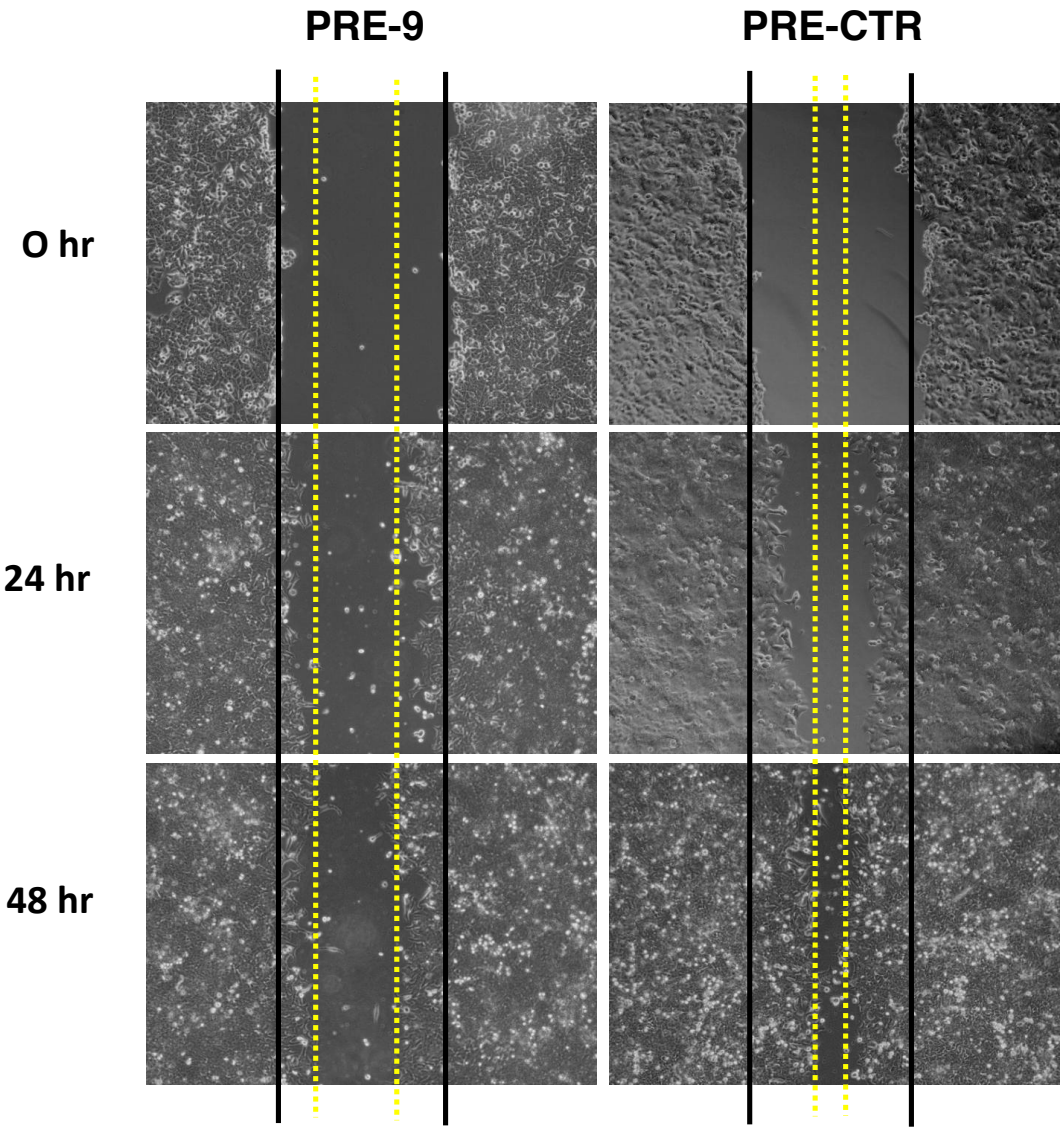

Figure 4.5: Pre-9 transfected MCF-7 cells migrate slower

Wound healing assay shows MCF-7 cells transfected with pre-9 display slower motility compared to pre-ctr transfected cells (24hr and 48hr post-transfection).

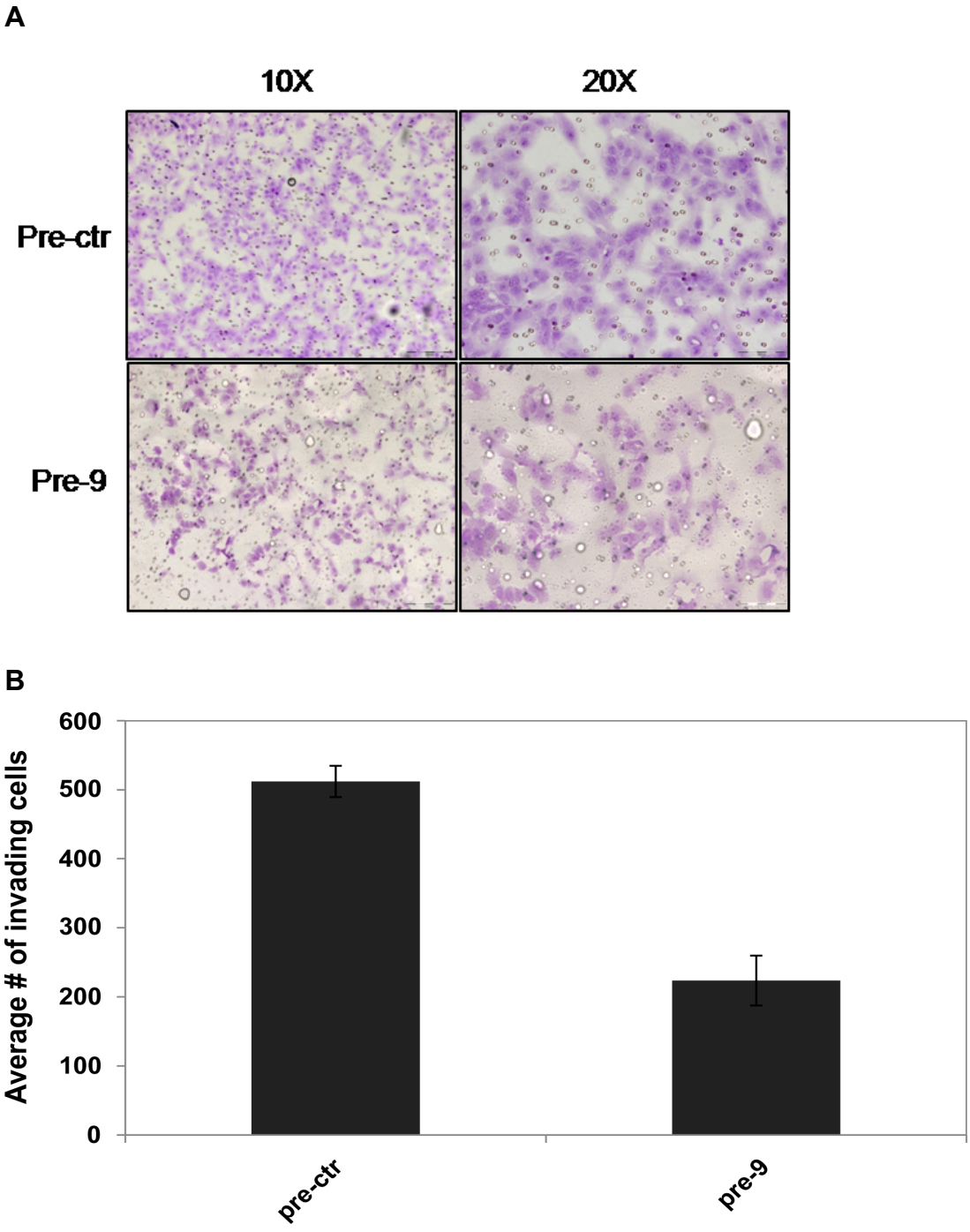

Figure 4.6: pre-9 transfected MDA-MB-231 invades slower.

Matrigel invasion assay shows **A)** Invasion images and **B)** average number of invading MDA-MB-231cells treated with pre-9 or pre-ctr 48 hr post-transfection.

4.3.4. Identification of genome-wide differentially expressed genes in mir-9 overexpressing MCF-7 cells by microarray profiling

To determine the global effects of mir-9 overexpression on the transcriptome of MCF-7, microarray profiling (Illumina bead arrays) was performed with samples expressing mir-9 in two dosages (1X = 12.5 nM and 2X = 25 nM). The quantitative analysis of mir-9 was conducted using Taqman miRNA assays and different levels of expression of mir-9 were confirmed. The expression experiment using 2X dosage did not increase endogenous levels two fold compared that of 1X treated samples. However, there was a significant increase in mir-9 levels up to 1.5 fold compared to 1X (data not shown) probably due to saturation of mir-9 expression levels. 48hr after transfection, samples overexpressing mir-9 in the two different dosages (1X pre-9, 2X pre-9) and controls (1X pre-ctr, 2X pre-ctr) were further processed and hybridized to whole human genome microarrays in triplicates. The data was normalized and differentially expressed genes were identified by moderated t-tests using the following comparisons: 1X pre-ctr vs. 1X pre-9 and 2X pre-ctr vs. 2X pre-9 ($p < 0.05$, fold change > 1.2).

In summary, a total of 516 differentially expressed genes were identified in mir-9 overexpressing cells compared to controls. Among these, 145 differentially expressed genes were specific to 1X and 121 genes were specific to 2X treatments **(Figure 4.7)**. 124 genes were upregulated and 126 genes were downregulated (total 250 genes) in both dosages showing a common profile of differential expression in both dosages as shown in the heat map **(section A.1.6.)**. The fold changes of common differentially expressed genes, (i.e. the probe intensities), did not correspond to expected dosage effects (i.e. gene1 in 1X mir-9 treatment does not show double expression level effects in 2X mir-9 treatment) **(section A.1.8.)**. Therefore, the union of the gene lists identified for both dosages (250 genes) was selected for further downstream analyses.

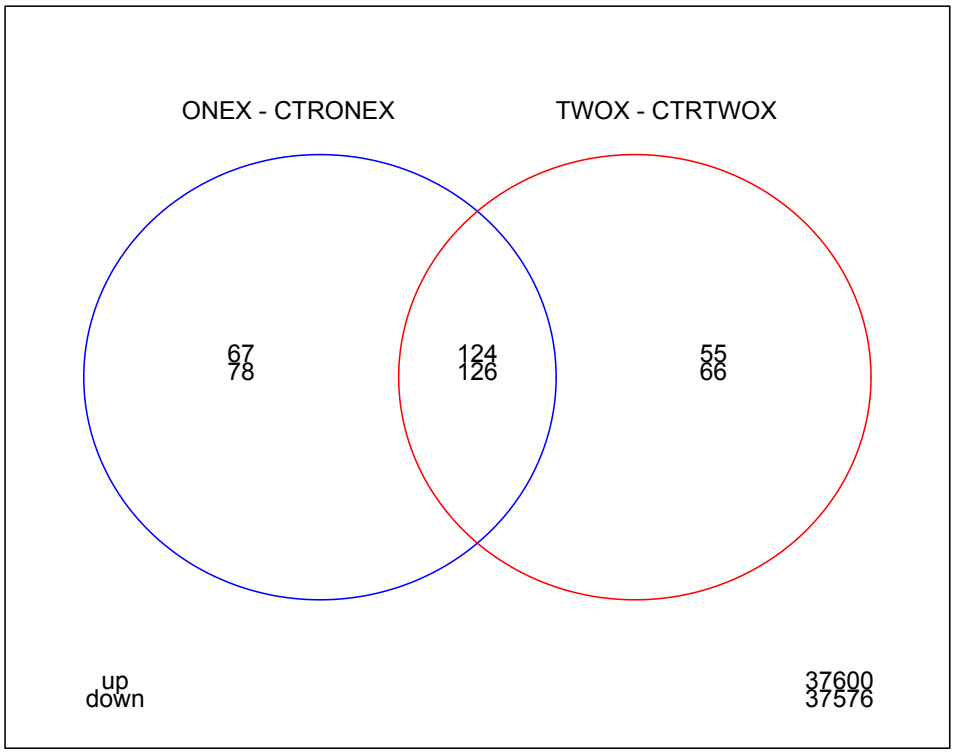

Figure 4.7: Venn diagram of up/downregulated genes.

Venn diagram of differentially expressed genes between 1X, 2X and corresponding controls identified in microarray is shown. Upper number represent upregulated, lower numbers represent downregulated genes.

4.3.5. Functional enrichment of cancer related terms and mir-9 seed sequence in mir-9 overexpressing cells

Downregulated genes in 1X treated samples were significantly enriched in GO terms (BP; biological processes) such as folic acid and derivative biosynthetic process, ncRNA processing and positive regulation of NK T cell differentiation. Similarly, downregulated genes in 2X samples were significantly enriched in same terms GO listed above as well as terms such as TOR signaling pathway, translational elongation (BP; biological processes) and cell-cell adherins junction (CC; Cellular Component).

On the other hand, upregulated genes in 1X treated samples were enriched in GO terms (BP; biological processes) such as regulation of apoptosis, cell death, and regulation of cell cycle. Upregulated genes in 2X treated samples showed enrichment in terms such as regulation of pathway-restricted SMAD protein phosphorylation and regulation of TGF-B pathway (BP; biological processes). For full list of GO enrichment see **section A.1.7.**

SylArray analysis of all the genes ranked according to t-statistics showed enrichment of mir-9 seed sequence (7-mer and 8-mer) in downregulated genes in both dosages **(Figure 4.8)**.

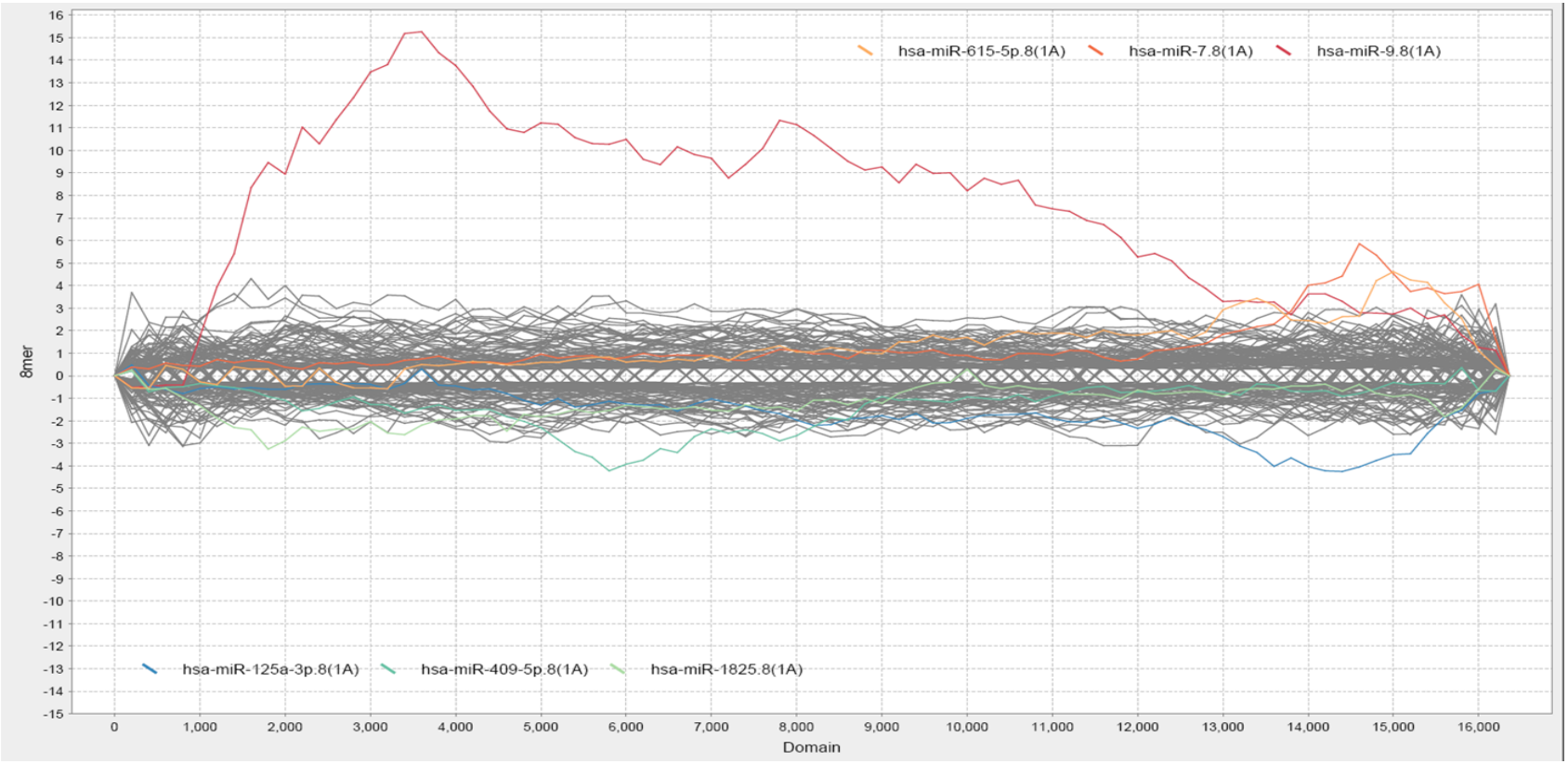

Figure 4.8: SylArray landscape plot for mir-9 8-mer seed region.

Genes are ranked from most downregulated to most upregulated according to t-statistics Peak (red) shows enrichment of mir-9 binding site in downregulated genes.

4.3.6. Mir-9 regulates 25 cancer associated or novel genes

To filter the differentially expressed genes (250) for further downstream analyses, the differentially expressed gene list was screened for functional enrichment using GO annotations and KEGG pathways. Filtering was done based on genes classified in cancer related terms (cell proliferation, apoptosis, and cell death). In addition, the top 20 genes with p-value < 0.001, downregulated or upregulated (in both dosages) compared to controls were included (independent of functional term). In total 47 genes were selected. The selected genes were screened for target prediction using MAMI microRNA meta-predictor (mami.med.harvard.edu) and this resulted in 17 predicted targets (16 downregulated, 1 upregulated). An additional 14 non-predicted genes were selected based on p-values and GO terms. As a final list for validations total 31 candidates (25 downregulated and 6 upregulated genes) were selected **(Table 4-1)**.

Among all the genes tested, differential regulation of 27 genes in pre-9 treated samples compared to pre-ctr treated samples was confirmed by quantitative real-time PCR (qPCR) method **(Figure 4.9)**. 21 of these genes were downregulated and 6 genes were upregulated when mir-9 was overexpressed. Downregulation NFKB1 as previously shown mir-9 target was also validated by qPCR. Most of the genes validated had GO terms that were significantly enriched in the list of differentially expressed genes; such as cell proliferation, apoptosis, etc. but also genes that are not previously reported in cancer and but are potential candidates as direct or indirect targets (secondary effects) of mir-9 ectopic expression in cancer cells were also validated.

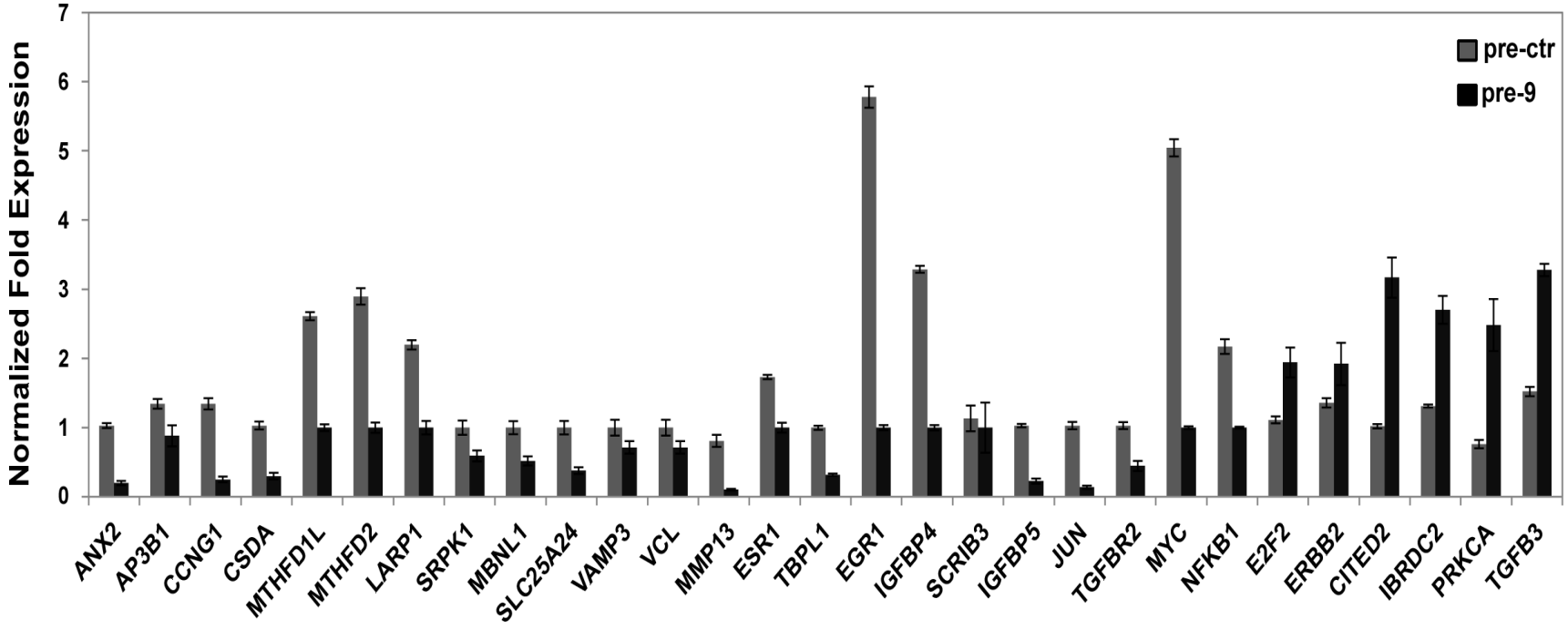

Figure 4.9: 29 out of 35 genes are validated as differentially expressed identified in microarray.
qRT-PCR analysis of 35 differentially expressed genes in microarray analysis confirms the downregulation or upregulation in pre-9 transfected MF-7 cells compared to pre-ctr transfected cells. Values represent normalized fold expression ±SD. GAPDH was used as housekeeping control in normalizations.

Table 4-1: qRT-PCR validated genes list

Downregulated genes (microarray)		*Selection based on:*	*Target prediction*	*UTR length: no. of binding sites (prediction program)*	*RNAi references*	*Breast cancer references*	*Other cancer references*
1	ANXA2	p<0.001	+	476:1 (TargetScan v5.1)	[333]; [334]; [335]	[336]; [337]	[333]; [334]; [338]; [339]; [340]
2	CSDA	p <0.001	+	599:2 (TargetScan v5.1)	[341];[342]	[343]	[344]; [345];[342]; [346]; [347]
3	LARP1	p<0.001	+	3505:1 (TargetScan v5.1)	[348]	[349]	[349]; [348]
4	CCNG1	Cell proliferation, cell death	+	1345:1 (TargetScan v5.1)	[350]	[351]; [350];	[351]; [350]; [352]
5	MTHFD1L	p<0.001 , GO: folic acid and derivative biosynthetic process	+	391:1 (TargetScan v5.1)	-	-	-
6	MTHFD2	p<0.001 , GO: folic acid and derivative biosynthetic process	+	1053:2 (TargetScan v5.1)	-	[353]	[354]; [355]
7	SRPK1	p <0.001 , Cell proliferation, cell death	+	2268:1 (TargetScan v5.1)	[356]	[356]	[357]; [356];[358]
8	AP3B1	GO: positive regulation of NK T cell	+	574:1 (TargetScan v5.1)	-	-	[359]; [360]; [361]

		differentiation					
9	ESR1	Cell proliferation, cell death	+	4307:1 (TargetScan v5.1)	[362] [363]	[364]; [365]; [366]; [367]	[368]; [369]; [370]
10	MYC	p-value, literature evidence	+	467:1 (PITA, RNAhybrid)	[371] [372]	mir-9 ref:[373]; [162]; [374]	[375];[376]; [377]
Downregulated genes (microarray)		***Selection based on:***	***Target prediction***	***UTR length: no. of binding sites (prediction program)***	***RNAi references***	***Breast cancer references***	***Other cancer references***
11	NFKB1	p-value, literature evidence (positive control)	+	709:1 (TargetScan v5.1)	[378]	[379] [380],[381] mir-9 ref: [382]; [321]	[321]; [383]
12	MBNL1	p<0.001	+	3410:1 (TargetScan v5.1)	[384, 385]	-	[386]
13	SLC25A24	p< 0.001	+	1827:1 (TargetScan v5.1)	-	-	-
14	VAMP3	p<0.001	+	1786:1 (TargetScan v5.1)	[387] [388]	-	[389]; [390]; [391]
15	TGFBR2	GO: positive regulation of NK T cell differentiation	-	-	[392]	[393]; [394]	[395]; [396]; [397]

16	MMP13	Cell proliferation, cell death	-	-	[398] [399]	[400]; [401]; [402] mir-9 ref :[403]	[399, 404-406] mir-9 ref:[403]
17	EGR1	Cell proliferation, cell death	-	-		[407]; [408]; [409]	[410]; [411]; [412]; [413]
18	IGFBP5	p <0.001	-	-		[414]; [415]; [416];[417]; [418]	[419]; [420]
19	IGFBP4	Cell proliferation, cell death	-	-		[421]; [422]	[423]; [419]; [424]
20	TBPL1	Cell proliferation, cell death	-	-	-	-	-
21	JUN	Cell proliferation, cell death	-	-	[425]	[426]; [427]; [323]	[426];[427];[323]
Upregulated genes (microarray)		***Selection based on:***	***Target prediction***	***UTR length: no. of binding site (prediction program)***	***RNAi references***	***Breast cancer references***	***Other cancer references***
1	E2F2	GO: cell death/apoptosis	-	-		**[428];[296]; [429]**	[430]; [431]; [432]; [433]; [434]
2	ERBB2	GO: cell death/apoptosis	-	-		[435]; [436]; [437]	[438]

3	TGFB3	GO: regulation of TGF-B receptor signaling pathway/apoptosis	-	-		[439]; [440]	[441]; [442]
4	CITED2	GO: apoptosis/cell death/regulation of TGF-B receptor signaling pathway	-	-		[443] [444]	[445]; [446]
5	IBRDC2	GO: apoptosis/cell death	-	-		-	[447]
6	PRKCA	GO: apoptosis/cell death	+	6701:1 (TargetScan v5.1)		[448]; [449]; [450]	[451]; [452]

4.3.7. Luciferase assay confirms eight genes as direct targets of mir-9

In most known cases, microRNAs negatively regulate gene expression (i.e. reduce levels of mRNAs/proteins) [44, 453]. Therefore, validated down-regulated genes were tested further for evidence of direct mir-9 targeting. ANXA2, CSDA, CCNG1, MTHFD2, LARP1 and SRPK1 were selected for target confirmation on the basis of their previous implications in breast cancer, and AP3B1 and MTHFD1L were selected for novelty (potential biomarkers) **(Table 4-1)**. Six of the genes had one mir-9 binding site and CSDA and MTHFD2 had two mir-9 predicted binding sites.

To identify whether these genes are directly regulated by mir-9 via putative sites on 3'UTR, we tested full-length 3'UTR luciferase reporter constructs (wt; wild type) (Switchgear genomics, US) and mutated UTR constructs (mut; mutant seed). 3'UTR constructs were co-transfected with pre-9 or pre-ctr mimics in MCF-7 cells and luciferase activity was determined as endogenous levels of mir-9 are low in MCF-7 cells.

Pre-9 overexpression significantly downregulated luciferase activity in 3'UTR constructs whereas in the mir-9 binding site mutated UTR constructs luciferase activity was partially restored **(Figure 4.10)** confirming the functionality of mir-9 binding sites in regulating the target genes. The pLight empty vector (EV) as a negative control also showed high luciferase activity. All measurements were normalized using pre-ctr (non-targeting miRNA) readings and represented as log2 ratio of targeting/non-targeting miRNA (pre-9/pre-ctr) luciferase activity. As shown in **Figure 4.11** the downregulation effect of mir-9 is also validated at protein level for MTHFD2, LARP1 and AP3B1. MYC showed no significant change. Taken together, these results indicate that ANXA2, AP3B1, CCNG1, CSDA, LARP1, MTHFD1L, MTHFD2, and SRPK1 are indeed direct targets and negatively regulated by mir-9 at the post-transcriptional level.

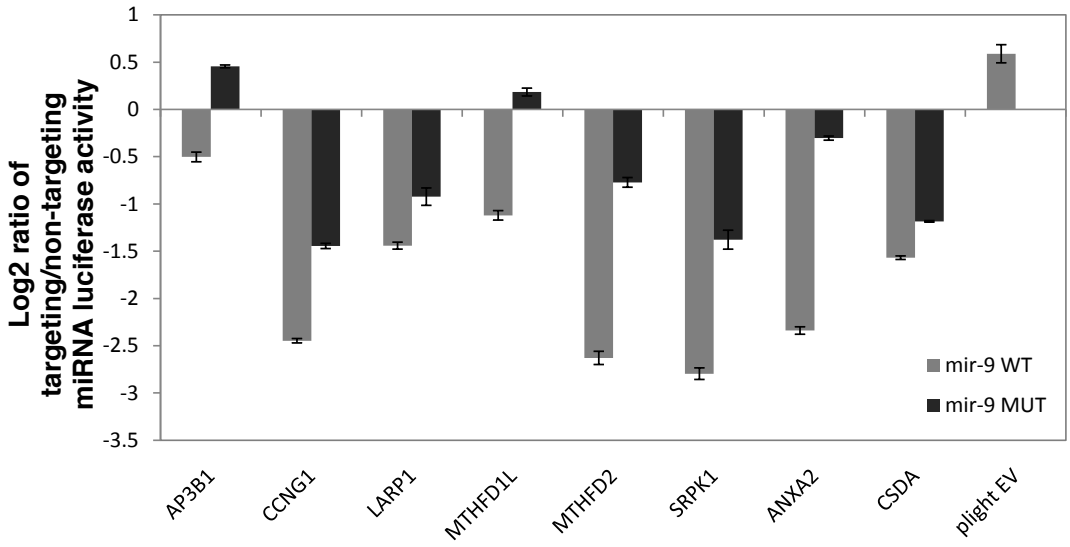

Figure 4.10: Mir-9 directly targets eight genes identified in microarray.

Luciferase analysis of pLight reporter constructs (wild type UTR and mutated UTR) for 8 predicted mir-9 targets are shown. Log2 ratios of pre-9/pre-ctr values are represented (in triplicates).

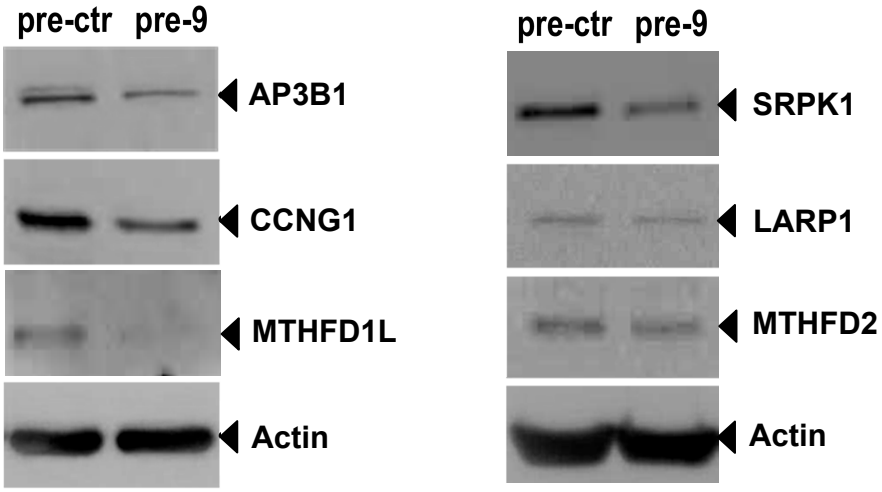

Figure 4.11: Mir-9 targets' protein levels are downregulated in mir-9 overexpressing MCF-7 cells.

Western blot analysis of six mir-9 predicted targets. LARP1 and MTHFD2 proteins show slight decrease, AP3B1, CCNG1, MTHFD1L and SRPK1 show significant decrease in protein levels in pre-9 transfected MCF-7 cells compared to pre-ctr transfected cells. β-Actin was detected as loading control.

4.3.8. SiRNA knockdown of MTHFD1L and MTHFD2 mimics apoptosis induced by mir-9 overexpression

To test whether the anti-proliferative effect of mir-9 overexpression is due to regulation of its identified targets, siRNA knockdown of AP3B1, MTHFD1L and MTHFD2 was performed in MCF-7 cells. QRT-PCR analysis of gene expressions in siRNA-transfected cells was compared to siRNA control (nonsense siRNA molecule). The results showed that all genes were knocked down successfully **(Figure 4.12)**. AP3B1 siRNA (siAP3B1) showed a 20-fold decrease, MTHFD1L siRNA (siMTHFD1L) showed a 5-fold decrease and similarly MTHFD2 siRNA (siMTHFD2) showed a 7-fold decrease in mRNA expression compared to siRNA control (siControl) **(Figure 4.12)**. In mir-9 overexpression, the level of suppression in AP3B1 was minimal (less than 20%) whereas MTHFD1L and MTHFD2 showed decrease around 40% equivalent of 2.5 fold **(Figure 4.9)**.

To test the functional effect of siRNA knockdown of these three genes on MCF-7 cells, an ApoTox-Glo assay was performed. The viability of siMTHFD1L and siMTHFD2 were decreased whereas siAP3B1 showed no change compared to siControl **(Figure 4.13)**. Analysis of caspase-3/7 activity indicated an increase only in siMTHFD2, while siAP3B1 and siMTHFD1L showed no significant change in caspase-7 activity compared to siControl **(Figure 4.13)**. Moreover, flow cytometry analysis of siRNA-knocked down cells showed increased apoptosis in siMTHFD1L (53.1% apoptotic) and siMTHFD2 (48.8% apoptotic) compared to siControl (41.8%) whereas AP3B1 showed slightly decreased apoptosis (35.9% apoptotic) **(section: A.1.9.)**.

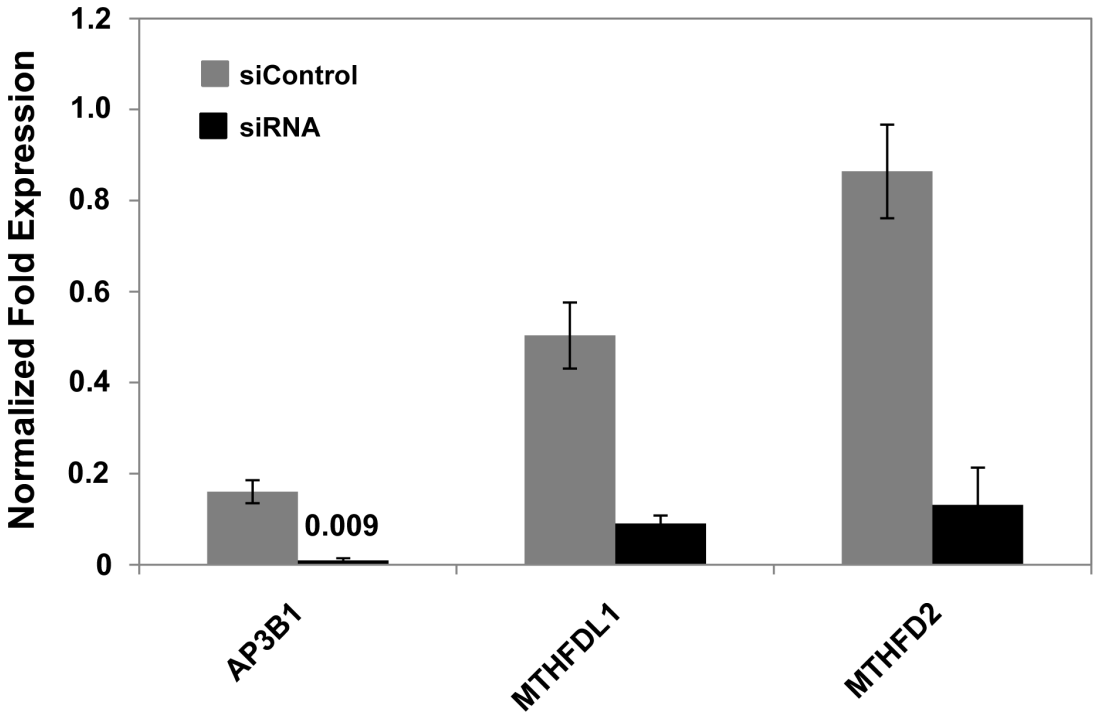

Figure 4.12: AP3B1, MTHFD1L and MTHFD2 mRNAs are knocked down using siRNAs.

qRT-PCR analysis of MCF-7 cells following siRNA transfections of AP3B1, MTHFD1L and MTHFD2 showed knockdown effect in mRNA expression compared to siControl transfected cells.

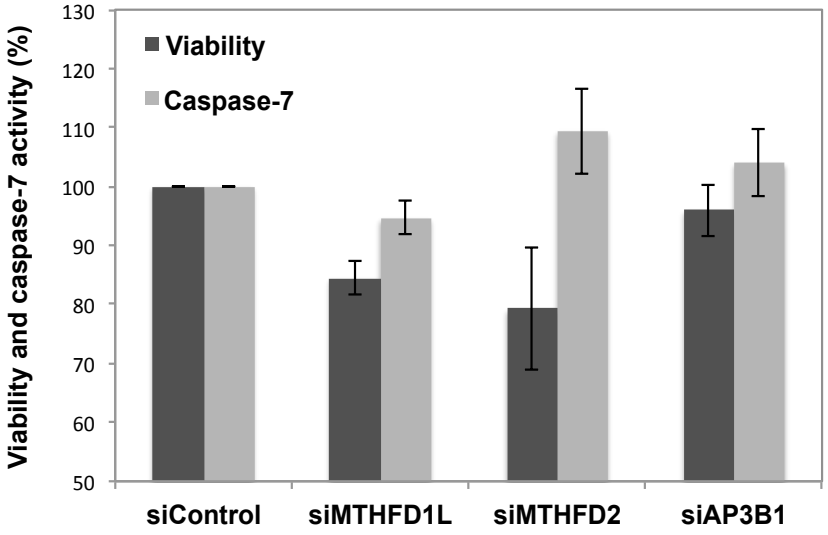

Figure 4.13: siRNA for MTHFD2 decreases viability and increases caspase-7 production in MCF-7 cells.

ApoTox-Glo assay for Viability and Caspase 7 activity of siRNA transfected MCF-7 cells are shown as percentages (%). SiControl transfection was used as negative control.

4.3.9. Mir-9 and MTHFD2 show inverse expression patterns in primary breast cancer samples

To test whether mir-9 and MTHFD2 expression profiles correlate in clinical cancer samples, qRT-PCR analysis of mir-9 (also described in **section 4.3.1.**) and MTHFD2 expression in primary cancer samples (n=20) and normal samples (n=5) was performed. For three of the cancer samples and one normal sample no expression was detectable. Therefore, relative fold changes of mir-9 and MTHFD2 in 17 cancer samples (8 non-metastatic and 9 metastatic) compared to 4 normal samples. The mean of 4 samples in mir-9 and MTHFD2 were taken independently and set to one. The relative fold changes in mir-9 and MTHFD2 were compared to corresponding controls (mean of normal samples) and presented as relative fold change (Log2 ± SE) in the graph **(Figure 4.14).** In six out of eight non-metastatic samples mir-9 and MTHFD2 show an inverse expression profile whereas in non-metastatic samples the trend was less obvious where four out of nine samples showed an inverse expression profile.

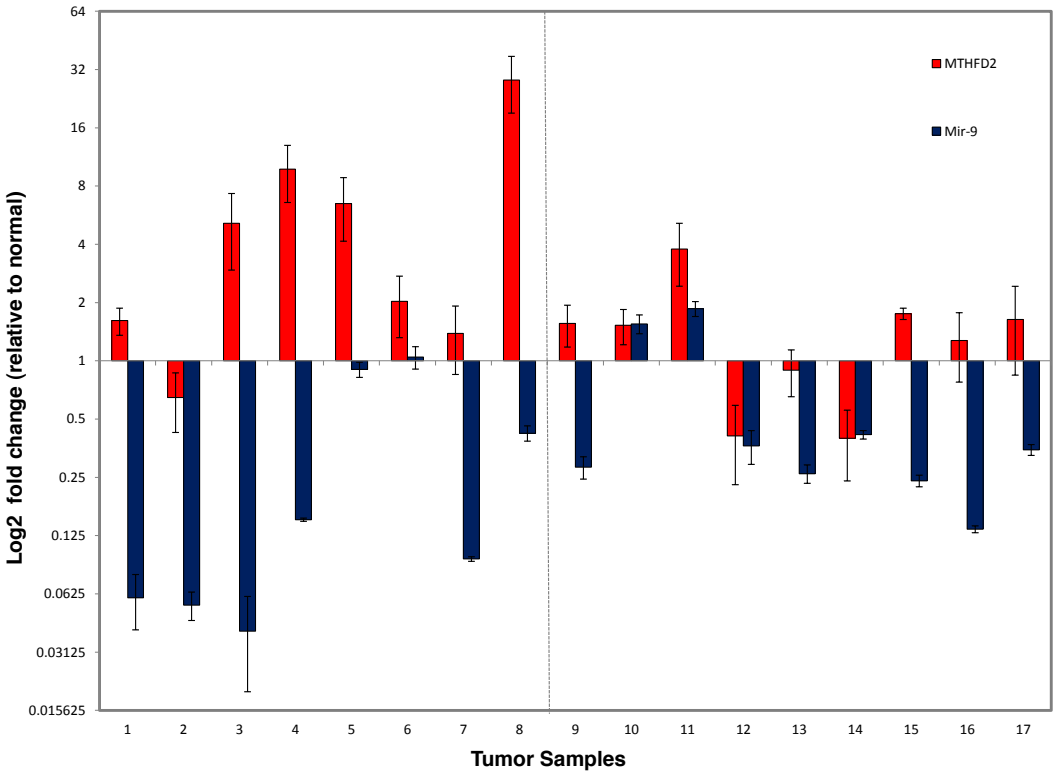

Figure 4.14: Mir-9 and MTHFD2 show inverse expression profiles in breast cancer samples.

qRT-PCR analysis of mir-9 and MTHFD2 in 17 primary breast cancer samples (8 non-metastatic; samples 1-8 and 9 metastatic; samples 9-17) are presented relative to normal samples (n=4). Values are represented as Log2 fold changes ±SE relative to normal samples (mean of 4 samples set to one). GAPDH and RNU6B were used as housekeeping controls in normalizations of MTHFD2 and mir-9 expressions, respectively.

4.3.10. ANXA2 and CSDA pseudogenes retain mir-9 seed region

In the microarray analysis results, described in **section 4.3.4**, in addition to ANXA2, one of its three pseudogenes ANXA2P1 was also identified as downregulated in mir-9 overexpressing MCF-7 cells. Similarly, in addition to CSDA downregulation, its single pseudogene CSDAP1 showed downregulation in mir-9 overexpressing MCF-7 cells. Recent findings suggest that pseudogenes with similar mRNA sequences to their parent genes' 3UTRs can also be targeted by microRNAs and act as microRNA decoys which limit the suppression of the gene by the microRNA [454, 455].

In total, ANXA2 has three known pseudogenes: ANXA2P1, ANXA2P2 and ANXA2P3. ANXA2P2 is not represented in the array (has no probes on the array) whereas ANXA2P1 and ANXA2P3 are represented. Although ANXA2P3 was downregulated in mir-9 overexpressing cells it was not significant after correcting for multiple testing. However, ANXA2P1 was significantly downregulated. All three pseudogenes were considered for further investigation in this study. Multiple sequence alignment of all isoforms of ANXA2 and its pseudogenes identified that the mir-9 seed region (CCAAAGA) was conserved in all of the pseudogene forms except ANXAP2. ANXA2P2 showed very divergent sequence such that a successful alignment was not possible and it did not contain a mir-9 seed region **(Figure 4.15)**. CSDA has only one pseudogene reported; CSDAP1. Both CSDA and CSDAP1 were identified as downregulated in mir-9 overexpressing MCF-7 cells (pre-9) in the microarray analysis. Multiple sequence alignment of all CSDA isoforms and CSDAP1 showed that the mRNA sequence of CSDAP1 is highly conserved including the mir-9 seed region **(Figure 4.16).**

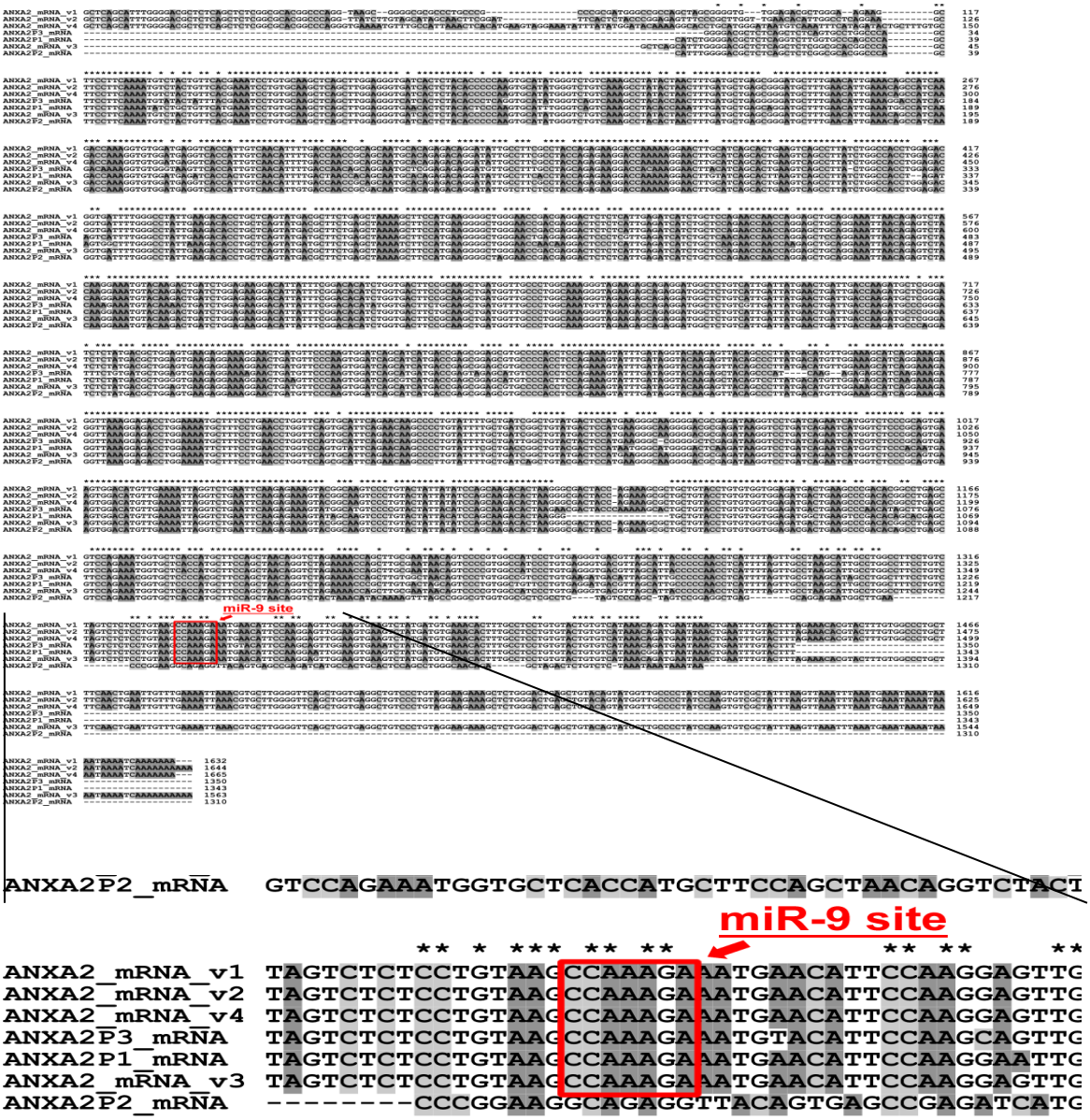

Figure 4.15: Mir-9 seed is conserved in ANXA2 and its two pseudogenes

Alignment of ANXA2 and its pseudogenes using ClustalW are shown. Mir-9 seed sequence is highlighted with red box.

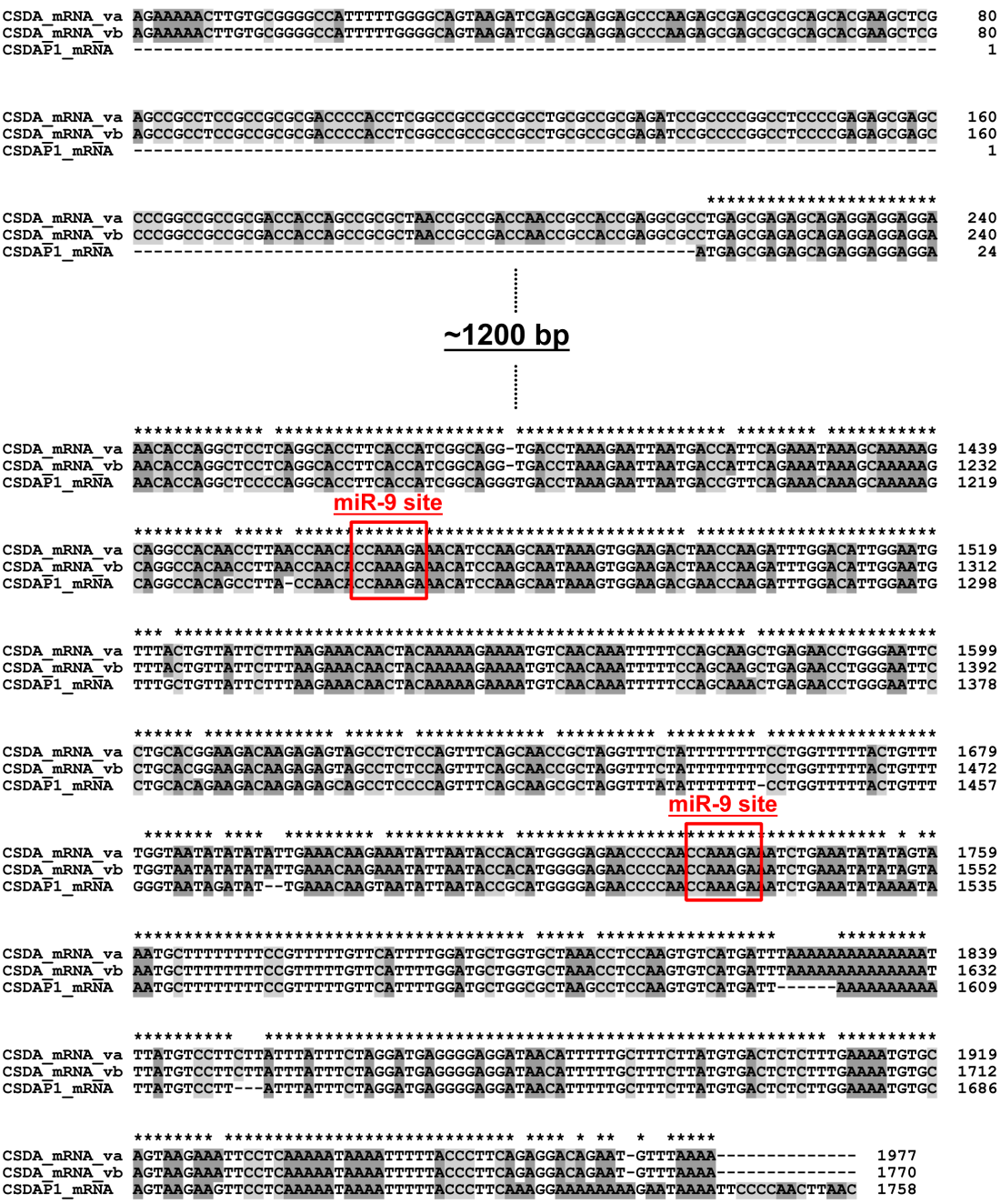

Figure 4.16: Mir-9 seed is conserved in CSDA and its pseudogene CSDAP1

Alignment of CSDA isoforms A and B and its pseudogene CSDAP1 using ClustalW are shown. Mir-9 seed sequence is highlighted with red box.

4.3.11. ANXA2 and CSDA pseudogenes are regulated by mir-9

To test whether the three ANXA2 pseudogenes (P1, P2 and P3) and CSDAP1 are regulated by mir-9, specific primers were designed **(primers: A.4.2.)** to selectively amplify ANXA2, CSDA and pseudogene sequences and qRT-PCR was performed. Primers designed specifically to detect expression of pseudogenes were analysed using regular PCR prior to qRT-PCR. MCF-7 cDNA was used as a template in the reaction and expected sizes were observed. However, non-specific bands were also visible on gel electrophoresis especially for ANXA2P1 and ANXA2P2 **(Figure 4.17A)**. ANXA2P3 and CSDAP1 showed single specific bands. Same primers were tested in qPCR using Sybr green assays and amplified products were separated in gel electrophoresis. Results showed that Sybr green-based amplification was specific to targeted products giving single bands with expected sizes **(Figure 4.17B)**. These results also confirmed the expression of these non-coding pseudogenes in MCF-7 cells.

QRT-PCR analysis showed that ANXA2 and ANXA2P3 endogenous levels (pre-ctr) were very similar whereas ANXA2P1 and ANXA2P2 showed much lower expression (pre-ctr) **(Figure 4.18)**. Results showed that as previously also shown in **Figure 4.9** ANXA2 expression was decreased in mir-9 overexpressing cells (pre-9) compared to control (pre-ctr). Similarly, ANXA2P3 expression showed decrease in response to mir-9 overexpression **(Figure 4.18)**. In contrast, ANXA2P1 and ANXA2P2 showed significant upregulation in response to mir-9 overexpression **(Figure 4.18)**. The decrease in ANXA2 protein levels is shown in **Figure 4.19**. CSDAP1 endogenous levels (pre-ctr) were similar to CSDA (pre-ctr) **(Figure 4.18).** Overexpression of mir-9 (pre-9) significantly decreased expression of CSDA as previously also shown in **Figure 4.9**. Similarly, CSDAP1 expression was decreased by mir-9 overexpression compared to pre-ctr down to the same levels as CSDA suppression **(Figure 4.18).** The decrease in CSDA protein levels is shown in **Figure 4.19.**

A

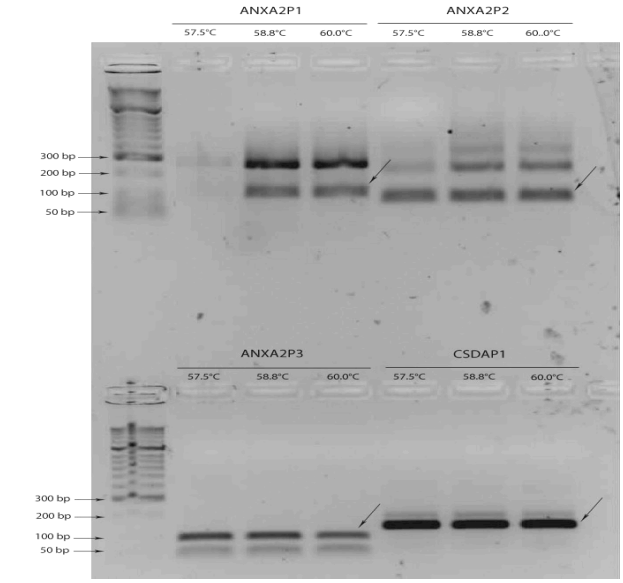

B

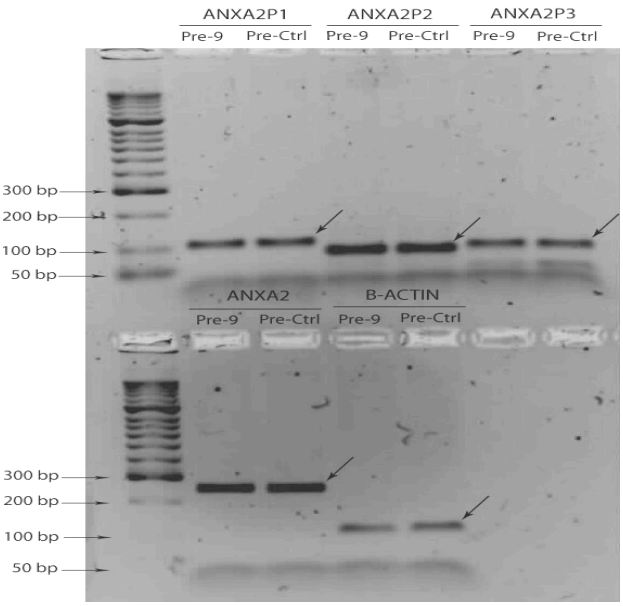

Figure 4.17: Gel electrophoresis of ANXA2 pseudogenes and CSDAP1.

Gel electrophoresis of **A)** PCR amplification of ANXA2 pseudogenes and CSDAP1 using 3 different melting temperatures and **B)** Sybr Green qRT-PCR amplification of ANXA2 pseudogenes and ANXA2. β-Actin was used as housekeeping control in Sybr Green qRT-PCR. Expected band are labeled with arrows.

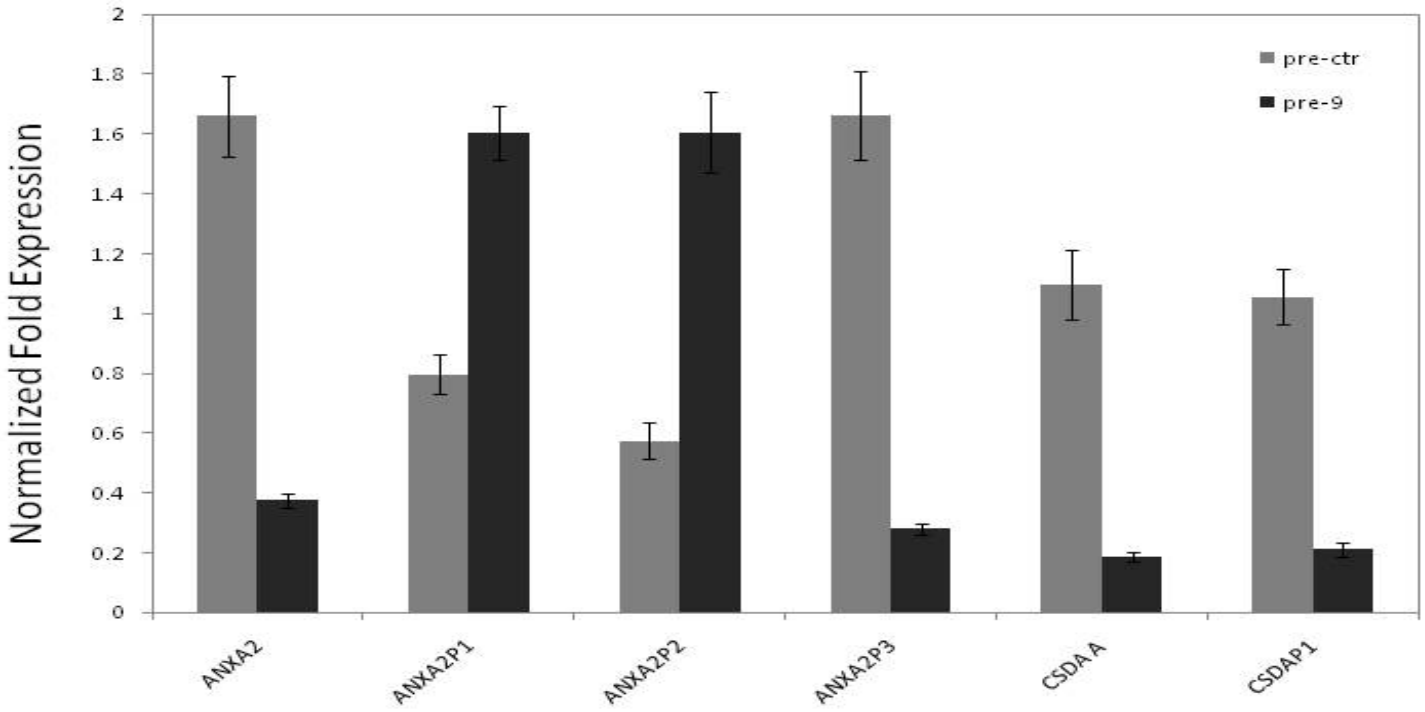

Figure 4.18: ANXA2, CSDA and their pseudogenes expressions change in mir-9 overexpressing MCF-7 cells.

qRT-PCR analysis of ANXA2, CSDA and their pseudogenes in pre-9 or pre-ctr transfected MCF-7 cells shows expression level changes as shown.

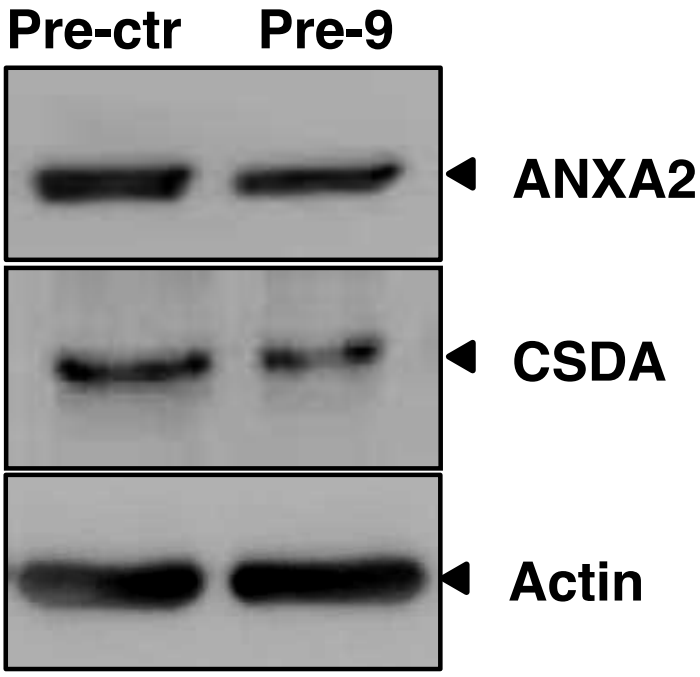

Figure 4.19: ANXA2 and CSDA proteins are downregulated in mir-9 overexpressing MCF-7 cells.

Western blot analysis of ANXA2 and CSDA proteins in pre-9 or pre-ctr treated MCF-7 cells is shown. β-Actin was used as loading control (lower lane).

4.3.12. Cloning of pseudogene mRNAs into pLight vector

To investigate whether the pseudogenes of ANXA2 and CSDAP1 are direct targets of mir-9 as well as their corresponding genes, luciferase reporter assays were performed. To clone the pseudogene mRNAs into reporter vector, first, specific primers were designed **(primers: A.4.1.)** and human genomic DNA was used as a template and products were amplified using a regular thermal cycler.

Gel electrophoresis of a gradient PCR was carried out to check the specificity of the primers and to optimize the reaction. An increase in the intensity of the expected bands (991 bp for ANXA2P1, 699 bp for ANXA2P2, 582 bp for ANXA2P3, 1085 bp for CSDAP1) with the increase of the temperature was observed. Increased annealing temperature also decreased the number of non-specific bands **(Figure 4.20A)**. The optimum temperature of annealing for PCR amplification of the pseudogene mRNAs (defined as 59.5°C) was used to amplify the samples before gel extraction **(Figure 4.20B)**. Following restriction enzyme digestion of an empty vector and PCR products with NheI and AvrII and gel extraction, the gel electrophoresis showed the specific bands of pseudogenes as well as empty vector samples before ligation. This confirmed the isolation of both specific inserts and empty vectors (**Figure 4.21**).

A

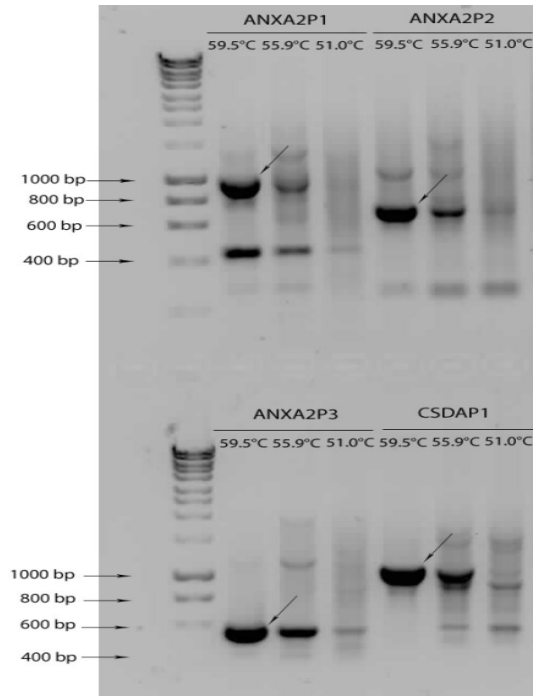

B

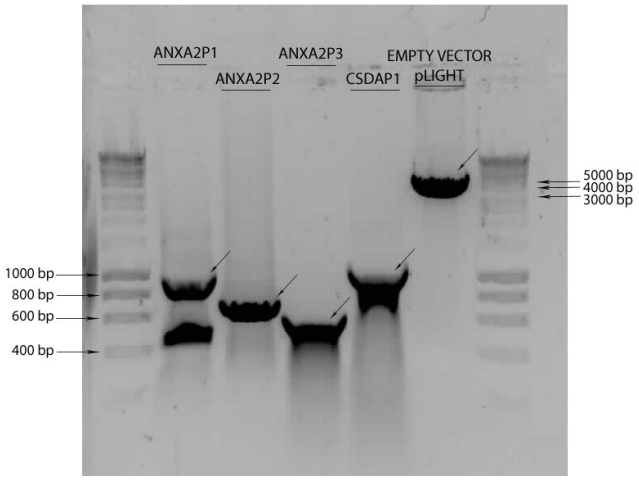

Figure 4.20: Gel electrophoresis of ANXA2 pseudogenes and CSDAP1 mRNA amplicons.

Gel electrophoresis of **A)** PCR amplified pseudogene mRNAs using three different annealing temperatures and **B)** Optimized PCR products after double digestion and before gel extraction. Expected sizes are labelled with arrows.

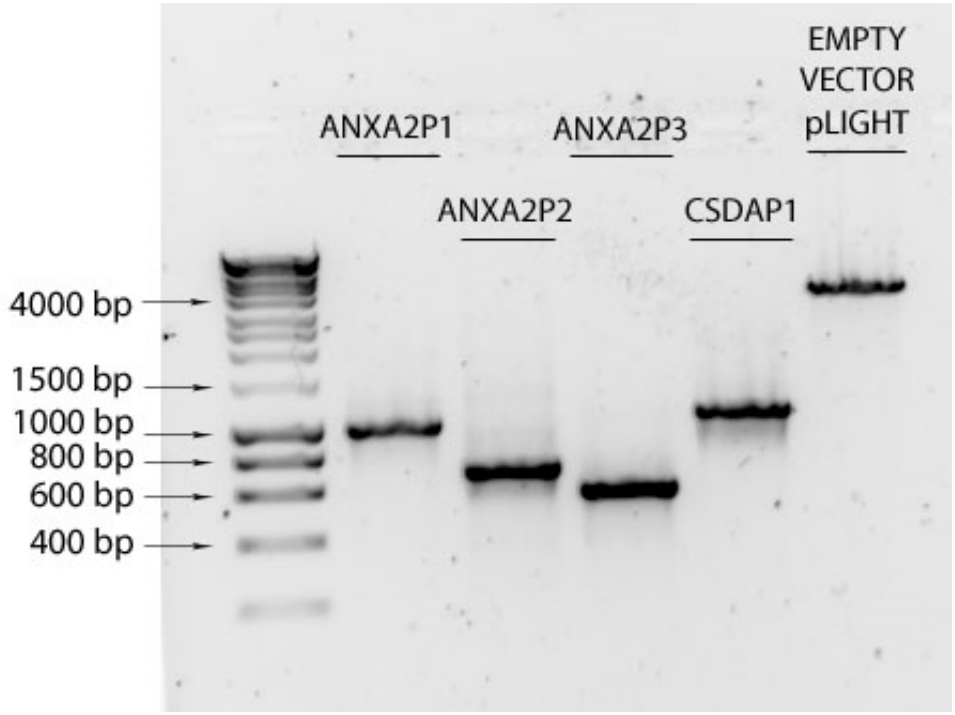

Figure 4.21: Gel electrophoresis of pseudogene mRNAs and pLight vector after double digestion.

Samples of 2 µl were run on the gel to check the specificity of the bands gel extracted before ligation is shown.

4.3.13. Positive colonies identified in colony PCR

Following cloning steps, some colonies were selected and tested in PCR reaction for the confirmation of insertion of the desired product into the pLight vector. Colony PCR showed a range of bands including expected sizes **(Figure 4.22)**. For the negative control, a pLight empty vector, an intense band was observed corresponding to the fragment amplified with the vector primers.

To confirm the presence of the insert, selected colonies were sent for sequencing. The obtained sequencing results were compared to the expected sequences and none of the ANXA2 pseudogenes gave the expected sequences. CSDAP1 was cloned successfully and the construct was designated as pLight/CSDAP1 UTR.

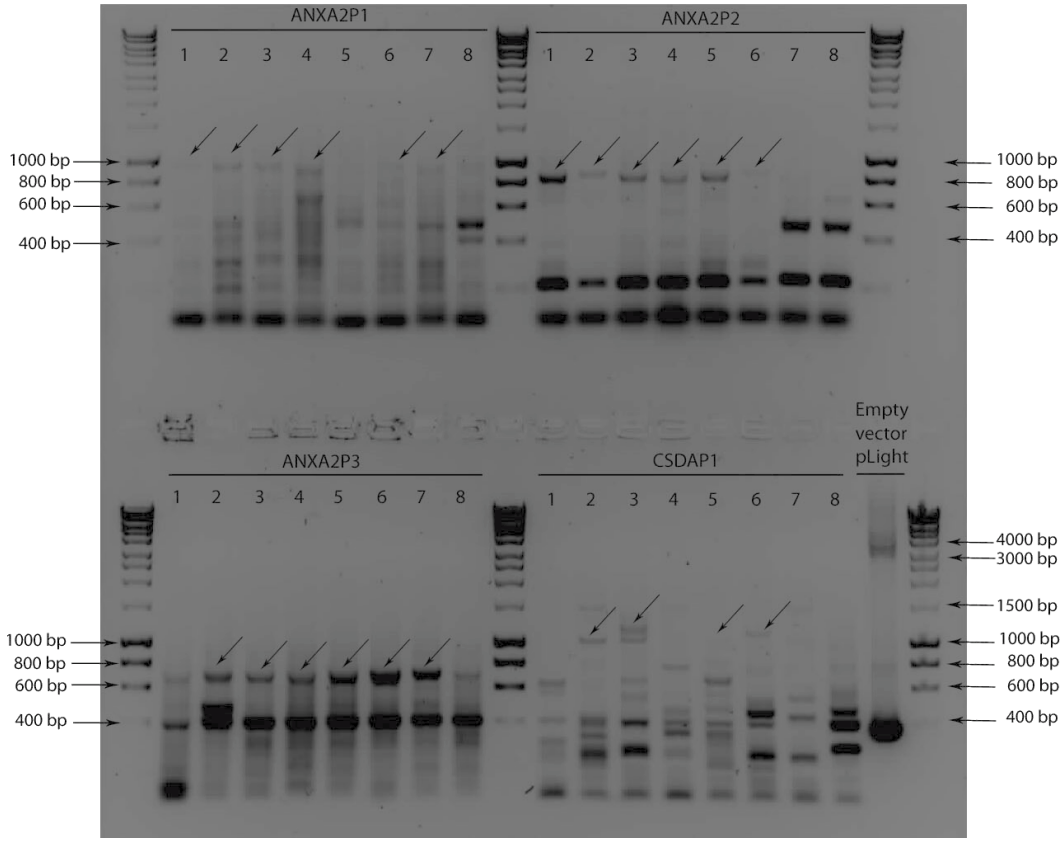

Figure 4.22: Gel electrophoresis of PCR of selected candidate colonies containing pseudogene mRNAs.

Colony PCR results for plasmids that contain pseudogene mRNAs are shown. Non-specific bands are observed and expected sizes for mRNAs are labeled with arrows.

4.3.14. CSDAP1 is a direct target of mir-9

Positive clones of CSDAP1 were grown and tested for mir-9 direct binding. The mir-9 seed region located in CSDAP1 mRNA was mutated generating a new construct designated as pLight/CSDAP1_mutUTR.

A Luciferase assay was performed in MCF-7 cells transfected with CSDAP1 mRNA reporter constructs containing wild type mir-9 seed and mutated mir-9 seed. Luciferase analysis showed significant decrease in luciferase reporter of CSDAP1 mRNA (CSDAP1 UTR) in mir-9 mimic (pre-9) compared to control (pre-ctr). This expression was restored significantly in the construct missing the mir-9 seed region (pLight/CSDAP1_mutUTR) **(Figure 4.23A)**. SiRNA knockdown of CSDAP1 significantly ($p<0.05$) reduced CSDAP1 and CSDA mRNA levels detected by qRT-PCR **(Figure 4.23B).**

A

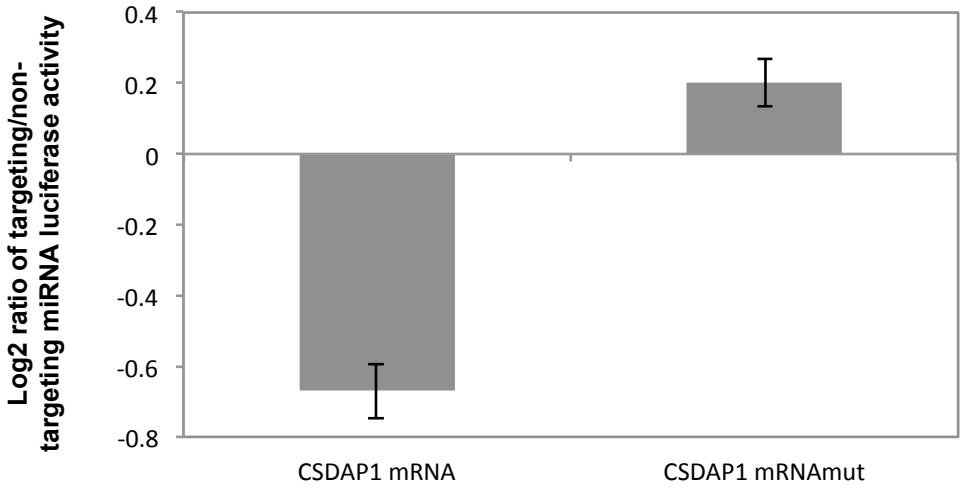

B

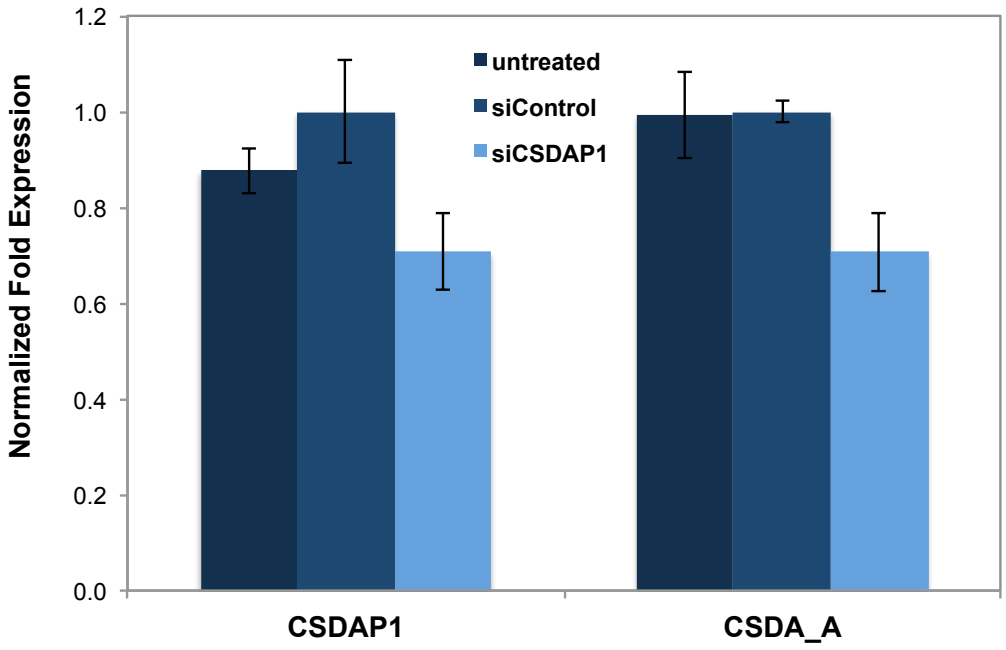

Figure 4.23: CSDAP1 mRNA is a direct target of mir-9 and acts as mir-9 sponge in MCF-7 cells.

(A) Log2 ratios of pre-9/pre-ctr are represented for CSDAP1 mRNA and CSDAP1mut (mir-9 seed mutated) constructs transfected into MCF-7 cells are shown. **(B)** qRT-PCR analysis of CSDAP1 and CSDA mRNAs following transfection with siControl or siCSDAP1 or untreated. T-test showed significant downregulation in both mRNAs ($p<0.05$). β-Actin was used as housekeeping control in normalizations.

4.4. Discussion

In the last decade dysregulation of miRNAs has been shown in several cancer types leading to overexpression of oncogenes or downregulation of tumor suppressors. In addition, the expression profiles of microRNAs can differentiate cancer cells from normal cells [75, 456, 457]. Detailed characterization of microRNAs and their targets involved in cancer networks is critical to elucidate their role in carcinogenesis and to identify novel cancer biomarkers for developing effective anti-cancer therapies [116, 458, 459].

In recent studies, although there are cases where overexpression of mir-9 in cancer cells/tissues is reported [315], mir-9 has emerged mainly as potential tumor suppressor miRNA and cancer biomarker due to its significant downregulation in many cancer types mostly due to aberrant methylation at the mir9 locus [163, 314]. It is important to study the mechanisms that mir-9 is involved to elucidate its potential in cancer therapeutics.

Endogenous mir-9 levels are lower in breast cancer cells compared to normal cells

The endogenous levels of mir-9 in breast cancer cell lines tested compared to normal breast tissue indicated that mir-9 levels are lower in cancer cell lines. Similarly, detection of mir-9 levels in primary cancer samples compared to normal breast tissues showed that in 16 out of 20 (80%) tumor samples mir9 levels were lower **(Figure 4.1)**. Four tumor samples showed significantly higher mir-9 expression compared to 4 normal cells tested (data not shown). However, this outlier behavior did not correlate to any of the background information provided (grade, disease stage, etc.) for those cell lines. This suggests evidence for heterogeneous expression of mir-9 in breast tumor samples where the majority (80%) of the samples show lower levels of mir-9 compared to

normal cells. The heterogeneity of mature mir-9 expression levels observed in previous studies on cancer has revealed a conflict as to whether mature mir-9 expression levels are higher or lower in cancer samples compared to normal samples [174, 314, 316]. This pilot experiment provided an initial screen of clinical cancer samples, and raised the need for testing larger number of samples to determine the extent of downregulation of mir-9 in breast tumor cells compared to normal.

In summary, mir-9 is downregulated in breast cancer cell lines. Similar or greater levels of mir9 expression can be achieved using synthetic oligonucleotides compared to plasmid driven ectopic expression with the tested concentrations in this study (50 nM precursor and 1 µg plasmid). However, to make a stronger claim for a general trend of downregulation of mir-9 in cancer cells and tissues, large number of samples should be considered.

Ectopic expression of mir-9 shows anti-proliferative activity

Mir-9 was overexpressed using two approaches; precursor plasmids and synthetic oligonucleotides. In plasmid based ectopic expression of mir-9 high levels of mature mir-9 was achieved that significantly decreased cell proliferation compared to controls. However, the plasmid transfections caused higher cell toxicity (high amounts of cell death) compared to synthetic oligonucleotides. In addition, the simultaneous expression of mir-9* that is processed from the precursor mir-9 plasmid was observed indicating that mir-9* is also processed from this precursor within the cells. However, mir-9* was expressed in much lower levels than mir-9 in pc-9-1 transfected cells, indicating that there may be differential regulation in processing of precursor mir-9 and mir-9* could be degraded or less stable as previously assumed for all miRNA star form [460]. Despite the low induced expression levels of mir-9* by precursor plasmid it cannot be neglected that this induction could have biological significance in the cells as is reported for some microRNA star forms [461-463]. Consequently, a

question is raised that whether the phenotypic effect observed is solely by mir-9 or a combinatorial effect of both mir-9 and mir-9*. This is a topic which has never been addressed in the literature before. Therefore, to investigate the individual effects of mir-9, synthetic oligonucleotides designed to overexpress specifically mir-9 were used in downstream experiments.

Cell viability was significantly decreased and caspase-3/7 activity increased as a hallmark of apoptosis indicating an anti-proliferative and apoptotic activity of mir-9 in cancer cells. No significant change in invasion of MCF-7 cells was observed when mir-9 was overexpressed. This can be due to poorly invasive nature of MCF-7 cells (ER+) [464] or incompetence of mir-9 to transform non-invasive cells to invasive phenotype. In contrast, mir-9 overexpression was able to reduce the invasiveness of MDA-MB-231 cells which is known to be highly invasive (ER-) confirming the potential of mir-9 as co-regulator in invasion process but not solely sufficient for transformation. The transformation process may require other or additional components (combinatorial) where mir-9 could only contribute to enhancing the process.

Microarray profiling of mir-9 overexpression identifies many direct and secondary targets

Although implicated in cancer by several studies, no genome-wide transcriptome analysis of mir-9 expression has to date been reported. This study demonstrates that mir-9 overexpression in breast cancer cells in two dosages (1X and 2X) identifies many mir-9 responsive genes including several predicted targets. The number of differentially expressed genes common in both dosages was higher than the individual effects of each dosage **(see Venn diagram Figure 4.7)**. The similar expression profile by both dosages confirms the accuracy of the experiment as can be considered as pseudo replicates. The fold changes identified in microarray for 1X or 2X treated samples did not show any linear dosage effect **(section A.1.8.).** This indicates that no linear dosage effect can be

detected in this platform using these two dosages. The lack of a linear correlated dosage effect could be due to saturation of mir-9 intake into cells or limitations of the platform. Considering the highly similar differential expression profile in both dosages and no linear dosage effect identified, the list of responsive genes independent of the dosages (intersection of both dosages) were taken for further downstream analyses.

SylArray enrichment analysis of the differentially expressed gene list showed enrichment for mir-9 seed region in downregulated genes. This provides a confirmation of the results that significant numbers of downregulated genes contain putative mir-9 binding sites (seed sequence) in 3'UTR. This is also consistent with the previous findings on microRNA-directed global mRNA downregulation [44]. The short list of 25 genes including predicted targets were validated using qRT-PCR.

Six genes are direct targets of mir-9 and suppression of MTHFD1L and MTHFD2 mimic the anti-proliferative effects of mir-9 overexpression in MCF-7 cells

Most of the genes that were confirmed by qRT-PCR were selected from cancer-relevant functional categories such as cell migration, cell proliferation, apoptosis, and cell death. Among those selected, six predicted targets (AP3B1, CCNG1, LARP1, MTHFD1L, MTHFD2 and SRPK1) were tested for mir-9 targeting and confirmed by reporter gene assays using seed region mutated constructs. In addition, all proteins tested showed negative correlation with mir-9 levels. These results showed that mir-9 binds to putative sites on the 3'UTR of these genes and transcriptionally downregulates mRNA levels that in turn reduced their protein levels.

Some of the targets identified in this study have been previously reported to function in carcinogenesis as potential oncogenes. For example, CCNG1 (Cyclin-G1), a p53 target, has been implicated in several cancer

types [350, 465-468]. Functional studies with siRNA knockdown of CCNG1 decreased growth rate and invasion [350]. LARP1 (La ribonucleoprotein domain family, member 1), functions in vesicle transport. Silencing of LARP1 increased apoptosis in HeLa cells [348]. Functioning in alternative splicing, SRPK1 (SRSF protein kinase 1) has been implicated in many cancer types [356, 358, 469-471] and siRNA knockdown of SRPK1 resulted in increased apoptotic potential in breast and colonic tumor cell lines [356], and decreased proliferative capacity in leukaemic cells [472]. These findings indicate the oncogenic potential of CCNG1, LARP1 and SRPK1 in cancer cells.

In contrast, AP3B1 (AP-3 complex subunit beta-1), involved in organelle biogenesis, has been reported in cancer in only a few studies [359, 361] but no knockdown experiments have been performed as of yet to define its functional role in cancer cells. These results are the first report on knock down of AP3B1 investigating potential effects on cancer cells.

MTHFD1L (methylenetetrahydrofolate dehydrogenase (NADP+ dependent) 1-like), functions in tetrahydrofolate synthesis in mitochondria, has been previously implicated in neural tube defects [473] and to date, no cancer link has been described for this gene. Here, loss-of-function analysis of MTHFD1L (siRNA) has been reported for the first time in mammalian cell lines.

MTHFD2 (methylenetetrahydrofolate dehydrogenase (NADP+ dependent) 2), a mitochondrial bifunctional enzyme, has been implicated in breast cancer recently [353] but no silencing experiments have been reported. In this study, the knockdown effects (siRNA) on MTHFD2 have been investigated for the first time.

The lack of experimental evidence on loss-of-function effects on cancer biology of these three genes (AP3B1, MTHFD1L and MTHFD2) make them ideal candidates to investigate these genes for their possible involvement in breast carcinogenesis using siRNA approach.

Based on ApoTox-Glo and flow cytometry analyses, siRNA knockdown of MTHFD1L, MTHFD2 and AP3B1 in MCF-7 cells indicated that MTHFD1L and MTHFD2 could be involved in regulating viability and apoptosis in cancer cells **(Figure 4.3.8. and section A.3.17)**. Downregulation of MTHFD2 showed decreased viability and increased apoptosis, which mimics the effect of mir-9 overexpression indicating that suppression of MTHFD2 by mir-9 could contribute in anti-proliferative effect observed in cells overexpressing mir-9. In contrast, MTHFD1L and AP3B1 showed no significant effect on viability and apoptosis analyzed by ApoTox-Glo assays.

In addition, flow cytometry analysis was performed in siRNA transfections. The mock (siControl) showed high levels of apoptotic cells (Annexin positive), which could be due to long exposure of cells to Annexin, stain during the process of flow cytometry. However, all the samples are stained for the same time and therefore the results are compared to siControl sample. SiMTHFD1L and siMTHFD2 showed significantly increased levels of apoptotic cells compared to the siControl. In contrast, siAP3B1 showed slightly decreased apoptosis compared to the siControl.

These results indicate that knockdown of MTHFD1L and MTHFD2 can recapitulate mir-9 overexpression effects on apoptosis, therefore mir-9 mediated suppression of MTHFD1L and MTHFD2 expression could contribute to anti-proliferative and apoptotic activity in MCF-7 cells. The no change or contradictory results obtained from both methods (ApoTox-Glo and flow cytometry) could indicate that individual suppression of MTHFD1l and AP3B1 may not be sufficient to change viability or apoptosis in cancer cells; however, in combination with suppression of other genes and factors these genes would still have potential in contributing tumorigenesis which requires further investigation.

In addition to the finding that MTHFD2 knockdown recapitulates mir-9 overexpression effects such as decreased viability and increased apoptosis, the mRNA expression levels of MTHFD2 and mir-9 were compared using qRT-PCR across the clinical cancer samples. The results

indicated a general trend of inverse correlation between mir-9 and MTHFD2 expression levels.

In the non-metastatic samples the inverse relationship between mir-9 and MTHFD2 expressions was more obvious compared to the non-metastatic samples. The results may indicate that the inverse correlation in mir-9 and MTHFD2 observed in cancer samples may hold promise as a potential biomarker for breast cancer. Although the trend did not apply to all samples where in some samples both mir-9 and MTHFD2 showed decrease or increase, these findings might provide preliminary results for highlighting the potential of this interaction in breast cancer that should be screened in larger sample groups (& likely in combination with other miRNAs which display probabilistic promise as biomarkers).

CSDAP1 acts as a mir-9 sponge in MCF-7 cells

In addition to six direct targets of mir-9 that have been validated in this study, ANXA2, its three pseudogenes P1, P2 and P3, and CSDA and its pseudogene CSDAP1 were also tested for mir-9 targeting in MCF-7 cells. The mir-9 seed region is conserved in two ANXA2 pseudogenes (ANXA2P1 and ANXAP3) and in CSDAP1. The qRT-PCR test for all these genes in mir-9 overexpressing MCF-7 cells (pre-9) showed decreased expression levels in ANXA2, ANXA2P3, CSDA and CSDAP1. The decrease in ANXA2 and CSDA was also confirmed at protein level. ANXA2P1 and ANXA2P2 mRNAs showed increased expression levels in mir-9 overexpression (pre-9) compared to control (pre-ctr). A decrease in CSDA, CSDAP1, ANXA2, ANXAP1 and ANXA2P3 expression would be expected due to presence of the mir-9 binding site. However, the observed increase in ANXAP1 and ANXAP2 may not necessarily be a direct effect of mir-9 but can be due to other regulatory mechanisms (i.e. interplay) between ANXA2 and its pseudogenes as a part of secondary effect of mir-9 overexpression.

A recent study on PTEN identified its pseudogene, PTENP1, as microRNA decoy, which can limit the access of microRNA to PTEN 3'UTR, keeping the PTEN levels still functional [454, 474]. Based on this evidence, the changes in ANXA2, CSDA and their pseudogenes may indicate a similar mechanism where these pseudogenes are acting as mir-9 sponges. This is the second report of such a case to be described.

To test whether CSDA, ANXA2 and their pseudogenes are targeted by mir-9, luciferase reporter constructs were generated. Cloning of ANXA2 pseudogenes was challenging and unsuccessful after several trials. Although colony PCR test showed positive clones the sequencing revealed the presence of unintended products. However, the cloning of ANXA2, CSDA 3'UTRs and CSDAP1 mRNA was successful and additional constructs were generated with mutated mir-9 binding sites. Luciferase reporter assays confirmed that ANXA2 is directly targeted by mir-9 in MCF-7 cells. Similarly, CSDA 3'UTR was directly regulated by mir-9. In addition, CSDAP1 showed direct targeting by mir-9 indicating that CSDAP1 acts as mir-9 decoy whereby availability of CSDAP1 mRNA for mir-9 regulation "sponges" mir-9 to lessen the suppression effect on CSDA. To prove this, siRNA knockdown of CSDAP1 mRNA followed by quantification of changes in CSDA (restoration of the expression) was performed. Knockdown of CSDAP1 also decreased CSDA mRNA levels mimicking the effect that mir-9 directed downregulation of CSDAP1 can reduce also CSDA levels. This indicates that CSDAP1 can act as mir-9 sponge saving CSDA from severe mir-9 directed downregulation and when knocked down the release of mir-9 from CSDAP1 mRNA cause stronger (more) binding of mir-9 to CSDA 3'UTR.

In summary, this is the first report identifying global effects of mir-9 overexpression on the breast cancer transcriptome. Here, a total of eight mir-9 predicted targets were confirmed as direct targets with an additional pseudogene mir-9 decoy (CSDAP1). Several other cancer-related genes were confirmed as indirectly regulated by mir-9. Given the established roles of ANXA2, CCNG1, SRPK1 and LARP1 in cancer, it is likely that loss

of mir-9 regulation in cancer cells is critical for these oncogenes to escape from mir-9 mediated suppression to promote tumorigenesis. In addition, novel potential oncogenes have been identified with their suppression by mir-9 linked to anti-proliferative and apoptotic activity of mir-9 overexpression. Ectopic expression of mir-9 in cancer cells holds great cancer biomarker and drug target potential in regulating these potential oncogenes to suppress cell proliferation and re-activate apoptotic pathways in breast cancer cells.

CHAPTER 5: Genome wide effects and functional analysis of mir-9* (mir-9 star) in breast cancer cells

5.1. Background: MiRNA* (star) forms and mir-9*

MicroRNA processing leads to a ~22 nucleotide duplex comprised of the mature microRNA derived from the 3' or 5' arm of the hairpin precursor. Initial findings on the fate of miRNA duplex indicated that one of the strands is favored and loaded in the RNA induced silencing complex (RISC) and leads to targeting of (primarily) 3'UTRs of mRNAs. The other strand which has a shorter half-life (or expressed at very low levels) incorporate into RISC less [475].

However, recent findings using next-generation sequencing have demonstrated significant accumulation of numerous miRNA* forms as well as their duplex partners ('active' miRNAs) during some developmental stages of the silkworm [20] and also in humans [476]. In addition to being found in the AGO complex, miRNA* have been shown to have conserved seed matches to 3'UTR of mRNAs [19, 22]. The target regulation by miRNA* species seems to be also related with their degree of nucleotide conservation with the target mRNA [21, 22]. Therefore, miRNAs* are also loaded into the RISC and therefore able to regulate target genes as well as their duplex partners [477, 478].

Mir-9 has been recently shown to be involved in cancer by several studies as reviewed in **sections 1.4 and 4.1**. The sequence from the opposing arm of the duplex cleaved from mir-9 precursor is called mir-9*. It is 22 nucleotides long with three mismatches compared to the mature mir-9 and a 2 nt overhang at 5' (http://www.mirbase.org/). Recently, Mir-9* was shown to involve in Huntington's disease and cancer. Mir-9* was first reported in Huntington's disease where a double negative feedback loop that involves mir-9 and mir-9* targeting two components of the REST complex (REST and CoREST, respectively) was described [326]. In addition, the conversion of human fibroblast into neurons was shown to be triggered by miR-9 and miR-9* in combination with miR-124b and neurogenic transcription factors [479].

Moreover, overexpression of mir-9* was shown in brain tumors and considered as a biomarker for brain primary tumors [18]. This followed another study showing that mir-9* expression was suppressed by inhibitor of differentiation 4 (ID4) which restored the expression of SOX2 (mir-9* target) and this consequently increased levels of ABC transporters which raised stemness potential and chemoresistance of glioma cells [480].

Burkitt's lymphoma is characterized by translocation of MYC gene under the control of immunoglobulin gene regulatory elements. Heterogeneous expression of mir-9 was observed in Burkitt's lymphoma tumors and mir-9* was shown to be strongly downregulated in Burkitt's lymphoma MYC translocation negative cases [481]. An inverse correlation between mir-9* and E2F1 was observed in determining the pathological role of mir-9* in MYC translocation negative Burkitt's lymphoma cases. Ectopic upregulation of mir-9* reduced E2F1 levels and conversely mir-9* silencing induces E2F1 expression, and thereby causing MYC overexpression [481].

MicroRNA profiling studies have shown higher levels of mir-92b and mir-9* in glioma tissues [327] and brain primary tumors compared to non-brain tumors [18]. In addition, a combination of mir-92 and mir-9* expression is sufficient to identify brain metastases from primary brain tumors with 88% sensitivity and 100% specificity [18]. Thus, together mir-92 and mir-9* expression represent potential biomarkers to classify primary and secondary brain malignancies.

5.1.1. Aim

To study microRNA function in cells, ectopic expression of microRNA precursors using mammalian expression vectors that contain stem-loop precursors is a common approach [482, 483]. However, ectopic expression of a precursor ensures processing of both strands (guide and

passenger) and passenger strands (miRNA*) may not necessarily be degraded (whether the precursor is generated from an endogenous locus or an ectopic construct). This may cause ectopic expression of both strands in cells and may interfere to analyze individual effects of each strand.

The research carried on mir-9, described in chapter 4, initially involved overexpression of mir-9 using precursor plasmids (pc-9-1). The qRT-PCR analysis of mir-9 and mir-9* in these cells identified a favored processing of mir-9 compared to mir-9*. However, compared to untreated cells the levels of mir-9* was increased to a level that may or may not be biologically significant. Therefore, to eliminate the possibility of interference by increased mir-9* expression, synthetic oligonucleotides (commercially available) were used to individually express each miRNA species (i.e. mir-9 versus mir-9*). The functional investigation of mir-9 has been described in chapter 4.

The aim of this chapter is to profile the individual effects of mir-9* ectopic expression in cancer genome using whole genome microarray profiling and to identify functional impact and direct targets of mir-9* in breast cancer cells.

5.2. Materials and Methods

5.2.1. Tissue culture and reagents

Human breast cancer cell lines MCF-7 and MDA-MB-231 were cultured in complete DMEM and maintained as described in **section 2.2.1**. Mir-9 overexpression synthetic oligonucleotides (pre-9*) and control oligonucleotide (pre-ctr) (ABI, UK, #AM17100) were used in 50nM final concentration in all experiments.

5.2.2. Mir-9* overexpression and transfections

To study the effect of overexpression of mature mir-9*, initially a pcDNA-9-1 construct was used in transfections as described in **section 4.2.2**. In addition, synthetic oligonucleotides were used to ectopically express mir-9* for final concentration of 50 nM. The day before transfections, cells were seeded at a density of $2x10^5$ cells per well in six-well plates. 48hr post-transfection of pre-9* or pre-ctr, cells were harvested using cell scrapers, snap frozen in liquid nitrogen for long term storage or proceeded with RNA and protein isolations.

5.2.3. RNA isolation and quantitative RT-PCR

Total RNA was isolated using a Nucleospin miRNA kit (Macherey-Nagel, Germany) **(protocol: A.3.13.)**. Quantity measurements of total RNA were performed using an Implen nano-photometer. Quality measurements prior to microarray experiments were done using a Bioanalyzer (Agilent Technologies, USA).

Mir-9* levels were quantified by real time microRNA RT-PCR as previously described in **section 2.2.7** using specifically designed primers and probes

(Taqman mir-9* assay, ABI, UK). A U6 small RNA (Taqman RNU6B assay, ABI) was used as housekeeping gene for Relative Quantification. For qPCR analysis of mir-9* predicted target, ITGB1, specific primers were designed **(protocol: A.3.1.)** and a Sybr green assay was used for detection as previously described in **section 2.2.8.** The data was analyzed by using the ΔΔCt method.

5.2.4. Microarray profiling and data analysis

For microarray analysis, $2x10^5$ cells were seeded on six-well plates the day before transfections. Following day, 50nM of pre-9* or pre-ctr were transfected **(protocol: A.3.10)**. 48hr post-transfection, cells were harvested using cell scrapers and total RNA isolation was performed **(protocol: A.3.13.).** 100ng of RNA was used as starting material in cDNA synthesis followed by labeling and hybridization into GeneChip Human U133A 2.0 arrays (#520065, Affymetrix Inc, USA) in triplicates. Arrays were washed and scanned according to manufacturer's protocol **(protocol: A.3.16)**.

Quality assessment of hgu133a2 arrays was performed using arrayQualityMetrics package in Bioconductor [255, 256]. The arrays were normalized using RMA method in the affy package in Bioconductor [257]. Probe set-to-locus mappings for the arrays were provided by the hgu133a2.db package [484]. Probe sets matching no or several loci were filtered out. Also, redundant probe sets that represent the same locus several times were counted only once (using the probe set with the greatest interquartile range) using featureFilter function in the genefilter package [259]. Differentially expressed genes were identified using linear modeling and moderated t-tests using the LIMMA package [260]. Adjusted p-values were calculated using FDR method [261]. Confidence thresholds of adjusted p-value < 0.05 and signal log ratio (SLR) > log2(1.2) were used. Putative microRNA targets and seed region enrichment was identified using SylArray [485] (http://www.ebi.ac.uk/enright-srv/sylarray/)

using the list of all genes ranked according to t-statistic. GO term enrichment analysis was performed using conditional hypergeometric tests.

5.2.5. Cell proliferation (Acid Phosphatase) and ApoTox-Glo Assays

The day before transfection $2x10^3$ MCF-7 cells per well were seeded in 96-well plates in eight technical replicates. Following day, for cell proliferation, cells were transiently transfected with one µg of pcDNA or pc-9-1 construct **(protocol: A.3.10)**. The rate of cell proliferation was assessed at 48hr post-transfection, using an acid phosphatase assay **(protocol: A.3.6.)**. For ApoTox-Glo assays, cells were transfected with 50 nM of pre-9* or pre-ctr oligonucleotides and 48hr post-transfection viability and caspase-3/7 activity were measured **(protocol A.3.7.)**.

5.2.6. Wound healing and invasion assays

To test migration of MCF-7 cells, cells were grown to full confluence and wounded by pipette tip. Following transfection with pre-9* or pre-ctr (50 nM) images of the cells were taken under an inverted microscope at 0, 24hr and 48hr. Three replicates of two independent experiments were performed. Only one of the experiments has been shown. For invasion assays, following transfection of pre-9* or pre-ctr, $2.5x10^4$ cells (in serum starving medium 0.1% FBS DMEM) were transferred into matrigel invasion chambers, 24-well plates (BD Biosciences, Germany, #354480) (matrigel coated membrane with 0.8 µm pore size). 10% FBS containing DMEM was added to the lower compartment and incubated at 37˚C. The non-invaded cells were removed from the insert by a cotton swab. The invaded cells were fixed in 100% methanol, stained by 0.5% crystal violet and counted. The number of stained cells from images was counted from multiple parts of the membrane **(protocol: A.3.9.).**

5.2.7. Cloning mir-9* predicted target ITGB1

ITGB1 has three putative mir-9* binding sites in its 3'UTR. These predicted binding sites are located at positions 52, 365 and 594 of ITGB1 3'UTR (www.microrna.org). Initially, to test mir-9* binding, the putative site starting at 365 was selected. ITGB1 3'UTR sequence was obtained from Ensembl database (www.ensembl.org). Primers were designed manually for maximum coverage of 3'UTR (1251 bp) and restriction sites for AvrII and XhoI were added to the 5' ends of the forward and reverse primers, respectively. Using the specific primers and human genomic DNA as a template, the ITGB1 3'UTR was amplified (1230 bp product size) and sub-cloned into pGEM-T vector. Sub-cloning protocol was used to amplify the RE digested insert and ligate into a pLight vector **(protocol: A.3.4.).** The construct was designated as ITGB1/plight and confirmed by sequencing.

Site directed mutagenesis of the mir-9* binding site was performed using a Quikchange Lightning Kit (Agilent Technologies, USA) **(protocol: A.3.5.).** The Mir-9* binding site 5'-TAGCTTTA-3'' was mutated to 5'-**A**A**C**C**A**T**A**T**T**-3' and the construct (ITGB1mut9/plight) was confirmed by sequencing with a pLight forward primer.

5.2.8. Luciferase assay

For luciferase analysis, cells were seeded in 24-well plates and co-transfected with 50 nM of pre-9* or pre-ctr and 100 ng of either of the UTR constructs (ITGB1/pLight, ITGB1mut9/pLight or pLight empty vector). 48hr post-transfection, cells were lysed in LightSwitch luciferase assay solution (Switchgear Genomics, USA, #L5010), incubated for 30 min at room temperature. Luminescence was read for 2 seconds in plate reader **(protocol: A.3.8.)**. Graphs are represented as changes in luminescence (log2) in pre-9* treatments, normalized to pre-ctr treatments.

5.3. Results

5.3.1. Endogenous and ectopic expression of mir-9*

To test the endogenous levels of mir-9* prior to microarray experiments, qRT-PCR was performed in MCF-7 cells and compared to normal breast RNA. Results showed that mir-9* levels were significantly higher in MCF-7 cells compared to normal breast tissue **(Figure 5.1A)**. To ectopically express mir-9*, pc-9-1 (mir-9 precursor) or pre-9* synthetic oligonucleotides were used. In plasmid based expressions, compared to pcDNA empty vector control, pc-9-1 transfection increased mir-9* levels up to 100 fold. Expression of mir-9* using synthetic oligonucleotides (50 nM) increased mir-9* levels much higher (up to 4000 fold) compared to pre-ctr control oligonucleotide **(Figure 5.1B)**. Pre-9* synthetic oligonucleotide was specific to mir-9* and it did not induce significant mir-9 expression in transfected cells **(Figure 5.1C).**

5.3.2. ApoTox-Glo Assay

To test the effect of mir-9* overexpression (pre-9*) on MCF-7 cell growth a ApoTox-Glo assay was performed. STS (Staurosporine) treated cells were used as a positive control. Compared to the control (pre-ctr) and STS treated cells the viability of the cells overexpressing mir-9* was significantly increased (30%) **(Figure 5.2A)** In contrast, mir-9* overexpressing MCF-7 cells showed decreased caspase-7 activity (30%) compared to pre-ctr treated samples. STS treated cells showed increased caspase-3/7 production confirming the sensitivity of the assay **(Figure 5.2B)**.

A

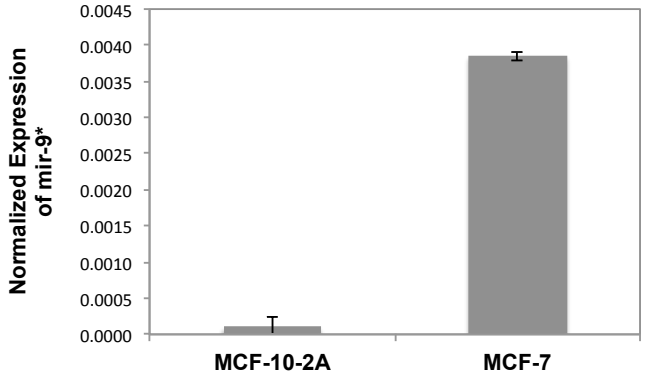

B

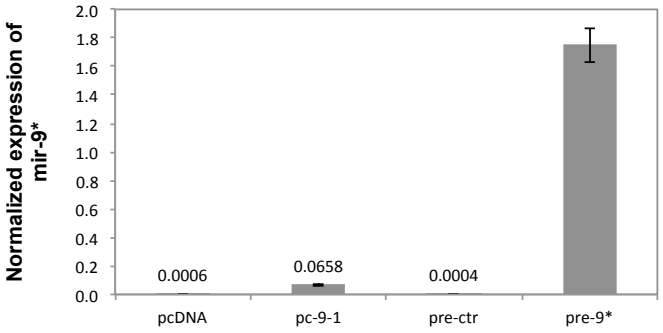

C

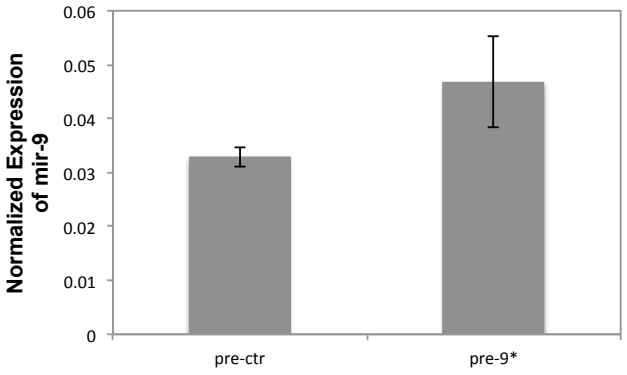

Figure 5.1: Endogenous and ectopic expression of mir-9* in MCF-7 cells.

qRT-PCR analysis (Taqman) of mir-9* in MCF-7 cells are shown. **A)** Endogenous mir-9* expression MCF-7 cells compared to normal breast tissue. **B)** Ectopic expression of mir-9* using pc-9-1 precursor plasmid or pre-9* oligonucleotide compared to controls (pcDNA or pre-ctr). **(C)** qRT-PCR analysis of mir-9 is MCF-7 cells transfected with pre-9* or pre-ctr. RNU6B was used as housekeeping control in normalizations.

A

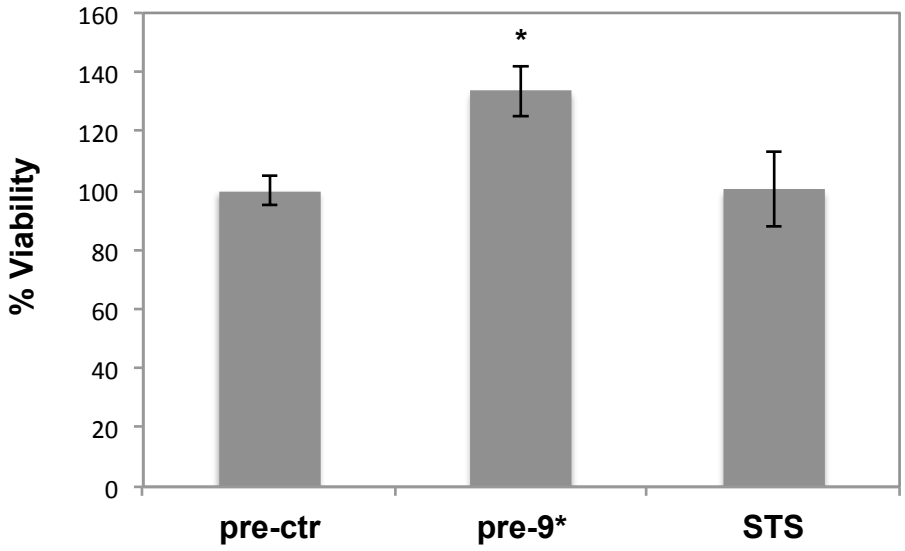

B

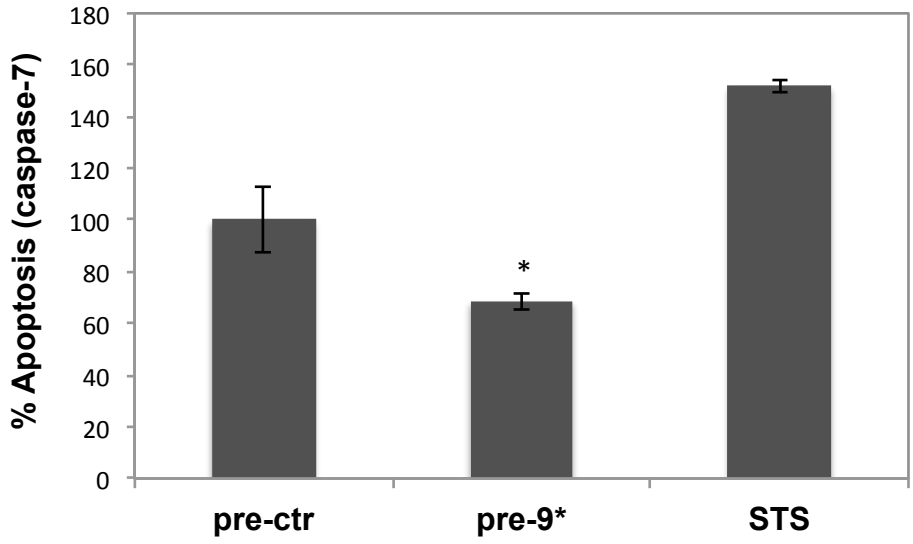

Figure 5.2: Pre-9* increases viability and decreases apoptosis in MCF-7 cells.

ApoTox-Glo analysis results for **A)** Percentage (%) viability (fluorescence) and **B)** percentage (%) caspase-7 activity (luminescence) in MCF-7 cells transfected with pre-9*, pre-ctr or STS (Staurosporine) are shown. Normalizations are done using the ratios to dead cell values (cytotoxicity; fluorescence). Statistical analysis (student's t-test) showed significant changes in both viability and caspase-7 production ($p<0.05$).

5.3.3. Mir-9* increases migration and invasion in breast cancer cells

To test the effects of mir-9* overexpression on cell migration and invasion, wound healing and matrigel invasion assays were performed. In contrast to mir-9 which displayed slower migration after wounding **(section 4.3.3)**, mir-9* overexpressing MCF-7 cells (pre-9*) showed faster migration (wound healing) compared to mock cells (pre-ctr). After 48hr post-transfection mir-9* overexpressing cells had moved significantly faster than the control cells **(Figure 5.3).**

To test the invasion effect, MCF-7 (non-invasive, ER+) and MDA-MB-231 (highly invasive, ER-) cells were transfected with pre-9* or pre-ctr synthetic oligonucleotides. No significant effect on invasion of MCF-7 cells was observed (data not shown). However, in contrast to mir-9 which displayed decreased invasiveness in MDA-MB-231 cells, mir-9* overexpression (pre-9*) significantly increased the number of invading cells in (the highly invasive) MDA-MB-231 cell line compared to control (pre-ctr). 10X and 20X magnification photos (inverted microscope) are shown in **Figure 5.4A.** Cell count was performed on the images of matrigel and represented as average number of invading cells in graph **(Figure 5.4B)**.

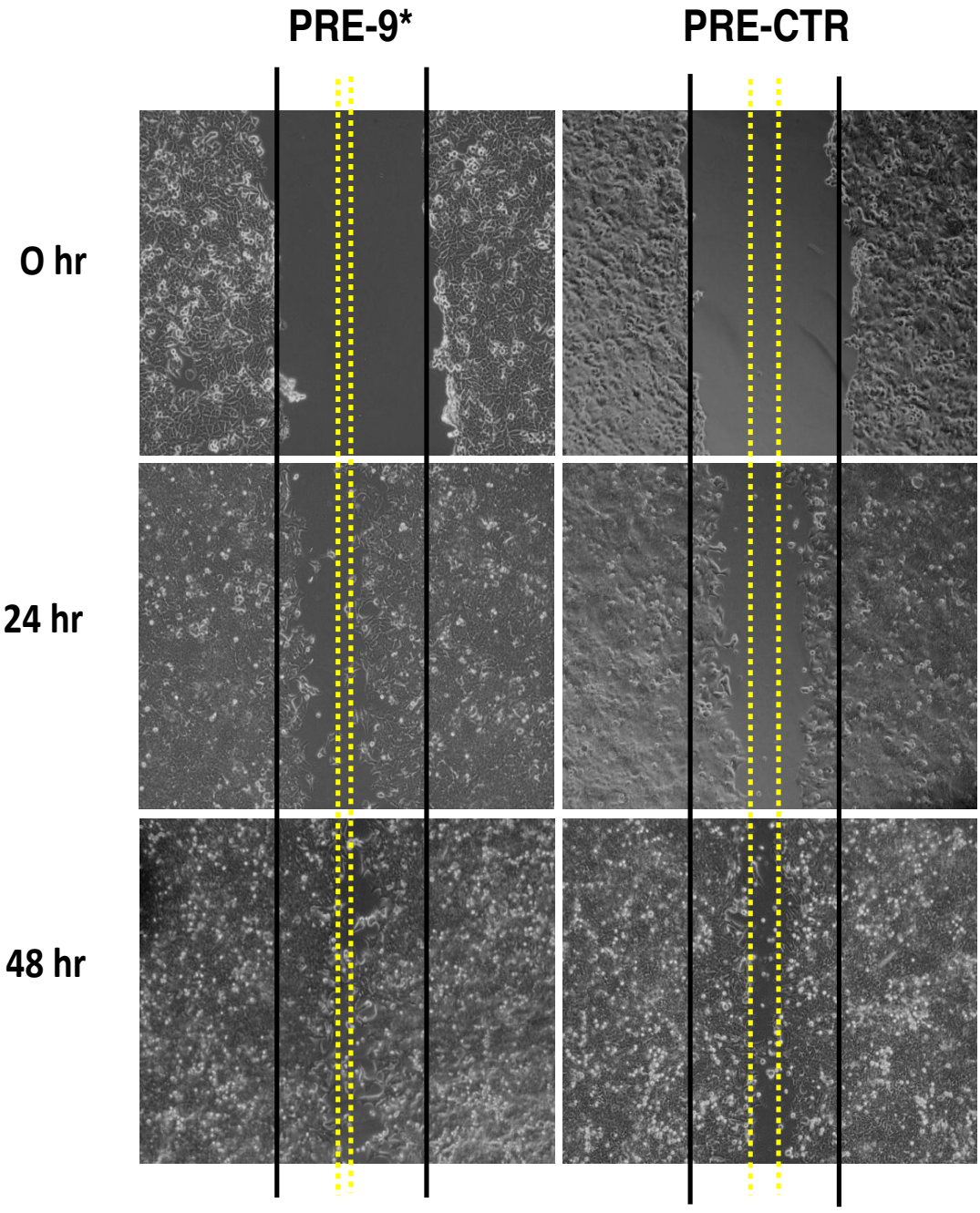

Figure 5.3: Pre-9* transfected MCF-7 cells migrate faster.

Wound healing assay in pre-9* or pre-ctr transfected MCF-7 cells 24hr and 48hr after wounding (0hr wounding). Yellow dashed lines show the healing of initial wound (black solid lines).

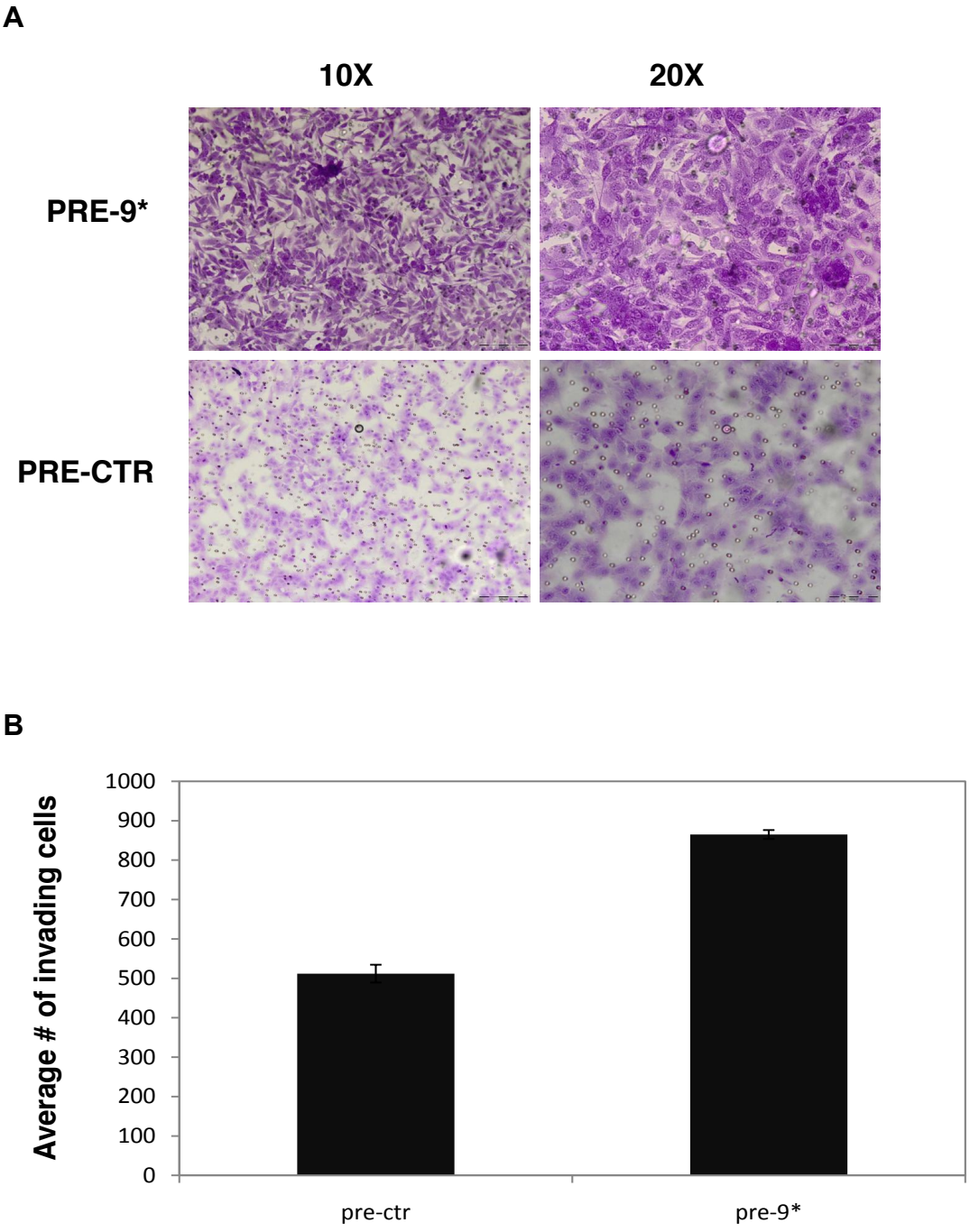

Figure 5.4: Pre-9* increases number of invaded cells in MDA-MB-231 cell line.

Matrigel invasion assay on highly invasive MDA-MB-231 cells transfected with pre-9* or pre-ctr is shown. **A)** Images of invaded cells; 10X and 20 X magnifications under inverted microscope **B)** Average number of cells invaded and counted in pre-9* or pre-ctr transfected MDA-MB-231 cells.

5.3.4. Microarray profiling of mir-9* overexpression identifies enriched GO terms

To identify genome-wide effects of mir-9* overexpression in MCF-7 cells microarray profiling was performed. Data analysis identified 217 upregulated and 137 downregulated genes in mir-9* overexpressing MCF-7 cells (pre-9*) compared to mock (pre-ctr). GO enrichment analysis showed that downregulated genes in mir-9* overexpressing cells were clustered in terms such as negative regulation of phosphorylation of STAT5 protein and LDL binding whereas upregulated genes were clustered in terms such as positive regulation of mitotic cell cycle, cell death and protein kinase inhibitor activity **(Table 5-1)**. SylArray analysis of the microarray results identified seed enrichment for mir-9* seed sequence **(Figure 5.5)**.

5.3.5. Selection of candidate mir-9* targets for downstream applications

To identify potential mir-9* direct targets, downregulated genes were selected with the assumption that microRNAs generally downregulate mRNA expression. Filtering the downregulated genes down based on different approaches. Using SylArray results, peak selection was performed on the landscape plot **(Figure 5.5)** to take the most downregulated genes that are enriched with mir-9* binding sites in 3'UTR. The peak that corresponds to first thousand genes left side of the peak (log10 > 10) was selected and the left of the peak gene list that is downregulated and enriched with mir-9* binding sites was obtained (total 797 downregulated genes). This list doesn't necessarily involve predicted mir-9* targets but rather a significant enrichment of targets compared to rest of the genes in microarray.

Tools for miRNA* target predictions are limited. The online programs that analyze miRNA* forms include MiRanda (www.microrna.org), MAMI

(mami.med.harvard.edu) and Microcosm (www.ebi.ac.uk/enright-srv/microcosm). Using the union of predicted mir-9* targets from these programs (limiting the MiRanda results to the top 100 hits) this list was compared to those genes identified as left of the peak on the landscape plot generated by SylArray giving an intersect of 90 genes. These 90 genes were then compared to those genes identified as significantly downregulated on the microarray, a total of 26 downregulated predicted targets. Sixteen of these genes were selected for validation along with an additional 13 genes downregulated on the array but not predicted as direct mir-9* targets. These additional 13 genes were selected based on functional GO annotations (i.e. cancer, cell migration, etc.). In total 29 downregulated genes were selected for validation, i.e. 16 predicted targets and 13 non-targets **(Table 5-2)**.

Table 5-1: GO enrichment in mir-9* downregulated and upregulated genes identified in microarray

Gene to GO Conditional test for over-representation (GOBP: Biological Processes, GOCC: Cellular Component, GOMF: Molecular Function)

Mir-9* DOWN

GOBPID	Pvalue	OddsRatio	ExpCount	Count	Size	Term
GO:0042524	0.000	Inf	0	2	2	negative regulation of tyrosine phosphorylation of Stat5 protein
GO:0070836	0.000	Inf	0	2	2	caveola assembly
GO:0033043	0.000	4.897	2	9	182	regulation of organelle organization
GO:0022411	0.001	6.445	1	6	92	cellular component disassembly
GO:0034623	0.001	7.914	1	5	63	cellular macromolecular complex disassembly
GO:0043242	0.001	10.73	0	4	38	negative regulation of protein complex disassembly
GOMFID	**Pvalue**	**OddsRatio**	**ExpCount**	**Count**	**Size**	**Term**
GO:0050750	0.000	45.496	0	3	9	low-density lipoprotein receptor binding

Mir-9* UP

GOBPID	Pvalue	OddsRatio	ExpCount	Count	Size	Term
GO:0065008	0.000	2.245	25	47	1383	regulation of biological quality
GO:0009636	0.000	8.282	1	7	55	response to toxin
GO:0006469	0.000	6.806	1	8	75	negative regulation of protein kinase activity
GO:0044092	0.000	3.302	5	16	299	negative regulation of molecular function
GO:0006882	0.000	55.799	0	3	6	cellular zinc ion homeostasis
GO:0051348	0.000	5.995	2	8	84	negative regulation of transferase activity
GO:0009725	0.000	3.05	6	17	343	response to hormone stimulus
GO:0008629	0.000	8.478	1	6	46	induction of apoptosis by intracellular signals
GO:0008219	0.000	2.133	18	34	1003	cell death
GO:0001890	0.000	7.704	1	6	50	placenta development
GO:0007584	0.000	4.586	2	9	121	response to nutrient
GO:0006915	0.000	2.123	16	31	910	apoptosis
GO:0007399	0.000	2.107	16	30	884	nervous system development
GO:0009991	0.001	3.605	3	11	186	response to extracellular stimulus
GO:0055066	0.001	3.285	4	12	222	di-, tri-valent inorganic cation homeostasis
GO:0033189	0.001	7.81	1	5	41	response to vitamin A
GO:0014070	0.001	4.455	2	8	110	response to organic cyclic substance
GO:0045931	0.001	20.914	0	3	11	positive regulation of mitotic cell cycle
GO:0002429	0.001	7.598	1	5	42	immune response-activating cell surface receptor signaling pathway
GO:0048523	0.001	1.825	26	42	1449	negative regulation of cellular process
GO:0007412	0.001	111.016	0	2	3	axon target recognition
GO:0007242	0.001	1.875	22	37	1231	intracellular signaling cascade
GOMFID	**Pvalue**	**OddsRatio**	**ExpCount**	**Count**	**Size**	**Term**
GO:0004860	0.000	10.317	1	5	32	protein kinase inhibitor activity
GO:0046870	0.000	33.149	0	3	8	cadmium ion binding
GO:0043565	0.000	2.533	9	20	478	sequence-specific DNA binding

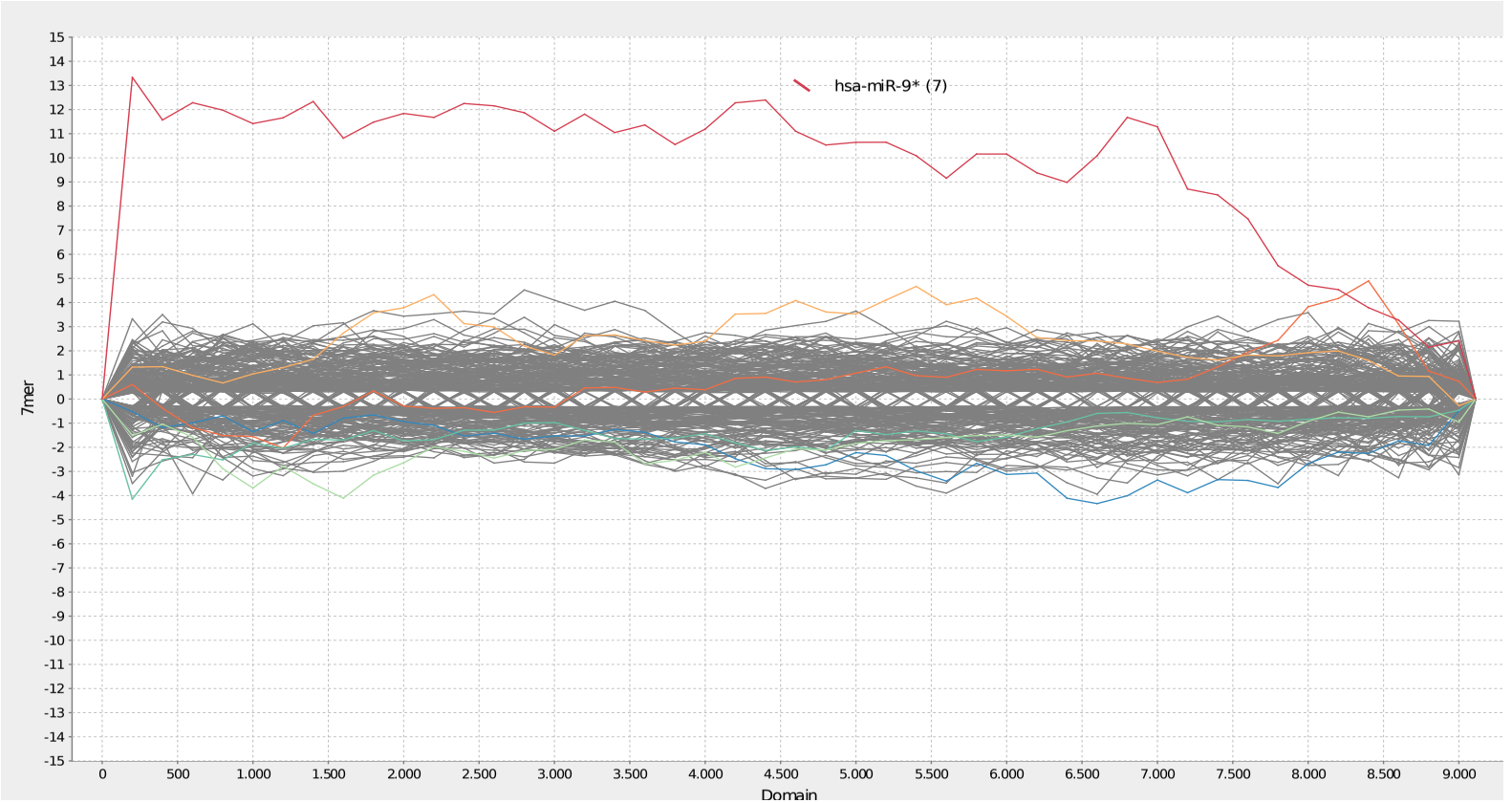

Figure 5.5: SylArray landscape plot for mir-9* 7-mer seed region.

Genes are ranked from most downregulated to most upregulated according to t-statistics Peak (red) shows enrichment of mir-9 binding site in downregulated genes.

Table 5-2: Downregulated genes selected from microarray results for qRT-PCR validation

	Predicted targets	Funtional annotation
1	ACTL6A	
2	ADIPOR1	
3	ITGB1	Cell Proliferation, migration
4	ELOVL6	
5	LIMA1	
6	CAPN2	
7	CLASP2	
8	DR1	
9	ID4	TGF-B pathway,cell proliferation, migration
10	MYH10	
11	NRP1	
12	PPP2R1B	TGF-B pathway
13	SYCP2	
14	TXNRD1	
15	WWTR1	
16	BLCAP	Apoptosis
	KEGG pathways	
17	ANXA1	Cell Proliferation, migration
18	CASP7	Apoptosis
19	APAF1	Apoptosis
20	CAPN2	Apoptosis
21	TNF	Apoptosis, TGF-B pathway
22	IL1R1	Apoptosis
23	INHBB	TGF-B pathway
24	PDZK1	Cell Proliferation, migration
25	CAV1	Cell Proliferation, migration
26	CAV2	Cell Proliferation, migration
27	PRKDC	Cell Proliferation, migration
28	NF2	Cell Proliferation, migration
29	STAT3	

5.3.6. Quantitative RT-PCR validates 12 out of 20 differentially expressed genes tested

Out of 29 selected candidates, 20 genes gave expected sizes and single bands in gel electrophoresis. Among these, 12 of them were validated as downregulated in pre-9* transfected cells compared to pre-ctr in qRT-PCR **(Figure 5.6)**. Adiponectin receptor 1 (ADIPOR1), Annexin A1 (ANXA1), Apoptotic peptidase activating factor 1 (APAF1), CBP/p300-interacting transactivator with ED-rich tail 2 (CITED2), Cytoplasmic linker associated protein 2 (CLASP2), Early Growth Response Protein 1 (EGR1), inhibitor of DNA-binding 4 (ID4), Inhibin, beta B (INHBB), protein kinase DNA-activated catalytic polypeptide (PRKDC), signal transducer and activator of transcription 3 (STAT3), tumor necrosis factor (TNF) and Integrin, beta 1 (ITGB1) showed significant downregulation in mir-9* overexpressing cells (pre-9*) compared to the control (pre-ctr). Among these, ADIPOR1, CLASP2, ID4 and ITGB1 were predicted targets. There results identify 12 genes as direct or indirect targets of mir-9* in MCF-7 breast cancer cells.

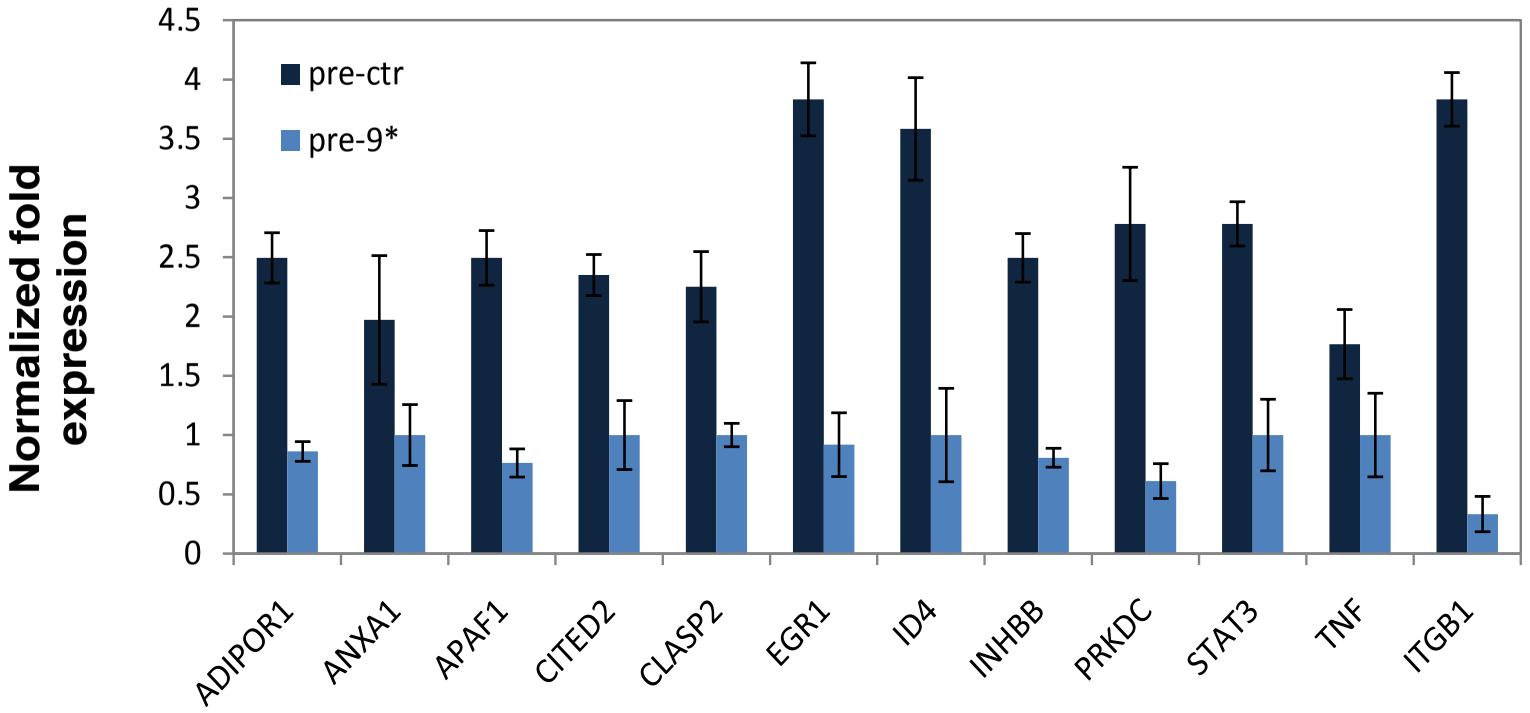

Figure 5.6: 12 out of 20 differentially expressed genes identified in mir-9* microarray are validated. qRT-PCR analysis of 12 differentially expressed genes in microarray analysis confirms the downregulation or upregulation in pre-9 transfected MF-7 cells compared to pre-ctr transfected cells. Values represented are normalized fold expression ±SD. GAPDH was used as housekeeping control in normalizations.

5.3.7. ITGB1 as predicted target of mir-9*

ITGB1 in which the strongest suppression by mir-9* **(Figure 5.6)** was observed is selected for further target validation by reporter assays. To test whether the 3'UTR of ITGB1 is regulated by mir-9* via putative binding site (starting at 365 bp) predicted by MiRanda (www.microrna.org), luciferase reporter constructs containing full length ITGB1 3'UTR (wild type) (pLight/ITGB1 UTR) or mutated mir-9* binding site (pLight/ITGB1 UTRmut9*) were co-transfected into MCF-7 with pre-ctr or pre-9* synthetic oligonucleotides.

All results were normalized against pre-ctr samples and represented as luciferase expression of UTR or UTRmut9* constructs in pre-9* treated samples. 48hr post-transfection luciferase analysis showed slightly restored expression in mut9* construct which lacks mir-9* binding site compared to wild type UTR. Statistical analysis (Student's t-test) showed this difference was statistically significant ($p < 0.001$) **(Figure 5.7)**.

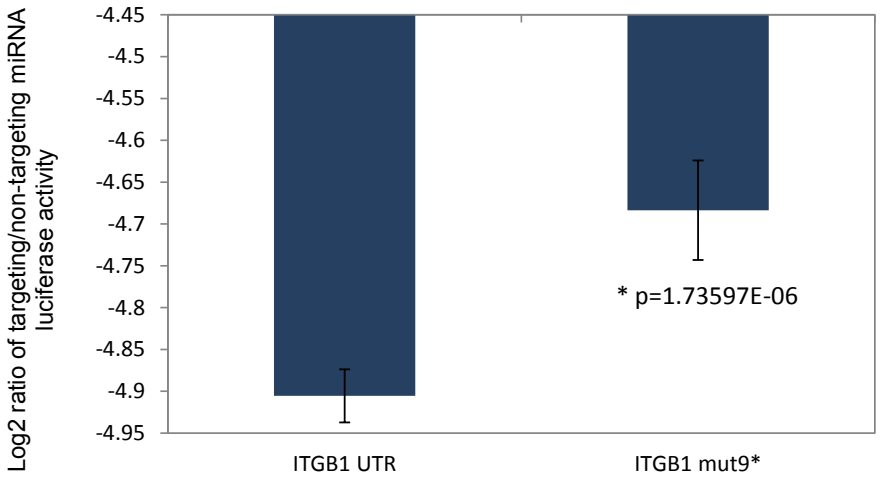

Figure 5.7: Luciferase assay for ITGB1 3'UTR in pre-9* overexpressing MCF-7 cells.

Graph represents normalized log2 ratio of targeting/non-targeting miRNA (pre-9*/pre-ctr) in ITGB1 UTR (wild type) or ITGB1 UTRmut9* (mir-9* seed mutated) constructs in mir-9* overexpressing (pre-ctr) MCF-7 cells. Statistical analysis (student's t-test) shows significant restoration of luciferase expression when mir-9* binding site is mutated ($p<0.001$).

5.4. Discussion

A growing body of evidence indicates that miRNA* forms (minor) have gene targets that they directly regulate [21, 331]. Mir-9* is one of the minor microRNAs that has been shown to have a function in the regulation of genes and diseases such as brain tumorigenesis [18]. Mir-9* is processed from the same precursor generating mir-9. Mir-9 has been recently indicated in breast carcinogenesis and the functional effects have been investigated and described in **chapter 4**. In contrast, mir-9*, has not been implicated in breast cancer and not much known about its function in cancer cells. Thus, its expression, genome-wide effects, functional role and direct targets have been investigated in this chapter.

Endogenous levels of mir-9* are higher in MCF-7 cells compared to normal breast tissue and the endogenous MIRN9 precursor processes into both mir-9 and mir-9* in the cells

Endogenous expression analysis of mir-9* in MCF-7 cells showed that mir-9* is expressed lower levels than mir-9, but compared to normal breast tissue the expression was higher. The analysis of mir-9* forced expression using plasmid-based precursor (pc-9-1) in MCF-7 cells showed that mir-9 expression was favoured which indicates a differential processing at precursor stage where mir-9* might be degraded or less stable. However, significant increase in mir-9* expression levels was observed indicating that mir-9* expression can be induced via plasmid precursors but this expression is limited compared to favourable mir-9 expression and it is not known whether the increase in mir-9* is biologically significant for studying its functional effects in the cells. As previously mentioned in **chapter 4**, to study the individual effects of mir-9 and mir-9* plasmid precursor is not suitable as generally miRNA precursors process into both forms in the cells and to avoid the interruption of either miRNA in studying the individual effects synthetic oligonucleotides were used. Ectopic expression of mir-9* via synthetic oligonucleotides (pre-9*) showed dramatic increase

in mir-9* levels in MCF-7 cells where by using this method the limitation of precursor processing is overcome and the functional effect of increased mir-9* can be studied.

Mir-9* overexpression promotes cell proliferation and invasiveness of breast cancer cells

Analysis of cell viability and caspase-3/7 production in MCF-7 cells indicated that mir-9* overexpression (pre-9*) has a role in cell proliferation and have anti-apoptotic activity on cancer cells. Staurosporine (STS), as a known apoptotic drug, treatment showed that the assay is accurate to measure the amount of caspase-3/7 activation induced by STS treatment (as minimum as 1nM) for 3 hours.

In addition to viability and apoptosis measurements, the motility and invasion effects were also tested using wound healing and matrigel invasion assays. Mir-9* overexpressing MCF-7 cells (pre-9*) showed increased motility compared to mock (pre-ctr) at 24 and 48 hours of treatments. In contrast, there was no effect observed in invasion of MCF-7 cells in pre-9* or pre-ctr treated samples. This could be due to non-invasive nature of MCF-7 cell line. The effect of mir-9* overexpression on invasion was shown in MDA-MB-231 cell line which is highly invasive. The invasiveness of the cells increased in pre-9* treated samples compared to pre-ctr treated samples.

Taken together, these results indicate that mir-9* might be involved in increasing the invasiveness (enhancing the process) but not solely sufficient to transform the cells from non-invasive to invasive phenotype which may strictly require activation of additional regulatory genes. Functional effect of microRNA* (star) forms has been reported in only a few studies [21, 477, 486]. These results contribute to the findings that microRNA* forms can have significant effects on cell migration and invasion.

Microarray profiling identified mir-9* sensitive transcriptome

To investigate the genome-wide effects of overexpressing mir-9* on the MCF-7 transcriptome, microarray profiling was performed in pre-9* and pre-ctr treated samples. SylArray analysis revealed significant enrichment of mir-9* seed sequence in the 3'UTR of downregulated genes indicating that mir-9* has a regulatory role in global expression patterns. This is the first report presenting the global effects of mir-9* on mammalian or cancer cells.

Assuming that potential mir-9* direct targets would be downregulated genes in mir-9* overexpressing cells, candidates were selected from the downregulated genes list. QRT-PCR analysis of 20 selected genes confirmed downregulation of 12 genes. From the predicted targets and validated genes initially ITGB1 was selected for further reporter assay confirmation due to the dramatic suppression effect of mir-9* on ITGB1 mRNA expression. ITGB1 (Integrin, beta 1) is a part of Integrin family members that are involved in cell adhesion and recognition (http://www.genecards.org/cgi-bin/carddisp.pl?gene=ITGB1). ITGB1 was reported recently to be linked to metastasis in gastric cancer [487] and significant expression was shown in stem-cell like bone cells [488].

Recently, ITGB1 was shown to be directly targeted by mir-124 and involve in oral squamous cell carcinoma progression [489]. Neither ITGB1 nor mir-9* have been extensively studied in cancer. However, independent reports indicating significance of both mir-9* [18, 490] and ITGB1 [489, 491, 492] raise the potential of this interaction to be investigated in detail.

ITGB1 has three predicted binding sites for mir-9* in its 3'UTR. Among these sites one of them (starting at 365 bp) was selected for testing direct binding. Reporter assays showed that ITGB1 3'UTR missing mir-9* binding site (ITGB1 UTRmut9*) has higher luciferase expression compared to construct containing wild type UTR (mir-9* binding site retained) **(Figure 5.7).** Although the increase in expression levels was not

a complete expression restoration it was statistically significant. This change does not assure biological significance, especially when the fold change is less than 10%. However, probably due to availability of its other two binding sites mir-9* has potential to strongly suppress ITGB1 UTRmut9*. The slight increase in luciferase expression may show the individual effect of this one binding site (starting 365 bp) on ITGB1 expression regulation. To fully understand the capability of mir-9* to suppress ITGB1 expression, a construct with all three binding sites should be generated and tested.

Overall, these results indicate that unlike mir-9, that has anti-proliferative activity on cancer cells, mir-9* has contrasting effects on breast cancer cells by increasing viability, migration and invasiveness which make it a candidate 'oncomir'. Genome-wide analysis of mir-9* overexpression identified several predicted targets of mir-9* to be tested and clarify the mechanisms and interactions that mir-9* is involved in the regulation of tumorigenesis.

Furthermore, when mir-9* is overexpressed it can target the 3'UTR of ITGB1 via a putative target site (starting at 365 bp) and can partially suppress ITGB1 expression. The partial restoration of ITGB1 indicates that mir-9* binding site at 365 bp contributes to but is not solely responsible for ITGB1 3'UTR suppression. Hence, two other binding sites (starting at 52 bp and 594 bp), together with the binding site tested in this study; potentially contribute to the suppression of ITGB1.

Conclusions

The potential of microRNAs as biomarkers and drug targets in diseases such as cancer is becoming more evident as a growing body of evidence proves the functional significance of the microRNAs encoded in the human genome. In this study, the phenotypic and genome-wide effects of three microRNAs in the breast cancer transcriptome, mir-21, mir-9 and mir-9* were investigated.

Mir-21 is a well-studied oncomir, yet much more remains to be discovered from genome-wide analysis of its effects on the cancer cell transcriptome. Here, global microarray profiling of mir-21 knockdown revealed the JAK-STAT pathway to be responsive to mir-21 dosage, which indicates that a direct or indirect communication exists between mir-21 and the components of this pathway. Analysis of predicted mir-21 targets identified STAT3 as a potential intermediary target of mir-21. An autoregulatory loop enhanced by, but not restricted to, IL-6 signaling, was identified between mr-21 and STAT3 in which their levels were positively correlated. Two putative mir-21 binding sites in the STAT3 3'UTR were also identified as active, which indicates a negative regulation of STAT3 expression as confirmed by reporter assays. This suggests a complex interaction between mir-21 and STAT3, which probably involves other regulatory components such as other JAK-STAT pathway genes, IL-6 and possibly other growth factors as well. These results represent a valuable starting point for further approaches to determine the mechanistic relationship of the regulatory loop between mir-21 and STAT3 to better elucidate the potential of this interaction in breast cancer therapeutics.

Analysis of predicted mir-21 targets identified and confirmed JAG1 as a direct mir-21 target dependent on mir-21 dosage. This interaction was shown to be dependent upon the genetic and epigenetic background as different cell lines showed different communications between mir-21, JAG1 and Estradiol. This study demonstrates that endogenous expression of mir-21 is important in regulation of JAG1 levels in breast cancer cells and that this interaction can be regulation via estrogen signaling. These

data indicate that estrogen receptor status in different breast cancer cell lines could determine the endogenous mir-21 levels which could in turn lead to differential regulation of its direct target, JAG1. Overall, these results contribute to the emerging realization that a particular microRNA:mRNA interaction is not necessarily a global (or axiomatic) phenomena and should be considered as valid only in the tested context (cell line, tissue, disease state, etc.). Extensive consideration of the genetic and epigenetic background of cell lines and tissues, complemented with extensive experimental testing are crucial for supporting any general claims that a microRNA targeting a particular mRNA is a common mechanism for all cell types.

Mir-9, initially reported as a neuron/brain-specific microRNA, has more recently been described to be deregulated in cancer. A small number of direct targets have been identified but the overall function of mir-9 in its wider cellular context has not been reported yet. This study is the first report of genome-wide effects of mir-9 on a cancer cell transcriptome. Here, anti-proliferative, anti-migration, anti-invasiveness and pro-apoptotic activities of mir-9 were demonstrated in breast cancer cells. Microarray analysis predicted many direct mir-9 targets of which eight have been confirmed. Among these targets, MTHFD1L and MTHFD2 showed evidence for contributing to the anti-proliferative activity of mir-9. In particular, MTHFD2 displayed an inverse expression level correlation profile with mir-9 levels in primary breast tumor samples and hence is a promising candidate to be investigated further in detail as a potential novel oncogene. Further investigation of mir-9* could potentially lead to identification of novel breast cancer biomarkers or targets. Among the eight genes confirmed as direct mir-9 targets, the gene CSDA has a pseudogene with high similarity at the mRNA sequence level with the 3'UTR of CSDA and which retains the putative mir-9 binding site. As this study had shown that mir-9 directly targets CSDA, it raised the question of whether the pseudogene CSDAP1 is also regulated by mir-9. Microarray analysis and quantitative RT-PCR results confirmed the downregulation of this pseudogene in mir-9 overexpressing cells. Reporter assays with

constructs containing the CSDAP1 mRNA sequence showed that mir-9 binds to the putative site and decreases the expression of the pseudogene CSDAP1. These results provide additional evidence in support of a recent report that pseudogenes can act as miRNA decoys and therefore protect the corresponding genes from severe suppression by the microRNAs [455]. Here, the results confirm that the CSDAP1 pseudogene acts as a mir-9 decoy and possibly limits the access of mir-9 to the CSDA 3'UTR. This could lead to reduced suppression of the CSDA gene which could keep CSDA mRNA expression at biologically functional levels.

Mir-9* has been reported in a few cases as the minor product processed from the same precursor as mir-9, and as mir-9 has recently been implicated in cancer mir-9* also holds great potential from this perspective. Although it has been shown that mir-9* is less stable and that mir-9 is favored in precursor processing, forcing higher expression levels (as could occur in a dysregulated cancer cell) could reveal any potential function in cancer cells. In contrast to the anti-proliferative (tumor suppressor) activity of mir-9, restoration of mir-9* expression triggered cell proliferation, migration and invasiveness and decreased apoptosis. Genome-wide analysis of mir-9* overexpression in MCF-7 cells identified many downregulated predicted targets and twelve of these genes were confirmed as direct or indirect targets. Among these, ITGB1 was shown to be a direct target of mir-9* in MCF-7 cells. Future experimental approaches should aim to elucidate the reasons why mir-9* expression is not favored over mir-9 in cancer cells, and what the consequences of mir-9* expression replacement and the mir-9*/ITGB1 interaction in cancer cells are. In summary, these results demonstrate that, although they are processed from the same precursor, the major and minor pre-miRNA products can have completely different functions and targets. This should be considered in future plasmid-based microRNA overexpression studies. This study also suggests that the functions of miRNA minor (*) forms should be studied in detail (both in combination and in isolation) in order to elucidate their distinct roles in biological processes and diseases.

Finally, this PhD study presents experimental research that identifies the global effects of three miRNAs; mir-21, mir-9 and mir-9* on cancer transcriptome. It identifies novel miRNA:mRNA interactions in the context of the cancer which contributes to our knowledge of the biological functions of the miRNAs. Additionally, this study elucidates the possible outcomes of miRNA dosage changes in cancer cells where the findings identify a need for further investigation to clarify the potential of these microRNAs in cancer diagnostics and therapeutic applications.

References

1. Calin, G.A., et al., *Human microRNA genes are frequently located at fragile sites and genomic regions involved in cancers.* Proc Natl Acad Sci U S A, 2004. **101**(9): p. 2999-3004.
2. Bartel, D.P. and C.Z. Chen, *Micromanagers of gene expression: the potentially widespread influence of metazoan microRNAs.* Nat Rev Genet, 2004. **5**(5): p. 396-400.
3. Lee, R.C., R.L. Feinbaum, and V. Ambros, *The C. elegans heterochronic gene lin-4 encodes small RNAs with antisense complementarity to lin-14.* Cell, 1993. **75**(5): p. 843-54.
4. Reinhart, B.J., et al., *MicroRNAs in plants.* Genes Dev, 2002. **16**(13): p. 1616-26.
5. Lagos-Quintana, M., et al., *Identification of novel genes coding for small expressed RNAs.* Science, 2001. **294**(5543): p. 853-8.
6. Kusenda, B., et al., *MicroRNA biogenesis, functionality and cancer relevance.* Biomed Pap Med Fac Univ Palacky Olomouc Czech Repub, 2006. **150**(2): p. 205-15.
7. Pfeffer, S., et al., *Identification of virus-encoded microRNAs.* Science, 2004. **304**(5671): p. 734-6.
8. Cai, X., C.H. Hagedorn, and B.R. Cullen, *Human microRNAs are processed from capped, polyadenylated transcripts that can also function as mRNAs.* Rna, 2004. **10**(12): p. 1957-66.
9. Lee, Y., et al., *MicroRNA genes are transcribed by RNA polymerase II.* Embo J, 2004. **23**(20): p. 4051-60.
10. Chen, C.Z., et al., *MicroRNAs modulate hematopoietic lineage differentiation.* Science, 2004. **303**(5654): p. 83-6.
11. Lee, Y., et al., *MicroRNA maturation: stepwise processing and subcellular localization.* Embo J, 2002. **21**(17): p. 4663-70.
12. Basyuk, E., et al., *Human let-7 stem-loop precursors harbor features of RNase III cleavage products.* Nucleic Acids Res, 2003. **31**(22): p. 6593-7.
13. Yi, R., et al., *Exportin-5 mediates the nuclear export of pre-microRNAs and short hairpin RNAs.* Genes Dev, 2003. **17**(24): p. 3011-6.
14. Tang, G., *siRNA and miRNA: an insight into RISCs.* Trends Biochem Sci, 2005. **30**(2): p. 106-14.
15. Hutvagner, G. and P.D. Zamore, *A microRNA in a multiple-turnover RNAi enzyme complex.* Science, 2002. **297**(5589): p. 2056-60.
16. Murchison, E.P. and G.J. Hannon, *miRNAs on the move: miRNA biogenesis and the RNAi machinery.* Curr Opin Cell Biol, 2004. **16**(3): p. 223-9.
17. Hammond, S.M., et al., *Argonaute2, a link between genetic and biochemical analyses of RNAi.* Science, 2001. **293**(5532): p. 1146-50.
18. Nass, D., et al., *MiR-92b and miR-9/9* are specifically expressed in brain primary tumors and can be used to differentiate primary from metastatic brain tumors.* Brain Pathol, 2009. **19**(3): p. 375-83.
19. Okamura, K., et al., *The regulatory activity of microRNA* species has substantial influence on microRNA and 3' UTR evolution.* Nat Struct Mol Biol, 2008. **15**(4): p. 354-63.
20. Jagadeeswaran, G., et al., *Deep sequencing of small RNA libraries reveals dynamic regulation of conserved and novel microRNAs and microRNA-stars during silkworm development.* BMC Genomics, 2010. **11**: p. 52.
21. Yang, J.S., et al., *Widespread regulatory activity of vertebrate microRNA* species.* RNA, 2011. **17**(2): p. 312-26.
22. Guo, L. and Z. Lu, *The fate of miRNA* strand through evolutionary analysis: implication for degradation as merely carrier strand or potential regulatory molecule?* PLoS One, 2010. **5**(6): p. e11387.
23. Griffiths-Jones, S., et al., *miRBase: microRNA sequences, targets and gene nomenclature.* Nucleic Acids Res, 2006. **34**(Database issue): p. D140-4.

24. Lewis, B.P., C.B. Burge, and D.P. Bartel, *Conserved seed pairing, often flanked by adenosines, indicates that thousands of human genes are microRNA targets.* Cell, 2005. **120**(1): p. 15-20.
25. Harfe, B.D., *MicroRNAs in vertebrate development.* Curr Opin Genet Dev, 2005. **15**(4): p. 410-5.
26. Zhao, Y. and D. Srivastava, *A developmental view of microRNA function.* Trends Biochem Sci, 2007. **32**(4): p. 189-97.
27. Bartel, D.P., *MicroRNAs: genomics, biogenesis, mechanism, and function.* Cell, 2004. **116**(2): p. 281-97.
28. Doench, J.G. and P.A. Sharp, *Specificity of microRNA target selection in translational repression.* Genes & development, 2004. **18**(5): p. 504-11.
29. He, L. and G.J. Hannon, *MicroRNAs: small RNAs with a big role in gene regulation.* Nature reviews. Genetics, 2004. **5**(7): p. 522-31.
30. Lytle, J.R., T.A. Yario, and J.A. Steitz, *Target mRNAs are repressed as efficiently by microRNA-binding sites in the 5′ UTR as in the 3′ UTR.* Proc Natl Acad Sci U S A, 2007. **104**(23): p. 9667-72.
31. Nielsen, A.F., J. Gloggnitzer, and J. Martinez, *MicroRNAs cross the line: the battle for mRNA stability enters the coding sequence.* Mol Cell, 2009. **35**(2): p. 139-40.
32. Kim, V.N., *MicroRNA biogenesis: coordinated cropping and dicing.* Nat Rev Mol Cell Biol, 2005. **6**(5): p. 376-85.
33. Zeng, Y., E.J. Wagner, and B.R. Cullen, *Both natural and designed micro RNAs can inhibit the expression of cognate mRNAs when expressed in human cells.* Mol Cell, 2002. **9**(6): p. 1327-33.
34. Yu, Z., T. Raabe, and N.B. Hecht, *MicroRNA Mirn122a reduces expression of the posttranscriptionally regulated germ cell transition protein 2 (Tnp2) messenger RNA (mRNA) by mRNA cleavage.* Biol Reprod, 2005. **73**(3): p. 427-33.
35. Yekta, S., I.H. Shih, and D.P. Bartel, *MicroRNA-directed cleavage of HOXB8 mRNA.* Science, 2004. **304**(5670): p. 594-6.
36. Mallory, A.C. and H. Vaucheret, *Functions of microRNAs and related small RNAs in plants.* Nat Genet, 2006. **38 Suppl**: p. S31-6.
37. Millar, A.A. and P.M. Waterhouse, *Plant and animal microRNAs: similarities and differences.* Funct Integr Genomics, 2005. **5**(3): p. 129-35.
38. Wu, L., J. Fan, and J.G. Belasco, *MicroRNAs direct rapid deadenylation of mRNA.* Proc Natl Acad Sci U S A, 2006. **103**(11): p. 4034-9.
39. Wakiyama, M., et al., *Let-7 microRNA-mediated mRNA deadenylation and translational repression in a mammalian cell-free system.* Genes Dev, 2007. **21**(15): p. 1857-62.
40. Standart, N. and R.J. Jackson, *MicroRNAs repress translation of m7Gppp-capped target mRNAs in vitro by inhibiting initiation and promoting deadenylation.* Genes Dev, 2007. **21**(16): p. 1975-82.
41. Eulalio, A., E. Huntzinger, and E. Izaurralde, *Getting to the Root of miRNA-Mediated Gene Silencing.* Cell, 2008. **132**(1): p. 9-14.
42. Moss, E.G., R.C. Lee, and V. Ambros, *The cold shock domain protein LIN-28 controls developmental timing in C. elegans and is regulated by the lin-4 RNA.* Cell, 1997. **88**(5): p. 637-46.
43. Wu, L. and J.G. Belasco, *Micro-RNA regulation of the mammalian lin-28 gene during neuronal differentiation of embryonal carcinoma cells.* Mol Cell Biol, 2005. **25**(21): p. 9198-208.
44. Lim, L.P., et al., *Microarray analysis shows that some microRNAs downregulate large numbers of target mRNAs.* Nature, 2005. **433**(7027): p. 769-73.
45. Grimson, A., et al., *MicroRNA targeting specificity in mammals: determinants beyond seed pairing.* Mol Cell, 2007. **27**(1): p. 91-105.
46. Krek, A., et al., *Combinatorial microRNA target predictions.* Nat Genet, 2005. **37**(5): p. 495-500.
47. John, B., et al., *Human MicroRNA targets.* PLoS Biol, 2004. **2**(11): p. e363.
48. Ovcharenko, D., et al., *Genome-scale microRNA and small interfering RNA screens identify small RNA modulators of TRAIL-induced apoptosis pathway.* Cancer Res, 2007. **67**(22): p. 10782-8.

49. Chen, Y. and R.L. Stallings, *Differential patterns of microRNA expression in neuroblastoma are correlated with prognosis, differentiation, and apoptosis.* Cancer Res, 2007. **67**(3): p. 976-83.
50. Kumar, M.S., et al., *Impaired microRNA processing enhances cellular transformation and tumorigenesis.* Nature genetics, 2007. **39**(5): p. 673-7.
51. Kumar, M.S., et al., *Impaired microRNA processing enhances cellular transformation and tumorigenesis.* Nat Genet, 2007. **39**(5): p. 673-7.
52. Selcuklu, S.D., M.C. Yakicier, and A.E. Erson, *An investigation of microRNAs mapping to breast cancer related genomic gain and loss regions.* Cancer Genet Cytogenet, 2009. **189**(1): p. 15-23.
53. He, L., et al., *A microRNA polycistron as a potential human oncogene.* Nature, 2005. **435**(7043): p. 828-33.
54. Calin, G.A., et al., *Frequent deletions and down-regulation of micro- RNA genes miR15 and miR16 at 13q14 in chronic lymphocytic leukemia.* Proc Natl Acad Sci U S A, 2002. **99**(24): p. 15524-9.
55. Zhang, B., et al., *microRNAs as oncogenes and tumor suppressors.* Dev Biol, 2007. **302**(1): p. 1-12.
56. Nelson, K.M. and G.J. Weiss, *MicroRNAs and cancer: past, present, and potential future.* Mol Cancer Ther, 2008. **7**(12): p. 3655-60.
57. Amin, R.P., et al., *Identification of putative gene based markers of renal toxicity.* Environ Health Perspect, 2004. **112**(4): p. 465-79.
58. Hanahan, D. and R.A. Weinberg, *The hallmarks of cancer.* Cell, 2000. **100**(1): p. 57-70.
59. Esquela-Kerscher, A. and F.J. Slack, *Oncomirs - microRNAs with a role in cancer.* Nat Rev Cancer, 2006. **6**(4): p. 259-69.
60. Jiang, S., et al., *MicroRNA-155 functions as an OncomiR in breast cancer by targeting the suppressor of cytokine signaling 1 gene.* Cancer Res, 2010. **70**(8): p. 3119-27.
61. Medina, P.P., M. Nolde, and F.J. Slack, *OncomiR addiction in an in vivo model of microRNA-21-induced pre-B-cell lymphoma.* Nature, 2010. **467**(7311): p. 86-90.
62. Wang, Z.Z. and N.Z. Xu, *[MiR-17-92 in cancer].* Sheng Li Ke Xue Jin Zhan, 2011. **42**(2): p. 91-4.
63. Reinhart, B.J., et al., *The 21-nucleotide let-7 RNA regulates developmental timing in Caenorhabditis elegans.* Nature, 2000. **403**(6772): p. 901-6.
64. Johnson, S.M., et al., *RAS is regulated by the let-7 microRNA family.* Cell, 2005. **120**(5): p. 635-47.
65. Bussing, I., F.J. Slack, and H. Grosshans, *let-7 microRNAs in development, stem cells and cancer.* Trends Mol Med, 2008. **14**(9): p. 400-9.
66. Zhao, Y., et al., *Let-7 family miRNAs regulate estrogen receptor alpha signaling in estrogen receptor positive breast cancer.* Breast Cancer Res Treat, 2011. **127**(1): p. 69-80.
67. Dalmay, T. and D.R. Edwards, *MicroRNAs and the hallmarks of cancer.* Oncogene, 2006. **25**(46): p. 6170-5.
68. Chan, J.A., A.M. Krichevsky, and K.S. Kosik, *MicroRNA-21 is an antiapoptotic factor in human glioblastoma cells.* Cancer Res, 2005. **65**(14): p. 6029-33.
69. Si, M.L., et al., *miR-21-mediated tumor growth.* Oncogene, 2007. **26**(19): p. 2799-803.
70. Asangani, I.A., et al., *MicroRNA-21 (miR-21) post-transcriptionally downregulates tumor suppressor Pdcd4 and stimulates invasion, intravasation and metastasis in colorectal cancer.* Oncogene, 2008. **27**(15): p. 2128-36.
71. Cimmino, A., et al., *miR-15 and miR-16 induce apoptosis by targeting BCL2.* Proc Natl Acad Sci U S A, 2005. **102**(39): p. 13944-9.
72. O'Donnell, K.A., et al., *c-Myc-regulated microRNAs modulate E2F1 expression.* Nature, 2005. **435**(7043): p. 839-43.
73. Lewis, B.P., et al., *Prediction of mammalian microRNA targets.* Cell, 2003. **115**(7): p. 787-98.
74. Bommer, G.T., et al., *p53-mediated activation of miRNA34 candidate tumor-suppressor genes.* Curr Biol, 2007. **17**(15): p. 1298-307.
75. Lu, J., et al., *MicroRNA expression profiles classify human cancers.* Nature, 2005. **435**(7043): p. 834-8.

76. Jay, C., et al., *miRNA profiling for diagnosis and prognosis of human cancer.* DNA Cell Biol, 2007. **26**(5): p. 293-300.
77. Iorio, M.V., et al., *MicroRNA gene expression deregulation in human breast cancer.* Cancer Res, 2005. **65**(16): p. 7065-70.
78. Zhang, L., et al., *microRNAs exhibit high frequency genomic alterations in human cancer.* Proc Natl Acad Sci U S A, 2006. **103**(24): p. 9136-41.
79. Asangani, I.A., et al., *MicroRNA-21 (miR-21) post-transcriptionally downregulates tumor suppressor Pdcd4 and stimulates invasion, intravasation and metastasis in colorectal cancer.* Oncogene, 2007.
80. Zhu, S., et al., *MicroRNA-21 targets the tumor suppressor gene tropomyosin 1 (TPM1).* J Biol Chem, 2007. **282**(19): p. 14328-36.
81. Mattie, M.D., et al., *Optimized high-throughput microRNA expression profiling provides novel biomarker assessment of clinical prostate and breast cancer biopsies.* Mol Cancer, 2006. **5**: p. 24.
82. Qian, B., et al., *High miR-21 expression in breast cancer associated with poor disease-free survival in early stage disease and high TGF-beta1.* Breast Cancer Res Treat, 2008.
83. Fujita, S., et al., *miR-21 Gene Expression Triggered by AP-1 Is Sustained through a Double-Negative Feedback Mechanism.* J Mol Biol, 2008.
84. Selcuklu, S.D., M.T. Donoghue, and C. Spillane, *miR-21 as a key regulator of oncogenic processes.* Biochemical Society transactions, 2009. **37**(Pt 4): p. 918-25.
85. Yan, L.X., et al., *Knockdown of miR-21 in human breast cancer cell lines inhibits proliferation, in vitro migration and in vivo tumor growth.* Breast cancer research : BCR, 2011. **13**(1): p. R2.
86. Folini, M., et al., *miR-21: an oncomir on strike in prostate cancer.* Molecular cancer, 2010. **9**: p. 12.
87. Volinia, S., et al., *A microRNA expression signature of human solid tumors defines cancer gene targets.* Proceedings of the National Academy of Sciences of the United States of America, 2006. **103**(7): p. 2257-61.
88. Calin, G.A., et al., *A MicroRNA signature associated with prognosis and progression in chronic lymphocytic leukemia.* The New England journal of medicine, 2005. **353**(17): p. 1793-801.
89. Garzon, R., et al., *MicroRNA signatures associated with cytogenetics and prognosis in acute myeloid leukemia.* Blood, 2008. **111**(6): p. 3183-9.
90. Garzon, R., et al., *Distinctive microRNA signature of acute myeloid leukemia bearing cytoplasmic mutated nucleophosmin.* Proceedings of the National Academy of Sciences of the United States of America, 2008. **105**(10): p. 3945-50.
91. Ciafre, S.A., et al., *Extensive modulation of a set of microRNAs in primary glioblastoma.* Biochemical and biophysical research communications, 2005. **334**(4): p. 1351-8.
92. Mendell, J.T., *miRiad roles for the miR-17-92 cluster in development and disease.* Cell, 2008. **133**(2): p. 217-22.
93. Ventura, A., et al., *Targeted deletion reveals essential and overlapping functions of the miR-17 through 92 family of miRNA clusters.* Cell, 2008. **132**(5): p. 875-86.
94. Iorio, M.V., et al., *MicroRNA gene expression deregulation in human breast cancer.* Cancer research, 2005. **65**(16): p. 7065-70.
95. Metzler, M., et al., *High expression of precursor microRNA-155/BIC RNA in children with Burkitt lymphoma.* Genes, chromosomes & cancer, 2004. **39**(2): p. 167-9.
96. Costinean, S., et al., *Pre-B cell proliferation and lymphoblastic leukemia/high-grade lymphoma in E(mu)-miR155 transgenic mice.* Proceedings of the National Academy of Sciences of the United States of America, 2006. **103**(18): p. 7024-9.
97. Voorhoeve, P.M., et al., *A genetic screen implicates miRNA-372 and miRNA-373 as oncogenes in testicular germ cell tumors.* Cell, 2006. **124**(6): p. 1169-81.
98. Yanaihara, N., et al., *Unique microRNA molecular profiles in lung cancer diagnosis and prognosis.* Cancer Cell, 2006. **9**(3): p. 189-98.

99. Akao, Y., Y. Nakagawa, and T. Naoe, *let-7 microRNA functions as a potential growth suppressor in human colon cancer cells.* Biological & pharmaceutical bulletin, 2006. **29**(5): p. 903-6.
100. Sampson, V.B., et al., *MicroRNA let-7a down-regulates MYC and reverts MYC-induced growth in Burkitt lymphoma cells.* Cancer research, 2007. **67**(20): p. 9762-70.
101. He, L., et al., *A microRNA component of the p53 tumour suppressor network.* Nature, 2007. **447**(7148): p. 1130-4.
102. Raver-Shapira, N., et al., *Transcriptional activation of miR-34a contributes to p53-mediated apoptosis.* Molecular cell, 2007. **26**(5): p. 731-43.
103. Chang, T.C., et al., *Transactivation of miR-34a by p53 broadly influences gene expression and promotes apoptosis.* Molecular cell, 2007. **26**(5): p. 745-52.
104. Chang, T.C., et al., *Widespread microRNA repression by Myc contributes to tumorigenesis.* Nature genetics, 2008. **40**(1): p. 43-50.
105. Mott, J.L., et al., *mir-29 regulates Mcl-1 protein expression and apoptosis.* Oncogene, 2007. **26**(42): p. 6133-40.
106. Fabbri, M., et al., *MicroRNA-29 family reverts aberrant methylation in lung cancer by targeting DNA methyltransferases 3A and 3B.* Proceedings of the National Academy of Sciences of the United States of America, 2007. **104**(40): p. 15805-10.
107. Scott, G.K., et al., *Coordinate suppression of ERBB2 and ERBB3 by enforced expression of micro-RNA miR-125a or miR-125b.* The Journal of biological chemistry, 2007. **282**(2): p. 1479-86.
108. Mattie, M.D., et al., *Optimized high-throughput microRNA expression profiling provides novel biomarker assessment of clinical prostate and breast cancer biopsies.* Molecular cancer, 2006. **5**: p. 24.
109. Calin, G.A., et al., *Frequent deletions and down-regulation of micro- RNA genes miR15 and miR16 at 13q14 in chronic lymphocytic leukemia.* Proceedings of the National Academy of Sciences of the United States of America, 2002. **99**(24): p. 15524-9.
110. Cimmino, A., et al., *miR-15 and miR-16 induce apoptosis by targeting BCL2.* Proceedings of the National Academy of Sciences of the United States of America, 2005. **102**(39): p. 13944-9.
111. Calin, G.A., et al., *MiR-15a and miR-16-1 cluster functions in human leukemia.* Proceedings of the National Academy of Sciences of the United States of America, 2008. **105**(13): p. 5166-71.
112. Cai, B., Z. Pan, and Y. Lu, *The roles of microRNAs in heart diseases: a novel important regulator.* Curr Med Chem, 2010. **17**(5): p. 407-11.
113. Lee, Y., et al., *Drosha in Primary MicroRNA Processing.* Cold Spring Harb Symp Quant Biol, 2006. **71**: p. 51-7.
114. Cheng, A.M., et al., *Antisense inhibition of human miRNAs and indications for an involvement of miRNA in cell growth and apoptosis.* Nucleic Acids Res, 2005. **33**(4): p. 1290-7.
115. Sempere, L.F., et al., *Altered MicroRNA expression confined to specific epithelial cell subpopulations in breast cancer.* Cancer Res, 2007. **67**(24): p. 11612-20.
116. Volinia, S., et al., *A microRNA expression signature of human solid tumors defines cancer gene targets.* Proc Natl Acad Sci U S A, 2006. **103**(7): p. 2257-61.
117. Feber, A., et al., *MicroRNA expression profiles of esophageal cancer.* J Thorac Cardiovasc Surg, 2008. **135**(2): p. 255-60; discussion 260.
118. Slaby, O., et al., *Altered expression of miR-21, miR-31, miR-143 and miR-145 is related to clinicopathologic features of colorectal cancer.* Oncology, 2007. **72**(5-6): p. 397-402.
119. Nam, E.J., et al., *MicroRNA expression profiles in serous ovarian carcinoma.* Clin Cancer Res, 2008. **14**(9): p. 2690-5.
120. Meng, F., et al., *Involvement of human micro-RNA in growth and response to chemotherapy in human cholangiocarcinoma cell lines.* Gastroenterology, 2006. **130**(7): p. 2113-29.
121. Lawrie, C.H., *MicroRNAs and haematology: small molecules, big function.* Br J Haematol, 2007. **137**(6): p. 503-12.

122. Connolly, E., et al., *Elevated expression of the miR-17-92 polycistron and miR-21 in hepadnavirus-associated hepatocellular carcinoma contributes to the malignant phenotype.* Am J Pathol, 2008. **173**(3): p. 856-64.
123. Meng, F., et al., *MicroRNA-21 regulates expression of the PTEN tumor suppressor gene in human hepatocellular cancer.* Gastroenterology, 2007. **133**(2): p. 647-58.
124. Kluiver, J., et al., *Lack of BIC and microRNA miR-155 expression in primary cases of Burkitt lymphoma.* Genes Chromosomes Cancer, 2006. **45**(2): p. 147-53.
125. Wang, T., et al., *A micro-RNA signature associated with race, tumor size, and target gene activity in human uterine leiomyomas.* Genes Chromosomes Cancer, 2007. **46**(4): p. 336-47.
126. Tran, N., et al., *MicroRNA expression profiles in head and neck cancer cell lines.* Biochem Biophys Res Commun, 2007. **358**(1): p. 12-7.
127. Fulci, V., et al., *Quantitative technologies establish a novel microRNA profile of chronic lymphocytic leukemia.* Blood, 2007.
128. Lee, E.J., et al., *Expression profiling identifies microRNA signature in pancreatic cancer.* Int J Cancer, 2007. **120**(5): p. 1046-54.
129. Wong, T.S., et al., *Mature miR-184 as Potential Oncogenic microRNA of Squamous Cell Carcinoma of Tongue.* Clin Cancer Res, 2008. **14**(9): p. 2588-92.
130. He, H., et al., *The role of microRNA genes in papillary thyroid carcinoma.* Proc Natl Acad Sci U S A, 2005. **102**(52): p. 19075-80.
131. Yan, L.X., et al., *MicroRNA miR-21 overexpression in human breast cancer is associated with advanced clinical stage, lymph node metastasis and patient poor prognosis.* RNA, 2008. **14**(11): p. 2348-60.
132. Feinberg, A.P., R. Ohlsson, and S. Henikoff, *The epigenetic progenitor origin of human cancer.* Nat Rev Genet, 2006. **7**(1): p. 21-33.
133. Zhu, S., et al., *MicroRNA-21 targets tumor suppressor genes in invasion and metastasis.* Cell Res, 2008. **18**(3): p. 350-9.
134. Loffler, D., et al., *Interleukin-6 dependent survival of multiple myeloma cells involves the Stat3-mediated induction of microRNA-21 through a highly conserved enhancer.* Blood, 2007. **110**(4): p. 1330-3.
135. Sathyan, P., H.B. Golden, and R.C. Miranda, *Competing interactions between micro-RNAs determine neural progenitor survival and proliferation after ethanol exposure: evidence from an ex vivo model of the fetal cerebral cortical neuroepithelium.* J Neurosci, 2007. **27**(32): p. 8546-57.
136. Martin, G., et al., *Prediction and validation of microRNA targets in animal genomes.* J Biosci, 2007. **32**(6): p. 1049-52.
137. Papadopoulos, G.L., et al., *The database of experimentally supported targets: a functional update of TarBase.* Nucleic Acids Res, 2009. **37**(Database issue): p. D155-8.
138. Zhu, S., et al., *MicroRNA-21 targets the tumor suppressor gene tropomyosin 1 (TPM1).* J Biol Chem, 2007.
139. Frankel, L.B., et al., *Programmed cell death 4 (PDCD4) is an important functional target of the microRNA miR-21 in breast cancer cells.* J Biol Chem, 2008. **283**(2): p. 1026-33.
140. Sayed, D., et al., *MicroRNA-21 targets Sprouty2 and promotes cellular outgrowths.* Mol Biol Cell, 2008. **19**(8): p. 3272-82.
141. Edwin, F., et al., *The tumor suppressor PTEN is necessary for human Sprouty 2-mediated inhibition of cell proliferation.* J Biol Chem, 2006. **281**(8): p. 4816-22.
142. Adams, B.D., H. Furneaux, and B. White, *The micro-RNA miR-206 Targets the Human Estrogen Receptor-{alpha}, and Represses ER{alpha} mRNA and Protein Expression in Breast Cancer Cell Lines.* Mol Endocrinol, 2007.
143. Papagiannakopoulos, T., A. Shapiro, and K.S. Kosik, *MicroRNA-21 targets a network of key tumor-suppressive pathways in glioblastoma cells.* Cancer Res, 2008. **68**(19): p. 8164-72.
144. Gabriely, G., et al., *MicroRNA 21 promotes glioma invasion by targeting matrix metalloproteinase regulators.* Mol Cell Biol, 2008. **28**(17): p. 5369-80.
145. Baek, D., et al., *The impact of microRNAs on protein output.* Nature, 2008. **455**(7209): p. 64-71.

146. Selbach, M., et al., *Widespread changes in protein synthesis induced by microRNAs.* Nature, 2008. **455**(7209): p. 58-63.
147. Vinther, J., et al., *Identification of miRNA targets with stable isotope labeling by amino acids in cell culture.* Nucleic Acids Res, 2006. **34**(16): p. e107.
148. Wagner, E.F. and K. Matsuo, *Signalling in osteoclasts and the role of Fos/AP1 proteins.* Ann Rheum Dis, 2003. **62 Suppl 2**: p. ii83-5.
149. Ozanne, B.W., et al., *Transcriptional regulation of cell invasion: AP-1 regulation of a multigenic invasion programme.* Eur J Cancer, 2000. **36**(13 Spec No): p. 1640-8.
150. Talotta, F., et al., *An autoregulatory loop mediated by miR-21 and PDCD4 controls the AP-1 activity in RAS transformation.* Oncogene, 2008.
151. Davis, B.N., et al., *SMAD proteins control DROSHA-mediated microRNA maturation.* Nature, 2008. **454**(7200): p. 56-61.
152. Roldo, C., et al., *MicroRNA expression abnormalities in pancreatic endocrine and acinar tumors are associated with distinctive pathologic features and clinical behavior.* J Clin Oncol, 2006. **24**(29): p. 4677-84.
153. Schetter, A.J., et al., *MicroRNA expression profiles associated with prognosis and therapeutic outcome in colon adenocarcinoma.* JAMA, 2008. **299**(4): p. 425-36.
154. Rossi, L., E. Bonmassar, and I. Faraoni, *Modification of miR gene expression pattern in human colon cancer cells following exposure to 5-fluorouracil in vitro.* Pharmacol Res, 2007. **56**(3): p. 248-53.
155. Iorio, M.V., et al., *MicroRNA signatures in human ovarian cancer.* Cancer Res, 2007. **67**(18): p. 8699-707.
156. Corsten, M.F., et al., *MicroRNA-21 knockdown disrupts glioma growth in vivo and displays synergistic cytotoxicity with neural precursor cell delivered S-TRAIL in human gliomas.* Cancer Res, 2007. **67**(19): p. 8994-9000.
157. Blower, P.E., et al., *MicroRNAs modulate the chemosensitivity of tumor cells.* Mol Cancer Ther, 2008. **7**(1): p. 1-9.
158. Lawrie, C.H., et al., *Detection of elevated levels of tumour-associated microRNAs in serum of patients with diffuse large B-cell lymphoma.* Br J Haematol, 2008. **141**(5): p. 672-5.
159. Lagos-Quintana, M., et al., *Identification of tissue-specific microRNAs from mouse.* Curr Biol, 2002. **12**(9): p. 735-9.
160. Laneve, P., et al., *A minicircuitry involving REST and CREB controls miR-9-2 expression during human neuronal differentiation.* Nucleic Acids Res, 2010. **38**(20): p. 6895-905.
161. Yuva-Aydemir, Y., et al., *MicroRNA-9: Functional evolution of a conserved small regulatory RNA.* RNA Biol, 2011. **8**(4).
162. Ma, L., et al., *miR-9, a MYC/MYCN-activated microRNA, regulates E-cadherin and cancer metastasis.* Nat Cell Biol, 2010. **12**(3): p. 247-56.
163. Hildebrandt, M.A., et al., *Hsa-miR-9 methylation status is associated with cancer development and metastatic recurrence in patients with clear cell renal cell carcinoma.* Oncogene, 2010. **29**(42): p. 5724-8.
164. Krichevsky, A.M., et al., *A microRNA array reveals extensive regulation of microRNAs during brain development.* RNA, 2003. **9**(10): p. 1274-81.
165. Deo, M., et al., *Detection of mammalian microRNA expression by in situ hybridization with RNA oligonucleotides.* Dev Dyn, 2006. **235**(9): p. 2538-48.
166. Krichevsky, A.M., et al., *Specific microRNAs modulate embryonic stem cell-derived neurogenesis.* Stem Cells, 2006. **24**(4): p. 857-64.
167. Shibata, M., et al., *MicroRNA-9 modulates Cajal-Retzius cell differentiation by suppressing Foxg1 expression in mouse medial pallium.* J Neurosci, 2008. **28**(41): p. 10415-21.
168. Delaloy, C., et al., *MicroRNA-9 coordinates proliferation and migration of human embryonic stem cell-derived neural progenitors.* Cell Stem Cell, 2010. **6**(4): p. 323-35.
169. Chen, X.M., *MicroRNA signatures in liver diseases.* World J Gastroenterol, 2009. **15**(14): p. 1665-72.

170. Thai, T.H., P.A. Christiansen, and G.C. Tsokos, *Is there a link between dysregulated miRNA expression and disease?* Discov Med, 2010. **10**(52): p. 184-94.
171. Kunej, T., et al., *Epigenetic regulation of microRNAs in cancer: An integrated review of literature.* Mutat Res, 2011.
172. Toyota, M., et al., *Epigenetic silencing of microRNA-34b/c and B-cell translocation gene 4 is associated with CpG island methylation in colorectal cancer.* Cancer Res, 2008. **68**(11): p. 4123-32.
173. Roman-Gomez, J., et al., *Epigenetic regulation of microRNAs in acute lymphoblastic leukemia.* J Clin Oncol, 2009. **27**(8): p. 1316-22.
174. Lehmann, U., et al., *Epigenetic inactivation of microRNA gene hsa-mir-9-1 in human breast cancer.* J Pathol, 2008. **214**(1): p. 17-24.
175. Omura, N., et al., *Genome-wide profiling of methylated promoters in pancreatic adenocarcinoma.* Cancer Biol Ther, 2008. **7**(7): p. 1146-56.
176. Bandres, E., et al., *Epigenetic regulation of microRNA expression in colorectal cancer.* Int J Cancer, 2009. **125**(11): p. 2737-43.
177. Trankenschuh, W., et al., *Frequent and distinct aberrations of DNA methylation patterns in fibrolamellar carcinoma of the liver.* PLoS One, 2010. **5**(10): p. e13688.
178. Lujambio, A., et al., *A microRNA DNA methylation signature for human cancer metastasis.* Proc Natl Acad Sci U S A, 2008. **105**(36): p. 13556-61.
179. Ebert, M.S., J.R. Neilson, and P.A. Sharp, *MicroRNA sponges: competitive inhibitors of small RNAs in mammalian cells.* Nat Methods, 2007. **4**(9): p. 721-6.
180. Franco-Zorrilla, J.M., et al., *Target mimicry provides a new mechanism for regulation of microRNA activity.* Nat Genet, 2007. **39**(8): p. 1033-7.
181. Poliseno, L., et al., *A coding-independent function of gene and pseudogene mRNAs regulates tumour biology.* Nature, 2010. **465**(7301): p. 1033-8.
182. Lacroix, M. and G. Leclercq, *Relevance of breast cancer cell lines as models for breast tumours: an update.* Breast Cancer Res Treat, 2004. **83**(3): p. 249-89.
183. Masters, J.R., *Human cancer cell lines: fact and fantasy.* Nat Rev Mol Cell Biol, 2000. **1**(3): p. 233-6.
184. Fogh, J., J.M. Fogh, and T. Orfeo, *One hundred and twenty-seven cultured human tumor cell lines producing tumors in nude mice.* J Natl Cancer Inst, 1977. **59**(1): p. 221-6.
185. Vargo-Gogola, T. and J.M. Rosen, *Modelling breast cancer: one size does not fit all.* Nat Rev Cancer, 2007. **7**(9): p. 659-72.
186. Perou, C.M., et al., *Molecular portraits of human breast tumours.* Nature, 2000. **406**(6797): p. 747-52.
187. Neve, R.M., et al., *A collection of breast cancer cell lines for the study of functionally distinct cancer subtypes.* Cancer Cell, 2006. **10**(6): p. 515-27.
188. Drexler, H.G., et al., *Pathobiology of NPM-ALK and variant fusion genes in anaplastic large cell lymphoma and other lymphomas.* Leukemia, 2000. **14**(9): p. 1533-59.
189. Wistuba, II, et al., *Comparison of features of human breast cancer cell lines and their corresponding tumors.* Clin Cancer Res, 1998. **4**(12): p. 2931-8.
190. Drexler, H.G., et al., *p53 alterations in human leukemia-lymphoma cell lines: in vitroartifact or prerequisite for cell immortalization?* Leukemia, 2000. **14**(1): p. 198-206.
191. *UKCCCR guidelines for the use of cell lines in cancer research.* Br J Cancer, 2000. **82**(9): p. 1495-509.
192. Soule, H.D., et al., *A human cell line from a pleural effusion derived from a breast carcinoma.* J Natl Cancer Inst, 1973. **51**(5): p. 1409-16.
193. Creighton, C.J., et al., *Genes regulated by estrogen in breast tumor cells in vitro are similarly regulated in vivo in tumor xenografts and human breast tumors.* Genome Biol, 2006. **7**(4): p. R28.
194. van Staveren, W.C., et al., *Human cancer cell lines: Experimental models for cancer cells in situ? For cancer stem cells?* Biochim Biophys Acta, 2009. **1795**(2): p. 92-103.
195. Ferlay, J., et al., *Estimates of worldwide burden of cancer in 2008: GLOBOCAN 2008.* Int J Cancer, 2010.

196. Ferlay, J., et al., *Estimates of worldwide burden of cancer in 2008: GLOBOCAN 2008.* Int J Cancer, 2010. **127**(12): p. 2893-917.
197. Wu, Q., et al., *Next-Generation Sequencing of MicroRNAs for Breast Cancer Detection.* J Biomed Biotechnol, 2011. **2011**: p. 597145.
198. Yamamichi, N., et al., *Locked nucleic acid in situ hybridization analysis of miR-21 expression during colorectal cancer development.* Clin Cancer Res, 2009. **15**(12): p. 4009-16.
199. Jorgensen, S., et al., *Robust one-day in situ hybridization protocol for detection of microRNAs in paraffin samples using LNA probes.* Methods, 2010. **52**(4): p. 375-81.
200. Chan, H.M., et al., *Direct quantification of single-molecules of microRNA by total internal reflection fluorescence microscopy.* Anal Chem, 2010. **82**(16): p. 6911-8.
201. Ali, S., et al., *Differentially expressed miRNAs in the plasma may provide a molecular signature for aggressive pancreatic cancer.* Am J Transl Res, 2010. **3**(1): p. 28-47.
202. Wei, J., et al., *Identification of plasma microRNA-21 as a biomarker for early detection and chemosensitivity of non-small cell lung cancer.* Chin J Cancer, 2011. **30**(6): p. 407-14.
203. Tsujiura, M., et al., *Circulating microRNAs in plasma of patients with gastric cancers.* Br J Cancer, 2010. **102**(7): p. 1174-9.
204. Yaman Agaoglu, F., et al., *Investigation of miR-21, miR-141, and miR-221 in blood circulation of patients with prostate cancer.* Tumour Biol, 2011. **32**(3): p. 583-8.
205. Xu, J., et al., *Circulating MicroRNAs, miR-21, miR-122, and miR-223, in patients with hepatocellular carcinoma or chronic hepatitis.* Mol Carcinog, 2010.
206. Laconti, J.J., et al., *Tissue and Serum microRNAs in the Kras Transgenic Animal Model and in Patients with Pancreatic Cancer.* PLoS One, 2011. **6**(6): p. e20687.
207. Wang, Z.X., et al., *Prognostic significance of serum miRNA-21 expression in human non-small cell lung cancer.* J Surg Oncol, 2011.
208. Ota, D., et al., *Identification of recurrence-related microRNAs in the bone marrow of breast cancer patients.* Int J Oncol, 2011. **38**(4): p. 955-62.
209. Ryu, J.K., et al., *Elevated microRNA miR-21 Levels in Pancreatic Cyst Fluid Are Predictive of Mucinous Precursor Lesions of Ductal Adenocarcinoma.* Pancreatology, 2011. **11**(3): p. 343-350.
210. Wang, J., et al., *MicroRNAs in plasma of pancreatic ductal adenocarcinoma patients as novel blood-based biomarkers of disease.* Cancer Prev Res (Phila), 2009. **2**(9): p. 807-13.
211. Pu, X.X., et al., *Circulating miR-221 directly amplified from plasma is a potential diagnostic and prognostic marker of colorectal cancer and is correlated with p53 expression.* J Gastroenterol Hepatol, 2010. **25**(10): p. 1674-80.
212. Vaz, C., et al., *Analysis of microRNA transcriptome by deep sequencing of small RNA libraries of peripheral blood.* BMC Genomics, 2010. **11**: p. 288.
213. Wang, F., et al., *Correlation and quantitation of microRNA aberrant expression in tissues and sera from patients with breast tumor.* Gynecol Oncol, 2010. **119**(3): p. 586-93.
214. Li, J., et al., *Expression of serum miR-221 in human hepatocellular carcinoma and its prognostic significance.* Biochem Biophys Res Commun, 2011. **406**(1): p. 70-3.
215. Asaga, S., et al., *Direct serum assay for microRNA-21 concentrations in early and advanced breast cancer.* Clin Chem, 2011. **57**(1): p. 84-91.
216. Krichevsky, A.M. and G. Gabriely, *miR-21: a small multi-faceted RNA.* J Cell Mol Med, 2009. **13**(1): p. 39-53.
217. Pan, X., Z.X. Wang, and R. Wang, *MicroRNA-21: a novel therapeutic target in human cancer.* Cancer Biol Ther, 2011. **10**(12): p. 1224-32.
218. Baffa, R., et al., *MicroRNA expression profiling of human metastatic cancers identifies cancer gene targets.* J Pathol, 2009. **219**(2): p. 214-21.
219. Li, J., et al., *MiR-21 indicates poor prognosis in tongue squamous cell carcinomas as an apoptosis inhibitor.* Clin Cancer Res, 2009. **15**(12): p. 3998-4008.

220. Giovannetti, E., et al., *MicroRNA-21 in pancreatic cancer: correlation with clinical outcome and pharmacologic aspects underlying its role in the modulation of gemcitabine activity.* Cancer Res, 2010. **70**(11): p. 4528-38.
221. Hwang, J.H., et al., *Identification of microRNA-21 as a biomarker for chemoresistance and clinical outcome following adjuvant therapy in resectable pancreatic cancer.* PLoS One, 2010. **5**(5): p. e10630.
222. Tomimaru, Y., et al., *MicroRNA-21 induces resistance to the anti-tumour effect of interferon-alpha/5-fluorouracil in hepatocellular carcinoma cells.* Br J Cancer, 2010. **103**(10): p. 1617-26.
223. Cervigne, N.K., et al., *Identification of a microRNA signature associated with progression of leukoplakia to oral carcinoma.* Hum Mol Genet, 2009. **18**(24): p. 4818-29.
224. Childs, G., et al., *Low-level expression of microRNAs let-7d and miR-205 are prognostic markers of head and neck squamous cell carcinoma.* Am J Pathol, 2009. **174**(3): p. 736-45.
225. Conti, A., et al., *miR-21 and 221 upregulation and miR-181b downregulation in human grade II-IV astrocytic tumors.* J Neurooncol, 2009. **93**(3): p. 325-32.
226. de Oliveira, P.E., et al., *Hypoxia-mediated regulation of Cdc25A phosphatase by p21 and miR-21.* Cell Cycle, 2009. **8**(19): p. 3157-64.
227. Nguyen, H.T., et al., *MicroRNA-7 modulates CD98 expression during intestinal epithelial cell differentiation.* J Biol Chem, 2010. **285**(2): p. 1479-89.
228. Feng, Y., X. Chen, and L. Gao, *Knockdown of miR-21 as a novel approach for leukemia therapy.* J Formos Med Assoc, 2010. **109**(9): p. 621-3.
229. Zhou, X., et al., *Reduction of miR-21 induces glioma cell apoptosis via activating caspase 9 and 3.* Oncol Rep, 2010. **24**(1): p. 195-201.
230. Bhatti, I., et al., *Knockdown of microRNA-21 inhibits proliferation and increases cell death by targeting programmed cell death 4 (PDCD4) in pancreatic ductal adenocarcinoma.* J Gastrointest Surg, 2011. **15**(1): p. 199-208.
231. Yan, L.X., et al., *Knockdown of miR-21 in human breast cancer cell lines inhibits proliferation, in vitro migration and in vivo tumor growth.* Breast Cancer Res, 2011. **13**(1): p. R2.
232. Finlayson, A.E. and K.W. Freeman, *A cell motility screen reveals role for MARCKS-related protein in adherens junction formation and tumorigenesis.* PLoS One, 2009. **4**(11): p. e7833.
233. Li, T., et al., *MicroRNA-21 directly targets MARCKS and promotes apoptosis resistance and invasion in prostate cancer cells.* Biochem Biophys Res Commun, 2009. **383**(3): p. 280-5.
234. Liu, X., et al., *MicroRNA profiling and head and neck cancer.* Comp Funct Genomics, 2009: p. 837514.
235. Connolly, E.C., et al., *Overexpression of miR-21 promotes an in vitro metastatic phenotype by targeting the tumor suppressor RHOB.* Mol Cancer Res, 2010. **8**(5): p. 691-700.
236. Loayza-Puch, F., et al., *Hypoxia and RAS-signaling pathways converge on, and cooperatively downregulate, the RECK tumor-suppressor protein through microRNAs.* Oncogene, 2010. **29**(18): p. 2638-48.
237. Jazdzewski, K., et al., *Thyroid hormone receptor beta (THRB) is a major target gene for microRNAs deregulated in papillary thyroid carcinoma (PTC).* J Clin Endocrinol Metab, 2011. **96**(3): p. E546-53.
238. Zheng, J., et al., *miR-21 downregulates the tumor suppressor P12 CDK2AP1 and stimulates cell proliferation and invasion.* J Cell Biochem, 2011. **112**(3): p. 872-80.
239. Huang, G.L., et al., *Clinical significance of miR-21 expression in breast cancer: SYBR-Green I-based real-time RT-PCR study of invasive ductal carcinoma.* Oncol Rep, 2009. **21**(3): p. 673-9.
240. Qi, L., et al., *Expression of miR-21 and its targets (PTEN, PDCD4, TM1) in flat epithelial atypia of the breast in relation to ductal carcinoma in situ and invasive carcinoma.* BMC Cancer, 2009. **9**: p. 163.
241. Hui, A.B., et al., *Robust global micro-RNA profiling with formalin-fixed paraffin-embedded breast cancer tissues.* Lab Invest, 2009. **89**(5): p. 597-606.

242. Du, J., et al., *BMP-6 inhibits microRNA-21 expression in breast cancer through repressing deltaEF1 and AP-1.* Cell Res, 2009. **19**(4): p. 487-96.
243. Huang, T.H., et al., *Up-regulation of miR-21 by HER2/neu signaling promotes cell invasion.* J Biol Chem, 2009. **284**(27): p. 18515-24.
244. Qian, B., et al., *High miR-21 expression in breast cancer associated with poor disease-free survival in early stage disease and high TGF-beta1.* Breast Cancer Res Treat, 2009. **117**(1): p. 131-40.
245. Ribas, J., et al., *miR-21: an androgen receptor-regulated microRNA that promotes hormone-dependent and hormone-independent prostate cancer growth.* Cancer Res, 2009. **69**(18): p. 7165-9.
246. Seike, M., et al., *MiR-21 is an EGFR-regulated anti-apoptotic factor in lung cancer in never-smokers.* Proc Natl Acad Sci U S A, 2009. **106**(29): p. 12085-90.
247. Terao, M., et al., *Induction of miR-21 by retinoic acid in estrogen receptor-positive breast carcinoma cells: biological correlates and molecular targets.* J Biol Chem, 2011. **286**(5): p. 4027-42.
248. Shin, V.Y., et al., *NF-kappaB targets miR-16 and miR-21 in gastric cancer: involvement of prostaglandin E receptors.* Carcinogenesis, 2011. **32**(2): p. 240-5.
249. Polytarchou, C., et al., *Akt2 Regulates All Akt Isoforms and Promotes Resistance to Hypoxia through Induction of miR-21 upon Oxygen Deprivation.* Cancer Res, 2011. **71**(13): p. 4720-31.
250. Frezzetti, D., et al., *Upregulation of miR-21 by Ras in vivo and its role in tumor growth.* Oncogene, 2011. **30**(3): p. 275-86.
251. Fix, L.N., et al., *MicroRNA expression profile of MCF-7 human breast cancer cells and the effect of green tea polyphenon-60.* Cancer Genomics Proteomics, 2010. **7**(5): p. 261-77.
252. Wickramasinghe, N.S., et al., *Estradiol downregulates miR-21 expression and increases miR-21 target gene expression in MCF-7 breast cancer cells.* Nucleic Acids Res, 2009. **37**(8): p. 2584-95.
253. Talotta, F., et al., *An autoregulatory loop mediated by miR-21 and PDCD4 controls the AP-1 activity in RAS transformation.* Oncogene, 2009. **28**(1): p. 73-84.
254. Cottonham, C.L., S. Kaneko, and L. Xu, *miR-21 and miR-31 converge on TIAM1 to regulate migration and invasion of colon carcinoma cells.* J Biol Chem, 2010. **285**(46): p. 35293-302.
255. Kauffmann, A. and W. Huber, *arrayQualityMetrics: Quality metrics on microarray data sets*, in *Bioconductor*.
256. Gentleman, R.C., et al., *Bioconductor: open software development for computational biology and bioinformatics.* Genome Biol, 2004. **5**(10): p. R80.
257. Gautier, L., et al., *affy--analysis of Affymetrix GeneChip data at the probe level.* Bioinformatics, 2004. **20**(3): p. 307-15.
258. Carlson, M., et al., *hgu133plus2.db: Affymetrix Human Genome U133 Plus 2.0 Array annotation data (chip hgu133plus2)*, in *Bioconductor*.
259. R. Gentleman, R., et al., *genefilter: methods for filtering genes from microarray experiments.*, in *Bioconductor*.
260. Smyth, G.K., *Limma: linear models for microarray data*, in *Bioinformatics and Computational Biology Solutions using R and Bioconductor*, W.H. R. Gentleman and V. Carey and S. Dudoit and R. Irizarry, Editor 2005, Springer: New York. p. 397-420.
261. Benjamini, Y. and Y. Hochberg, *Controlling the False Discovery Rate: A Practical and Powerful Approach to Multiple Testing.* Journal of The Royal Statistical Society. Series B (Methodological), 1995. **57**(1): p. 289-300.
262. Falcon, S. and R. Gentleman, *Using GOstats to test gene lists for GO term association.* Bioinformatics, 2007. **23**(2): p. 257-8.
263. Gentleman, R., S. Falcon, and D. Sarkar, *Category: Category Analysis*, in *Bioconductor*.
264. Kawashima, H., et al., *Glucocorticoid attenuates brain-derived neurotrophic factor-dependent upregulation of glutamate receptors via the suppression of microRNA-132 expression.* Neuroscience, 2010. **165**(4): p. 1301-11.

265. Zhao, Y., et al., *[Identification of metastasis-related microRNAs of hepatocellular carcinoma in hepatocellular carcinoma cell lines by quantitative real time PCR].* Zhonghua Gan Zang Bing Za Zhi, 2009. **17**(7): p. 526-30.
266. Niles, A.L., R.A. Moravec, and T.L. Riss, *Multiplex caspase activity and cytotoxicity assays.* Methods Mol Biol, 2008. **414**: p. 151-62.
267. !!! INVALID CITATION !!!
268. Bowman, T., et al., *STATs in oncogenesis.* Oncogene, 2000. **19**(21): p. 2474-88.
269. Inghirami, G., et al., *New and old functions of STAT3: a pivotal target for individualized treatment of cancer.* Cell Cycle, 2005. **4**(9): p. 1131-3.
270. Tumang, J.R., et al., *IL-6 rescues the hyporesponsiveness of c-Rel deficient B cells independent of Bcl-xL, Mcl-1, and Bcl-2.* Cell Immunol, 2002. **217**(1-2): p. 47-57.
271. Brock, M., et al., *Interleukin-6 modulates the expression of the bone morphogenic protein receptor type II through a novel STAT3-microRNA cluster 17/92 pathway.* Circ Res, 2009. **104**(10): p. 1184-91.
272. Yang, C.H., et al., *IFN induces miR-21 through a signal transducer and activator of transcription 3-dependent pathway as a suppressive negative feedback on IFN-induced apoptosis.* Cancer Res, 2010. **70**(20): p. 8108-16.
273. Iliopoulos, D., et al., *STAT3 activation of miR-21 and miR-181b-1 via PTEN and CYLD are part of the epigenetic switch linking inflammation to cancer.* Mol Cell, 2010. **39**(4): p. 493-506.
274. Ren, Y., et al., *MicroRNA-21 inhibitor sensitizes human glioblastoma cells U251 (PTEN-mutant) and LN229 (PTEN-wild type) to taxol.* BMC Cancer, 2010. **10**: p. 27.
275. Vasudevan, S., Y. Tong, and J.A. Steitz, *Switching from repression to activation: microRNAs can up-regulate translation.* Science, 2007. **318**(5858): p. 1931-4.
276. Place, R.F., et al., *MicroRNA-373 induces expression of genes with complementary promoter sequences.* Proc Natl Acad Sci U S A, 2008. **105**(5): p. 1608-13.
277. Yang, J., et al., *Unphosphorylated STAT3 accumulates in response to IL-6 and activates transcription by binding to NFkappaB.* Genes Dev, 2007. **21**(11): p. 1396-408.
278. Iliopoulos, D., et al., *STAT3 activation of miR-21 and miR-181b-1 via PTEN and CYLD are part of the epigenetic switch linking inflammation to cancer.* Molecular cell, 2010. **39**(4): p. 493-506.
279. Hofmann, J.J. and M. Luisa Iruela-Arispe, *Notch expression patterns in the retina: An eye on receptor-ligand distribution during angiogenesis.* Gene Expr Patterns, 2007. **7**(4): p. 461-70.
280. Katoh, M., *Notch ligand, JAG1, is evolutionarily conserved target of canonical WNT signaling pathway in progenitor cells.* Int J Mol Med, 2006. **17**(4): p. 681-5.
281. Li, L., et al., *Alagille syndrome is caused by mutations in human Jagged1, which encodes a ligand for Notch1.* Nat Genet, 1997. **16**(3): p. 243-51.
282. Krantz, I.D., D.A. Piccoli, and N.B. Spinner, *Clinical and molecular genetics of Alagille syndrome.* Curr Opin Pediatr, 1999. **11**(6): p. 558-64.
283. Colliton, R.P., et al., *Mutation analysis of Jagged1 (JAG1) in Alagille syndrome patients.* Hum Mutat, 2001. **17**(2): p. 151-2.
284. Palacios, R., et al., *A network analysis of the human T-cell activation gene network identifies JAGGED1 as a therapeutic target for autoimmune diseases.* PLoS One, 2007. **2**(11): p. e1222.
285. Zavadil, J., et al., *Integration of TGF-beta/Smad and Jagged1/Notch signalling in epithelial-to-mesenchymal transition.* EMBO J, 2004. **23**(5): p. 1155-65.
286. Weller, M., et al., *Jagged1 ablation results in cerebellar granule cell migration defects and depletion of Bergmann glia.* Dev Neurosci, 2006. **28**(1-2): p. 70-80.
287. Hashimi, S.T., et al., *MicroRNA profiling identifies miR-34a and miR-21 and their target genes JAG1 and WNT1 in the coordinate regulation of dendritic cell differentiation.* Blood, 2009. **114**(2): p. 404-14.
288. Reedijk, M., et al., *JAG1 expression is associated with a basal phenotype and recurrence in lymph node-negative breast cancer.* Breast Cancer Res Treat, 2008. **111**(3): p. 439-48.

289. Xing, Y., et al., *[Expression changes of Notch-related genes during the differentiation of human mesenchymal stem cells into neurons].* Sheng Li Xue Bao, 2007. **59**(3): p. 267-72.
290. Tiezzi, D.G., S.V. Fernandez, and J. Russo, *Epithelial mesenchymal transition during the neoplastic transformation of human breast epithelial cells by estrogen.* Int J Oncol, 2007. **31**(4): p. 823-7.
291. Snijders, A.M., et al., *Rare amplicons implicate frequent deregulation of cell fate specification pathways in oral squamous cell carcinoma.* Oncogene, 2005. **24**(26): p. 4232-42.
292. Reedijk, M., et al., *High-level coexpression of JAG1 and NOTCH1 is observed in human breast cancer and is associated with poor overall survival.* Cancer Res, 2005. **65**(18): p. 8530-7.
293. Dickson, B.C., et al., *High-level JAG1 mRNA and protein predict poor outcome in breast cancer.* Mod Pathol, 2007. **20**(6): p. 685-93.
294. Cohen, B., et al., *Cyclin D1 is a direct target of JAG1-mediated Notch signaling in breast cancer.* Breast Cancer Res Treat, 2010. **123**(1): p. 113-24.
295. Soares, R., et al., *Evidence for the notch signaling pathway on the role of estrogen in angiogenesis.* Mol Endocrinol, 2004. **18**(9): p. 2333-43.
296. Bhat-Nakshatri, P., et al., *Estradiol-regulated microRNAs control estradiol response in breast cancer cells.* Nucleic Acids Res, 2009. **37**(14): p. 4850-61.
297. Shimizu, M., et al., *Plasminogen activator uPA is a direct transcriptional target of the JAG1-Notch receptor signaling pathway in breast cancer.* Cancer Res, 2011. **71**(1): p. 277-86.
298. Selcuklu, S.D., M.T. Donoghue, and C. Spillane, *miR-21 as a key regulator of oncogenic processes.* Biochem Soc Trans, 2009. **37**(Pt 4): p. 918-25.
299. Friedland, D.R., et al., *Cholesteatoma growth and proliferation: posttranscriptional regulation by microRNA-21.* Otology & neurotology : official publication of the American Otological Society, American Neurotology Society [and] European Academy of Otology and Neurotology, 2009. **30**(7): p. 998-1005.
300. Zheng, S., et al., *17beta-Estradiol enhances breast cancer cell motility and invasion via extra-nuclear activation of actin-binding protein ezrin.* PLoS One, 2011. **6**(7): p. e22439.
301. Sanchez, A.M., et al., *Estrogen receptor-alpha promotes breast cancer cell motility and invasion via focal adhesion kinase and N-WASP.* Molecular endocrinology, 2010. **24**(11): p. 2114-25.
302. Ariazi, E.A., et al., *Estrogen induces apoptosis in estrogen deprivation-resistant breast cancer through stress responses as identified by global gene expression across time.* Proceedings of the National Academy of Sciences of the United States of America, 2011. **108**(47): p. 18879-86.
303. Lobanova, Y.S., et al., *Mechanism of estrogen-induced apoptosis in breast cancer cells: role of the NF-kappaB signaling pathway.* Biochemistry. Biokhimiia, 2007. **72**(3): p. 320-7.
304. Croxtall, J.D. and K. McKeage, *Fulvestrant: a review of its use in the management of hormone receptor-positive metastatic breast cancer in postmenopausal women.* Drugs, 2011. **71**(3): p. 363-80.
305. Manni, A. and B.M. Arafah, *Tamoxifen-induced remission in breast cancer by escalating the dose to 40 mg daily after progression on 20 mg daily: a case report and review of the literature.* Cancer, 1981. **48**(4): p. 873-5.
306. Gaur, A., et al., *Characterization of microRNA expression levels and their biological correlates in human cancer cell lines.* Cancer Res, 2007. **67**(6): p. 2456-68.
307. Chen, L., et al., *The role of microRNA expression pattern in human intrahepatic cholangiocarcinoma.* J Hepatol, 2009. **50**(2): p. 358-69.
308. Liu, H. and I.S. Kohane, *Tissue and process specific microRNA-mRNA co-expression in mammalian development and malignancy.* PLoS One, 2009. **4**(5): p. e5436.
309. Wang, Z., et al., *Down-regulation of Notch-1 and Jagged-1 inhibits prostate cancer cell growth, migration and invasion, and induces apoptosis via inactivation of Akt, mTOR, and NF-kappaB signaling pathways.* J Cell Biochem, 2010. **109**(4): p. 726-36.

310. Zhang, Y., et al., *Down-regulation of Jagged-1 induces cell growth inhibition and S phase arrest in prostate cancer cells.* Int J Cancer, 2006. **119**(9): p. 2071-7.
311. Song, B., et al., *MicroRNA-21 regulates breast cancer invasion partly by targeting tissue inhibitor of metalloproteinase 3 expression.* J Exp Clin Cancer Res, 2010. **29**: p. 29.
312. Martino, C.F., et al., *Reduction of the Earth's magnetic field inhibits growth rates of model cancer cell lines.* Bioelectromagnetics, 2010. **31**(8): p. 649-55.
313. Bane, A.L., et al., *Expression profiling of familial breast cancers demonstrates higher expression of FGFR2 in BRCA2-associated tumors.* Breast Cancer Res Treat, 2009. **117**(1): p. 183-91.
314. Luo, H., et al., *Down-regulated miR-9 and miR-433 in human gastric carcinoma.* J Exp Clin Cancer Res, 2009. **28**: p. 82.
315. Zhu, L., et al., *MicroRNA-9 up-regulation is involved in colorectal cancer metastasis via promoting cell motility.* Med Oncol, 2011.
316. Khew-Goodall, Y. and G.J. Goodall, *Myc-modulated miR-9 makes more metastases.* Nat Cell Biol, 2010. **12**(3): p. 209-11.
317. Sun, Y., et al., *Expression profile of microRNAs in c-Myc induced mouse mammary tumors.* Breast Cancer Res Treat, 2009. **118**(1): p. 185-96.
318. Song, G., et al., *MicroRNAs control hepatocyte proliferation during liver regeneration.* Hepatology, 2010. **51**(5): p. 1735-43.
319. Tan, H.X., et al., *MicroRNA-9 reduces cell invasion and E-cadherin secretion in SK-Hep-1 cell.* Med Oncol, 2010. **27**(3): p. 654-60.
320. Wan, H.Y., et al., *Regulation of the transcription factor NF-kappaB1 by microRNA-9 in human gastric adenocarcinoma.* Mol Cancer, 2010. **9**: p. 16.
321. Guo, L.M., et al., *MicroRNA-9 inhibits ovarian cancer cell growth through regulation of NF-kappaB1.* FEBS J, 2009. **276**(19): p. 5537-46.
322. Laios, A., et al., *Potential role of miR-9 and miR-223 in recurrent ovarian cancer.* Mol Cancer, 2008. **7**: p. 35.
323. Guled, M., et al., *CDKN2A, NF2, and JUN are dysregulated among other genes by miRNAs in malignant mesothelioma -A miRNA microarray analysis.* Genes Chromosomes Cancer, 2009. **48**(7): p. 615-23.
324. Zhao, C., et al., *A feedback regulatory loop involving microRNA-9 and nuclear receptor TLX in neural stem cell fate determination.* Nat Struct Mol Biol, 2009. **16**(4): p. 365-71.
325. Hsu, P.Y., et al., *Xenoestrogen-induced epigenetic repression of microRNA-9-3 in breast epithelial cells.* Cancer Res, 2009. **69**(14): p. 5936-45.
326. Packer, A.N., et al., *The bifunctional microRNA miR-9/miR-9* regulates REST and CoREST and is downregulated in Huntington's disease.* J Neurosci, 2008. **28**(53): p. 14341-6.
327. Chao, T.F., et al., *[MiR-9 regulates the expression of CBX7 in human glioma].* Zhongguo Yi Xue Ke Xue Yuan Xue Bao, 2008. **30**(3): p. 268-74.
328. Rotkrua, P., et al., *MiR-9 down-regulates CDX2 expression in gastric cancer cells.* Int J Cancer, 2011.
329. Smirnova, L., et al., *Regulation of miRNA expression during neural cell specification.* Eur J Neurosci, 2005. **21**(6): p. 1469-77.
330. Diederichs, S. and D.A. Haber, *Dual role for argonautes in microRNA processing and posttranscriptional regulation of microRNA expression.* Cell, 2007. **131**(6): p. 1097-108.
331. Ro, S., et al., *Tissue-dependent paired expression of miRNAs.* Nucleic Acids Res, 2007. **35**(17): p. 5944-53.
332. Xue, L.Y., S.M. Chiu, and N.L. Oleinick, *Staurosporine-induced death of MCF-7 human breast cancer cells: a distinction between caspase-3-dependent steps of apoptosis and the critical lethal lesions.* Exp Cell Res, 2003. **283**(2): p. 135-45.
333. Huang, Y., et al., *Involvement of Annexin A2 in p53 induced apoptosis in lung cancer.* Mol Cell Biochem, 2008. **309**(1-2): p. 117-23.
334. Bao, H., et al., *Overexpression of Annexin II affects the proliferation, apoptosis, invasion and production of proangiogenic factors in multiple myeloma.* Int J Hematol, 2009. **90**(2): p. 177-85.

335. Braden, A.R., et al., *Polymeric nanoparticles for sustained down-regulation of annexin A2 inhibit prostate tumor growth.* J Nanosci Nanotechnol, 2009. **9**(5): p. 2856-65.
336. Cortesi, L., et al., *Identification of protein clusters predictive of response to chemotherapy in breast cancer patients.* J Proteome Res, 2009. **8**(11): p. 4916-33.
337. Zhang, F., et al., *Anxa2 plays a critical role in enhanced invasiveness of the multidrug resistant human breast cancer cells.* J Proteome Res, 2009. **8**(11): p. 5041-7.
338. Nedjadi, T., et al., *S100A6 binds to annexin 2 in pancreatic cancer cells and promotes pancreatic cancer cell motility.* Br J Cancer, 2009. **101**(7): p. 1145-54.
339. Das, S., et al., *Signal transducer and activator of transcription 6 (STAT6) is a novel interactor of annexin A2 in prostate cancer cells.* Biochemistry, 2010. **49**(10): p. 2216-26.
340. Naryzhny, S.N. and H. Lee, *Proliferating cell nuclear antigen in the cytoplasm interacts with components of glycolysis and cancer.* FEBS Lett, 2010.
341. Tobita, H., et al., *Gene expression profile of DNA binding protein A transgenic mice.* Int J Oncol, 2006. **29**(3): p. 673-9.
342. Wang, G.R., et al., *Upregulation of human DNA binding protein A (dbpA) in gastric cancer cells.* Acta Pharmacol Sin, 2009. **30**(10): p. 1436-42.
343. Crawford, N.P., et al., *The metastasis efficiency modifier ribosomal RNA processing 1 homolog B (RRP1B) is a chromatin-associated factor.* J Biol Chem, 2009. **284**(42): p. 28660-73.
344. Dormeyer, W., et al., *Plasma membrane proteomics of human embryonic stem cells and human embryonal carcinoma cells.* J Proteome Res, 2008. **7**(7): p. 2936-51.
345. Saito, Y., et al., *Cold shock domain protein A represses angiogenesis and lymphangiogenesis via inhibition of serum response element.* Oncogene, 2008. **27**(13): p. 1821-33.
346. Buchert, M., et al., *Symplekin promotes tumorigenicity by up-regulating claudin-2 expression.* Proc Natl Acad Sci U S A, 2010. **107**(6): p. 2628-33.
347. Matsumoto, G., et al., *Cold shock domain protein A (CSDA) overexpression inhibits tumor growth and lymph node metastasis in a mouse model of squamous cell carcinoma.* Clin Exp Metastasis, 2010. **27**(7): p. 539-47.
348. Burrows, C., et al., *The RNA binding protein Larp1 regulates cell division, apoptosis and cell migration.* Nucleic Acids Res, 2010. **38**(16): p. 5542-53.
349. Andersen, J.N., et al., *Pathway-based identification of biomarkers for targeted therapeutics: personalized oncology with PI3K pathway inhibitors.* Sci Transl Med, 2010. **2**(43): p. 43ra55.
350. Fornari, F., et al., *MiR-122/cyclin G1 interaction modulates p53 activity and affects doxorubicin sensitivity of human hepatocarcinoma cells.* Cancer Res, 2009. **69**(14): p. 5761-7.
351. Ohtsuka, T., et al., *The negative role of cyclin G in ATM-dependent p53 activation.* Oncogene, 2004. **23**(31): p. 5405-8.
352. Shimizu, S., et al., *The let-7 family of microRNAs inhibits Bcl-xL expression and potentiates sorafenib-induced apoptosis in human hepatocellular carcinoma.* J Hepatol, 2010. **52**(5): p. 698-704.
353. Xu, X., et al., *Quantitative proteomics study of breast cancer cell lines isolated from a single patient: discovery of TIMM17A as a marker for breast cancer.* Proteomics, 2010. **10**(7): p. 1374-90.
354. Li, J.L., et al., *Correlation between methylation profile of promoter cpg islands of seven metastasis-associated genes and their expression states in six cell lines of liver origin.* Ai Zheng, 2004. **23**(9): p. 985-91.
355. Andrew, A.S., et al., *Bladder cancer SNP panel predicts susceptibility and survival.* Hum Genet, 2009. **125**(5-6): p. 527-39.
356. Hayes, G.M., P.E. Carrigan, and L.J. Miller, *Serine-arginine protein kinase 1 overexpression is associated with tumorigenic imbalance in mitogen-activated protein kinase pathways in breast, colonic, and pancreatic carcinomas.* Cancer Res, 2007. **67**(5): p. 2072-80.

357. Schenk, P.W., et al., *Resistance to platinum-containing chemotherapy in testicular germ cell tumors is associated with downregulation of the protein kinase SRPK1.* Neoplasia, 2004. **6**(4): p. 297-301.
358. Krishnakumar, S., et al., *SRPK1: a cisplatin sensitive protein expressed in retinoblastoma.* Pediatr Blood Cancer, 2008. **50**(2): p. 402-6.
359. Petrenko, A.A., et al., *Downregulation of genes encoding for subunits of adaptor complex-3 in cervical carcinomas.* Biochemistry (Mosc), 2006. **71**(10): p. 1153-60.
360. Lewis-Wambi, J.S., et al., *Overexpression of CEACAM6 promotes migration and invasion of oestrogen-deprived breast cancer cells.* Eur J Cancer, 2008. **44**(12): p. 1770-9.
361. Mantripragada, K.K., et al., *Genome-wide high-resolution analysis of DNA copy number alterations in NF1-associated malignant peripheral nerve sheath tumors using 32K BAC array.* Genes Chromosomes Cancer, 2009. **48**(10): p. 897-907.
362. Zhai, Y., et al., *Loss of estrogen receptor 1 enhances cervical cancer invasion.* Am J Pathol, 2010. **177**(2): p. 884-95.
363. Godinho, M., et al., *Characterization of BCAR4, a novel oncogene causing endocrine resistance in human breast cancer cells.* J Cell Physiol, 2010.
364. Pandey, D.P. and D. Picard, *miR-22 inhibits estrogen signaling by directly targeting the estrogen receptor alpha mRNA.* Mol Cell Biol, 2009. **29**(13): p. 3783-90.
365. Tchatchou, S., et al., *A variant affecting a putative miRNA target site in estrogen receptor (ESR) 1 is associated with breast cancer risk in premenopausal women.* Carcinogenesis, 2009. **30**(1): p. 59-64.
366. Di Leva, G., et al., *MicroRNA cluster 221-222 and estrogen receptor alpha interactions in breast cancer.* J Natl Cancer Inst, 2010. **102**(10): p. 706-21.
367. O'Day, E. and A. Lal, *MicroRNAs and their target gene networks in breast cancer.* Breast Cancer Res, 2010. **12**(2): p. 201.
368. Duale, N., et al., *Molecular portrait of cisplatin induced response in human testis cancer cell lines based on gene expression profiles.* Mol Cancer, 2007. **6**: p. 53.
369. Garzon, R., et al., *MicroRNA-29b induces global DNA hypomethylation and tumor suppressor gene reexpression in acute myeloid leukemia by targeting directly DNMT3A and 3B and indirectly DNMT1.* Blood, 2009. **113**(25): p. 6411-8.
370. Loven, J., et al., *MYCN-regulated microRNAs repress estrogen receptor-alpha (ESR1) expression and neuronal differentiation in human neuroblastoma.* Proc Natl Acad Sci U S A, 2010. **107**(4): p. 1553-8.
371. Butt, A.J., et al., *The estrogen and c-Myc target gene HSPC111 is over-expressed in breast cancer and associated with poor patient outcome.* Breast Cancer Res, 2008. **10**(2): p. R28.
372. Musgrove, E.A., et al., *Identification of functional networks of estrogen- and c-Myc-responsive genes and their relationship to response to tamoxifen therapy in breast cancer.* PLoS One, 2008. **3**(8): p. e2987.
373. Almeida, M.I., R.M. Reis, and G.A. Calin, *MYC-microRNA-9-metastasis connection in breast cancer.* Cell Res, 2010. **20**(6): p. 603-4.
374. Papanikolaou, V., et al., *Survivin regulation by HER2 through NF-kappaB and c-myc in irradiated breast cancer cells.* J Cell Mol Med, 2010.
375. Albihn, A., J.I. Johnsen, and M.A. Henriksson, *MYC in oncogenesis and as a target for cancer therapies.* Adv Cancer Res, 2010. **107**: p. 163-224.
376. Bui, T.V. and J.T. Mendell, *Myc: Maestro of MicroRNAs.* Genes Cancer, 2010. **1**(6): p. 568-575.
377. Zhang, L., et al., *The impact of C-MYC gene expression on gastric cancer cell.* Mol Cell Biochem, 2010.
378. Bernal-Mizrachi, L., C.M. Lovly, and L. Ratner, *The role of NF-{kappa}B-1 and NF-{kappa}B-2-mediated resistance to apoptosis in lymphomas.* Proc Natl Acad Sci U S A, 2006. **103**(24): p. 9220-5.
379. Lerebours, F., et al., *NF-kappa B genes have a major role in inflammatory breast cancer.* BMC Cancer, 2008. **8**: p. 41.
380. Van Laere, S.J., et al., *Nuclear factor-kappaB signature of inflammatory breast cancer by cDNA microarray validated by quantitative real-time reverse*

transcription-PCR, immunohistochemistry, and nuclear factor-kappaB DNA-binding. Clin Cancer Res, 2006. **12**(11 Pt 1): p. 3249-56.
381. Zhang, J., et al., *NFkappaB1/p50 is not required for tumor necrosis factor-stimulated growth of primary mammary epithelial cells: implications for NFkappaB2/p52 and RelB.* Endocrinology, 2007. **148**(1): p. 268-78.
382. Bazzoni, F., et al., *Induction and regulatory function of miR-9 in human monocytes and neutrophils exposed to proinflammatory signals.* Proc Natl Acad Sci U S A, 2009. **106**(13): p. 5282-7.
383. Iliopoulos, D., H.A. Hirsch, and K. Struhl, *An epigenetic switch involving NF-kappaB, Lin28, Let-7 MicroRNA, and IL6 links inflammation to cell transformation.* Cell, 2009. **139**(4): p. 693-706.
384. Dansithong, W., et al., *MBNL1 is the primary determinant of focus formation and aberrant insulin receptor splicing in DM1.* J Biol Chem, 2005. **280**(7): p. 5773-80.
385. Vajda, N.A., et al., *Muscleblind-like 1 is a negative regulator of TGF-beta-dependent epithelial-mesenchymal transition of atrioventricular canal endocardial cells.* Dev Dyn, 2009. **238**(12): p. 3266-72.
386. Goh, X.Y., et al., *Integrative analysis of array-comparative genomic hybridisation and matched gene expression profiling data reveals novel genes with prognostic significance in oesophageal adenocarcinoma.* Gut, 2011.
387. Luftman, K., et al., *Silencing of VAMP3 inhibits cell migration and integrin-mediated adhesion.* Biochem Biophys Res Commun, 2009. **380**(1): p. 65-70.
388. Feldmann, A., et al., *Transport of the major myelin proteolipid protein is directed by VAMP3 and VAMP7.* J Neurosci, 2011. **31**(15): p. 5659-72.
389. Janoueix-Lerosey, I., et al., *Gene expression profiling of 1p35-36 genes in neuroblastoma.* Oncogene, 2004. **23**(35): p. 5912-22.
390. Pontes, E.R., et al., *Auto-antibodies in prostate cancer: humoral immune response to antigenic determinants coded by the differentially expressed transcripts FLJ23438 and VAMP3.* Prostate, 2006. **66**(14): p. 1463-73.
391. Kean, M.J., et al., *VAMP3, syntaxin-13 and SNAP23 are involved in secretion of matrix metalloproteinases, degradation of the extracellular matrix and cell invasion.* J Cell Sci, 2009. **122**(Pt 22): p. 4089-98.
392. Schultz, N., et al., *Off-target effects dominate a large-scale RNAi screen for modulators of the TGF-beta pathway and reveal microRNA regulation of TGFBR2.* Silence, 2011. **2**: p. 3.
393. Forrester, E., et al., *Effect of conditional knockout of the type II TGF-beta receptor gene in mammary epithelia on mammary gland development and polyomavirus middle T antigen induced tumor formation and metastasis.* Cancer Res, 2005. **65**(6): p. 2296-302.
394. Hembruff, S.L., et al., *Loss of transforming growth factor-beta signaling in mammary fibroblasts enhances CCL2 secretion to promote mammary tumor progression through macrophage-dependent and -independent mechanisms.* Neoplasia, 2010. **12**(5): p. 425-33.
395. Xu, J.B., et al., *Defective expression of transforming growth factor beta type II receptor (TGFBR2) in the large cell variant of non-small cell lung carcinoma.* Lung Cancer, 2007. **58**(1): p. 36-43.
396. Bellam, N. and B. Pasche, *Tgf-beta signaling alterations and colon cancer.* Cancer Treat Res, 2010. **155**: p. 85-103.
397. Mamiya, T., et al., *Reduced transforming growth factor-beta receptor II expression in hepatocellular carcinoma correlates with intrahepatic metastasis.* Lab Invest, 2010. **90**(9): p. 1339-45.
398. Meierjohann, S., et al., *MMP13 mediates cell cycle progression in melanocytes and melanoma cells: in vitro studies of migration and proliferation.* Mol Cancer, 2010. **9**: p. 201.
399. Rizki, A., et al., *A human breast cell model of preinvasive to invasive transition.* Cancer Res, 2008. **68**(5): p. 1378-87.
400. Kondratiev, S., et al., *Expression and prognostic role of MMP2, MMP9, MMP13, and MMP14 matrix metalloproteinases in sinonasal and oral malignant melanomas.* Hum Pathol, 2008. **39**(3): p. 337-43.
401. Kumamoto, K., et al., *ING2 is upregulated in colon cancer and increases invasion by enhanced MMP13 expression.* Int J Cancer, 2009. **125**(6): p. 1306-15.

402. Lederle, W., et al., *MMP13 as a stromal mediator in controlling persistent angiogenesis in skin carcinoma.* Carcinogenesis, 2010. **31**(7): p. 1175-84.
403. Jones, S.W., et al., *The identification of differentially expressed microRNA in osteoarthritic tissue that modulate the production of TNF-alpha and MMP13.* Osteoarthritis Cartilage, 2009. **17**(4): p. 464-72.
404. Chang, H.J., et al., *MMP13 is potentially a new tumor marker for breast cancer diagnosis.* Oncol Rep, 2009. **22**(5): p. 1119-27.
405. Nannuru, K.C., et al., *Matrix metalloproteinase (MMP)-13 regulates mammary tumor-induced osteolysis by activating MMP9 and transforming growth factor-beta signaling at the tumor-bone interface.* Cancer Res, 2010. **70**(9): p. 3494-504.
406. Ellsworth, R.E., et al., *A gene expression signature that defines breast cancer metastases.* Clin Exp Metastasis, 2009. **26**(3): p. 205-13.
407. Liu, J., et al., *Concurrent down-regulation of Egr-1 and gelsolin in the majority of human breast cancer cells.* Cancer Genomics Proteomics, 2007. **4**(6): p. 377-85.
408. Zhu, L., C. Johnson, and M. Bakovic, *Stimulation of the human CTP:phosphoethanolamine cytidylyltransferase gene by early growth response protein 1.* J Lipid Res, 2008. **49**(10): p. 2197-211.
409. Parra, E. and J. Ferreira, *The effect of siRNA-Egr-1 and camptothecin on growth and chemosensitivity of breast cancer cell lines.* Oncol Rep, 2010. **23**(4): p. 1159-65.
410. Ferraro, B., et al., *EGR1 predicts PTEN and survival in patients with non-small-cell lung cancer.* J Clin Oncol, 2005. **23**(9): p. 1921-6.
411. Yang, S.Z., I.A. Eltoum, and S.A. Abdulkadir, *Enhanced EGR1 activity promotes the growth of prostate cancer cells in an androgen-depleted environment.* J Cell Biochem, 2006. **97**(6): p. 1292-9.
412. Zheng, C., et al., *E2F1 Induces tumor cell survival via nuclear factor-kappaB-dependent induction of EGR1 transcription in prostate cancer cells.* Cancer Res, 2009. **69**(6): p. 2324-31.
413. Fang, L., et al., *Downregulation of stathmin expression is mediated directly by Egr1 and associated with p53 activity in lung cancer cell line A549.* Cell Signal, 2010. **22**(1): p. 166-73.
414. Butt, A.J., et al., *Insulin-like growth factor-binding protein-5 inhibits the growth of human breast cancer cells in vitro and in vivo.* J Biol Chem, 2003. **278**(32): p. 29676-85.
415. Akkiprik, M., et al., *Multifunctional roles of insulin-like growth factor binding protein 5 in breast cancer.* Breast Cancer Res, 2008. **10**(4): p. 212.
416. Wang, H., et al., *IGFBP2 and IGFBP5 overexpression correlates with the lymph node metastasis in T1 breast carcinomas.* Breast J, 2008. **14**(3): p. 261-7.
417. Akkiprik, M., et al., *The subcellular localization of IGFBP5 affects its cell growth and migration functions in breast cancer.* BMC Cancer, 2009. **9**: p. 103.
418. Ahn, B.Y., et al., *Genetic screen identifies insulin-like growth factor binding protein 5 as a modulator of tamoxifen resistance in breast cancer.* Cancer Res, 2010. **70**(8): p. 3013-9.
419. Walker, G., et al., *Insulin-like growth factor binding proteins IGFBP3, IGFBP4, and IGFBP5 predict endocrine responsiveness in patients with ovarian cancer.* Clin Cancer Res, 2007. **13**(5): p. 1438-44.
420. Chang, K.W., et al., *Curcumin upregulates insulin-like growth factor binding protein-5 (IGFBP-5) and C/EBPalpha during oral cancer suppression.* Int J Cancer, 2010. **127**(1): p. 9-20.
421. Mita, K., et al., *Prognostic significance of insulin-like growth factor binding protein (IGFBP)-4 and IGFBP-5 expression in breast cancer.* Jpn J Clin Oncol, 2007. **37**(8): p. 575-82.
422. Ryan, A.J., et al., *Expression of a protease-resistant insulin-like growth factor-binding protein-4 inhibits tumour growth in a murine model of breast cancer.* Br J Cancer, 2009. **101**(2): p. 278-86.
423. Durai, R., et al., *Insulin-like growth factor binding protein-4 gene therapy increases apoptosis by altering Bcl-2 and Bax proteins and decreases angiogenesis in colorectal cancer.* Int J Oncol, 2007. **30**(4): p. 883-8.

424. Yu, J.Z., et al., *Assessing the clinical utility of measuring Insulin-like Growth Factor Binding Proteins in tissues and sera of melanoma patients.* J Transl Med, 2008. **6**: p. 70.
425. Zhang, Y., et al., *Critical role of c-Jun overexpression in liver metastasis of human breast cancer xenograft model.* BMC Cancer, 2007. **7**: p. 145.
426. Maeno, K., et al., *Altered regulation of c-jun and its involvement in anchorage-independent growth of human lung cancers.* Oncogene, 2006. **25**(2): p. 271-7.
427. Xia, H.H., et al., *Induction of apoptosis and cell cycle arrest by a specific c-Jun NH2-terminal kinase (JNK) inhibitor, SP-600125, in gastrointestinal cancers.* Cancer Lett, 2006. **241**(2): p. 268-74.
428. Shen, Q., et al., *The AP-1 transcription factor regulates breast cancer cell growth via cyclins and E2F factors.* Oncogene, 2008. **27**(3): p. 366-77.
429. Justenhoven, C., et al., *Polymorphic loci of E2F2, CCND1 and CCND3 are associated with HER2 status of breast tumors.* Int J Cancer, 2009. **124**(9): p. 2077-81.
430. Reimer, D., et al., *Heterogeneous cross-talk of E2F family members is crucially involved in growth modulatory effects of interferon-gamma and EGF.* Cancer Biol Ther, 2006. **5**(7): p. 771-6.
431. Sylvestre, Y., et al., *An E2F/miR-20a autoregulatory feedback loop.* J Biol Chem, 2007. **282**(4): p. 2135-43.
432. Timmers, C., et al., *E2f1, E2f2, and E2f3 control E2F target expression and cellular proliferation via a p53-dependent negative feedback loop.* Mol Cell Biol, 2007. **27**(1): p. 65-78.
433. Dong, Q., et al., *MicroRNA let-7a inhibits proliferation of human prostate cancer cells in vitro and in vivo by targeting E2F2 and CCND2.* PLoS One, 2010. **5**(4): p. e10147.
434. Pusapati, R.V., et al., *E2F2 suppresses Myc-induced proliferation and tumorigenesis.* Mol Carcinog, 2010. **49**(2): p. 152-6.
435. Wang, D., et al., *Differential protein expression in MCF7 breast cancer cells transfected with ErbB2, neomycin resistance and luciferase plus yellow fluorescent protein.* Proteomics, 2004. **4**(7): p. 2175-83.
436. Strasser, S., et al., *5-FdUrd-araC heterodinucleoside re-establishes sensitivity in 5-FdUrd- and AraC-resistant MCF-7 breast cancer cells overexpressing ErbB2.* Differentiation, 2006. **74**(9-10): p. 488-98.
437. Liu, N., et al., *Erbin-regulated sensitivity of MCF-7 breast cancer cells to TRAIL via ErbB2/AKT/NF-kappaB pathway.* J Biochem, 2008. **143**(6): p. 793-801.
438. Epis, M.R., et al., *miR-331-3p regulates ERBB-2 expression and androgen receptor signaling in prostate cancer.* J Biol Chem, 2009. **284**(37): p. 24696-704.
439. Ghellal, A., et al., *Prognostic significance of TGF beta 1 and TGF beta 3 in human breast carcinoma.* Anticancer Res, 2000. **20**(6B): p. 4413-8.
440. Figueroa, J.D., et al., *Expression of TGF-beta signaling factors in invasive breast cancers: relationships with age at diagnosis and tumor characteristics.* Breast Cancer Res Treat, 2010. **121**(3): p. 727-35.
441. Bolat, F., et al., *Expression of vascular endothelial growth factor (VEGF), hypoxia inducible factor 1 alpha (HIF-1alpha), and transforming growth factors beta1 (TGFbeta1) and beta3 (TGFbeta3) in gestational trophoblastic disease.* Pathol Res Pract, 2010. **206**(1): p. 19-23.
442. Joseph, D.S., et al., *Myometrial cells undergo fibrotic transformation under the influence of transforming growth factor beta-3.* Fertil Steril, 2010. **93**(5): p. 1500-8.
443. Lau, W.M., et al., *Identification of prospective factors promoting osteotropism in breast cancer: a potential role for CITED2.* Int J Cancer, 2010. **126**(4): p. 876-84.
444. Bakker, W.J., I.S. Harris, and T.W. Mak, *FOXO3a is activated in response to hypoxic stress and inhibits HIF1-induced apoptosis via regulation of CITED2.* Mol Cell, 2007. **28**(6): p. 941-53.
445. Bai, L. and J.L. Merchant, *A role for CITED2, a CBP/p300 interacting protein, in colon cancer cell invasion.* FEBS Lett, 2007. **581**(30): p. 5904-10.
446. Haase, M., et al., *CITED2 is expressed in human adrenocortical cells and regulated by basic fibroblast growth factor.* J Endocrinol, 2007. **192**(2): p. 459-65.

447. Benard, G., et al., *IBRDC2, an IBR-type E3 ubiquitin ligase, is a regulatory factor for Bax and apoptosis activation.* EMBO J, 2010. **29**(8): p. 1458-71.
448. Lindemann, R.K., et al., *Protein kinase Calpha regulates Ets1 transcriptional activity in invasive breast cancer cells.* Int J Oncol, 2003. **22**(4): p. 799-805.
449. Tan, M., et al., *Upregulation and activation of PKC alpha by ErbB2 through Src promotes breast cancer cell invasion that can be blocked by combined treatment with PKC alpha and Src inhibitors.* Oncogene, 2006. **25**(23): p. 3286-95.
450. Lonne, G.K., et al., *PKCalpha expression is a marker for breast cancer aggressiveness.* Mol Cancer, 2010. **9**: p. 76.
451. Kang, J.H., et al., *Plasma protein kinase C (PKC)alpha as a biomarker for the diagnosis of cancers.* Carcinogenesis, 2009. **30**(11): p. 1927-31.
452. Chiang, C.W., et al., *PKCalpha mediated induction of miR-101 in human hepatoma HepG2 cells.* J Biomed Sci, 2010. **17**: p. 35.
453. Sun, R., et al., *Global gene expression analysis reveals reduced abundance of putative microRNA targets in human prostate tumours.* BMC Genomics, 2009. **10**: p. 93.
454. Ebert, M.S. and P.A. Sharp, *Emerging roles for natural microRNA sponges.* Curr Biol, 2010. **20**(19): p. R858-61.
455. Rigoutsos, I. and F. Furnari, *Gene-expression forum: Decoy for microRNAs.* Nature, 2010. **465**(7301): p. 1016-7.
456. Kent, O.A. and J.T. Mendell, *A small piece in the cancer puzzle: microRNAs as tumor suppressors and oncogenes.* Oncogene, 2006. **25**(46): p. 6188-96.
457. Croce, C.M., *Causes and consequences of microRNA dysregulation in cancer.* Nat Rev Genet, 2009. **10**(10): p. 704-14.
458. Iguchi, H., N. Kosaka, and T. Ochiya, *Versatile applications of microRNA in anti-cancer drug discovery: from therapeutics to biomarkers.* Curr Drug Discov Technol, 2010. **7**(2): p. 95-105.
459. Sotillo, E. and A. Thomas-Tikhonenko, *Shielding the messenger (RNA): microRNA-based anticancer therapies.* Pharmacol Ther, 2011.
460. Hardin, C., et al., *Understanding the biologic mechanisms responsible for breast-cancer progression during tamoxifen or fulvestrant treatment.* American journal of surgery, 2004. **188**(4): p. 426-8.
461. Calhoun, K., et al., *The effect of high dehydroepiandrosterone sulfate levels on tamoxifen blockade and breast cancer progression.* American journal of surgery, 2003. **185**(5): p. 411-5.
462. Visscher, D.W., et al., *Tamoxifen suppresses histologic progression to atypia and DCIS in MCFIOAT xenografts, a model of early human breast cancer.* Breast cancer research and treatment, 2001. **65**(1): p. 41-7.
463. *Longer time to tumor progression with exemestane vs tamoxifen in advanced breast cancer.* Oncology, 2000. **14**(9): p. 1291, 1294.
464. Fox, B.P. and R.P. Kandpal, *Invasiveness of breast carcinoma cells and transcript profile: Eph receptors and ephrin ligands as molecular markers of potential diagnostic and prognostic application.* Biochem Biophys Res Commun, 2004. **318**(4): p. 882-92.
465. Gramantieri, L., et al., *Cyclin G1 is a target of miR-122a, a microRNA frequently down-regulated in human hepatocellular carcinoma.* Cancer Res, 2007. **67**(13): p. 6092-9.
466. Perez, R., et al., *A better cell cycle target for gene therapy of colorectal cancer: cyclin G.* J Gastrointest Surg, 2003. **7**(7): p. 884-9.
467. Gordon, E.M., et al., *Inhibition of metastatic tumor growth in nude mice by portal vein infusions of matrix-targeted retroviral vectors bearing a cytocidal cyclin G1 construct.* Cancer Res, 2000. **60**(13): p. 3343-7.
468. Liang, J., et al., *Relationship between cyclin G1 and human papilloma virus infection in cervical intraepithelial neoplasia and cervical carcinoma.* Chin Med Sci J, 2006. **21**(2): p. 81-5.
469. Schenk, P.W., et al., *SKY1 is involved in cisplatin-induced cell kill in Saccharomyces cerevisiae, and inactivation of its human homologue, SRPK1, induces cisplatin resistance in a human ovarian carcinoma cell line.* Cancer Res, 2001. **61**(19): p. 6982-6.

470. Plasencia, C., et al., *Expression analysis of genes involved in oxaliplatin response and development of oxaliplatin-resistant HT29 colon cancer cells.* Int J Oncol, 2006. **29**(1): p. 225-35.
471. Thorsen, K., et al., *Alternative splicing of SLC39A14 in colorectal cancer is regulated by the Wnt pathway.* Mol Cell Proteomics, 2011. **10**(1): p. M110 002998.
472. Sanidas, I., et al., *The ratio of SRPK1/SRPK1a regulates erythroid differentiation in K562 leukaemic cells.* Biochim Biophys Acta, 2010. **1803**(12): p. 1319-31.
473. Parle-McDermott, A., et al., *A common variant in MTHFD1L is associated with neural tube defects and mRNA splicing efficiency.* Hum Mutat, 2009. **30**(12): p. 1650-6.
474. Bonomi, P., et al., *Quantitative estrogen and progesterone receptor levels related to progression-free interval in advanced breast cancer patients treated with megestrol acetate or tamoxifen.* Seminars in oncology, 1988. **15**(2 Suppl 1): p. 26-33.
475. Khvorova, A., A. Reynolds, and S.D. Jayasena, *Functional siRNAs and miRNAs exhibit strand bias.* Cell, 2003. **115**(2): p. 209-16.
476. Schotte, D., et al., *Discovery of new microRNAs by small RNAome deep sequencing in childhood acute lymphoblastic leukemia.* Leukemia, 2011.
477. Zhou, H., et al., *miR-155 and its star-form partner miR-155* cooperatively regulate type I interferon production by human plasmacytoid dendritic cells.* Blood, 2010. **116**(26): p. 5885-94.
478. Mah, S.M., et al., *miRNA*: a passenger stranded in RNA-induced silencing complex?* Crit Rev Eukaryot Gene Expr, 2010. **20**(2): p. 141-8.
479. Yoo, A.S., et al., *MicroRNA-mediated conversion of human fibroblasts to neurons.* Nature, 2011. **476**(7359): p. 228-31.
480. Jeon, H.M., et al., *ID4 imparts chemoresistance and cancer stemness to glioma cells by derepressing miR-9*-mediated suppression of SOX2.* Cancer Res, 2011. **71**(9): p. 3410-21.
481. Onnis, A., et al., *Alteration of microRNAs regulated by c-Myc in Burkitt lymphoma.* PLoS One, 2010. **5**(9).
482. Bian, H.B., et al., *Upregulation of microRNA-451 increases cisplatin sensitivity of non-small cell lung cancer cell line (A549).* J Exp Clin Cancer Res, 2011. **30**: p. 20.
483. Chen, S., et al., *Construction and identification of a human liver specific microRNA eukaryotic expression vector.* Cell Mol Immunol, 2007. **4**(6): p. 473-7.
484. Carlson, M., et al., *hgu133a2.db: Affymetrix Human Genome U133A 2.0 Array annotation data (chip hgu133a2)*, in *Bioconductor*.
485. Bartonicek, N. and A.J. Enright, *SylArray: a web server for automated detection of miRNA effects from expression data.* Bioinformatics, 2010. **26**(22): p. 2900-1.
486. Johnson, R. and N.J. Buckley, *Gene dysregulation in Huntington's disease: REST, microRNAs and beyond.* Neuromolecular Med, 2009. **11**(3): p. 183-99.
487. Zhao, Z.S., et al., *Expression and prognostic significance of CEACAM6, ITGB1, and CYR61 in peripheral blood of patients with gastric cancer.* J Surg Oncol, 2011. **104**(5): p. 525-9.
488. Sununliganon, L. and W. Singhatanadgit, *Highly osteogenic PDL stem cell clones specifically express elevated levels of ICAM1, ITGB1 and TERT.* Cytotechnology, 2011.
489. Hunt, S., et al., *MicroRNA-124 suppresses oral squamous cell carcinoma motility by targeting ITGB1.* FEBS Lett, 2011. **585**(1): p. 187-92.
490. Schraivogel, D., et al., *CAMTA1 is a novel tumour suppressor regulated by miR-9/9(*) in glioblastoma stem cells.* EMBO J, 2011.
491. Mori, R., et al., *Targeting beta1 integrin restores sensitivity to docetaxel of esophageal squamous cell carcinoma.* Oncol Rep, 2008. **20**(6): p. 1345-51.
492. Li, G., et al., *Targeting of integrin beta1 and kinesin 2alpha by microRNA 183.* J Biol Chem, 2010. **285**(8): p. 5461-71.

Appendices

A.1. Supplementary Data

A.1.1. Heat Map of mir-21 microarray differentially expressed genes

Decreased genes (blue) in anti-21 treatment compared to untreated samples (red).

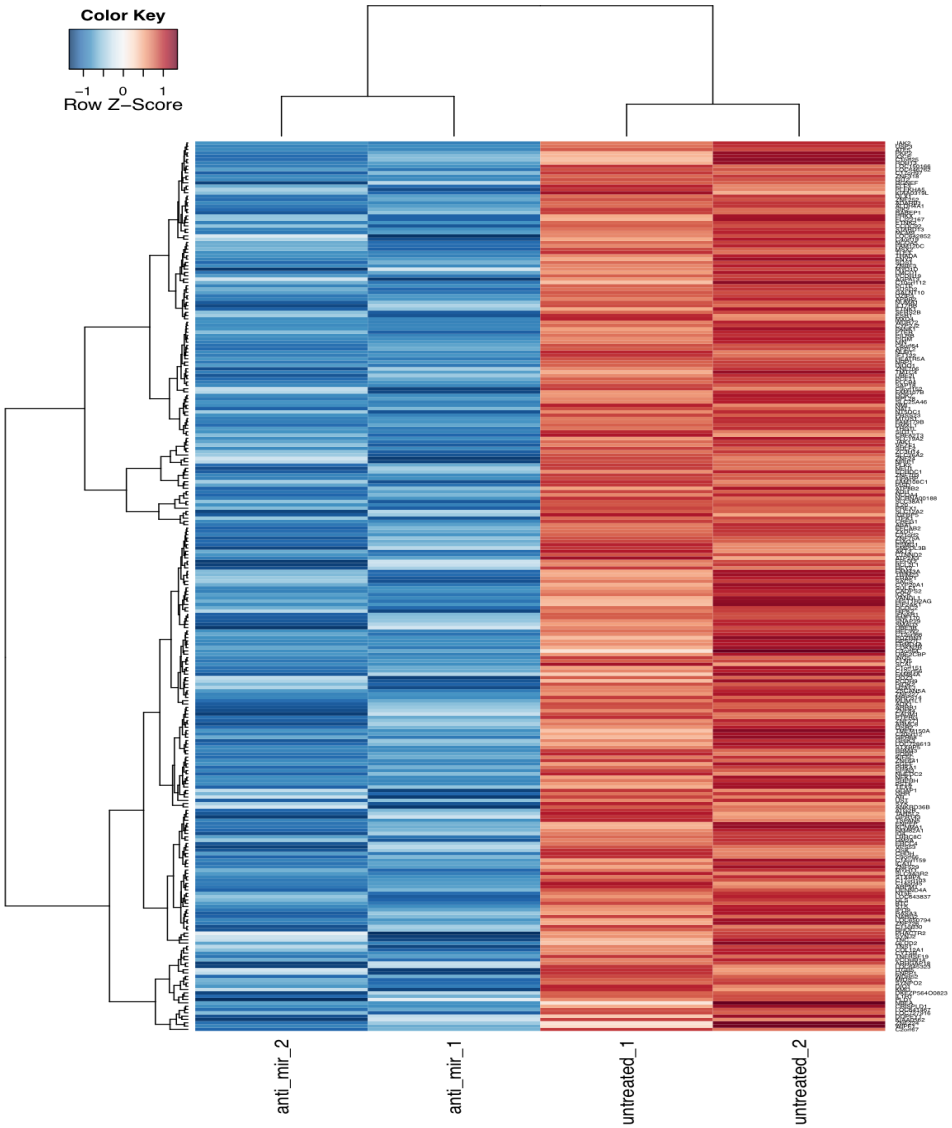

A.1.2. Heat Map of mir-21 microarray differentially expressed genes

Increased genes (red) in anti-21 treatment compared to untreated samples (blue).

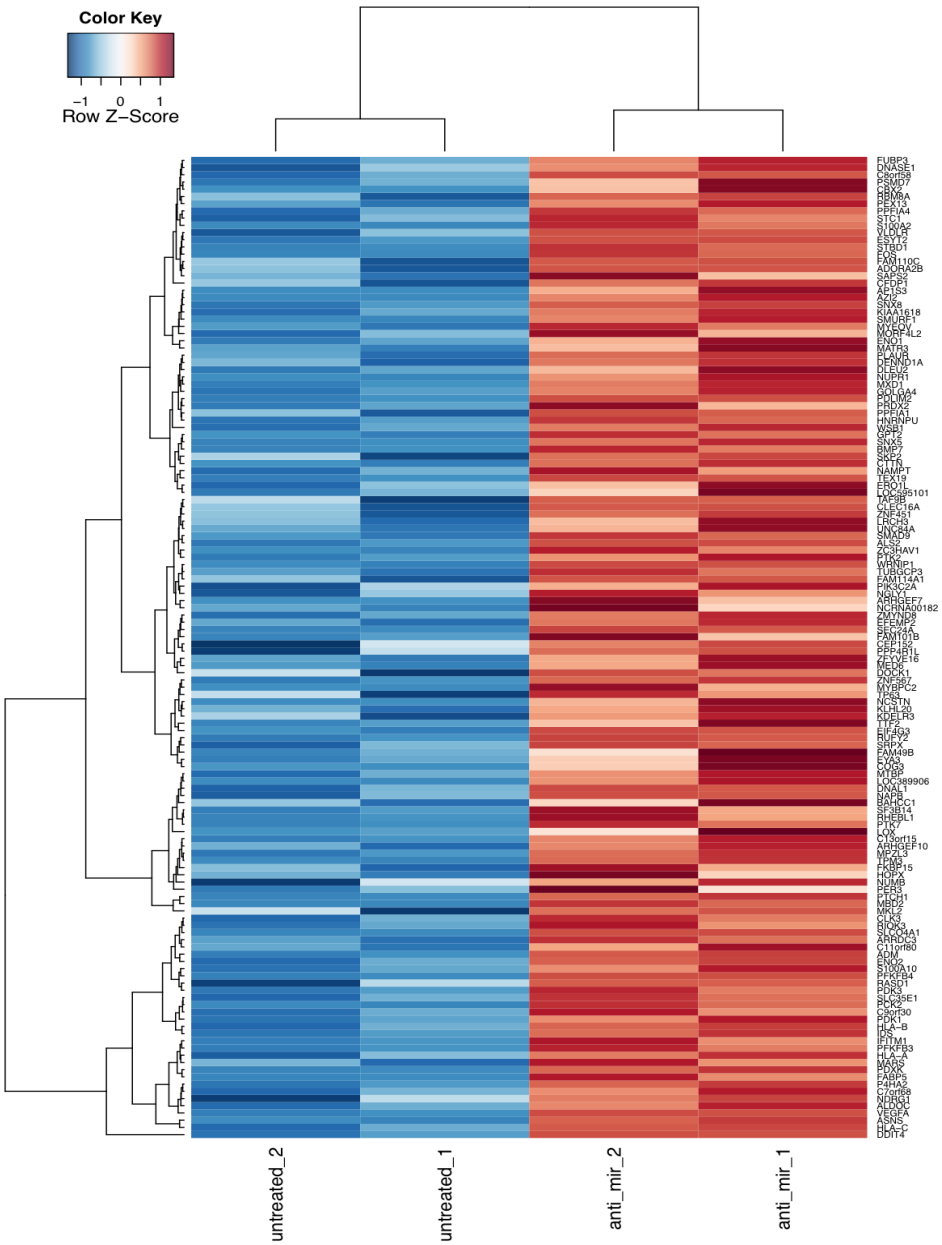

A.1.3. Cell-cycle network of differentially expressed genes identified by IPA (Ingenuity Pathway Analysis)

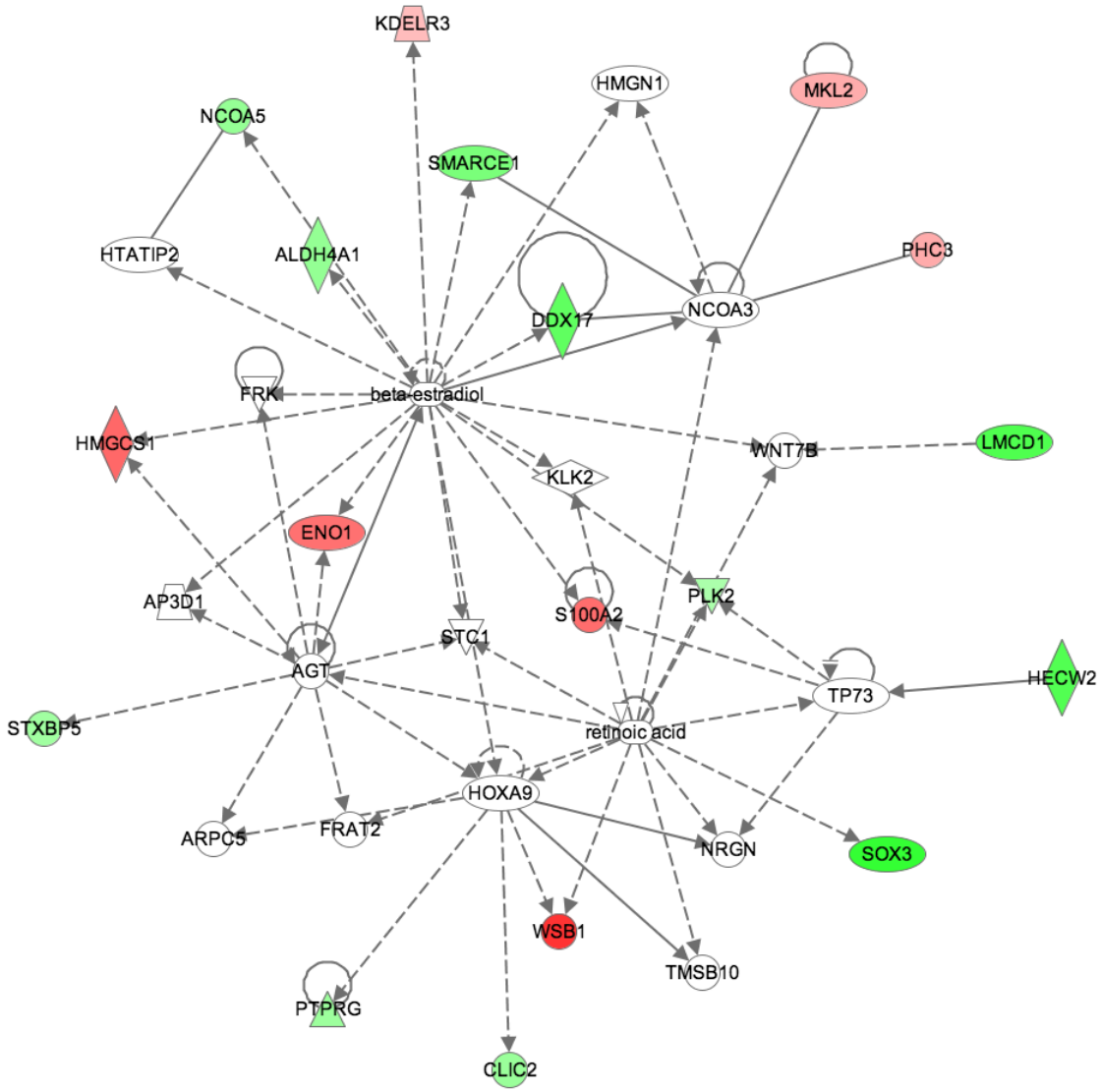

A.1.4. Cellular growth and proliferation network of differentially expressed genes identified by IPA (Ingenuity Pathway Analysis)

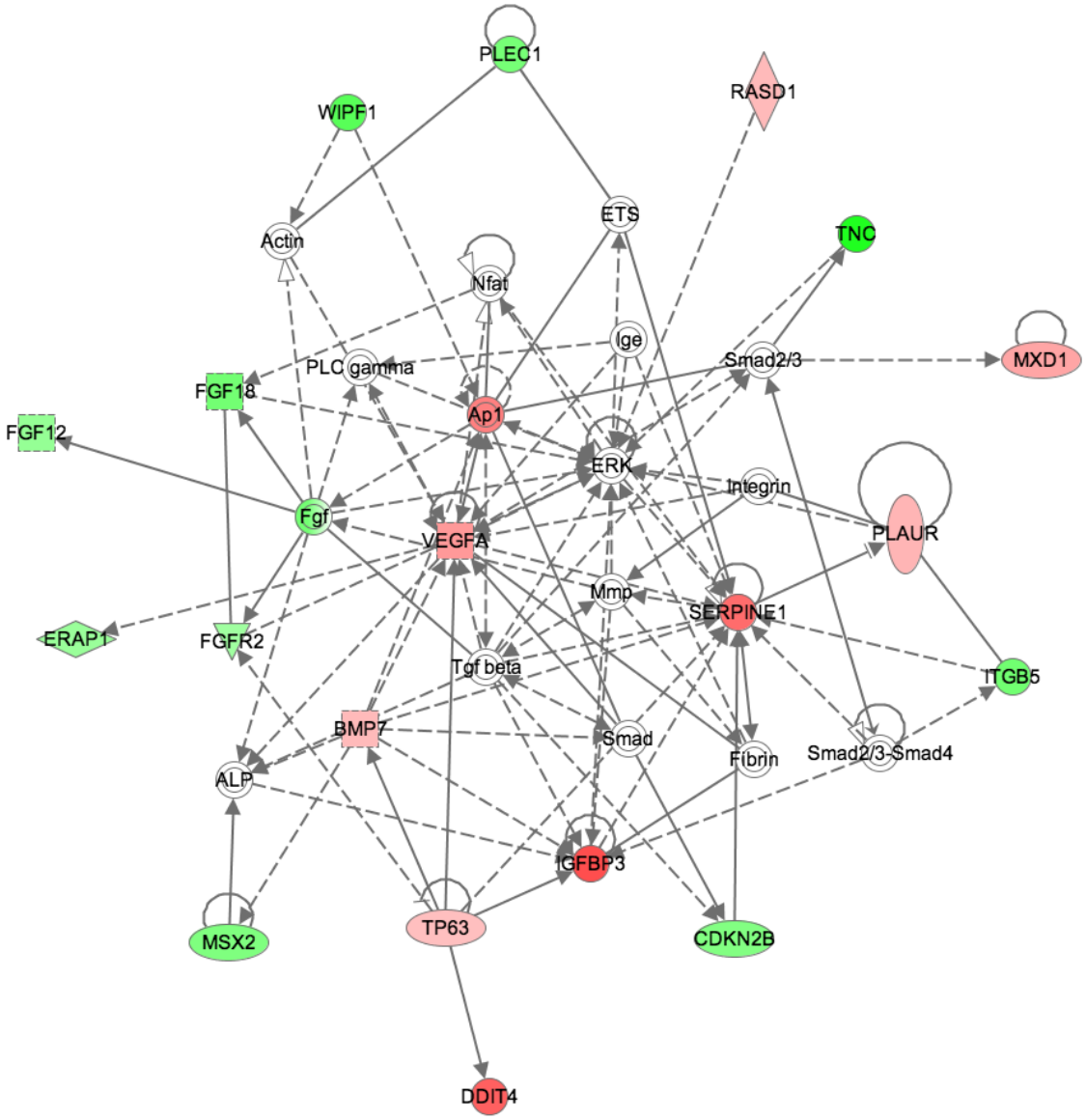

A.1.5. Tumor morphology network of differentially expressed genes identified by IPA (Ingenuity Pathway Analysis)

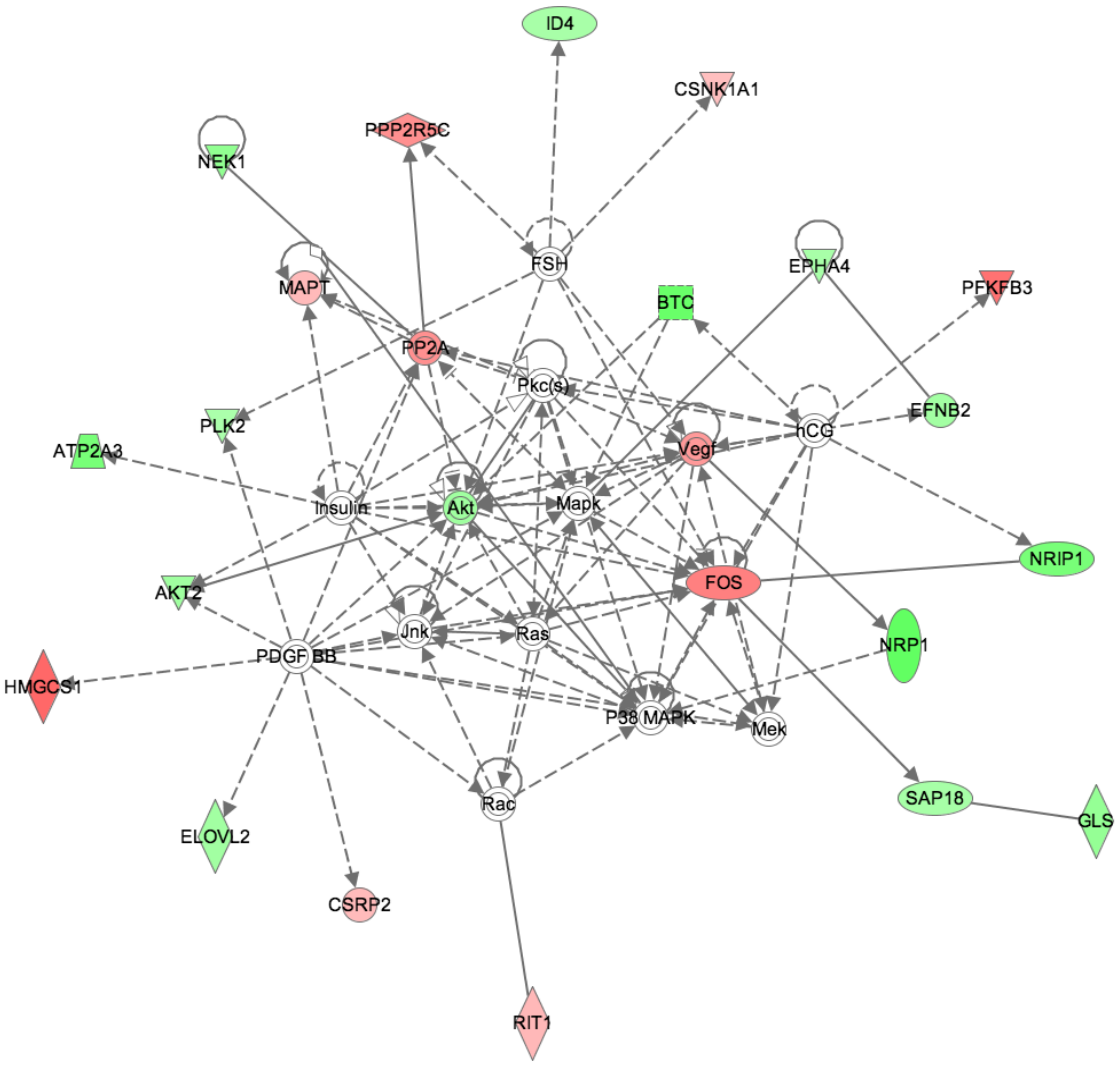

A.1.6. Heat map of mir-9 microarray

Downregulated (blue) and upregulated (red) genes are represented. Mir-9 overexpression samples (both dosages) are clustered together compared to controls.

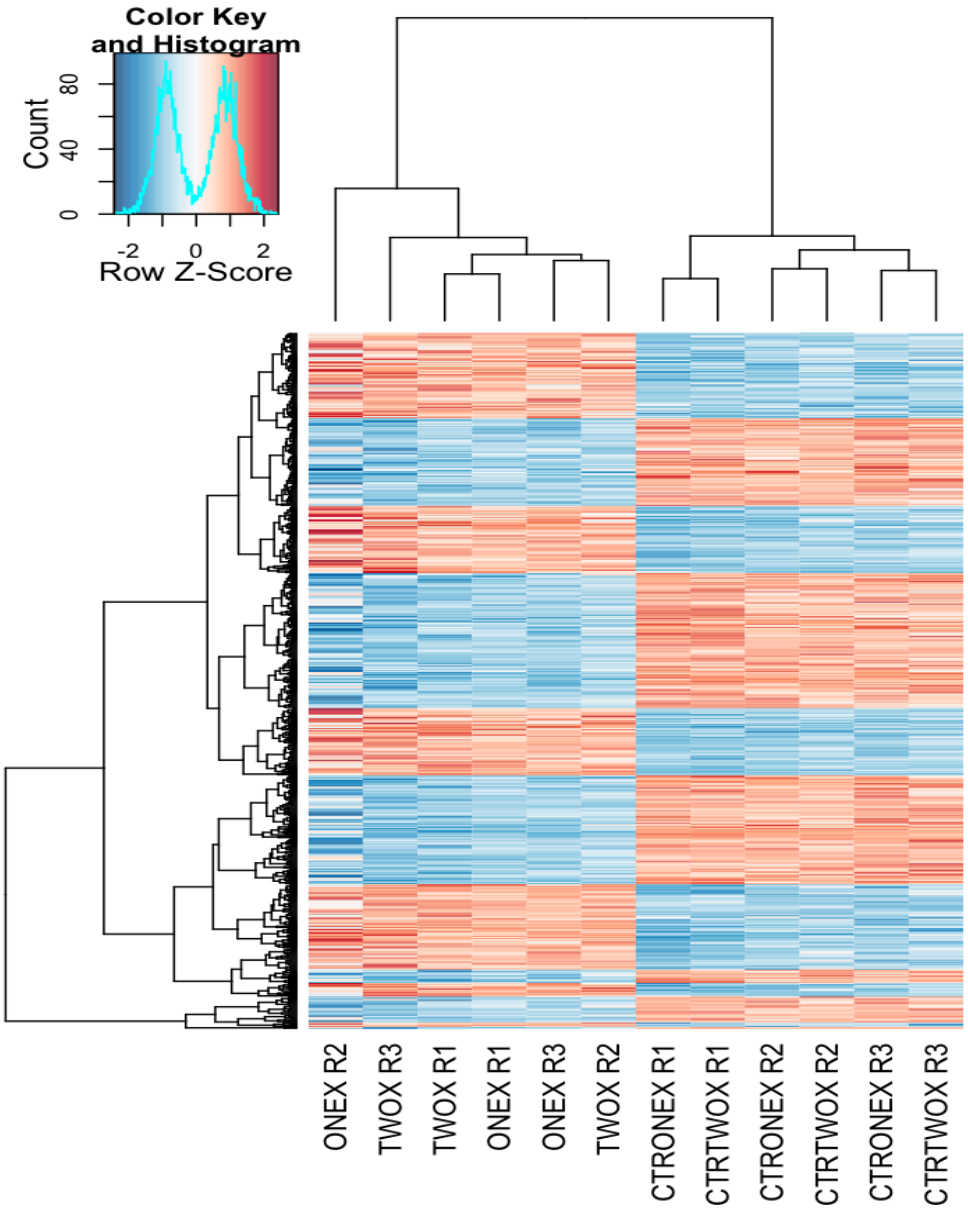

A.1.7. GO terms enriched in mir-9 microarray analysis

1X downregulated and 1X upregulated GO terms

Gene to GO Conditional test for over-representation (GOBP: Biological Processes, GOCC: Cellular Component, GOMF: Molecular Function)

1X DOWN

GOBPID	Pvalue	OddsRatio	ExpCount	Count	Size	Term
GO:000939	0	102.731	0	4	8	folic acid and derivative biosynthetic process
GO:004665	0	102.731	0	4	8	tetrahydrofolate metabolic process
GO:005118	0	8.032	1	7	98	cofactor biosynthetic process
GO:001594	0	Inf	0	2	2	formate metabolic process
GO:000675	0	18.654	0	4	26	group transfer coenzyme metabolic process
GO:000641	0	3.587	4	13	401	translation
GO:001604	0	1.989	26	43	2596	cellular component organization
GO:005113	0	202.485	0	2	3	positive regulation of NK T cell differentiation
GO:003466	0	4.258	2	9	231	ncRNA metabolic process
GO:003447	0.001	4.646	2	8	188	ncRNA processing
GO:000667	0.001	11.388	0	4	40	ceramide metabolic process

GOCCID	Pvalue	OddsRatio	ExpCount	Count	Size	Term
GO:001593	0	9.539	1	5	60	small ribosomal subunit
GO:000573	0	2.419	10	22	1035	mitochondrion
GO:003052	0.001	2.962	5	13	487	ribonucleoprotein complex

1X UP

GOBPID	Pvalue	OddsRatio	ExpCount	Count	Size	Term
GO:004232	0	14.023	0	5	41	negative regulation of phosphorylation
GO:006102	0	3.693	4	14	413	membrane organization
GO:001056	0	12.941	0	5	44	negative regulation of phosphorus metabolic process
GO:000739	0	2.561	11	24	1045	nervous system development
GO:001619	0	3.046	6	17	610	vesicle-mediated transport
GO:009009	0	8.114	1	6	81	regulation of transmembrane receptor protein serine/threonine kinase signaling pathway
GO:000821	0	2.445	12	25	1140	cell death
GO:004819	0	33.232	0	3	12	vesicle targeting, to, from or within Golgi
GO:000691	0	2.454	11	23	1036	apoptosis
GO:005172	0	3.76	3	11	314	regulation of cell cycle
GO:000689	0	8.843	1	5	62	receptor-mediated endocytosis
GO:001086	0	24.918	0	3	15	positive regulation of pathway-restricted SMAD protein phosphorylation
GO:000704	0.001	99.029	0	2	4	lysosomal lumen acidification
GO:003461	0.001	99.029	0	2	4	response to laminar fluid shear stress
GO:005066	0.001	99.029	0	2	4	homocysteine metabolic process
GO:002261	0.001	21.356	0	3	17	gland morphogenesis
GO:003050	0.001	19.93	0	3	18	positive regulation of bone mineralization
GO:000703	0.001	10.549	0	4	42	vacuole organization
GO:001032	0.001	3.909	2	9	245	membrane invagination

GOCCID	Pvalue	OddsRatio	ExpCount	Count	Size	Term
GO:000013	0	3.42	4	14	433	Golgi membrane
GO:004446	0	6.754	147	157	14208	cell part
GO:003013	0	4.817	2	8	174	coated vesicle
GO:000579	0	2.492	9	20	853	Golgi apparatus
GO:003404	0.001	97.185	0	2	4	pre-autophagosomal structure membrane
GO:000573	0.001	1.686	75	95	7239	cytoplasm
GO:000577	0.001	19.545	0	3	18	autophagic vacuole
GO:000577	0.001	5.886	1	6	107	vacuolar membrane

2X downregulated and 2X upregulated GO terms

2X DOWN

GOBPID	Pvalue	OddsRatio	ExpCount	Count	Size	Term
GO:000939	0	66.658	0	3	8	folic acid and derivative biosynthetic process
GO:004665	0	66.658	0	3	8	tetrahydrofolate metabolic process
GO:004348	0	Inf	0	2	2	cellular pigment accumulation
GO:004423	0	2.018	65	86	7109	cellular metabolic process
GO:005113	0	220.48	0	2	3	positive regulation of NK T cell differentiation
GO:003192	0	30.286	0	3	14	TOR signaling pathway
GO:003466	0	4.658	2	9	231	ncRNA metabolic process
GO:001604	0	2.019	24	40	2596	cellular component organization
GO:000641	0	7.069	1	6	102	translational elongation
GO:000673	0	5.684	1	7	147	coenzyme metabolic process
GO:000803	0.001	8.028	1	5	75	tRNA processing
GO:003057	0.001	18.499	0	3	21	collagen catabolic process

GOCCID	Pvalue	OddsRatio	ExpCount	Count	Size	Term
GO:003327	0	6.917	1	7	119	ribosomal subunit
GO:000573	0	2.941	6	17	682	nucleolus
GO:000591	0	15.021	0	4	33	cell-cell adherens junction
GO:002262	0.001	7.813	1	5	75	cytosolic ribosome

GOMFID	Pvalue	OddsRatio	ExpCount	Count	Size	Term
GO:000373	0	5.603	1	7	151	structural constituent of ribosome

2X UP

GOBPID	Pvalue	OddsRatio	ExpCount	Count	Size	Term
GO:004632	0	16.397	0	4	30	regulation of fatty acid oxidation
GO:006043	0	210.29	0	2	3	bronchus development
GO:003444	0	9.081	1	5	64	lipid oxidation
GO:003461	0.001	105.137	0	2	4	response to laminar fluid shear stress
GO:006043	0.001	105.137	0	2	4	trachea development
GO:001604	0.001	3.316	4	12	412	cellular membrane organization
GO:003018	0.001	3.129	5	13	474	neuron differentiation
GO:006039	0.001	21.169	0	3	18	regulation of pathway-restricted SMAD protein phosphorylation
GO:003250	0.001	1.868	30	47	3165	developmental process
GO:004828	0.001	19.845	0	3	19	lung alveolus development
GO:006042	0.001	70.087	0	2	5	lung epithelium development
GO:006044	0.001	70.087	0	2	5	branching involved in lung morphogenesis
GO:000739	0.001	2.335	10	21	1045	nervous system development
GO:001701	0.001	10.139	0	4	46	regulation of transforming growth factor beta receptor signaling pathway

GOCCID	Pvalue	OddsRatio	ExpCount	Count	Size	Term
GO:000573	0	1.894	68	90	7239	cytoplasm
GO:000562	0	2.031	100	118	10670	intracellular
GO:000562	0.001	6.097	133	142	14209	cell
GO:000576	0.001	7.813	1	5	75	lysosomal membrane
GO:003130	0.001	6.049	1	6	115	integral to organelle membrane
GO:000032	0.001	4.434	2	8	208	lytic vacuole
GO:001971	0.001	7.491	1	5	78	synaptosome

A.1.8. Expected fold changes of 1X, 1.5X and 2X mir-9 treatments in microarray

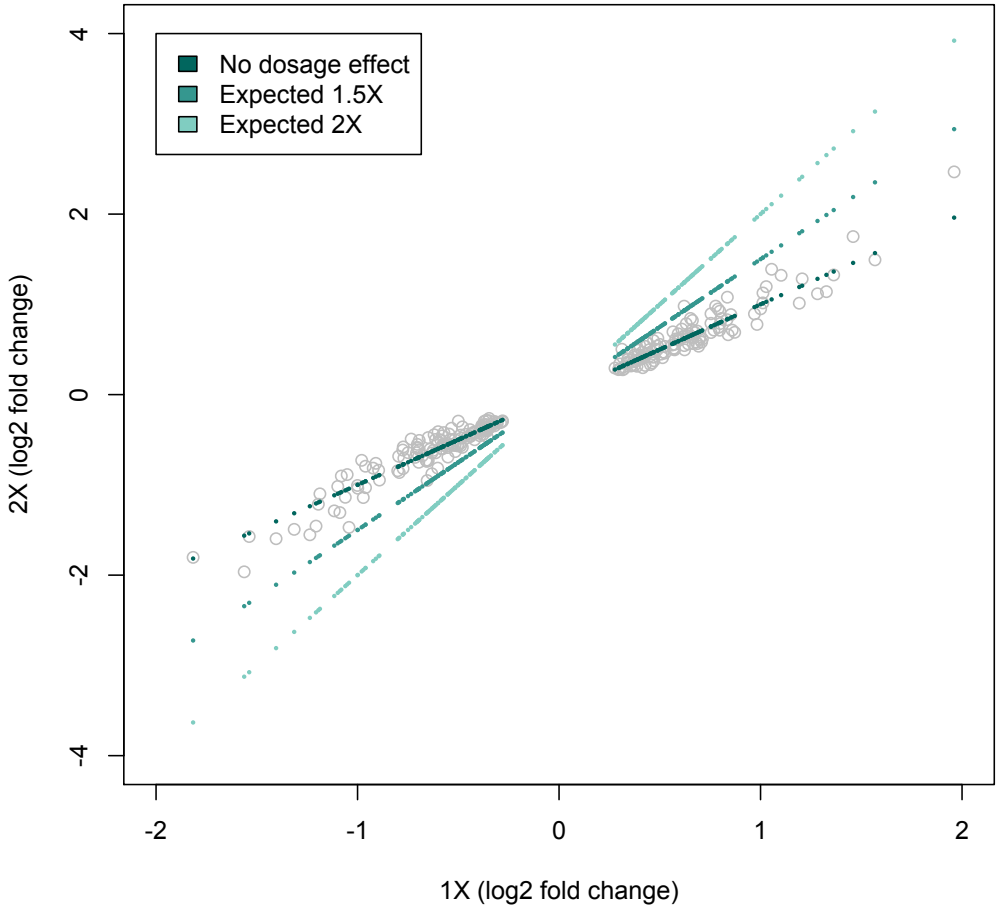

A.1.9. Flow cytometry analysis results for siRNA knockdown experiments

siRNA control: 41.8% Annexin positive (apoptotic) cells

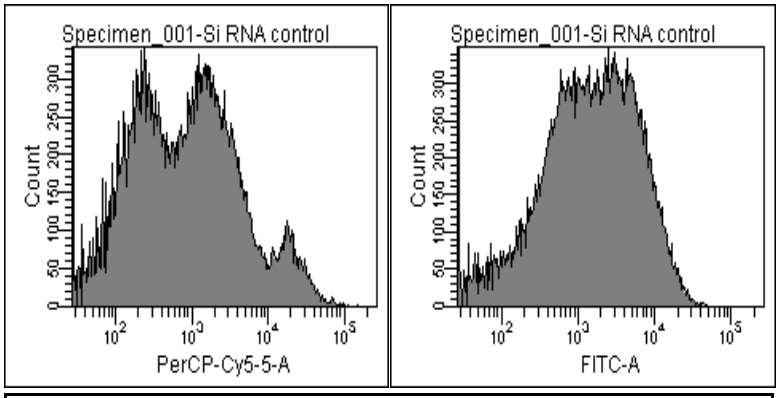

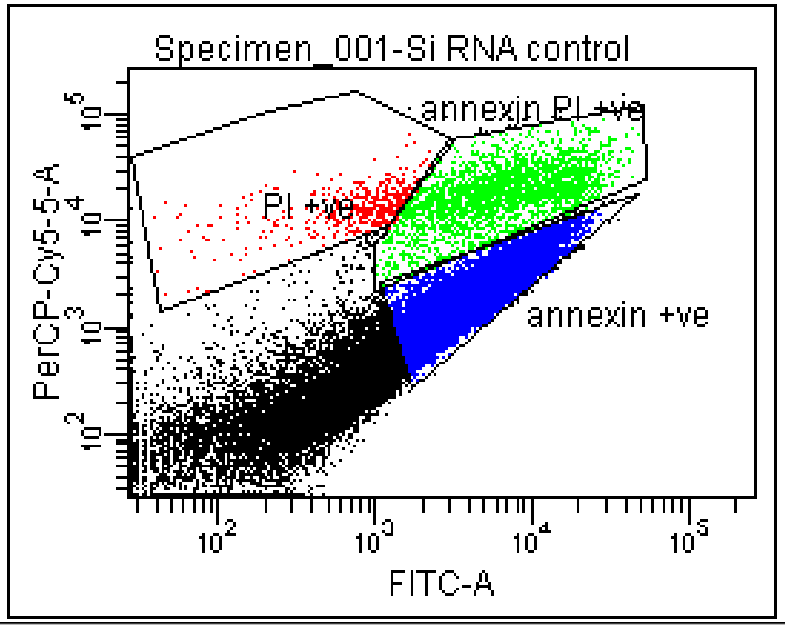

Tube: Si RNA control

Population	#Events	%Parent	%Total
All Events	34,960		100.0
PI +ve	539	1.5	1.5
annexin +ve	14,611	41.8	41.8
annexin PI +ve	2,656	7.6	7.6

AP3B1 siRNA: 35.9% Annexin positive (apoptotic) cells

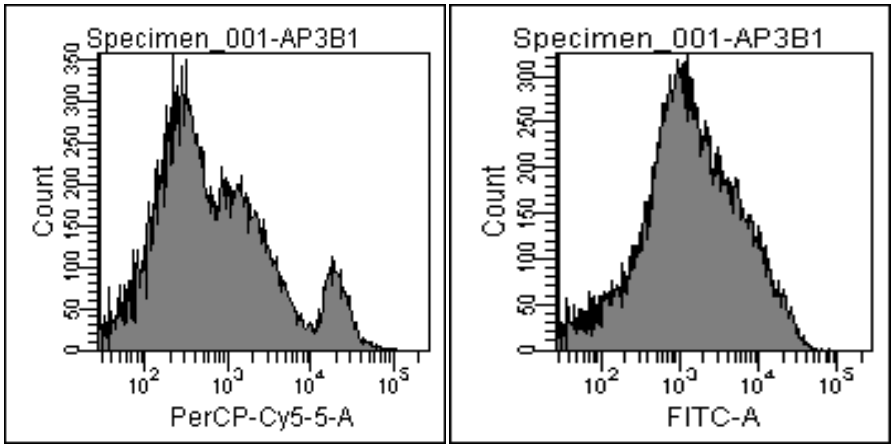

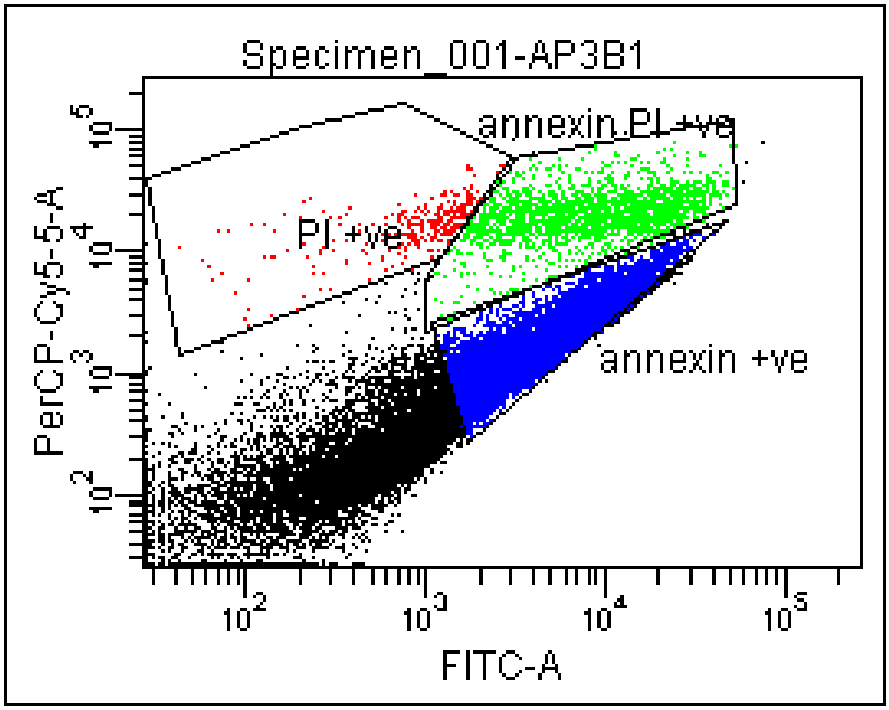

Tube: AP3B1

Population	#Events	%Parent	%Total
All Events	27,106		100.0
PI +ve	342	1.3	1.3
annexin +ve	9,729	35.9	35.9
annexin PI +ve	2,138	7.9	7.9

MTHFD1L siRNA: 53.1% Annexin positive (apoptotic) cells

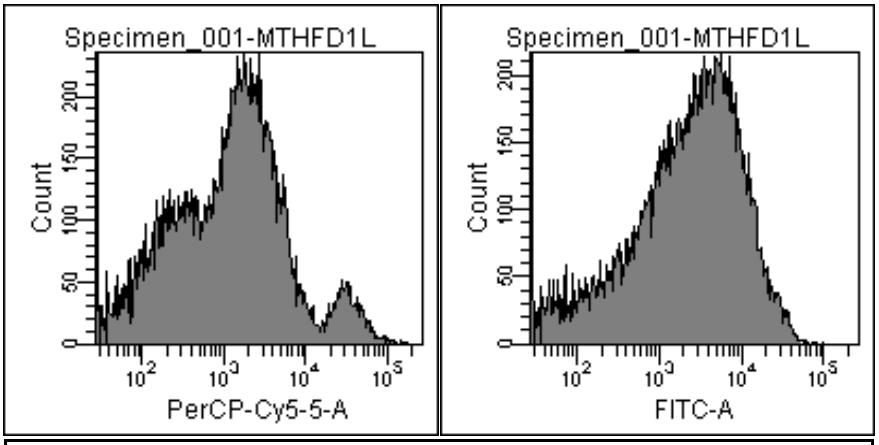

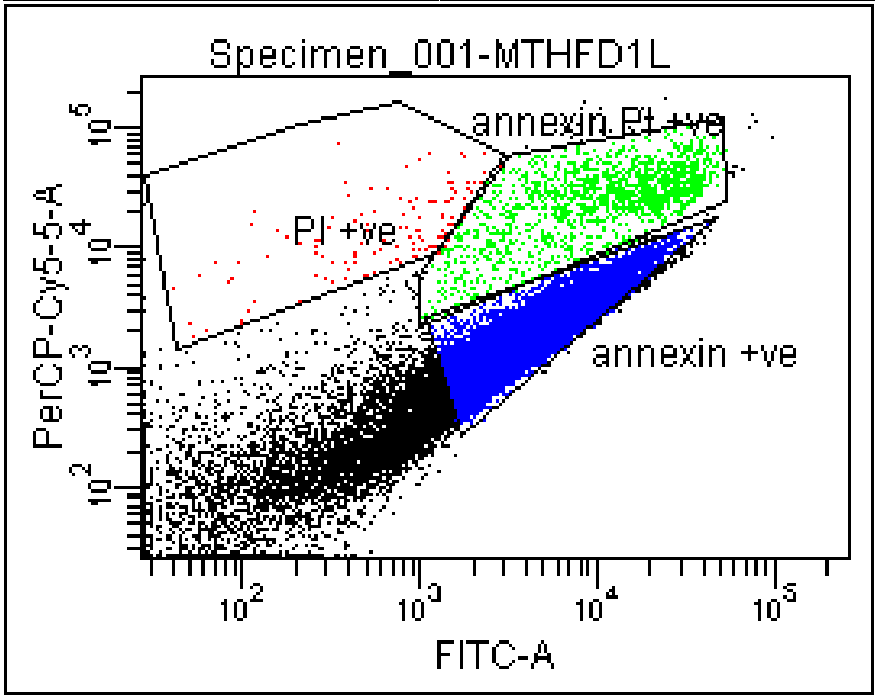

Tube: MTHFD1L

Population	#Events	%Parent	%Total
All Events	20,027		100.0
PI +ve	151	0.8	0.8
annexin +ve	10,644	53.1	53.1
annexin PI +ve	1,505	7.5	7.5

MTHFD2 siRNA: 48.8% Annexin positive (apoptotic) cells

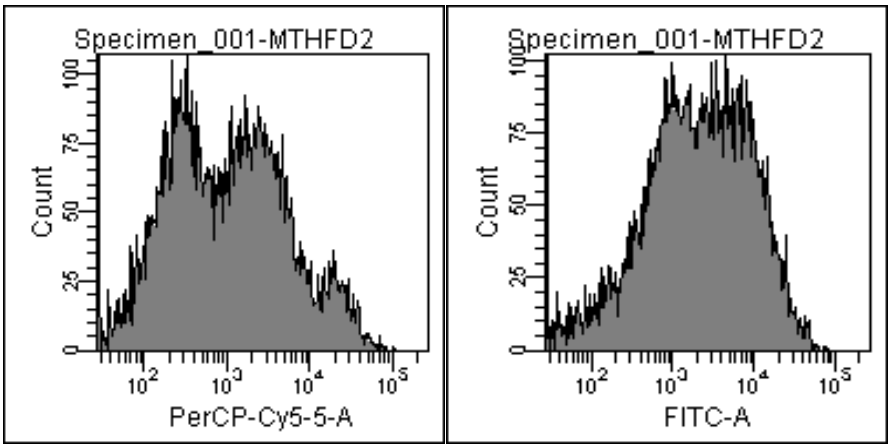

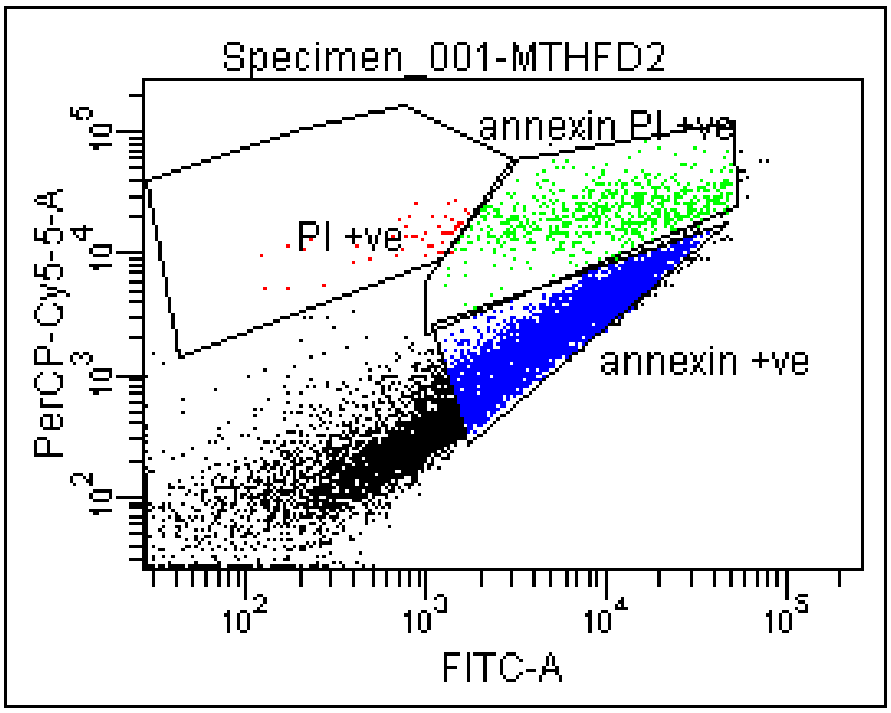

Tube: MTHFD2

Population	#Events	%Parent	%Total
All Events	10,000		100.0
PI +ve	69	0.7	0.7
annexin +ve	4,881	48.8	48.8
annexin PI +ve	730	7.3	7.3

A.1.10. Primary tumor and normal samples information

Patient no	Hospital patient no	Shire No	Tissue Type	Reason for referral	Subtype	Stage	Grade	Patient status
1	4	R09-0561	Tumour	Breast Cancer	Luminal A	2A	2	**alive with no record of disease progression**
2	9	R09-0541	Tumour	Breast Cancer	Luminal B	2B	2	**alive with no record of disease progression**
3	28	R06-1467	Tumour	Breast Cancer	Luminal A	2A	1	**alive with no record of disease progression**
4	37	R09-0563	Tumour	Breast Cancer	Luminal A	2B	3	**alive with no record of disease progression**
5	50	R09-0569	Tumour	Breast Cancer	Luminal A	2B	3	**alive with no record of disease progression**
6	145	R06-0187	Tumour	Breast Cancer	Her 2	2A	3	**alive with no record of disease progression**
7	147	R06-0189	Tumour	Breast Cancer	Luminal A	2A	3	**alive with no record of disease progression**
8	149	R06-0191	Tumour	Breast Cancer	Luminal A	2A	3	**alive with no record of disease progression**
9	316	R09-0546	Tumour	Breast Cancer	sal Medulla	2B	3	**alive with no record of disease progression**
10	319	R09-0553	Tumour	Breast Cancer	Luminal A	2B	3	**alive with no record of disease progression**
11	392	R07-0118	Tumour	Breast Cancer	Unknown	4		**alive M1 at presentation**
12	21	R07-0137	Tumour	Breast Cancer	Luminal A	4		**RIP M1 at presentation**
13	456	R07-0117	Tumour	Breast Cancer	Luminal A	4		**RIP M1 at presentation**
14	331	R07-0139	Tumour	Breast Cancer	Unknown	4		**RIP M1 at presentation**
15	348	R07-0116	Tumour	Breast Cancer	Unknown	4		**RIP M1 at presentation**
16	418	R07-0115	Tumour	Breast Cancer	Unknown	4		**RIP M1 at presentation**
17	433	R07-0138	Tumour	Breast Cancer	Unknown	4		**RIP M1 at presentation**
18	108	R07-0146	Tumour	Breast Cancer	Luminal A	4		**alive M1 at presentation**
19	262	R07-0141	Tumour	Breast Cancer	Luminal A	4		**alive M1 at presentation**
20	1338	R09-0557	Tumour	Breast Cancer	Her 2	4		**alive M1 at presentation**
21	285	R09-0592	Normal	Mastopexy	n/a	n/a	n/a	**n/a**
22	3351	R09-1883	Normal	Mastopexy	n/a	n/a	n/a	**n/a**
23	3206	R09-1886	Normal	Mastopexy	n/a	n/a	n/a	**n/a**
24	3349	R09-1887	Normal	Mastopexy	n/a	n/a	n/a	**n/a**
25	3206	R09-1986	Normal	Mastopexy	n/a	n/a	n/a	**n/a**

A.1.11. pcDNA3/pre-9-1 construct map

Figure taken from Dr. Prasad Kovvuru's PhD thesis (Genetics & Biotechnology Lab, UCC, Ireland).

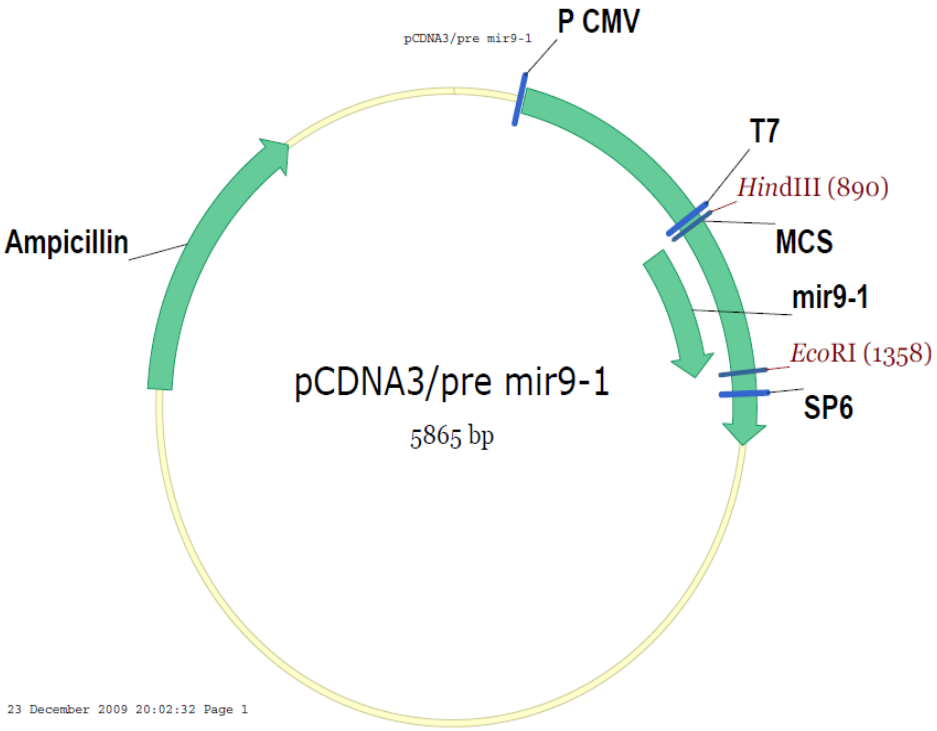

A.2. Recipes

A.2.1. Buffers and solutions

1.5 M Tris-HCl, pH 8.8

Tris base 27.23 gm
80 mL water
Adjust to pH 8.8 with 6N HCl.
Make to 150 mL with water.
Store at 4° C.

0.5 M Tris-HCl, pH 6.8

Tris base 6.1 gm
80 mL water
Adjust to pH 6.8 with 6N HCl.
Make to 100 mL with water.
Store at 4° C.

Protein Lysis Buffer

0.1% SDS
1% Triton X-100
0.5% Deoxycholic acid (DOC)
In 10ml PBS

TGS Running Buffer (TBS) (10X)

Trisbase 30.3g

Glycine 144g

SDS 10g

Water to 1L

Dilute 1:10 for running gels

Store at 4C

TG Wet transfer Buffer (1X)

Trisbase 3.03g

Glycine 14.4g

100ml methanol

Water to 1L

Protein loading buffer (6X)

440mM Tris-HCl pH 6.8

12% w/v SDS

30% v/v glycerol

0.1% bromophenol blue

Add 600ul of 2-mercaptoethanol per 1.4 ml aliquot of 6X dye.

A.2.2. Media

LB Broth

Dissolve 20 g of LB broth in 1 L water

Autoclave immediately and store at 4˚C.

For LBamp broth (ampicillin selection) add 500 ul of 100 mg/ml ampicillin into 1 L of LB broth, store at 4˚C.

LB Agar

Dissolve 37g of LB agar in 1L water.

Autoclave immediately and once it is cool down add 500ul of 100mg/ml ampicillin into 1L of LB broth (for LBamp selection plates).

Pour the media into petri dishes and store at 4˚C laying the plates up-side down.

Phosphatase Substrate for cell proliferation assay

Resuspend phosphatase buffer in 0.1M NaAc, 0.1% Triton X-100 pH 5.5 for a final concentration of 10mM.

A.3. Protocols

A.3.1. RT primer design protocol for mammalian genomes

- Primers should be located in exon-exon boundaries so that in any case of DNA contamination correct product (mRNA) is amplified.
- Possible genomic amplicon should be kept >1000bp.
- For Sybr green based assays product size should be >70bp and <250bp
- Primers can be selected from online databases (part 1) or can be designed manually (part 2) or using online tools (part 3)
- Proceed to Quality control checks (part 4).

Part 1: Use of available online databases

There are some databases available for ready to order RT primers for many human genes. The primers taken from these databases must be tested for quality check points listed in part 4.

qPrimerDepot: http://primerdepot.nci.nih.gov/

RTprimerDB: http://medgen.ugent.be/rtprimerdb/

Part 2: Manual design

Manual design allows picking primers from exon-exon boundaries so that only targeted mRNA will be amplified with no possible genomic amplicon.

- Find the transcript sequence (make sure it belongs to *Homo sapiens*) from Ensembl website (http://www.ensembl.org/index.html)
- Pick 2-3 exons that have large intronic region (>1000bp) in between
- Select 20-25nt from the first junction-forward primer and select 20-25 nt from 2nd or 3rd exon-exon junction (depending on the size of the middle exon and intended product size) as a reverse primer (keep the junction points in the center of the primer)

- Proceed to Quality control checks (part 4).

Part 3: Primer design using PRIMER3 online tool

This design allows amplifying mRNA sequences with large genomic amplicons.

- Find the transcript sequence (make sure it belongs to *Homo sapiens*) from Ensembl website (http://www.ensembl.org/index.html)
- Select 2 exons that have large intronic region (>1000bp) in between
- Paste the sequence to word file and delete intronic sequences (in silico splicing) label different exons with different color
- Add "[" to end of the first exon (10-15bp before) and add "]" to the beginning of the second exon (10-15bp ahead). This avoids picking primers from this region and allowing exon-exon boundary region to be amplified

- Paste the sequence to primer3 program (http://frodo.wi.mit.edu/)
- Define the product size: 100-250
- Primer size: 18-25
- Tm optimum: 60C
- GC% optimum:50
- Number to return:15 (to get 15 different options of primer sets)
- Change other options if necessary and select the primers

Check the output file and pick the proper primer set (product size, Tm, GC% and having G/C at 3' would be a criteria)

Proceed to quality control check (Part 4).

Part 4: Quality Control check

Primer Specificity/genomic amplicon

Paste the fwd and reverse primer to UCSC in silico PCR program** (http://genome.ucsc.edu/cgi-bin/hgPcr)

- Select the most current available genome database and product size to 500000 (This allows to see large genomic amplicons by the primer set) and Run
- The output file gives the genomic amplicon by primer set, make sure its >1000bp
- The ready primers taken from databases may give same genomic amplicon as the mRNA product size as the primers might have been designed in one exon, make sure the product size in mRNA and genomic are different.
- If the intronic region has been selected large in step 2 above the output amplicon will be large and be neglected. If the amplicon size is small (<1000bp) redesign of primers from different exon-exon should be considered.
- Also check the primer specificity from NCBI BLASTN (http://blast.ncbi.nlm.nih.gov/Blast.cgi) so that you ensure the primers bind 100% only to intended mRNA.

Primer sequence

- Ta (Annealing temp.): close to 60C (Most RT PCR programs are set to Ta=60 so designed primers should have 58<Tm<65 so that it works at Tm=60C)
- Size should be 18-25 nt
- 3' should end with G/C for high stability
- Primer set shouldn't form a primer dimer and secondary structure
- To control these use sigma primer calculator (http://www.sigma-genosys.com/calc/DNACalc.asp)

- Make sure Tm, GC% are in range and forming no secondary structure (can be weak or moderate if there is no other option) and no primer dimmer

A.3.2. Preparation of ultra competent DH5α cells for routine molecular cloning

Materials Required:

Solution I: $CaCl_2$ (100mM)
Solution II: $CaCl_2$ (100mM +15% Glycerol)
LB Broth
E.coli Starter Culture

- Prepare $CaCl_2$ I &II solution a day before and store it at 4°C.
- Sterile conditions must be kept during the procedure, and all the items used during preparation must be ice cold.
- Start a pre-culture of 5-10ml of the *E.coli* strain without antibiotics, and let it grow overnight.

Day of preparation:

- Inoculate 400ml of LB media with overnight grown starter culture (0.5%) (2 x 200ml in 1000ml flask)
- After 4 hrs hours of growth check the OD of the culture. The OD_{600} should not be higher than 0,600E measured against LB as a blank.
- Allow the flasks with bacterial culture to cool down by placing them in Cold room.
- Divide the bacterial culture 4 x 100ml into the four pre cooled centrifuge bottles.
- Centrifuge the cells for 10 min at 6000g at 4°C.

- Pour off the supernatant and resuspend the pellets with sterile pipettes with 100mM $CaCl_2$-solution gently (1/10 volume of culture medium in each tube).
- Keep resuspended cells on ice for 30 minutes.
- Centrifuge the cells at 4000g, 4°C for 5 min, remove the supernatant and resuspend each pellet in 1.5ml $CaCl_2$+15% glycerol solution (II) gently.
- Keep the resuspended cells on ice for 4 hrs
- Aliquot the cells 100 - 200µl in ice cold 1.5ml eppendorf tubes and store at -80^{0}C.

Transformation Efficiency Check

- Thaw competent cells on ice.
- Add 10ng of PUC18 DNA to 100µl of cells and keep on ice for 30minutes.
- Heat shock at 42^{0}C (in water bath) for 90 seconds and chill by immediately replacing the tubes on ice.
- After 2min, add warm 900µl LB, and incubate at 37°C for 1hr and plate 5,10,20µl on LB-Amp plates
- Count the colonies of the appropriate plate and calculate the efficiency

No. of Colonies/ µl of Cells plated X10^5= per µg of DNA

A.3.3. Direct cloning protocol

Day 1:

- PCR amplification of the insert (optimized PCR for specific band)
- Double digestions of PCR insert and host vector (37˚C overnight)

Plasmid (3-5 ug) or PCR insert	**10ul**
NEB Buffer 4	**2ul**
BSA(10X)	**2ul**
RE 1	**1.5ul**
RE 2	**1.5ul**
water	**3ul**
TOTAL	**20ul**

Day 2:

- Add 1 ul of SAP (Shrimp alkaline phosphatase) to the vector digestion to eliminate self ligation (37˚C for 2 hours)
- Gel extraction of double digested vector and purify PCR insert and ligation of the vector and insert (4˚C overnight)

Cut Plasmid (50ng)	1ul
Cut insert (3:1 molar ratio*)	10ul
10X Lligase Buffer	1.5 ul
T4 Ligase	1 ul
Water	1.5ul
TOTAL	**15ul**

***ng of insert = ng of vector X bp insert / vector bp X molar ratio**

Day 3:

Transformation into DH5a cells

- Thaw competent cells on ice (DH5a)
- Add 5ul of ligation mix into 50ul competent cells
- Incubate on ice for 45 min
- Heat shock at 42˚C for 45 sec
- Incubate on ice for 2 min
- Add 500ul LB broth
- Incubate at 37˚C with 200rpm shaking for 1-1.5 hours
- To plate all mixture, centrifuge at 7000g for 3 min and resuspend the pellet with 200ul LB and spread on the plate under sterile conditions.

- Incubate overnight at 37˚C

Day 4:

Colony PCR

It allows a quick screen for positive clones before miniprep plasmid isolation and sequencing. Forward primer of vector and reverse primer of insert can be used screen positive clones.

- Using sterile tip pick half of the colony and inoculate into LB amp broth for plasmid isolation and inoculate into PCR mixture for colony PCR
- Grow the colonies showing correct sizes in 3-5ml LB amp broth overnight at 37˚C with 200rpm shaking
- Isolate the plasmid (miniprep) and send to sequencing for confirmation.

A.3.4. Sub-cloning protocol

This protocol can be used for large inserts or inserts difficult for direct cloning. TOPO PCRII (Invitrogen, USA) or pGEM-T (Promega, USA) vectors can be used in sub-cloning **(vector maps: section A.5)**. The steps are similar to direct cloning described in section A.3.3 except first cloning into sub-cloning vector and then cloning into intended vector is used.

- Following PCR amplification, ligate 3ul of PCR into sub-cloning vector (4˚C overnight)
- Transform the ligation into competent cells overnight
- Grow the colonies and isolate plasmid (miniprep)
- Double digest the insert and intended vector using the RE used in primer design
- Gel extract the released inserts (double digested with sticky ends)
- Ligate the insert and plasmid (4˚C overnight)

- Transform 3ul of ligation mixture into 50ul of competent cells overnight
- Perform colony PCR to test positive clones
- Grown and isolate plasmid from positive clones
- Send sequencing for confirmation

A.3.5. Site directed mutagenesis (SDM) protocol

Using Quikchange Lightning SDM kit (# 210513, Agilent Technologies, USA)

The mutagenesis protocol uses 125 ng of each oligonucleotide primer.

To convert nanograms to picomoles of oligo, following formula is used:

X pmoles of oligo = 125 ng of oligo/ (330x #of based in oligo) x1000

- Perform a qRT-PCR reaction using the template construct to be mutated

10X multi reaction buffer	2.5 ul
plasmid template (50ng)	1 ul
SDM primer F	X (according to formula)
SDM primer R	X (according to formula)
dNTP mix	1ul
water	X (for final 25ul)
Quickchange enzyme	1 ul
TOTAL	25 ul

95˚C	2:00 min	
95˚C	0:20 min	X18
55-65˚C	0:30 min	
65˚C	0:30 min /kb plasmid	
65˚C	5 min	
10˚C	Hold	

- Digest the parental plasmid with 1ul DpnI enzyme for 5 in at 37˚C
- Transform 3ul of PCR reaction into XL10-Gold Ultra competent cells as described in section A.3.3
- Candidate colonies picked should be confirmed by sequencing.

A.3.6. Cell Proliferation (Acid Phosphatase) Assay

For cell proliferation assays, cells were grown in 96-well plates.

- Following treatments remove the medium from the wells and wash with 100ul PBS. Remove the PBS.
- Add 100ul of freshly prepared phosphatase substrate and wrap the plate with aluminum foil, incubate at 37˚C for 2 hours.
- Stop the enzymatic reaction by adding 50ul of 1M NaOH to each well
- Read the wells in plate reader at 405nm with reference (background correction) at 620nm.

A.3.7. ApoTox-Glo Assay

For ApoTox-Glo assays, cells were grown in 96-well plates.

- Prepare GF-AFC and bis-AAF-R110 substrates for viability and cytotoxicity (10ul of each substrate in 2ml assay buffer).
- Add 20ul of substrate mixtures directly onto cells (in medium), shake for 30sec and incubate for 30min-2 hours at 37˚C.
- Measure fluorescence in plate reader using the filters for $405_{EX}/505_{EM}$ (Viability) and $485_{EX}/520_{EM}$ (Cytotoxicity)
- Add 100ul of Caspase-Glo 3/7 reagent on to wells, mix by shaking for 30sec
- Incubate at room temperature for 30min-2hours.
- Measure Luminescence (caspase activation)

- For normalization of well-to-well differences take the ratio of viability/cytotoxicity.

A.3.8. Luciferase Assays

Dual-luciferase Protocol (Promega, USA)

This assay allows detecting firefly and renilla luciferase separately. Renilla luciferase vector is used for normalization of transfection efficiency. Both luciferase experiments were performed in 24-well plates

- Following transfections (usually 48 hours later) remove the medium and wash the cells with PBS, remove medium
- Prepare 1X Passive lysis buffer (PLB); add 100ul of PLB on wells.
- Incubate by shaking for 15 min
- Prepare LARII (luciferase assay reagent) by resuspend the lyophilized substrate in 10ml assay buffer II.
- Prepare Stop-Glo reagent by adding 1V of substrate into 50V of stop-glo buffer.
- Transfer 20ul cells (lysed in PLB) into black plates with flat bottom in five replicates.
- Place the solutions into injector holders in dual injector system.
- Place the plate and read the luminescence with set up of dispensing 50ul each substrate to each well. Analyze the data by taking the ratios of firefly/renilla.

LightSwitch luciferase Protocol (Switchgear genomics, USA)

This kit is designed only for pLight constructs (renilla) and does not require additional vector for transfection normalization. The original protocol is optimized for less reagent use.

- Remove the medium form 24-well plates and add 150ul of fresh medium
- Reconstitute 100X substrate by adding 100ul solvent to lyophilized substrate.
- Add 100ul of reconstituted substrate into 10ml assay buffer.
- Add 150ul of the assay mix onto 150ul of cells + medium in wells.
- Transfer 50ul of the cell + substrate mixture into half-area 96 well plates in 6 replicates.
- Read the luminescence 2 sec in Luminometer (plate reader)

A.3.9. Matrigel invasion assay protocol

Protocol for BD Matrigel Invasion Chamber (Cat#354480)

Day 1:

Following transfections;

- Remove the matrigel plate from packaging and allow to room temperature.
- Rehydrate; add 37˚C DMEM (without FBS) in interior of inserts (500ul) and bottom of the wells (500ul), keep 2hr in incubator
- Trypsinize and count the cells and dilute in DMEM (no FBS or 0.1-1%) for $5x10^4$ /ml. Cells should be max 70-80% confluent.
- Remove the medium from both top and bottom
- Add 750ul of DMEM+FBS to bottom well
- Immediately, add 500ul of cell suspension on upper chamber
- Incubate for 24 hours in incubator

Day 2:

- Remove the cells on top of the insert that are not invaded by using moistened cotton tipped swabs. Do not use pressure.
- Check the bottom of the wells if there are invaded cells. (take photo)

- Fixation; transfer inserts into 100% methanol for 5 min in a companion 24 well.
- Staining; transfer inserts into staining solution (0.5% crystal violet in 20%methanol) for 5 min
- Washing; transfer the inserts into distilled water twice.
- Remove the membrane from insert with sharp scalpel. Leave very small point of attachment.
- Put oil on slide and place the membrane bottom side down on microscope slide, add drop of oil on top and place cover slip.
- Take photo at 10-40X magnifications under inverted microscope in triplicates.
- Count the invaded cells from the photo.

A.3.10. Transfection of cell lines

For transfection of plasmids and oligonucleotides liposome based agent was used (Lipofectamine 2000, Invitrogen, USA).
For 96-well plates 0.3ul, 24-well plates 1ul and for 6-well plates 3ul of Lipofectamine 2000 reagent was used.

- Grow the cells in appropriate tissue culture plate so that on the day of transfection, cells are in 50-70% confluency, As an example the transfection protocol for 24-well plates for 1 well transfection is given below:
- On the day of transfection, wash the cells with PBS and replace it with 400ul of fresh DMEM medium without Pen/Strep.
- Prepare the plasmid/oligo mixtures. Mix appropriate amount of plasmid or oligo in OPTIMEM I medium (in dark) for a final volume of 50ul.
- Prepare the transfection mixture. Mix 1ul of Lipofectamine in 49ul OPTIMEM I. Incubate both mixtures for 5 min at room temperature.
- Combine both mixtures and Incubate for 20 min at room temperature.

- Add the combined mixture on to wells drop-wise.

A.3.11. Protein isolation and quantification protocol

Protein Isolation

- Following treatments in cell culture, cells can be harvested by trypsinization or by the help of cell scraper. Centrifuge the cells and remove the supernatant.
- Resuspend the pellet in protein lysis buffer (30-70ul) and incubate on ice for 30 min.
- Centrifuge at 20,000rpm for 20 min
- The supernatant contains the protein. Proceed to protein quantification. Keep the proteins on ice.

Bradford Protein Quantification:

Prepare BSA (1mg/ml) standard dilutions (to be used as a known conc. standard to construct a curve).

Final conc. ug/100ul	***0***	***0.5***	***1.25***	***2.5***	***3.75***	***5***	***7.5***	***10***
H2O (ul)	990	985	977.5	965	952.5	940	915	890
BSA (ul)	0	5	12.5	25	37.5	50	75	100
Lysis buffer(ul)	10	10	10	10	10	10	10	10
TOTAL (ul)	100	100	100	100	100	100	100	100

- Prepare Bradford reagent mix by diluting 2ml reagent in 3 ml water, total 5ml (enough for 4-5 samples)
- Prepare protein sample mix to be measured

4.5ul in 450ul water (3 replicates x 1ul + excess makes 4.5ul protein to be used)

- Aliquot 100ul Bradford mix onto 96 well plates
- Add 100ul BSA standards mix onto wells
- Add 100ul samples mix onto corresponding wells
- Read the plate in plate reader (check the settings→ endpoint analysis, 1 wavelength 595nm and check the plate template/std/sample),
- Using the standard curve formula (equation obtained from the standard curve), dilute the proteins to same final concentration each so that in western same volume input can be used
- Mix the appropriate amount of protein with protein loading buffer, incubate at 100˚C for 15 min and store at -20C or proceed to western blot protocol.

A.3.12. Western Blot Protocol

Day1: Running protein samples

Prepare the proteins for same final concentration before starting western blot.

- Prepare 10% Acrylamide Gel (add reagents below order)

REAGENT	**1 GEL**	**2 GELS**	**4 GELS**
ddH2O	2.66ml	5.6ml	11.2ml
30% Acrylamide	2.38ml	4.62ml	9.24ml
1.5 M Tris (pH 8.8)	1.82ml	3.5ml	7ml
10% SDS	70 ul	140 ul	280 ul
10% APS	70 ul	140 ul	280 ul
TEMED	2.8 ul	5.6 ul	11.2 ul
TOTAL	**7.028 ml**	**14.056 ml**	**28.112 ml**

- Pour/pipette the gel into prepared glass plates, leave space for stacking gel and comb (1cm lower than the tip of comb). It solidifies in 20-25 min.

- Prepare 5 % Stacking Gel in 50 ml falcon tube

REAGENT	1 GEL	2 GELS	4 GELS
ddH2O	0.9ml	1.8ml	3.6ml
30% Acrylamide	330 ul	660 ul	1.32 ml
0.5 M Tris (pH 6.8)	750 ul	1.5ml	3 ml
10% SDS	20 ul	40 ul	80 ul
10% APS	20 ul	40 ul	80 ul
TEMED	2 ul	4 ul	8 ul

- Place the combs and pour Stacking gel until it covers the comb. Wait for 15-20 min to solidify.
- Prepare protein samples. Vortex before taking the sample. Mix 30-50ug protein with loading dye.
- Heat the samples at 100˚C for 5-10min, spin and directly load into wells.
- Remove the comb from the glass before put into solution.
- Prepare the running set up, pour running buffer into system, correct each well with a thin tip, flush if any acrylamide remained in the wells.
- Load protein ladder to the beginning and proteins to following wells.
- Run for around 2 hours until the lowest ladder (25kD) comes to edge. Run at 0.04A for 1 gel.

Gel transfer to PVDF membrane using wet transfer

- Take the gels out of the running apparatus and separate the glass plates. Put the gels into wet buffer.
- Wet filter pads and filter papers and membrane just before making the sandwich. Roll each layer with the help of pipette to be sure there is no bubble left in between.
- Prepare the sandwich with the following order;

Black base (goes with the black current)

Filter pad

3 whatman (3mm) papers

Acrylamide Gel

PVDF Membrane

3 whatman (3mm) papers

Filter pad

White base (goes with the red current)

- Close the sandwich and place into wet transfer apparatus run at 0.14A for 1 hour.

Primary antibody binding

- Remove the sandwich and membrane (mind the side of the protein in membrane, keep it up side)
- Put it into a small tray and pour some red Ponceau S solution to cover the membrane and put into shaker for a min. The protein bands will be stained in red bands.
- Wash the red solution couple of times until the membrane goes whitish.
- Pour blocking solution onto it
- Block in shaking for 1 hour
- Prepare the primary antibody solution

1/1000 diluted antibody in milk-TBS-T

- When blocking is done remove the solution and add antibody mix and incubate in 4˚C with gentle shaking.

Day 2:

Washing and secondary antibody binding

- Remove the primary antibody solution into a falcon tube (keep it at -20˚C, to be reused)
- Add TBS-T solution to clear the membrane from antibody.

- Add TBS-T solution x3 for 10 min in a shaker
- Prepare secondary antibody solution while incubation of 3rd wash. Dilute Ab in 1/10,000 in 0.05% milk-TBS-T.
- Remove the washing solution and add secondary antibody solution onto the membrane.
- Incubate 1-2 hours in a shaker.
- Discard the secondary antibody solution
- Add TBS-T solution to clear the membrane from antibody.
- Add TBS-T solution x2 for 10 min in a shaker
- Add TBS 1X solution for 5 min

Chemiluminescence and scanning

- Following secondary antibody binding and final washing, add chemiluminescence mixture (equal amounts of Enhanced Luminol Reagent and Oxidizing Reagent) (0.125ml each per cm^2 of membrane)
- Incubate the membrane with the mixture for 1 min with gentle agitation
- Visualize the membrane in Chemi exposure of G:Box system.

A.3.13. RNA isolation protocols

Using Trizol Reagent (Invitrogen, USA)

- To the cell pellet 7 ml of Trizol reagent was added (1 ml of Trizol reagent to 3.5 cm diameter dish or 1ml per 10 cm^2)
- Incubate the samples for 5 minutes at 15 to 30°C for complete dissociation of nucleoprotein complexes.
- Add 1.4 ml of chloroform to the Trizol reagent (0.2 ml per 1 ml of Trizol).
- Shake the tube for 15 seconds and incubate it for 2 to 3 minutes at room temperature.
- Centrifuge the samples at 2000 rpm at 4°C for 15minutes by gradient centrifuge without brake.

- Following centrifugation, the mixture separates into 3 phases, lower red phenol chloroform (protein), an interphase (DNA) and a colourless upper aqueous layer (RNA).RNA remains exclusively on the aqueous layer.
- Transfer the aqueous phase to a fresh tube and save the organic phase for isolation of DNA.
- 3.5 ml of isopropyl alcohol is added (0.5 ml per 1 ml of Trizol).incubate the samples at 4°C for 30 minutes.
- Centrifuge the samples at 3000 rpm for 20 minutes at 4°C.
- Wash the RNA pellet with 75% ethanol(1 ml per 1ml of Trizol reagent)
- Mix the sample for vortexing and centrifuge at 8000 rpm for 10 min at 4°C. Dissolve the RNA pellet with RNase free water.

DNase treatment (Turbo Dna-free, Ambion, USA) and isopropanol precipitation of RNA isolated with Trizol method

- Add 0.1V Turbo DNase buffer 10X
- Add 1ul Turbo DNase, mix gently
- Incubate at 37˚C for 30 min
- Add 0.1V DNase inactivating reagent
- Incubate at room temperature for 5 min, mix occasionally
- Centrifuge at 10,000g for 1.5min
- Transfer RNA to fresh tube
- Add 1V of isopropanol to RNA sample, store at -20˚C for 1hr.
- Centrifuge and wash the pellet with EtOH
- Resuspend the pellet in nuclease free water

Using Nucleospin microRNA kit (Macherey-Nagel, Germany)

This kit allows isolation of total RNA and small RNA at separate fractions. In this thesis, total RNA + small RNA in single fractions were isolated.

- Add 300ul of Buffer ML to cell pellet, vortex and load the mixture into violet ring filter and centrifuge at 11,000g for 1 min
- Discard the filter and add 150ul of 100% ethanol to lysate. Incubate for 5min at room temperature.
- Load the mixture into blue or green ring filter and centrifuge at 14,000g for 1 min. Save the flow-through
- Add 350ul MDB buffer on to blue ring, centrifuge at 11,000g for 1 min, and discard the flow-through.
- Add 10ul rDNase onto blue ring membrane; incubate at room temperature for at least 15min.
- Add 300ul MP Buffer to saved flow through, vortex, centrifuge at 11,000g for 3 min.
- Pour the supernatant into white filter, centrifuge at 11,000g for 1 min. Keep the flow through.
- Add 800ul MX buffer, vortex and load 600ul of sample onto blue ring, centrifuge at 11,000g for 30sec.Repeat twice.
- Add 600ul MW1 buffer, centrifuge at 11,000g for 30sec and discard the flow-through
- Add 700ul MW2 buffer, centrifuge at 11,000g for 30sec and discard the flow-through
- Add 250ul MW2 buffer, centrifuge at 11,000g for 2min and discard the flow-through
- Elute the RNA by adding 30-50ul water onto blue ring membrane, incubate open lid for 1 min, centrifuge at 11,000g for 1 min

A.3.14. Plasmid Isolation

Miniprep using the kit Nucleospin Plasmid (Macherey-Nagel, Germany)

- Use 1-5ml LB culture grown overnight. Centrifuge at 11,000g for 30sec.
- Add 250ul buffer A1 for cell lysis, vortex.
- Add 25ul Buffer A2 and invert the tube 6-8 times. Add 300ul Buffer A3 and invert the tube 6-8 times.
- Clarify the lysate by centrifugation at 11,000g for 5 min
- Bind the supernatant onto columns (750ul) and centrifuge at 11,000g for 1 min and discard the flow-through.
- Wash the silica membrane with 500ul Buffer AW, centrifuge at 11,000g for 1 min. Discard the flow-through.
- Add 600ul Buffer A4, centrifuge at 11,000g for 1 min. Discard the flow-through.
- Centrifuge at 11,000g for 2 min to dry the membrane. Discard the flow-through.
- Elute the plasmid with 40-50ul water, centrifuge at 11,000g for 1 min.

Midiprep using NucleoBond Xtra Midi kit (Macherey-Nagel, Germany)

- Previous day, grow a started culture (5ml), dilute in LB (ampicillin) for 1:1000 v/v and grow overnight (100ml).
- Harvest the cells by centrifugation at 6000g for 10 min at 4˚C
- Resuspend the pellet in 8ml RES buffer, vortex
- Add 8ml LYS buffer for lysis and invert the tube 5 times. Incubate at room temperature for 5min
- Add 12 ml Buffer EQU on column filter and allow emptying by gravity.

- Add 8ml NEU for neutralization, invert 10 times.
- Centrifuge the mixture at high speed for 5 min to collect and clarify the lysate. Load the supernatant on the column.
- Wash the column with 5ml Buffer EQU and discard the inside column filter. Wash the column with 8ml Buffer WASH
- Elute the DNA with 5ml Buffer ELU; collect the DNA in fresh tube.
- Add 3.5ml room temperature isopropanol to precipitate the plasmid, vortex, and incubate 2 min. Centrifuge at 15,000g for 30 min at 4˚C, discard the supernatant.
- Add 2ml 70% ethanol to pellet and Centrifuge at 15,000g for 5 min at room temperature.
- Remove the ethanol and allow the pellet to air-dry and resuspend the DNA in water (500ul).

A.3.15. Gel Extraction and PCR Purification protocol

Using the kit Nucleospin Extract II (Macherey-Nagel, Germany)

PCR cleanup

- Mix 1 V of sample with 2V of Buffer NT
- Bind the sample to DNA to column and centrifuge at 11,000g for 1min and discard the flow-through.
- Add 700ul Buffer NT3 to column and centrifuge at 11,000g for 1min, discard the flow-through.
- Dry the membrane by centrifugation at 11,000g for 2 min and discard the flow-through.
- Elute the DNA into fresh tube by 40ul water.

Gel Extraction

- Excise DNA fragment with scalpel and weigh. For each 100mg agarose add 200ul Buffer NT.
- Load the sample onto the column and centrifuge at 11,000g for 1min. Discard the flow-through.

- Add 700ul Buffer NT3 to column and centrifuge at 11,000g for 1min, discard the flow-through.
- Dry the membrane by centrifugation at 11,000g for 2 min and discard the flow-through and elute the DNA into fresh tube by 40ul water.

A.3.16. Microarray Profiling (Affymetrix)

Using GeneChip Human Genome Arrays (Affymetrix, Inc., USA)

For detailed protocol refer to link below:
http://media.affymetrix.com/support/downloads/manuals/3_ivt_express_kit_manual.pdf

Kits and materials required:

- 3' IVT Express Kit (#901228, Affymetrix, Inc, USA)
- Hybridization, Wash, and Stain Kit (#900720, Affymetrix, Inc, USA)
- Magnetic Stand for 96-well plates (#AM10050, Ambion, USA)
- Other regular molecular biology tools / equipment
- GeneChip® Hybridization Oven 640 (#800138, Affymetrix, Inc, USA)
- GeneChip® Fluidics Station 450 (#00-0079, Affymetrix, Inc, USA)
- GeneChip® Scanner 3000

aRNA Amplification

RNA integrity should be checked with Bioanalyzer prior to the experiment.

1. Diltue poly-A Control stock with dilution buffer with following dilutions (1:20 > 1:50 > 1:50 >1:10)
2. Add 2 ul of diluted Poly-A controls to 100ng RNA sample for final 5ul volume.
3. Mix 4ul first-strand master mix and 1ul first-strand enzyme mix (final 5ul volume) and add 5ul of RNA/polyA mix, vortex and spin.

4. Incubate 2 hours at 42˚C.
5. Prepare second-strand master mix by combining 5 ul second-strand master mix and 2 ul first-strand enzyme mix and 13ul water to 20ul.
6. Transfer 20ul of second-strand mix onto first cDNA mix (10ul), vortex and spin.
7. Incubate the reaction at 16˚C for 1 hour followed by 65˚C for 10 min.
8. Proceed to IVT reaction or store at -20˚C.
9. Mix 4ul IVT Biotin label, 20ul IVT labeling buffer and 6ul IVT enzyme mix for final 30ul volume, vortex and spin.
10. Transfer 30ul of labeling mixture to 30ul of cDNA sample.
11. Incubate IVT reaction at 40˚C for overnight (16 hours).

aRNA Purification

1. Prepare aRNA binding mix by combining 10ul of RNA binding beads and 50ul aRNA binding buffer concentrate.
2. Add 60ul of aRNA binding mix to samples and transfer to a U bottom 96-well plate, mix by pipetting several times
3. Add 120ul of 100% ethanol to each sample; shake for 2 min at setting.
4. Move the plate to magnetic stand and capture the beads for 5 min.
5. Discard supernatant and wash the beads with 100ul aRNA wash solution, shake for 1 min at setting 7.
6. Move the plate to magnetic stand and capture the beads for 5 min.
7. Discard supernatant and wash the beads with 100ul aRNA wash solution again, shake for 1 min at setting 7.
8. Discard the supernatant, move the plate to magnetic stand and dry the beads for 1 min, shaking at setting 10.
9. Elute aRNA by adding 50ul preheated (50˚C) aRNA elution solution on the beads.
10. Vigorously shake the plate at setting 10 for 3 min.
11. Move the plate to magnetic stand and capture the beads for 5 min.

12. Transfer the supernatant, which contains the aRNA to fresh tubes.
13. Keep on ice, store at -20˚C or proceed to fragmentation.

aRNA Fragmentation:

1. Quantify the RNA in nanospectrophotometer
2. For 49/64 format of arrays prepare the fragmentation reaction by mixing 15 ug of aRNA (1-32 ul), 8ul fragmentation buffer and water for final 40ul volume.
3. Incubate the reaction at 94˚C for 35 min.
4. Run the sample on the agarose gel to check the fragmented samples (50-200nt).

Hybridization:

1. Combine 12.5ug of fragmented aRNA, 4.2ul control oligonucleotide B2, 12.5ul 20X hybridization controls, 125ul 2X hybridization mix, 25ul DMSO and water to final 250ul volume.
2. Heat the hyb cocktail at 99˚C for 5min.
3. Wet the array with 200ul pre-hyb mix and incubate at 45˚C for 10 min with rotation.
4. Spin the cocktail for 5 min at maximum speed.
5. Remove the array from the oven and pre-hyb mix from the array.
6. Refill the array with hyb cocktail. Incubate at 45˚C overnight with rotation (60rpm) for 16 hours.

Washing/Staining and Scanning:

Fluidics station should be connected to computer and samples should be registered. For detailed protocol refer to link below:
http://media.affymetrix.com/support/downloads/manuals/wash_stain_scan_cartridge_arrays_manual.pdf

1. After hybridization, remove the hyb cocktail and refill the array with 250ul WashA buffer.
2. Place the stain cocktails to fluidics station (600ul stain cocktail 1, 600ul stain cocktail 2 and 800ul of array holding buffer).
3. Place the WashA, WashB and Water bottles to fluidics station.
4. Select the suitable washing and staining protocol for the array type. Follow the LCD window.
5. After washing and staining check if there is any bubble in the array screen, if so, refill with array buffer to get rid of the bubble.
6. Scan the arrays and save the raw files .DAT, .CEL and .CHP for data analysis.

A.3.17. Flow Cytometry analysis (FACS)

Using Annexin-V-FLUOS Staining Kit (#11858777001, Roche, USA)

This kit is used for detection and quantification of apoptosis and differentiation from necrosis at single cell level.

1. Following treatment of the cells, remove the supernatant and save.
2. Wash the cells with 1X PBS gently and detach the cells using EDTA/PBS solution. Incubate for 5 min at 37C incubator.
3. Spin the tubes containing cells and supernatant at 200g for 5 min.
4. Remove the supernatants and add freshly prepared staining solutions.
5. For dual staining (Annexin-V and PI) mix 10ul of annexin dye and 10ul of PI dye in 500ul solution provided in the kit.
6. For single staining (Annexin-V or PI) add 1ul of each dye in 50ul solution. These will be used as controls for determining background noise in data analysis.
7. Resuspend the cell pellets in 50ul of staining solution.
8. Also include untreated cells as negative control

9. Incubate at room temperature for 10-15min

10. Add 200ul solution on the cells and transfer them into tubes to be used in BD Facs Canto machine.

A.4. Primers

All the primers used in this thesis are listed in the following sections;

A.4.1. Cloning primers

A.4.2. qRT-PCR primers

A.4.1. CLONING PRIMERS						
Final construct name	**Target Amplicon**	**Primer Name**	**Primer Sequence (5'>3')**	**Tm (˚C)**	**Insert (bp)**	**Notes**
pc-21	mir-21 precursor	MIR21_OVEREXP_F	GGATGTTTTTGATT**AAGCTT**GT TCA	63.9	490	**modified HindIII site**
		MIR21_OVEREXP_R	GAAGACTA TCCC**GAATTC**TCCATA	63.1		**modified EcoRI site**
pc-9-1	mir-9 precursor	Fmir-9	AT**GAATTC**GTGACTCCTACCTGTGCCAA	74.2	462	**modified HindIII site**
		Rmir-9	CTG**TAAGCT**TTGTATCTCCGTGTCTGAGG	69.9		**modified EcoRI site**
pCMV-STAT3-UTRfull	STAT3 3'UTR 1.5kb	STAT3_UTR2_F_1577	ACAGTCTGAGACTCTGTCTCAAAA	61.1	1577	STAT3 3'UTR additional 1.5kb
		STAT3_UTR2&RT_R_1577	CCTCTAGATTTTACGGTTCCTATATAAC	60.4		
pCMV-STAT3-UTRdel1	STAT3 3'UTR del1	STAT3_UTR_DEL1_F	CTCCAGCAACACTCTTCAGTACATATAACTGATAA ACAGAATATTTA	78.1	1571	mir-21 seed 1 deletion
		STAT3_UTR_DEL1_R	TAAATATTCTGTTTATCAGTTATATGTACTGAAGAG TGTTGCTGGAG	78.1		
pCMV-STAT3-UTRdel2	STAT3 3'UTR del2	STAT3_UTR_DEL2_F	CTTACCTACCTATAAGGTGGTTTGCTGTCCTGGCC	80.4	1571	mir-21 seed 2 deletion
		STAT3_UTR_DEL2_R	GGCCAGGACAGCAAACCACCTTATAGGTAGGTAG	80.4		
pMIR-STAT3-UTRfull	STAT3 3'UTR full	STAT3_UTR_full_F	*C***GAGCTC***G*GAGCTGAGAACGGAAGCTGC	76.0	2422	*Recognition sites* and **SacI sited added**
		STAT3_UTR_full_R	*CCC***AAGCTT***GGG*TTTTTACGGTTCCTATATAACG	71.0		*Recognition sites* and **HindIII sited added**

pMIR-STAT3-UTRdel1	STAT3 3'UTRdel1	PMIR_STAT3_DEL1_F	CTCCAGCAACACTCTTCAGTACATATAACTGATAAACAGAATATTTA	78.1	2416	mir-21 seed 1 deletion in pMIR
		PMIR_STAT3_DEL1_R	TAAATATTCTGTTTATCAGTTATATGTACTGAAGAGTGTTGCTGGAG	78.1		
pMIR-STAT3-UTRdel2	STAT3 3'UTRdel2	PMIR_STAT3_DEL2_F	CTTACCTACCTATAAGGTGGTTTGCTGTCCTGGCC	80.4	2416	mir-21 seed 2 deletion in pMIR
		PMIR_STAT3_DEL2_R	GGCCAGGACAGCAAACCACCTTATAGGTAGGTAG	80.4		
pMIR-JAG1-UTR	JAG1 3' UTR	JAG1_UTR_F	GTACATAATACTGAACC**ACTAGT**AGATTTG	59.4	632	**modified SpeI site**
		JAG1_UTR_R	GTTTATTC**AAGCTT**TATTCACACTTG	60.8		**modified HindIII site**
pMIR-JAG1-UTRdel	JAG1 3' UTRdel	JAG1_UTR_SDM_F	TCTACTGCATTTAGGGAGTATTCTAAGTTGAATACTTGAACCATAAA	73.3	626	mir-21 seed deletion in pMIR
		JAG1_UTR_SDM_R	TTTATGGTTCAAGTATTCAAGTATTCAACTTAGAATACTCCCTAAATGCAGTAGA	73.3		
pLight-MTHFD1L-UTRmut	MTHFD1L 3'UTRmut	MTHFD1L_mutF	AATGCTGGAGACATGGTGAAATAGGGCTATGTTTTCTTCTTCGTTCAAGATGAATTC	83.2	498	mir-9 seed mutation in pLight
		MTHFD1L_mutR	GAATTCATCTTGAACGAAGAAGAAAACATAGCCCTATTTCACCATGTCTCCAGCATT	83.2		
pLight-ANXA2-UTRmut	ANXA2 3'UTRmut	ANXA2_mutF	CCTGTCTAGTCTCTCCTGTAAGGCTATGTAATGAACATTCCAAGGAGTTGG	80.4	657	mir-9 seed mutation in pLight
		ANXA2_mutR	CCAACTCCTTGGAATGTTCATTACATAGCCTTACAGGAGAGACTAGACAGG	80.4		
pLight-AP3B1-UTRmut	AP3B1 3'UTRmut	AP3B1_mutF	TATGCAATACTTTCCCCCTTTTTGCTTTGCTAAGCTATGTGCATATATTTTACTGTCAGTTG	81.3	696	mir-9 seed mutation in pLight
		AP3B1_mutR	CAACTGACAGTAAAATATATGCACATAGCTTAGCAAAGCAAAAAGGGGGAAAGTATTGCATA	81.3		

pLight-CSDA-UTRmut1	CSDA 3'UTRmut1	CSDA_mut1_F	CAGGCCACAACCTTAACCAACAGCTATGTAACATC CAAGCAATAAAGTGGA	83.0	699	mir-9 seed 1 mutation in pLight
		CSDA_mut1_R	TCCACTTTATTGCTTGGATGTTACATAGCTGTTGGT TAAGGTTGTGGCCTG	83.0		
pLight-CSDA-UTRmut2	CSDA 3'UTRmut2	CSDA_mut2_F	AAATATTAATACCACATGGGGAGAACCCCAAGCTA TGTAATCTGAAATATATAGTAAATGCTTTTTTTTC	79.0	699	mir-9 seed 2 mutation in pLight
		CSDA_mut2_R	GAAAAAAAAGCATTTACTATATATTTCAGATTACAT AGCTTGGGGTTCTCCCCATGTGGTATTAATATTT	79.0		
pLight-MTHFD2-UTRmut1	MTHFD2 3'UTRmut1	MTHFD2_mut1_F	CCAAACCTTTTGAGTTCAACTGATCAAAGCTATGT AAAAGTGTTGCTAGAGAAAATTAGGGAA	81.3	1144	mir-9 seed 1 mutation in pLight
		MTHFD2_mut1_R	TTCCCTAATTTTCTCTAGCAACACTTTTACATAGCT TTGATCAGTTGAACTCAAAAGGTTTGG	81.3		
pLight-MTHFD2-UTRmut2	MTHFD2 3'UTRmut2	MTHFD2_mut2_F	GGGTAAGTACGCAACTTACTTTTCCAGCTATGTAC TGTCAGCAGCTGC	80.9	1144	mir-9 seed 2 mutation in pLight
		MTHFD2_mut2_R	GCAGCTGCTGACAGTACATAGCTGGAAAAGTAAG TTGCGTACTTACCC	80.9		
pLight-CCNG1-UTRmut	CCNG1 3'UTRmut	CCNG1_mutF	TTGACATCACGTTATGGATCAGTACACAATGAAAA AGCTATGTACCACAGTATATCTTATTC	79.3	1399	mir-9 seed mutation in pLight
		CCNG1_mutR	GAATAAGATATACTGTGGTACATAGCTTTTTCATTG TGTACTGATCCATAACGTGATGTCAA	79.3		
pLight-SRPK1-UTRmut	SRPK1 3'UTRmut	SRPK1_mutF	ATTTGGCCTTGGTTGGGCTCTGGCTATGTCTAATG GACTAAAATGTGAAAC	83.1	2398	mir-9 seed mutation in pLight
		SRPK1_mutR	GTTTCACATTTTAGTCCATTAGACATAGCCAGAGC CCAACCAAGGCCAAAT	83.1		
pLight-LARP1-UTRmut	LARP1 3'UTRmut	LARP1_mutF	GCCATCTTCTGGGAGAAGGAATCGAATGCATCTAA AACTGGGGTTTGGG	86.3	3608	mir-9 seed mutation in pLight
		LARP1_mutR	CCCAAACCCCAGTTTTAGATGCATTCGATTCCTTC TCCCAGAAGATGGC	86.3		

pLight-ID4-UTR	ID4 3'UTR	ID4_UTR_F_1415	*GAGA***GCTAGC**GAGCCAGGAGCACTAGA	73.1	1415	*extra GAGA* and **NheI site added**
		ID4_UTR_R_1415	*GAGA***CCTAGG**GTTACACATCACAAGAGATGGG	73.3		*extra GAGA* and **AvrII site added**
pLight-ITGB1-UTR	ITGB1 3'UTR	ITGB1_UTR_F_1210	*GAGA***CCTAGG**AAATCCCACAACACTGAATGC	74.1	1210	*extra GAGA* and **AvrII site added**
		ITGB1_UTR_R_1210	*GAGA***CTCGAG**AAATTTCATGCACACAACCTG	74.5		*extra GAGA* and **XhoI site added**
pLight-CSDAP1-UTR	CSDAP1 mRNA	CSDAP1_mRNA_Nhe_F	**GCTAGC**AGTCGTTACGCGCTGATTG	73.0	1085	**NheI site added**
		CSDAP1_mRNA_Avr_R	**CCTAGG**ATCATGACACTTGGAGGCTTAG	70.0		**AvrII site added**
pLight-CSDAP1-UTRmut1	CSDAP1 mRNA mut1	CSDAP1_SDM_1_F	CAGGCCACAGCCTTACCAACAGCTATGTAACATCCAAGCAATAAAGTGG	83.4	1085	mir-9 seed 1 mutation
		CSDAP1_SDM_1_R	CCACTTTATTGCTTGGATGTTACATAGCTGTTGGTAAGGCTGTGGCCTG	83.4		
pLight-CSDAP1-UTRmut2	CSDAP1 mRNA mut2	CSDAP1_SDM_2_F	TAATATTAATACCGCATGGGGAGAACCCCAAGCTATGTAATCTGAAATATAAAATAAATGCTTTTTTTTC	80.2	1085	mir-9 seed 2 mutation
		CSDAP1_SDM_2_R	GAAAAAAAGCATTTATTTTATATTTCAGATTACATAGCTTGGGGTTCTCCCCATGCGGTATTAATATTA	80.2		
pLight	pLight insert	pLight_InsertSeq_F	GGGAAGTACATCAAGAGCTTCGT	64.5	N/A	sequencing primers
		pLight_InsertSeq_R	CCCCCTGAACCTGAAACATAAA	65.7		
pMIR	pMIR insert	pMIR_F	GGCGATTAAGTTGGGTAAC	58.7	215	sequencing primers
		pMIR_R	CGAGTGATGAAAGCTGCG	63.4		

LARP1	LARP1 3'UTR insert	LARP1_seq_F	GTTAATTTTTAGCCTGTGCCC	61.3	N/A	sequencing primer
pcDNA	pcDNA insert	T7	TAATACGACTCACTATAGGG	50.8	N/A	sequencing primer
		SP6	TATTTAGGTGACACTATAG	43.3		
pCMV	pCMV insert	pCMV6_F_521	GCTATTGGCCATTGCATACG	65.0	521	for testing plasmid contamination (pCMV6 specific)
		pCMV6_R_521	AAATCCCCGTGAGTCAAACC	64.9		
pCMV-STAT3	pCMV-STAT3	pCMV_STAT3_qRT-PCR_F_302	AGCAGAGCTCGTTTAGTGAAC	60.2	302	amplifies plasmid induced STAT3
		pCMV_STAT3_qRT-PCR_R_302	GGAAGCTGTCACTGTAGAGC	59.2		

A.4.2. qRT-PCR PRIMERS				
Target Amplicon	**Primer Name**	**Sequence 5'>3'**	**Tm(˚C)**	**Insert (bp)**
AKT2 mRNA	AKT2_F_231	TCACTGCGCTGAAGTATGCCTT	68.0	231
	AKT2_R_231	TGTGGCCATCTTTGTCCAGCAT	70.8	
BCL2L1 mRNA	BCL2L1_RT_F	ACCCCAGGGACAGCATATCA	66.6	159
	BCL2L1_RT_R	TGCGATCCGACTCACCAATA	66.5	
IL20 mRNA	IL20_F123	CTTCACAACTGCTGCCTGAG	63.9	123
	IL20_R123	AAGAAGGACCTCCGGCTCT	64.2	
IFNAR1 mRNA	IFNAR1_RT_F	ACTCATCGCTCCTGTTCCAC	64.3	137
	IFNAR1_RT_R	GACCCTAGTGCTCGTCGC	63.7	
SOCS2 mRNA	SOCS2_F132	GCTCTTTCTCCCCAGATCCT	63.7	132
	SOCS2_R132	GCGACAGTTTCGAGAACCC	64.8	
JAK1 mRNA	JAK1_RT_F_139	CTGCTCATTGTCGTTGGTTC	63.3	139
	JAK1_RT_R_139	TGCCCTGTATGACGAGAAC	61.4	
JAK2 mRNA	JAK2_RT_F_139	CCCTCCATTTCTGTCATCG	63.1	139
	JAK2_RT_R_139	AGCAGGCAACAGGAACAAG	63.1	
STAT3 mRNA	STAT3_qPCR_F_73	GATCCAGTCCGTGGAACCAT	66.1	73
	STAT3_qPCR_R_73	ATAGCCCATGATGATTTCAGCAA	66.3	
JAG1 mRNA	JAG1_qPCR_F_126	GATCATGCCCGAGTGAGAA	64.0	126
	JAG1_qPCR_R_126	ATCGTGCTGCCTTTCAGTTT	63.7	
Beta-Actin mRNA	ACTB_qPCR_F_112	GCACAGAGCCTCGCCTT	64.6	112
	ACTB_qPCR_R_112	CCTTGCACATGCCGGAG	66.9	
GAPDH mRNA	GAPDH_qPCR_F_144	CTCTGCTCCTCCTGTTCGAC	64.2	144
	GAPDH_qPCR_R_144	TTAAAAGCAGCCCTGGTGAC	64.0	
B2MG mRNA	B2mG_F_276	CCAGCAGAGAATGGAAAGTC	61.4	276
	B2mG_R_276	CCTCCATGATGCTGCTTACA	63.8	
ADIPOR1 mRNA	ADIPOR1_qPCR_F_148	GACATCTGGCTGGTACCTCAA	64.0	148
	ADIPOR1_qPCR_R_148	GATGTAGCGCGGGGGAC	66.8	
ANXA1 mRNA	ANXA1_qPCR_F_88	TGGATGAAGCAACCATCATT	62.9	88
	ANXA1_qPCR_R_88	CCTGTTTCCTGGAGATATGC	61.1	
APAF1 mRNA	APAF1_qPCR_F_81	ACAATGCTCTACTACATGAAGGATATAAAGA	63.8	81
	APAF1_qPCR_R_81	CACTGGAAGAAGAGACAACAGGAA	65.6	

EGR1 mRNA	EGR1_qPCR_F_73	GCCTGCGACATCTGTGGAA	67.7	73
	EGR1_qPCR_R_73	GCCGCAAGTGGATCTTGGTA	67.2	
ID4 mRNA	ID4_qPCR_F_116	CCGAGCCAGGAGCACTAGAG	66.4	116
	ID4_qPCR_R_116	CTTGGAATGACGAATGAAAACG	65.3	
INHBB mRNA	INHBB_qPCR_F_70	GAAGGTGCGGGTCAAAGTGT	66.3	70
	INHBB_qPCR_R_70	CCTCTTCTCCACCATGTTCCA	66.3	
PRKDC mRNA	PRKDC_qPCR_F_83	ACAAGAGGGAGAAAGGTACAACTACAG	64.6	83
	PRKDC_qPCR_R_83	AGGTGTTTAGCAGAGTCGTGGTAA	64.8	
TNF mRNA	TNF_qPCR_F_81	CCTGCCCCAATCCCTTTATT	65.7	81
	TNF_qPCR_R_81	CCCTAAGCCCCCAATTCTCT	65.2	
CSDA isoform A mRNA	CSDA_isoA_qPCR_F_125	GAGTCGTTACGCTGCAGATT	62.0	125
	CSDA_isoA_qPCR_R_125	GGTCAAATCCTTCACTGCTG	62.3	
CSDAP1 mRNA	CSDAP1_qPCR_F_138	GCAGAAGCAGCCAGTGTGACTG	69.6	138
	CSDAP1_qPCR_R_138	TCCTCCTCCTCCCAGCGTAATC	69.5	
ITGB1 mRNA	ITGB1_qPCR_F_105	CTACCAACACGCCCTTCATT	63.8	105
	ITGB1_qPCR_R_105	ATGTGAATGCCAAAGCGAAG	65.0	
MTHFD1L mRNA	MTHFD1L_qPCR_F_148	TAGGCGCTGGGTTCATTTAC	63.8	148
	MTHFD1L_qPCR_R_148	GGTCCTGTGAGAGCCTTGTC	63.9	
MTHFD2 mRNA	MTHFD2_qPCR_F_81	GATGGCCTCCTTGTTCAGTTG	65.8	81
	MTHFD2_qPCR_R_81	ATCCTTGTCTGGAGAAACAGCATT	65.9	
VCL mRNA	VCL_qPCR_F_137	AGCCATTCCTGACCTCACC	64.2	137
	VCL_qPCR_R_137	CCTTAATAAATGCTGGTGGCA	63.5	
VAMP3 mRNA	VAMP3_qPCR_F_146	CTACAGGTCCAACTGCTGCC	64.8	146
	VAMP3_qPCR_R_146	TGCACGGTCGTCTAACTCAG	64.1	
NFKB1 mRNA	NFKB1_qPCR_F_131	GTGGACTACCTGGTGCCTCT	63.2	131
	NFKB1_qPCR_R_131	GGCATGCAGGTGGATATTTT	63.5	
PRKCA mRNA	PRKCA_qPCR_F_126	CGACTTCATCTGGGGGTTT	63.9	126
	PRKCA_qPCR_R_126	TCAGTGTCGGGTCCCTTATC	63.9	
IBRDC2 mRNA	IBDRC2_qPCR_F_108	GGAATGCCAGTGCATCTTTT	63.9	108
	IBDRC2_qPCR_R_108	TTTAGGCACACCATGTCAGG	63.6	
SLC25A24 mRNA	SLC25A24_qPCR_F_112	TTGAGGCTTCAGAAATTGTCC	63.0	112
	SLC25A24_qPCR_R_112	TCCACTGTCATTGTCCCATC	63.6	
MBNL1 mRNA	MBNL1_qPCR_F_146	GGCCAGACACGGAATGTAAA	64.7	146
	MBNL1_qPCR_R_146	CGTTTTTAAATGTGGGGGTG	63.7	

MMP13 mRNA	MMP13_qPCR_F_136	GCAGCTGTTCACTTTGAGGA	63.2	136
	MMP13_qPCR_R_136	CACCAATTCCTGGGAAGTCT	62.9	
MYC mRNA	MYC_qPCR_F_144	GCTGCTTAGACGCTGGATTT	63.3	144
	MYC_qPCR_R_144	CTCCTCCTCGTCGCAGTAGA	64.7	
E2F2 mRNA	E2F2_qPCR_F_143	CTACACACCGCTGTACCCG	64.6	143
	E2F2_qPCR_R_143	CCAGATCCAGCTTCCTTTTG	66.9	
ERBB2 mRNA	ERBB2_qPCR_F_145	AGCCCTACGAGCACCTGAC	63.4	145
	ERBB2_qPCR_R_145	GGAAAAGCGGCCAGTATAGG	63.7	
ESR1 mRNA	ESR1_qPCR_F_145	AAGCTTCGATGATGGGCTTA	63.5	145
	ESR1_qPCR_R_145	AGGATCTCTAGCCAGGCACA	63.9	
IGFBP4 mRNA	IGFBP4_qPCR_F_98	CACCCTCGTCCTTGTCAGAG	64.9	98
	IGFBP4_qPCR_R_98	CCTGCACACACTGATGCAC	64.4	
IGFBP5 mRNA	IGFBP5_qPCR_F_141	CTACCGCGAGCAAGTCAAG	63.7	141
	IGFBP5_qPCR_R_141	ACTGCTTCAGCCTTCAGCTC	63.8	
JUN mRNA	JUN_qPCR_F_141	TAACAGTGGGTGCCAACTCA	64.2	141
	JUN_qPCR_R_141	TTTTCTCTCCGTCGCAACTT	63.8	
LARP1 mRNA	LARP_mRNA_F_137	TGCATCTCCAAAGTCACCAA	64.4	137
	LARP_mRNA_R_137	GTGACAGGGAGAAGCCATTG	64.7	
SRPK1 mRNA	SRPK1_qPCR_F_132	AGAAAAGGACCAAGGCCAAG	64.3	132
	SRPK1_qPCR_R_132	GCTCATCATCATCAGATCCCA	65.1	
TBPL1 mRNA	TBPL1_qPCR_F_141	CATCCTTGTCCTCCAGCTTC	63.8	141
	TBPL1_qPCR_R_141	CATCCATTGGGGTGGTTTTA	64.2	
TGFB3 mRNA	TGFB3_qPCR_F_132	AAATTCGACATGATCCAGGG	63.6	132
	TGFB3_qPCR_R_132	TTCTGCTCGGAATAGGTTGG	64.0	
TGFBR2 mRNA	TGFBR2_qPCR_F_135	GCACGTTCAGAAGTCGGTTA	62.9	135
	TGFBR2_qPCR_R_135	CAGTTGCTCATGCAGGATTT	62.8	
ANXA2 mRNA	ANXA2_qPCR_F_144	CGGGATGCTTTGAACATTG	64.1	144
	ANXA2_qPCR_R_144	TGCAAGTTCCTTTTTGGTCC	63.9	
AP3B1 mRNA	AP3B1_qPCR_F_141	CTTCCCACACCAGCTCTTTC	63.8	141
	AP3B1_qPCR_R_141	TCCACTCATTCGATGAAGCA	64.5	
CCNG1 mRNA	CCNG1_qPCR_F_116	CAGTTCTTTGGCTTTGACACA	62.8	116
	CCNG1_qPCR_R_116	AAGCAGCTCAGTCCAACACA	63.8	
CITED2 mRNA	CITED2_qPCR_F_109	AAGGTCCCCTCTATGTGCTG	63.0	109
	CITED2_qPCR_R_109	CATATGGTCTGCCATTTCCA	63.3	

CSDA mRNA	CSDA_qPCR_F_141	TACCACGTGGGACAGACCTT	64.4	141
	CSDA_qPCR_R_141	AGTTGGATTTCGATGAACCG	63.8	
ANXA2P3 mRNA	ANXA2P3_mRNA_ NheI_R_582	GCTAGCTACAGCCCATCAAGAGAGAGC	70.7	582
	ANXA2P3_mRNA_ AvrII_F_582	CCTAGGACAGTACACAGGAGGCAAAGTG	71	
ANXA2P2 mRNA	ANXA2P2_mRNA_ NheI_R_699	GCTAGCGAACTGATTGACCAAGATG	68.6	699
	ANXA2P2_mRNA_ AvrII_F_699	CCTAGGATTTAGAGACAGAGTCTAGCTC	63.0	
ANXA2P1 mRNA	ANXA2P1_mRNA_ NheI_R_1085	GCTAGCACCTAGATAGTGGCTTTGGG	69.2	1085
	ANXA2P1_mRNA_ AvrII_F_1085	CCTAGGACAGTACACAGGAGGCAAAGTG	71.0	

A.5. Vector Maps

Original vector maps

A.5.1. pcDNA3 Mammalian Expression Vector (Invitrogen, USA)

Comments for pcDNA3:
5446 nucleotides

CMV promoter: bases 209-863
T7 promoter: bases 864-882
Polylinker: bases 889-994
Sp6 promoter: bases 999-1016
BGH poly A: bases 1018-1249
SV40 promoter: bases 1790-2115
SV40 origin of replication: bases 1984-2069
Neomycin ORF: bases 2151-2945
SV40 poly A: bases 3000-3372
ColE1 origin: bases 3632-4305
Ampicillin ORF: bases 4450-5310

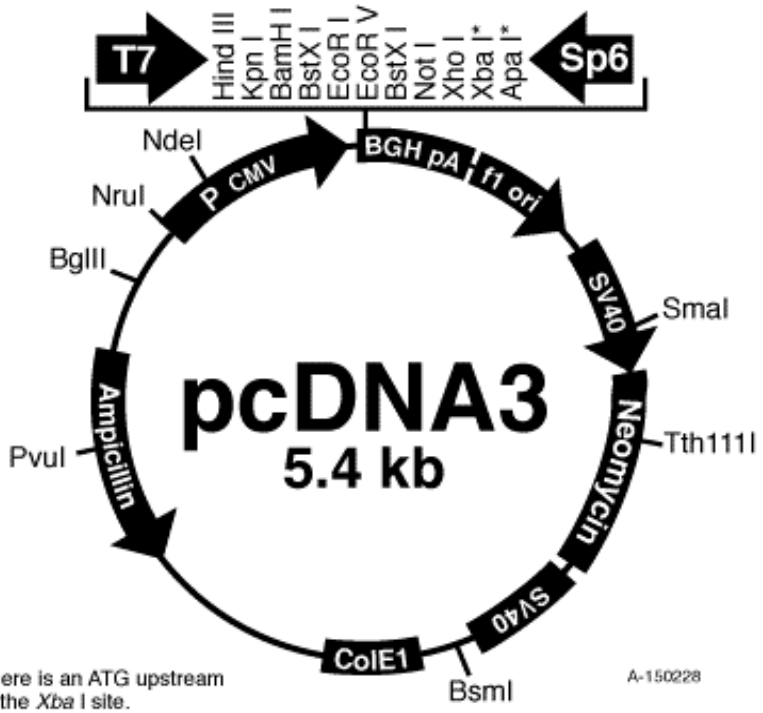

* There is an ATG upstream of the *Xba* I site.

A.5.2. pCRII-TOPO TA Cloning Vector (Invitrogen, USA)

Comments for pCR®II-TOPO
3950 nucleotides

LacZα gene: bases 1-588
M13 Reverse priming site: bases 205-221
Sp6 promoter: bases 239-256
Multiple Cloning Site: bases 269-399
T7 promoter: bases 406-425
M13 (-20) Forward priming site: bases 433-448
M13 (-40) Forward priming site: bases 453-468
f1 origin: bases 590-1004
Kanamycin resistance ORF: bases 1338-2132
Ampicillin resistance ORF: bases 2150-3010
ColE1 origin: bases 3155-3828

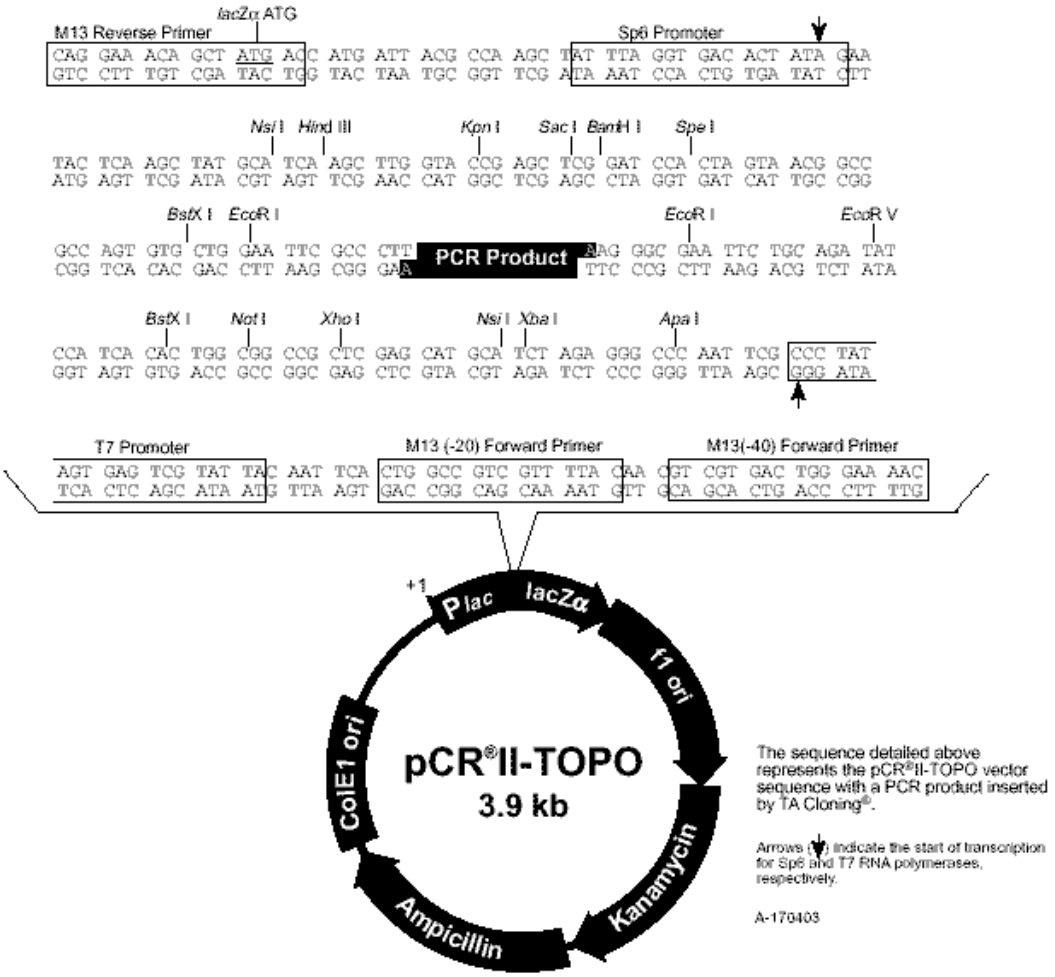

The sequence detailed above represents the pCR®II-TOPO vector sequence with a PCR product inserted by TA Cloning®.

Arrows (▼) indicate the start of transcription for Sp6 and T7 RNA polymerases, respectively.

A-170403

A.5.3. pMIR-REPORT miRNA Expression Vector (Ambion, USA)

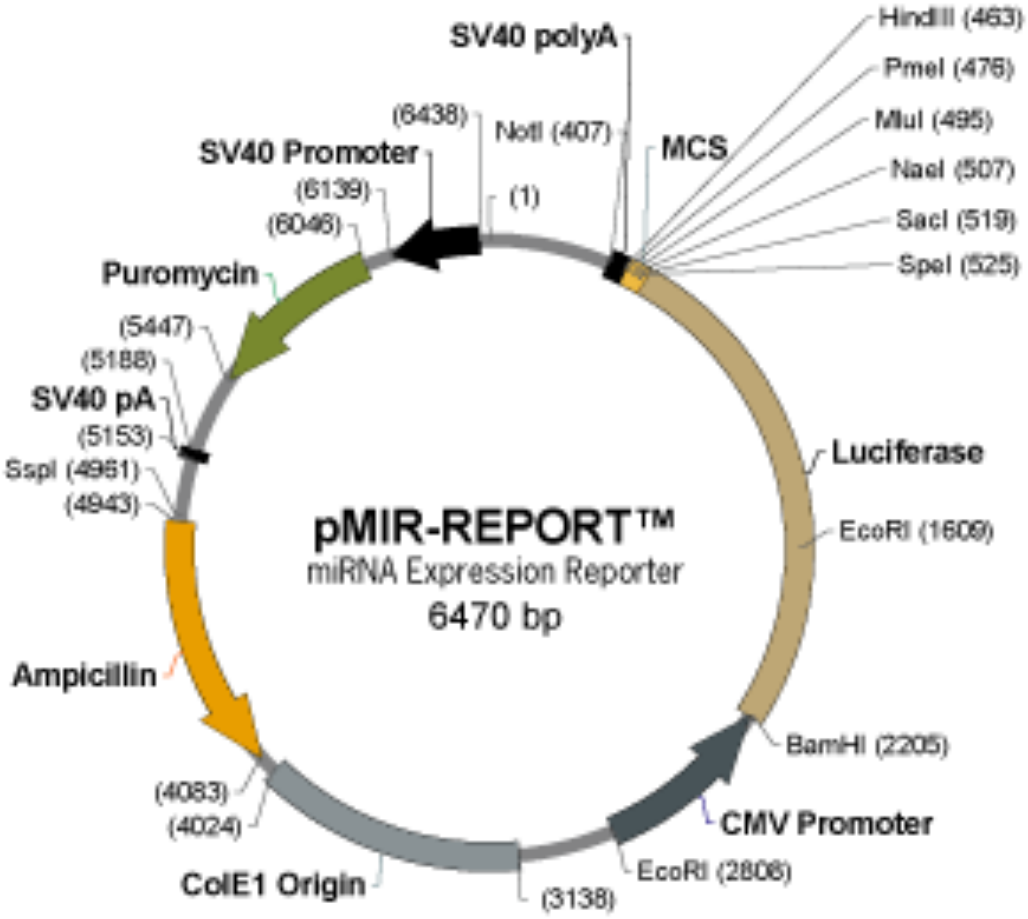

A.5.4. pRL-SV40 Renilla Luciferase Vector (Promega, USA)

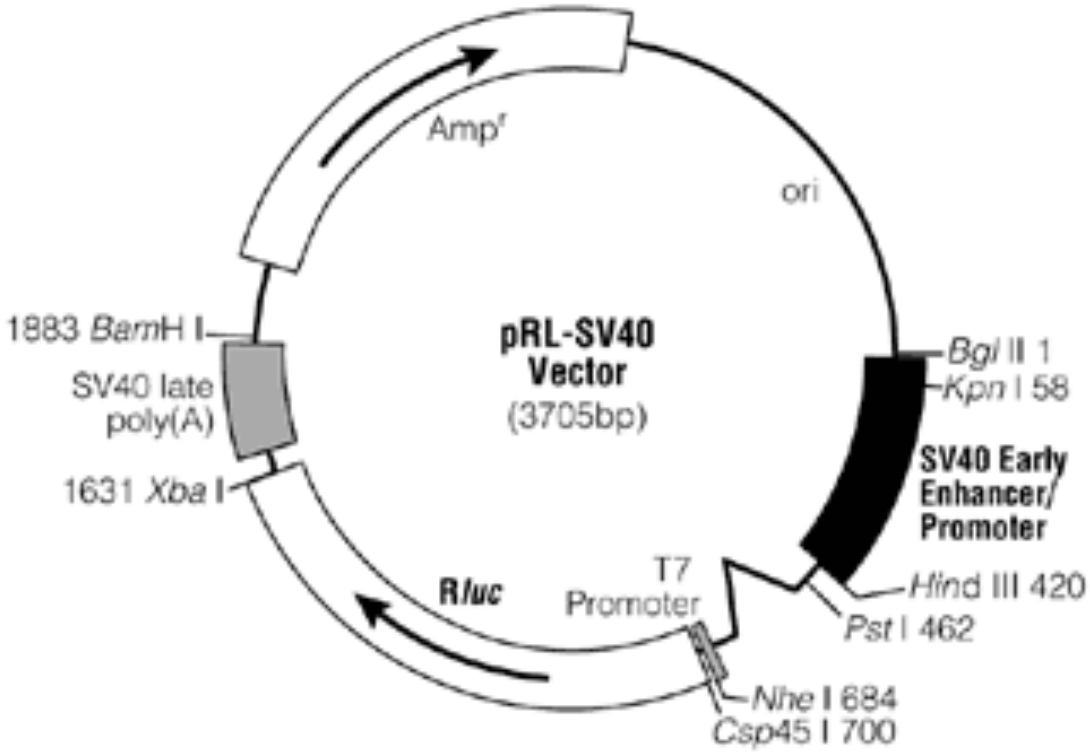

A.5.5. pLightSwitch luciferase vector (Switchgear Genomics, USA)

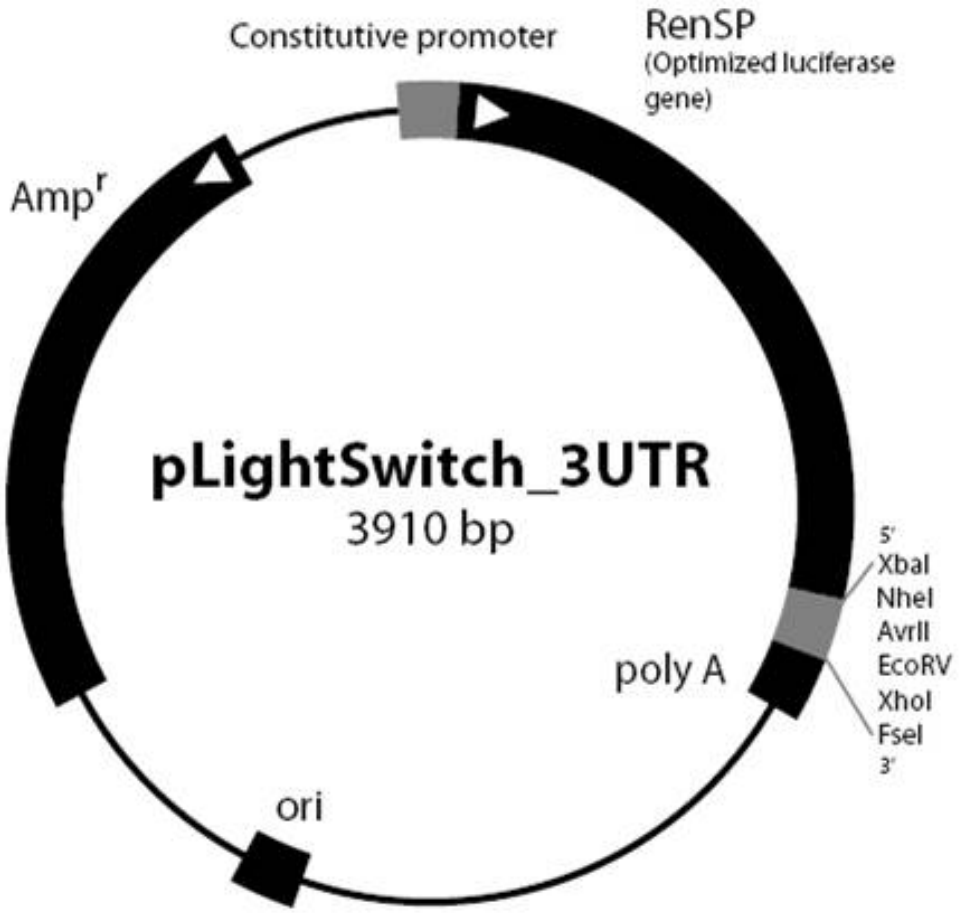

pLightSwitch Luciferase Construct Maps (Vector NTI)

A.5.6. pLight/ANXA2

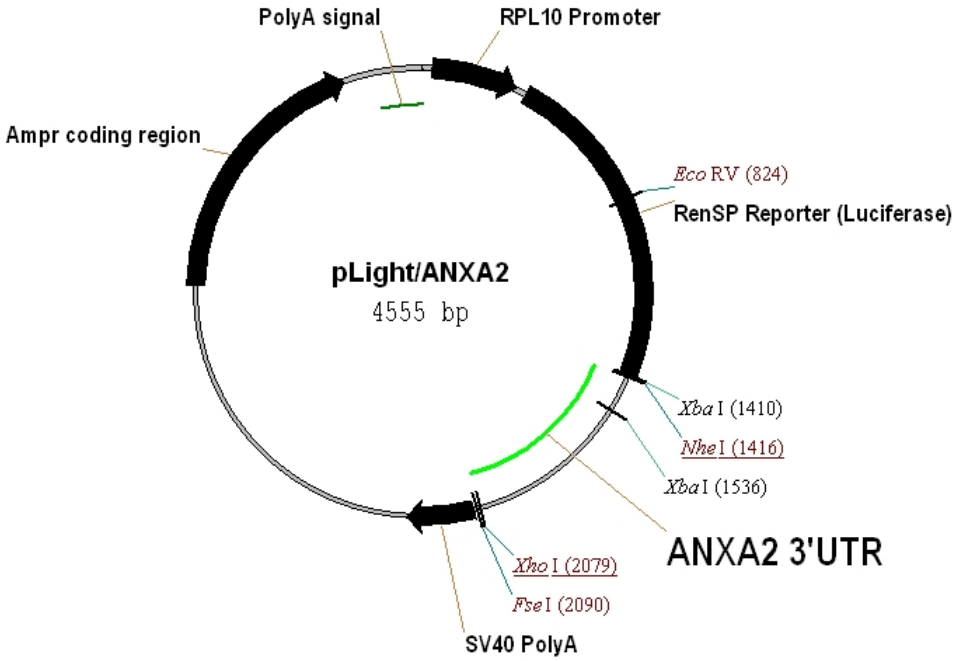

A.5.7. pLight/AP3B1

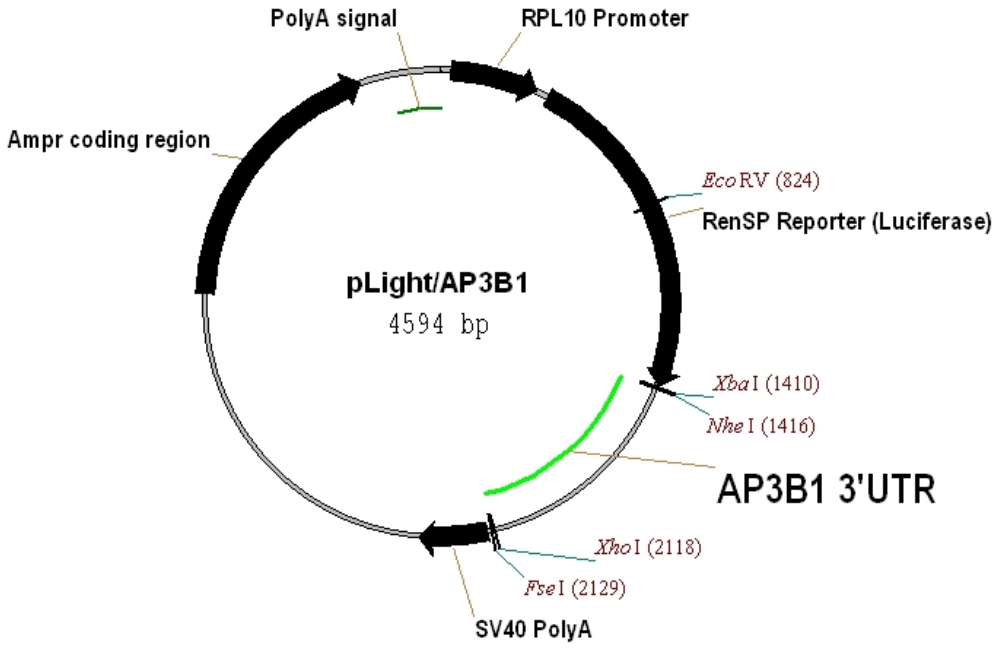

A.5.8. pLight/CCNG1

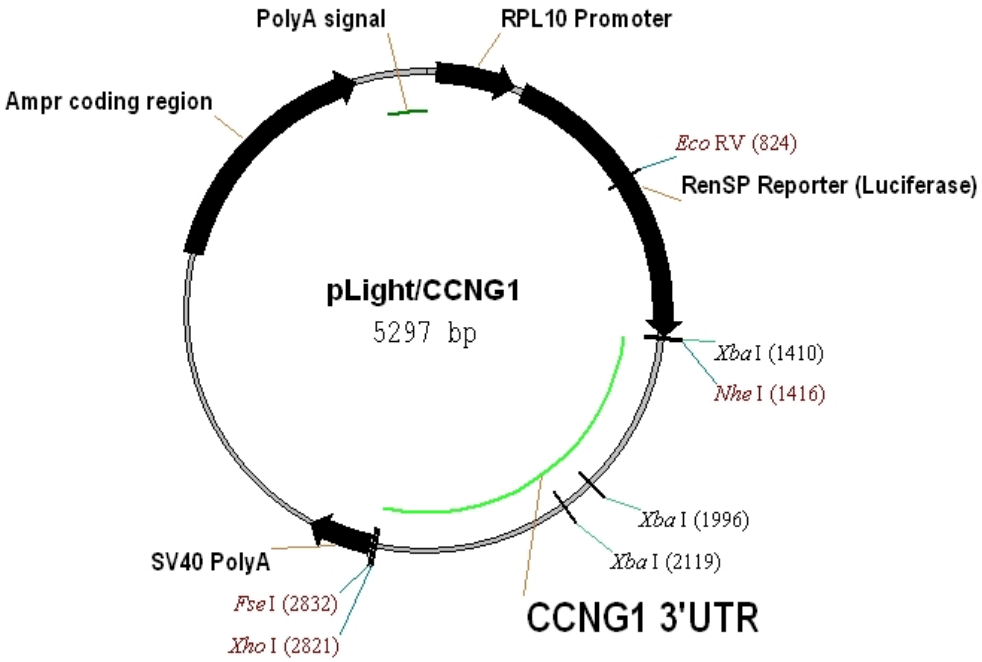

A.5.9. pLight/CSDA

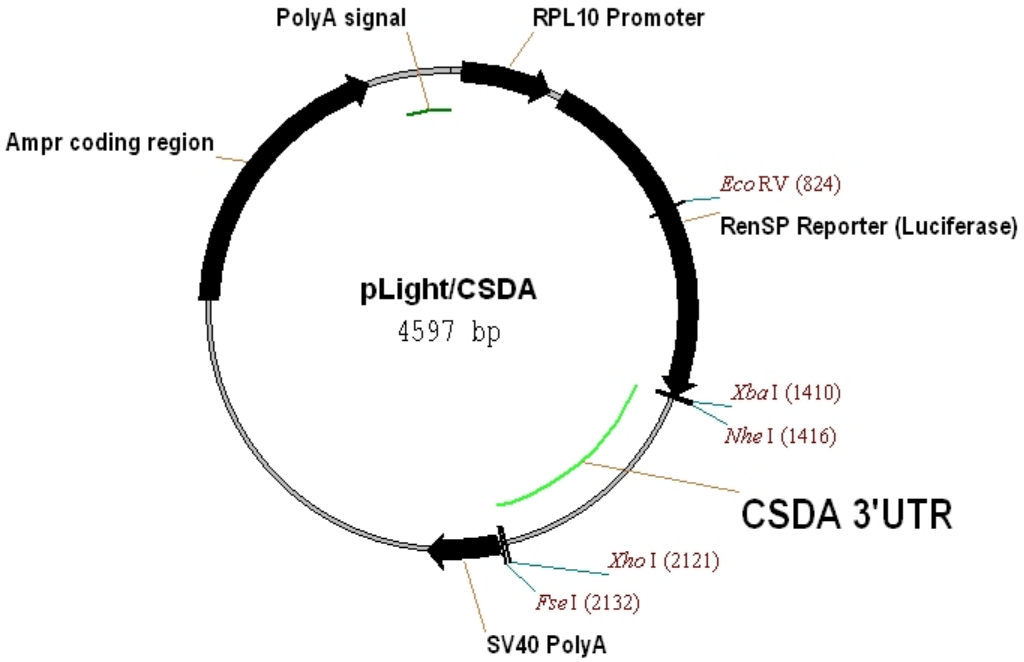

A.5.10. pLight/CSDAP1

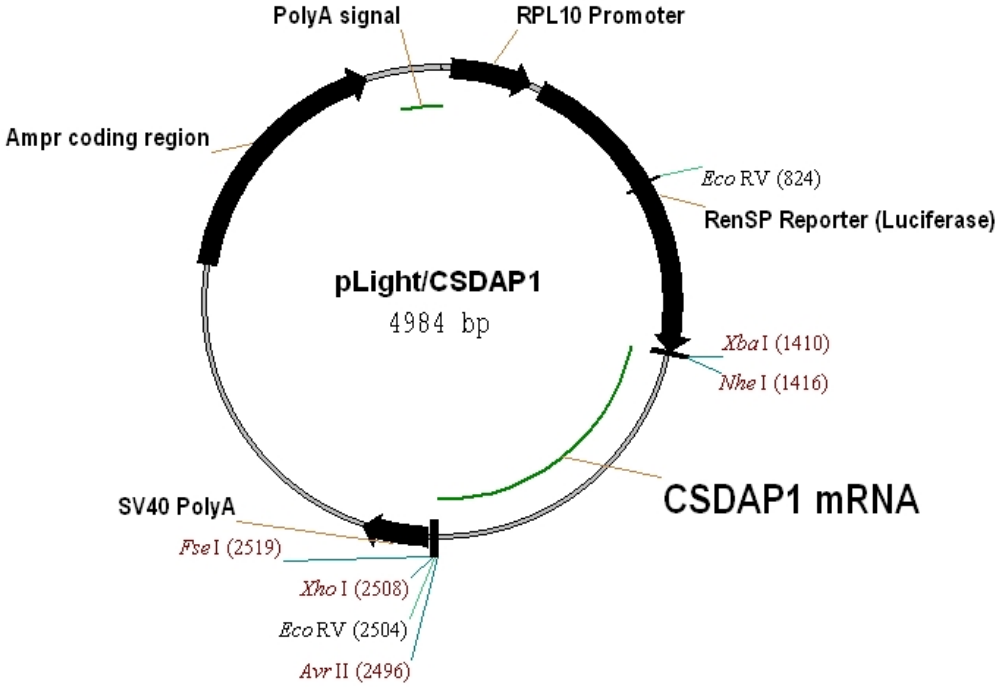

A.5.11. pLight/LARP1

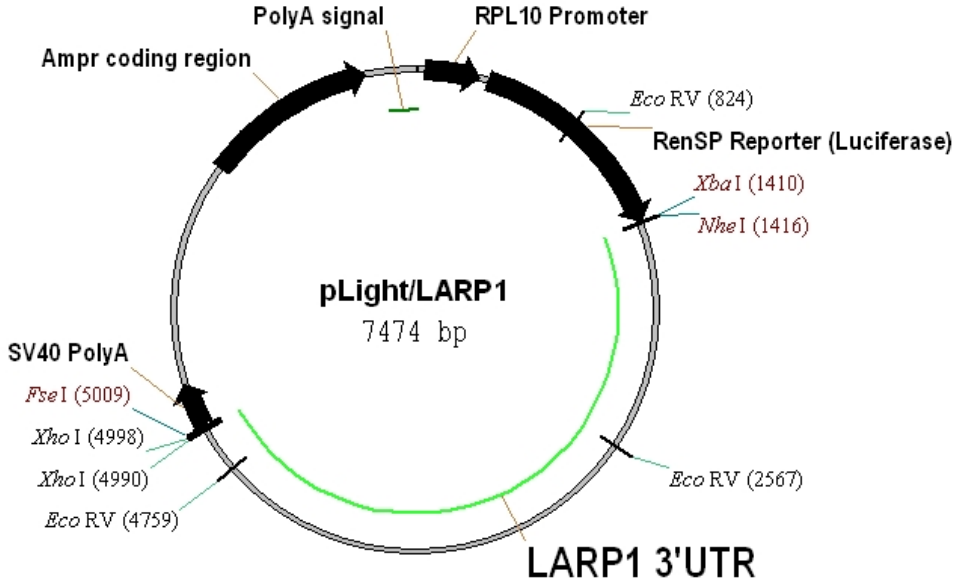

A.5.12. pLight/MTHFD1L

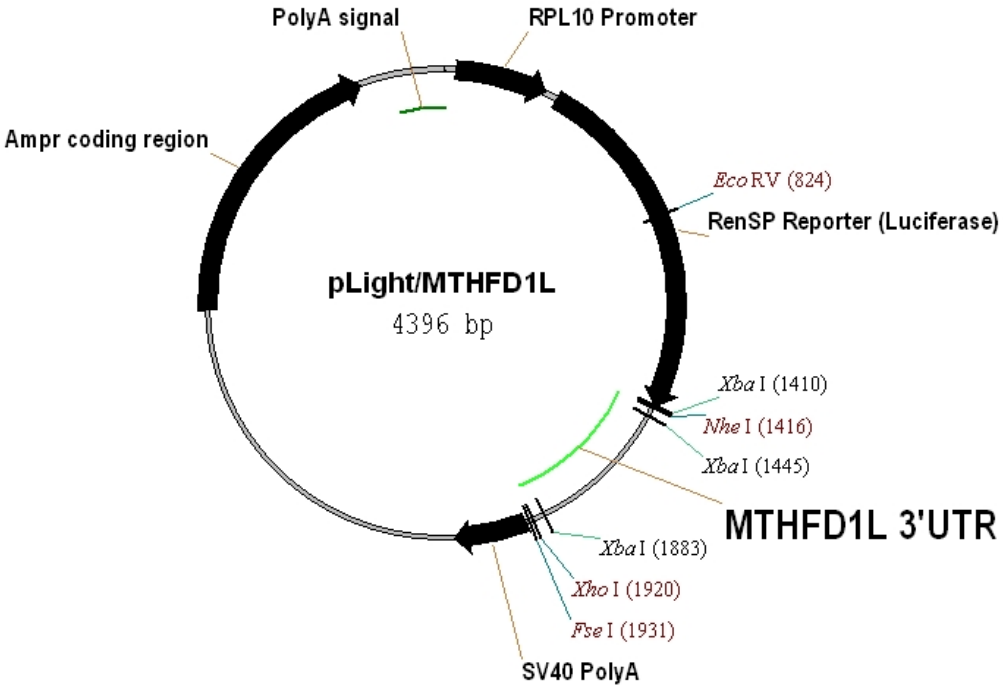

A.5.13. pLight/MTHFD2

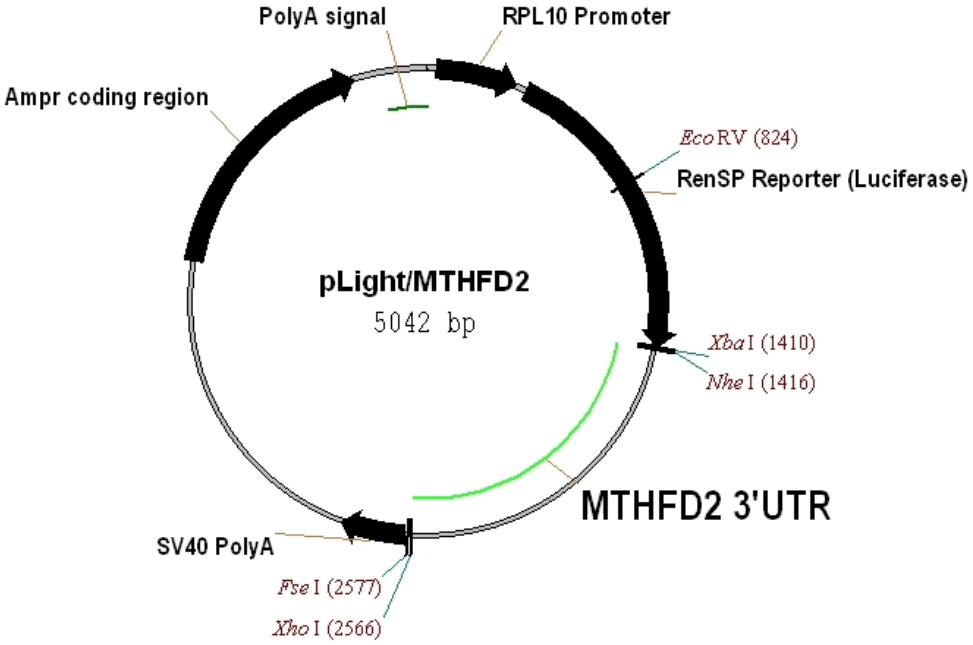

A.5.14. pLight/SRPK1

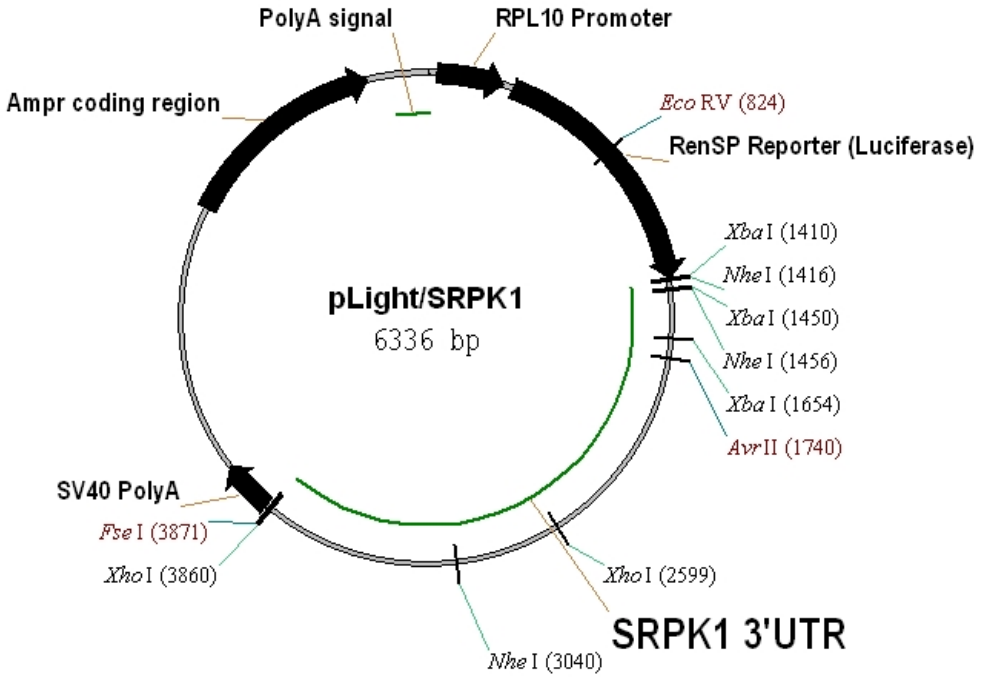

A.5.15. pLight/ITGB1